Construction of the new lock in Terneuzen using pneumatic caissons

A construction alternative to conventional construction methods

T.A.W. van Corven

Master of Science Thesis

TU Delft Delft University of Technology

Lievense CSO infra water milieu

Faculty of Civil Engineering and Geosciences

Construction of the new lock in Terneuzen using pneumatic caissons

A construction alternative to conventional construction methods

T.A.W. van Corven
6 March 2015

Educational institution:
Delft University of Technology
Faculty of Civil Engineering and Geosciences
.

Stevinweg 1
2628CN Delft
Netherlands

Company:
LievenseCSO
Tramsingel 2
4814 AB Breda

Postbus 3199
4800 DD Breda

Graduation committee:

Prof. Ir. A.F. van Tol	Delft University of Technology
Ir. W.F. Molenaar	Delft University of Technology
Dr.ir. K.J. Bakker	Delft University of Technology
Ir. W.O. Molendijk	LievenseCSO

PREFACE

This is the final report for the thesis: *Construction of the new lock in Terneuzen using pneumatic caissons: A construction alternative to conventional construction methods*. The thesis is part of the master's program Hydraulic Engineering, specialization Hydraulic Structures and has been completed at Delft University of Technology. The report describes the construction method for the design of a new lock in Terneuzen. The study has been performed in collaboration with LievenseCSO in Breda.

I would like to thank my company supervisor ir. W.O. Molendijk for his supervision during my time at LievenseCSO. I would also like to express my gratitude to my supervisors Prof. Ir. A.F. van Tol, Ir. W.F. Molenaar and Dr.ir. K.J. Bakker for their input, guidance and sharing their knowledge. At last I would like to thank Brigitte van Kronenburg for her valuable assistance during my graduation period.

Tim van Corven

Breda, 6 March 2015

ABSTRACT

The lock complex at Terneuzen is the main entrance for ships coming from the Westerscheld and navigating towards the cities of Terneuzen and Ghent. The construction of a new large lock at the lock complex of Terneuzen is planned to increase its capacity. This lock will be built between the existing locks. See figure i.

The ground level is situated at NAP +6 meter. The minimum normative sea water level occurring twice a year is NAP -2.85 meter. The new lock will have larger dimensions than the current locks. It is assumed that a ship with a draft of 13.1 meter must be able to use the lock tide independently. Because of the large allowable draft the lock must be founded to a depth of NAP -17.26 m. It is becoming increasingly difficult to construct the new lock with traditional building methods like combi– or diaphragm walls to such extent. In this master thesis the use of pneumatic caissons as alternative construction method for the new lock in Terneuzen has been elaborated.

Pneumatic caissons have been used for many times as construction method. However, pneumatic caissons have never been used with the dimensions required for the new lock head. ($l = 132m$, $w = 45m$ & $h = 33m$) The pneumatic caisson method involves the construction of a relative rigid concrete box at ground level that is lowered into the ground by excavating the soil underneath it. Under the bottom slab of a pneumatic caisson an air-pressurized space, called the working chamber, is present which is made up of tapering walls around the perimeter of the

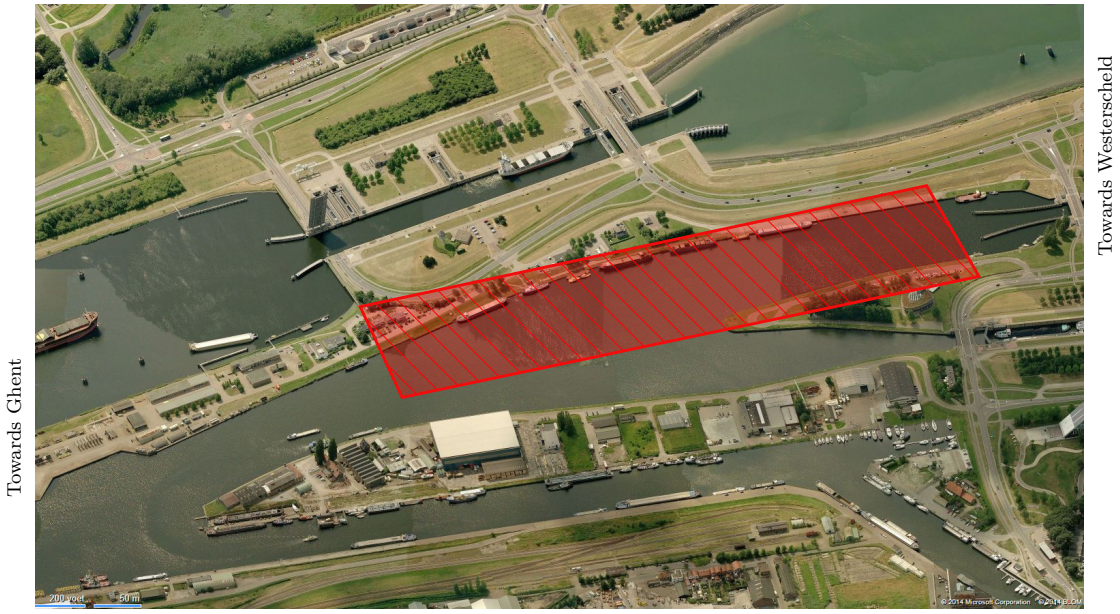

Figure i: *Aerial photo of the lock complex, the location of the new lock is indicated in red*

caisson base slab. These tapering walls are called the cutting edges of the caisson. The working chamber is kept dry by the presence of air pressure. Due to the air pressure, groundwater is not able to enter the working chamber. The deeper the caisson is located below the water table, the higher the air pressure should be.

In this master thesis two construction alternatives for the lock heads with help of pneumatic caissons are elaborated:

1. The construction of one large pneumatic caisson with a length of 132 meter, width of 45 meter and a height of 33 meter containing the complete lock head including the gate chamber and gate recess. The working chamber is divided into 14 compartments.

2. The construction of two (compartmentalized–) pneumatic caissons which can be subsided independently. One caisson with a length of 10 meter, width of 45 meter and a height of 33 meter is covering the gate recess and the other caisson with a length of 67 meter, width of 45 meter and a height of 33 meter is covering the gate chamber. Between the pneumatic caisson an immersible caisson is located. This caisson acts as foundation for the guiding rail and moving equipment and prevents piping below the lock gates.

With help of SCIA Engineer, a software package for structural calculations, the structural feasibility of the caisson is analyzed and worked out. Due to the lack of bending and torsional stiffness in the first construction alternative the occurring forces and moments are up to 2 times larger in comparison to the second construction alternative.

The use of pneumatic caissons to construct the lock head has some advantages over the use of a traditional building pit. The building time of 22 months is 8 months shorter in duration compared with the building pit and the building costs are with respectively €48.300.000 and €37.700.000 much lower than the building costs of a building pit which is estimated at €52.600.000. Moreover the pneumatic caissons can be constructed in controlled conditions above the surface level. Despite of the advantages the construction method has a large number of disadvantages.

Different conclusions can be drawn up. Some conclusions are in favor of the construction with pneumatic caisson. On the other hand the construction method has some important disadvantages that can not be neglected. A considerably large working space is required for the sedimentation basin and bentonite de-sanding installation during subsidence of the caisson(s). The possibility of rotation of the caisson during subsidence and working under an overpressure increase the associated risks. It should be taken into account that about 50% of the surface area of the bottom slab must be reinforced against shear. Also a large amount of bending reinforcement (101 kg/m^3–219 kg/m^3) is required. Moreover there is less practical experience with the construction of pneumatic caissons.

A comparison between the options on *feasibility, safety, risk, required materials, building time* and *costs* shows that the reference design, the use of a traditional building pit to construct the lock head, is the best conceivable option.

TABLE OF CONTENTS

Part I

INTRODUCTION

1

INTRODUCTION

1.1 OBJECTIVE AND SCOPE

At this moment the lock complex at Terneuzen is the main entrance for ships coming from the Westerscheld and navigating towards the cities of Terneuzen and Ghent. The channel Terneuzen-Ghent is part of the Seine-Schelde connection which connects the French waterways network with the waterway networks of The Netherlands, Belgium and Germany. The Netherlands and Flanders are planning the construction together of a new lock at Terneuzen. The new lock will be constructed between the existing locks. In this master thesis the use of pneumatic caissons as construction alternative has been elaborated.

1.2 RESEARCH QUESTIONS

The main aim of this master thesis is to examine the technical and economic feasibility of the use of pneumatic caissons for the construction of the new lock in Terneuzen. Hence the main question to be answered is: Are there possibilities to use pneumatic caissons for the construction of the new lock at Terneuzen?

A number of sub-questions would have to be answered:

- What are the underlying principle behind a pneumatic caisson.
- What are the acting forces and required dimensions for the design of a pneumatic caisson?
- What are the advantages and disadvantages of a design with pneumatic caissons in comparison to a traditional building pit?

1.3 REPORT STRUCTURE

The objective of this document is to present a continuous, readable report of a feasible design process. Additional background information for the design process and calculations for a variety of issues are presented in the appendices. For this reason the appendices cannot be seen separately from the main report.

In this first part and chapter an introduction to the thesis subject was given. Further the research aim and the report structure are elaborated.

Part I - Introduction Chapter 1 - Introduction

In the second part of the report an introduction to the lock complex at Terneuzen is given. The report continuous with site specific and site non-site specific characteristics. The combination of boundary conditions, requirements and assumptions serves as the input for the design steps and leads to a first consideration of the future structure.

Part II - Analysis of local circumstances and conditions	Chapter 2 - Lock Complex Terneuzen Chapter 3 - Boundary conditions Chapter 4 - Requirements and assumptions

In the third part pneumatic caissons are elaborated. The technique behind, components and the methods of excavation are described.

Part III - Analysis of construction method	Chapter 5 - Pneumatic Caissons

In the fourth part of the report the design process, based on a global-to-detailed design methodology, starts. The general construction planning and mode of operation will be stated. Subsequently the construction of a pneumatic caisson for the lock head is worked out for two different variants.

Part IV - New lock Terneuzen
Chapter 6 - Concept development of pneumatic caissons
Chapter 7 - Variant 1 - One large caisson divided in multiple compartments
Chapter 8 - Variant 2 -Two caissons which can be subsided individually divided into several compartments
Chapter 9 - Reference design - Traditional building pit
Chapter 10 - Consideration between the variants

In part five of the report the conclusions is drawn and recommendations for future research are given.

Part V - Conclusions and recommendations	Chapter 11 - Conclusions - Recommendations

Subsequently after the conclusion and recommendations the bibliography as well as the appendices are given. Different construction methods, general information about caissons, soil information, planning and calculations are described herein.

Part VI - References and Appendices

Part II

ANALYSIS OF LOCAL CIRCUMSTANCES AND CONDITIONS

2

LOCK COMPLEX TERNEUZEN

This chapter starts with a global description of the lock complex at Terneuzen wherein the location of the current locks and possibilities for a new lock are described. The location of the new lock is in fact the result of previous studies. Those studies are also describing the function of the new lock which will be elaborated.

2.1 CURRENT SITUATION

The Westerscheld is connected with the city of Ghent through a channel that is situated between the cities of Terneuzen and Ghent. A lock complex at Terneuzen connects the Westerscheld with this channel. The lock complex consists out of three separated locks. Called the western lock, middle lock and the eastern lock. The western lock is built in 1968 and is suitable for big seagoing vessels where the other two locks are only appropriate for smaller inland vessels. The maximum tide-independent normative vessel allowed on the channel Terneuzen-Ghent has a length of 265 meter, is 34 meter wide and has a draft of 12.5 meter in fresh water. Vessels with larger dimensions have to ask permission first to navigate on the channel, and have to fit in the lock. Vessels with a larger draft can use the lock only tide dependent. Due to up-scaling nowadays the western lock is used both by inland– and seagoing vessels. The eastern lock, also build in 1968, is only used by inland vessels through there limited dimensions. The middle lock, build in 1910 and completely renovated in 1986, is used for both inland vessels and tugboats using the lock to cross the lock complex quickly. The dimensions are given in table 2.1.

Table 2.1: *Overview of the current lock dimensions and maximum ship dimensions*

	Lock dimensions			**Maximum ship dimensions**		
	Length [m]	**Width** [m]	**Depth** [m]	**Length** [m]	**Width** [m]	**Draft** [m]
Western lock	290	40	13.5	265	34	12.5
Middle lock	140	18	8.6	140	17.4	6.5
Eastern lock	280	23	4.0	200	23	4.3

The city of Terneuzen is located on the eastern side of the lock complex. The entrance of the Westerscheld tunnel, which connects Zeelandic Flanders with South Beveland on the northern side of the tunnel. In figure 2.1 an overview of the lock complex is shown.

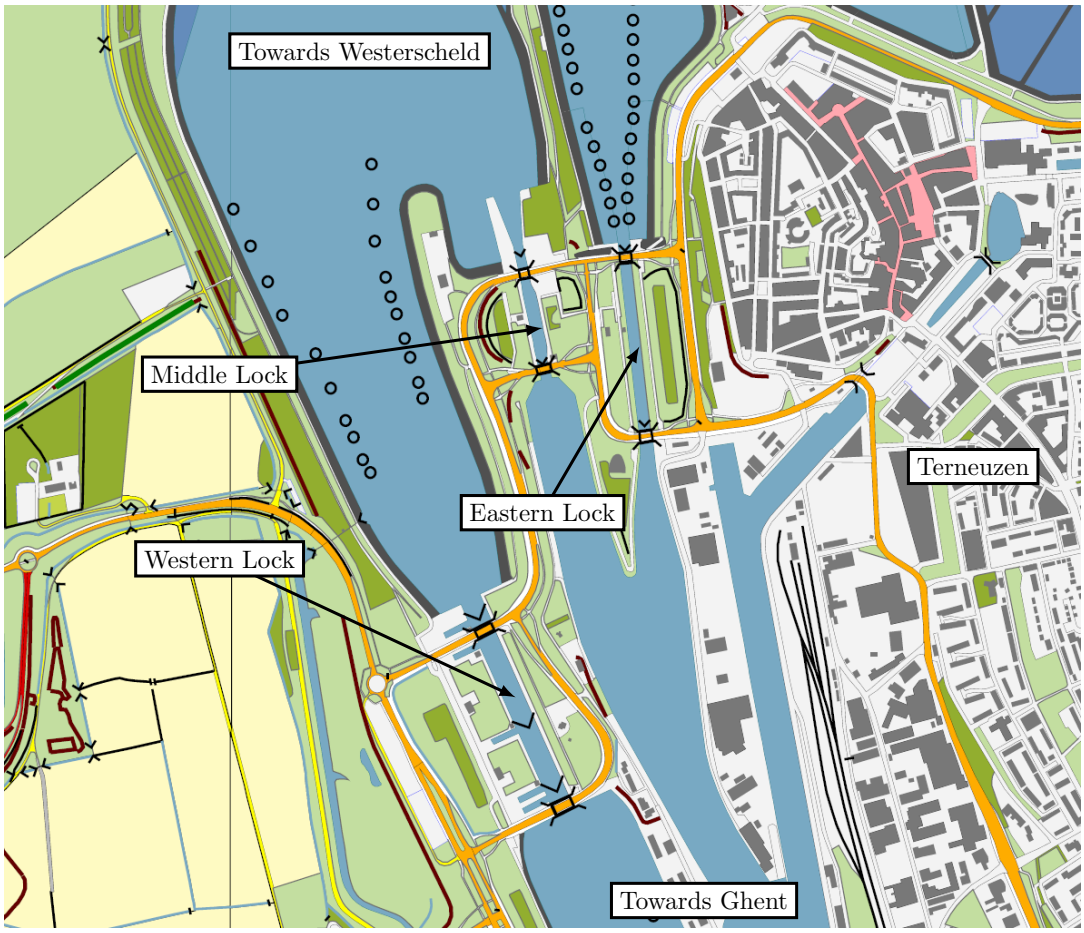

Figure 2.1: *Overview of the lock complex near Terneuzen.*

2.2 INCREASE LOCK CAPACITY

At this moment the lock complex at Terneuzen is the main entrance for ships coming from the Westerscheld and navigating towards the cities of Terneuzen and Ghent. Besides the complex is part of the maritime route between The Netherlands, Belgium and France. The channel Terneuzen-Ghent is part of the Seine-Schelde connection which connects the French waterways network with the waterway networks of The Netherlands, Belgium and Germany. At present economic hard times companies are moving production facilities towards low-wage counties. This underlines the importance of a strong logistic and distribution networks. At this moment the target value of the maximum waiting time for traversing the lock-complex in Terneuzen is 30 minutes. In practice the waiting time for crossing one of the locks is regularly more than one hour. At present time the lock complex at Terneuzen doesn't realize this target value of a maximum waiting time of 30 minutes. In the period 2007-2008 research has been done towards the maritime accessibility of the channel zone. From this research several problems emerged.

One of the bottlenecks is the robustness for big seagoing vessels. Through the large sizes of these vessels the only option to pass the lock complex at Terneuzen is by making use of the western lock facility. When maintenance of the lock is required or an accident occurred in or

near to the lock, the western lock will close and there is no possibility for these seagoing vessels to enter or leave the channel. Only smaller (inland) vessels can use the other two locks. Because of up scaling effects ships are growing in time and the portion of ships that can only use the western lock is growing in the future. In future there is also more inland ship activity expected due to the opening of the connection towards the Seine-Nord. When inland vessels are using the western locks due to capacity problems in the other two locks a conflict with seagoing vessels will occur. Because of that reason waiting times for passing the lock complex will increase even more. In 2011 more than 70.000 vessels have used one of the locks.

A solution to the problems above is already given. Both the Netherlands and Flanders are preparing the building of a new lock. This lock will be built between the existing eastern and western lock. The new lock will have larger dimensions than the current western lock.

Not only more ships can be handled in time by use of this new lock also larger ships are in the future able to pass the lock complex where this was not possible in the past. The system of locks will become more robust since the big seagoing vessels that make already use of the current western lock have in the future the possibility to use one of the two existing sealocks. As the passing options for the seagoing vessels increase, also the smaller inland vessels will benefit from an increase in capacity. Both the region of Zeeland and Flanders and thereby both investing countries, can make profit of a significant economic impulse.

2.3 LOCATION OF THE NEW LOCK

In this report the assumptions and underlying principles of the report [Notitie Reikwijdte en Detailniveau LievenseCSO, 2014f] are used. Therefore the new lock will be located at the eastern side of the west lock, below the middle lock. In the future situation the middle lock will be removed. An overview of the current lock complex and the proposed location of the new lock is given in figure 2.2.

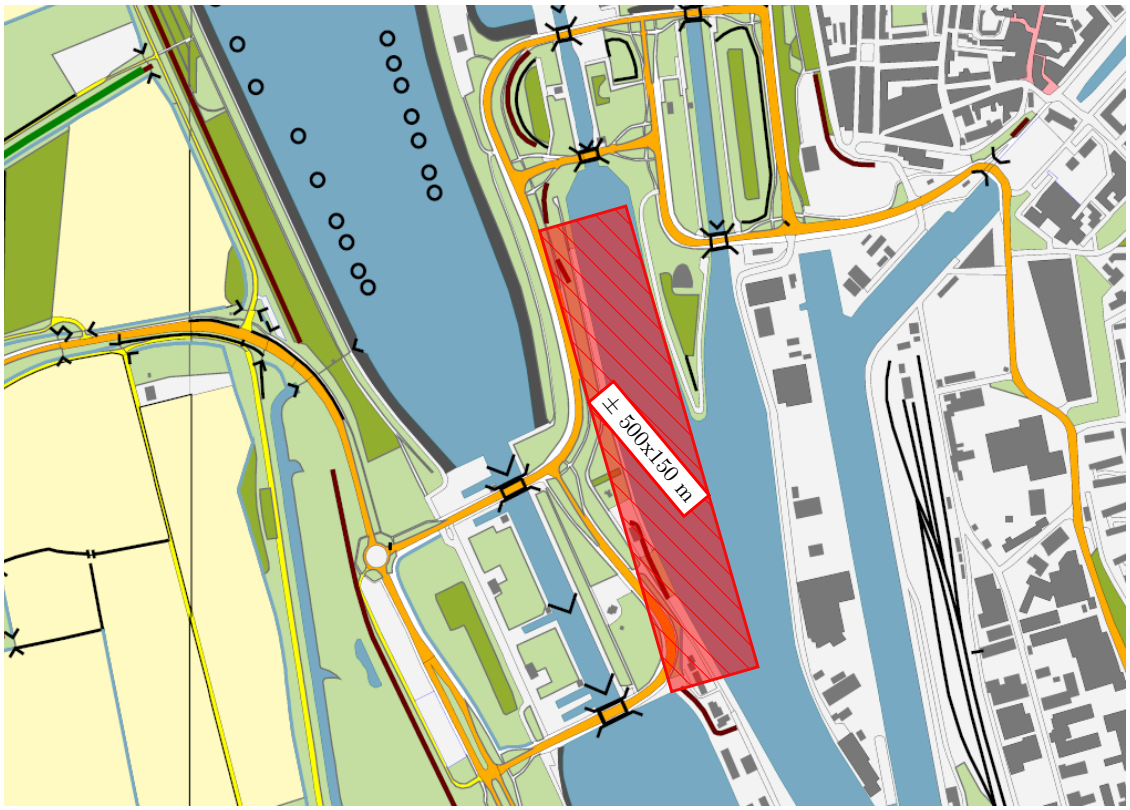

Figure 2.2: *Map of the lock complex, in red the location of the new lock is indicated roughly*

2.4 LOCK FUNCTIONS

In the world there are a lot of different types of locks, each with different properties and environmental characteristics. In Terneuzen the already existing locks and the new lock full fill roughly three main functions. [Molenaar, 2011]

- **Water retention** - The lock is a boundary between two different water levels. On the outer side of the lock the Westerscheld is located, on the inner side the channel Terneuzen-Ghent is situated. The lock maintains the different water levels on both side.
- **Ship passage** - Because of shipping the lock complex must be a passage for smaller inland vessels and larger seagoing vessels.
- **Water quality control** - On the outer side of the lock complex salt water is present, on the inner side of the complex fresh water is flowing towards the Westerscheld. In times of low discharge the lock complex must prevent the inflow of salt water towards the channel which can cause problems for the industry which uses the water in the channel as process water.

To accomplish the above mentioned functions, a standard lock design exist out of multiple elements. Together these elements perform the function of the lock. The main elements of the lock are:

1. Waiting– or lay-by berths
2. Guide wall or lead-in jetty
3. Lock gates
4. Lock heads
5. Loch chamber
6. Filling and emptying system
7. Cut-off walls and screens to prevent piping
8. Bottom protection

The above main elements are schematised in figure 2.3.

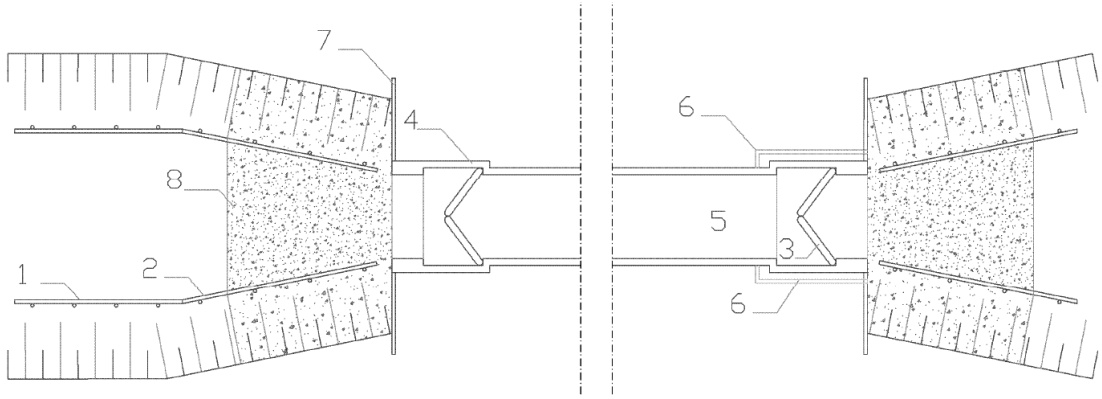

Figure 2.3: *Top view of a standard lock design [Molenaar, 2011]*

For the lock head– and chamber a construction method with pneumatic caissons can be considered.

2.4.1 LOCK HEADS

The design, shape and lay out of the lock head depends on the type of gate and the used filling and emptying system. [Vrijburcht, 2000] The lock heads must be large enough to enclose the space through which a vessel should be able to sail into and out of the chamber. The lock heads must also provide space for the gates and their operating mechanisms in such a way that the lock gates remain outside the free profile for navigation when they are in an opened condition. In the lock head, additional space is required for all additional equipment required for the operation of the lock gates. Apart from the operating mechanisms there must also be space for the turning points for mitre and pivot gates, space for guiding facilities for a rolling, sliding or lift gate and space for the electrical equipment. This togheter determines the size of the pneumatic caisson(s) when they are used to construct parts of the lock.

2.4.2 LOCK CHAMBER

The construction of the lock chamber has to enclose the space that ships needed to sail into, moor and remain moored during the levelling of the lock chamber. After the locking process, the vessels have to be able to sail away out of the lock chamber and leave the navigation lock. Inside the lock chamber, vessels are moored to prevent vessel collision. The coping beam on top of the lock chamber walls are equipped with mooring rings and bollards. [Vrijburcht, 2000] One can choose to construct the entire width of the lock chamber or to construct only the lock chamber walls in separate caissons.

3

BOUNDARY CONDITIONS

In the previous chapter the location of the lock complex and the proposed location of the new lock were given . In this chapter the boundary conditions which the new lock must satisfy are discussed. This chapter starts with the surface elevation in section 3.1. The corresponding soil properties are discussed in section 3.2. The water levels at both side of the lock are determined in section 3.3. At last, the hydraulic head will be elaborated in section 3.4.

3.1 SURFACE ELEVATION

The new lock is situated on the eastern side of the western lock. The current surface level next to the western lock is situated between NAP +5.5 meter and NAP +6.5 meter. Where NAP in Dutch stands for *Normaal Amsterdams Peil* (Geodetic Reference Level). In figure 3.1 an overview of the lock complex is given. The different colors indicates here different surface elevations. The blue tint indicates the depth of the channel and the green tint indicates the surface elevation on land.

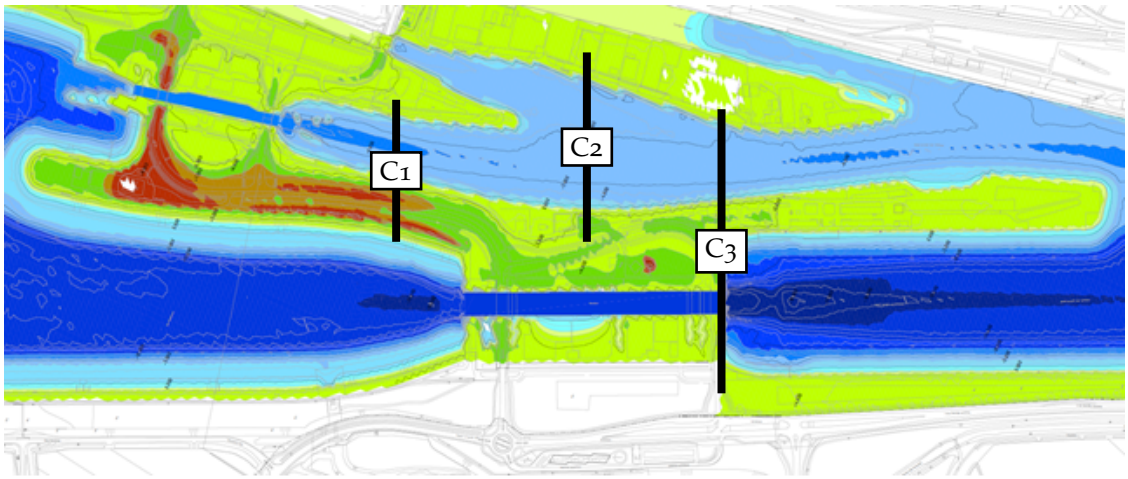

Figure 3.1: *Height of the surface level and location of cross section C1, C2 and C3 [AHN]*

A cross section of the elevation is made at different locations. These can be found in appendix A.1.

3.2 SOIL PROPERTIES

The underground at the proposed position of the new lock consists out of multiple different soil layers. The soil properties are not only changing in depth but are also spatially distributed over the lock complex. To simplify the calculations no spatial distribution of soil profiles is presumed. Only one soil profile is supposed to be present.

When looking at the upper layer, the first layer consist out of a Holocene top layer called the Formation of Nieuwkoop. Below this layer a layer of clay can be found. Subsequently multiple layers consisting out of sand and combinations of sand with clayey layers in it can be found. Below these layers Boom Clay can be found, corresponding to the Formation of Rupel and below this layer a glauconite sand layer related to the Formation of Breda can be found. In appendix A.2 the results of a CPT (Cone Penetration Test) is given and in appendix B.1 more information about Boom clay and glauconite containing sand is given.

On basis of previous research, the in table 3.1 mentioned soil parameters are assumed, where γ/γ_{sat} are the dry and saturated volumetric weights, ϕ the angle of internal friction and c the cohesion. These are actually characteristic for the southern lock head but it is considered that these parameters are uniform over the entire length of the lock.

Table 3.1: *Assumed soil parameters*

Top level [m]	**Description**	γ/γ_{sat} [kN/m^3]	ϕ [°]	**c** [kPa]
NAP +6	Top layer	17/18.2	25	-
NAP +2.5	Clay	16	21	3
NAP -3	Sand including clay layers	16/17.1	32	-
NAP -9	Sand	17.1/19.1	37	-
NAP -12.5	Sand including clay layers	16/17.1	32	-
NAP -13.5	Sand	17.1/19.1	37	-
NAP -20.5	Boom Clay	18.8/19	23	90
NAP -38	Glauconite containing sand	19.1/19.4	17	85

Special attention has to be given presence of glauconite containing sands in the subsoil. Background information about the properties of glauconite containing sands is given in appendix B.2.

3.3 WATERLEVELS

It is assumed that vessels with a draft of 13.1 meter must be able to use the lock except when the design water levels are subceeded. This happens on average twice a year. In figure 3.2 a graph with the probability of occurrence of an extreme minimum and maximum water levels has been shown.

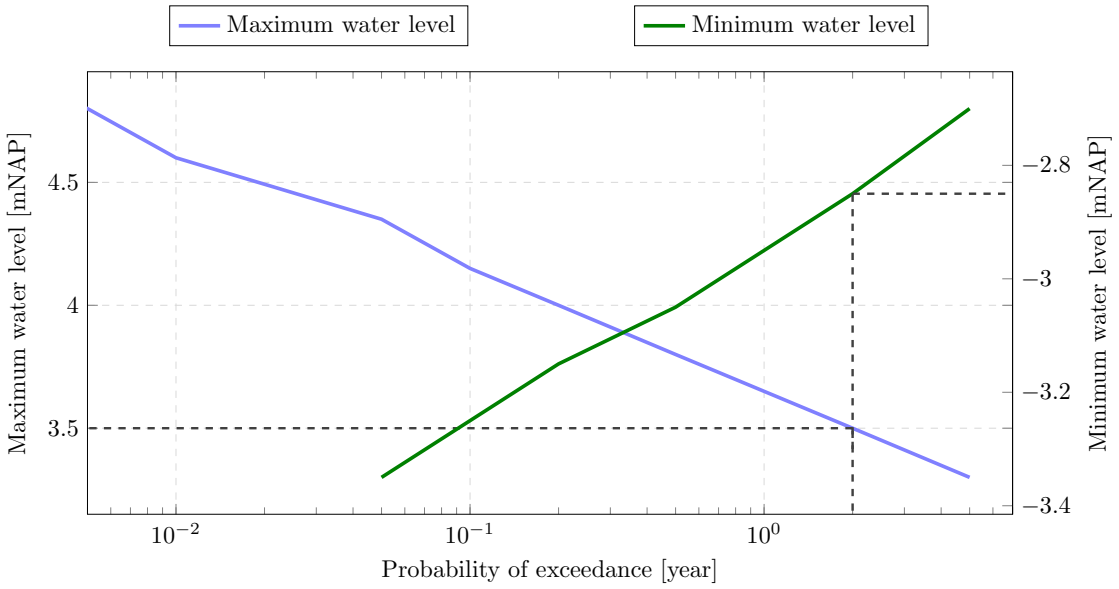

Figure 3.2: *Extreme water levels and occurrence probability [Rijkswaterstaat, 2011]*

From the graph it can be concluded that the minimum design water level is NAP -2.85 meter. The maximum design water level in contrast is NAP +3.5 meter. The water level at the channel Terneuzen Ghent is kept constant at a level of NAP +2.13 meter.

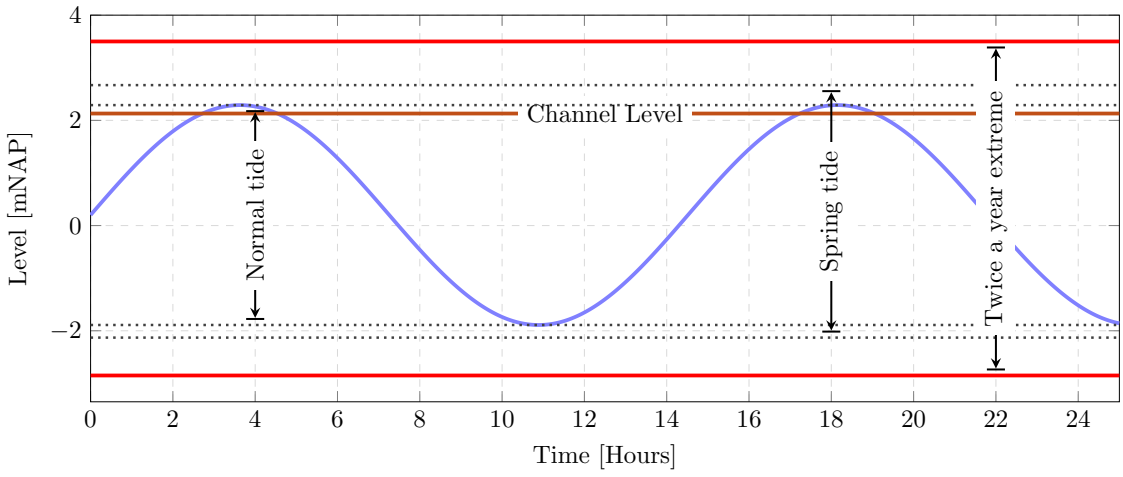

Figure 3.3: *Progress of the tide [Rijkswaterstaat, 2011]*

3.4 HYDRAULIC HEAD

The hydraulic head is depending of the depth and on the permeability of the different soil layers. There are two different locations with different hydraulic heads. Namely at the inner side of the

water defense system and at the outer side of the water defense system. In table 3.2 three layers with different hydraulic heads are given. In the table the first aquifer stands for the sand layers between NAP -3m and NAP -20.5 m which is closed off by a clay layer above. The second aquifer stands for the glauconite sand layer below NAP -38m which is separated to the soil above by the Boom Clay layer.

Table 3.2: *Average hydraulic head at the current situation [LievenseCSO, 2014g]*

Layer	Inner side [m + NAP]	Outer side [m + NAP]
Top layer	2–2.5	1–1.5
First aquifer	1–2.5	0.5–1
Second aquifer	1–2	0.5–1

4

REQUIREMENTS AND ASSUMPTIONS

The boundary conditions which the design has to fulfill were enclosed already. In this chapter assumptions are made to simplify the considerations and calculations in this research. Section 4.1 starts with the water levels at the location of the new lock. Subsequently in section 4.2 the different types of possible gate designs for the specific lock are elaborated and the chapter will be closed by a first consideration of alternatives in section 4.3.

4.1 DIMENSIONS

Prior studies [LievenseCSO, 2014f] have shown that the optimal lock has a length of 427 meter and a width of 55 meter. During any stage of the tide, except twice a year, a vessel with a maximum draught of 13.1 meter must be able to use the lock. The derivation of these values will not be elaborated in this thesis. As determined in the previous chapter a minimal water level of NAP -2.85 meter in the lock is assumed. For the keel clearance a margin of 10% of the draft is assumed. The minimal construction depth, h_{req}, is calculated in equation 4.1:

$$h_{req} = 13.1 + 0.1 \cdot 13.1 = 14.41 \text{ m} \tag{4.1}$$

The minimal depth of the top side of the lock head or –chamber is situated at $-2.85 - 14.41 = \text{NAP} - 17.26$ m. All vertical dimensions and the water levels around the lock are given once again in figure 4.1 and figure 4.2

During the initial design the parameters of the inner side of the water defense system will be used for reasons of simplicity. For simplicity a hydraulic head of 2 meter is assumed for all layers. This assumption is permitted because the piezometric levels in the different layers are very close to each other. In section 3.1 it was determined that the surface level on land is situated between NAP +6.5 and +7.5 meter. In the rest of the research a surface level of NAP +6 meter will be used.

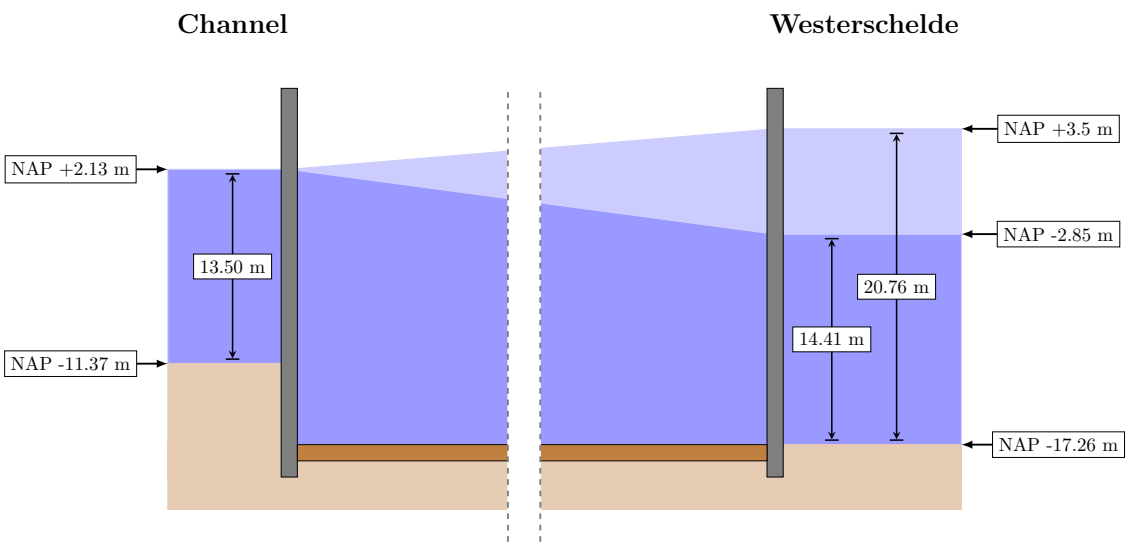

Figure 4.1: *Cross-section over the length of the lock with corresponding water levels*

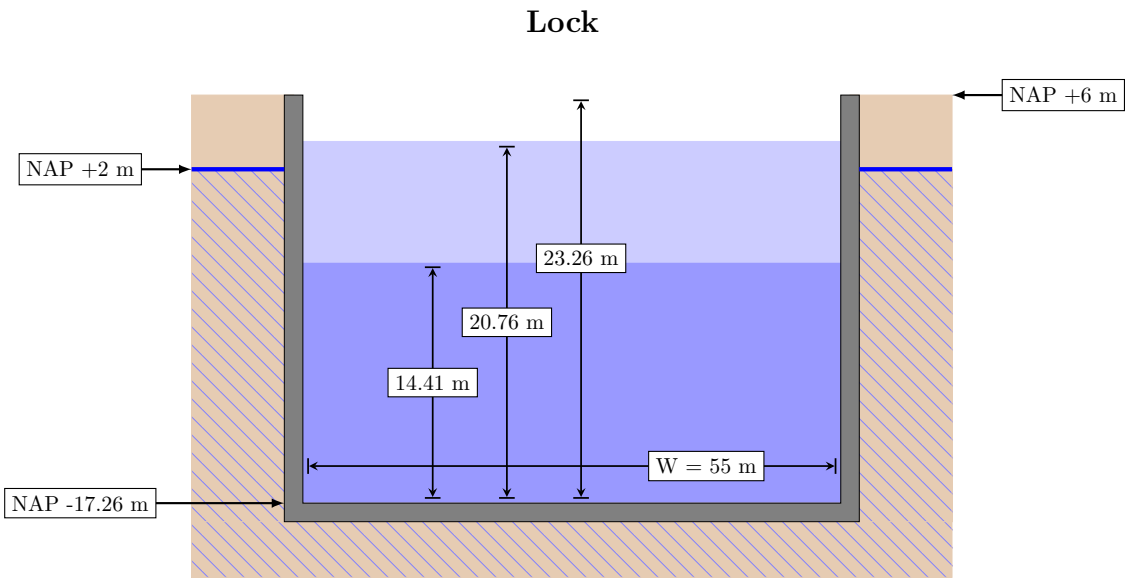

Figure 4.2: *Cross-section over the width of the lock chamber with corresponding water levels*

4.2 LOCK GATES

The water level differences influences the gate type design. Because of the dual retaining function, the lock gates must retain water in both directions. Three different types of lock gates are considered which are all elaborated in section A.3. The corresponding dimensions of the lock heads are based on the project of the Deurganckdoksluis near Antwerp. More information about the project is given in appendix D.3.

All the different gate designs and thereby the lock heads do all have the same functions: Retaining water, ship passage and water quality control. The options differ in operating mechanisms, guiding rails, possibilities for maintenance etc. which are all out of the scope of this research. The major difference between the three designs are the length and width of the corresponding lock head. For the continuation of this study the rolling doors and adjacent dimensions are assumed:

Table 4.1: *Overview of the lock head dimensions*

Gate design	**Length** [m]	**Width** [m]
Rolling doors	132	45

4.3 FIRST CONSIDERATION OF CONSTRUCTION

An overview of possible building methods have been given in appendix C. Due to the function of the lock-head as water retaining structure, where lock gates, turning points, recesses and guiding rails must be placed within very small tolerances, strict requirements are demanded for the final position of those elements. Because of this reason construction below the water surface is not considered as feasible option and is therefore not taken into account in this master thesis. Therefore the remaining options are: a temporary building pit, construct out of a diaphragm– or combi-wall, where in the final construction can be build or a permanent structure which is part of the lock head, these can be construct out of diaphragm walls or pneumatic caissons. Often pneumatic caissons are designed as box-shaped constructions. however by building a lock-head, a U-shaped construction without end- and front walls is needed. Because of this fact a pneumatic lock head construction is torsion weak and during subsidence major stresses may occur during unequal supports and settlements. For the lock chamber in can be concluded from previous research, [LievenseCSO, 2014b], that there is no need for dewatering and the use of pneumatic caissons which creates a dry working space is therefore not taken into account.

In chapters 7–8 a construction of the lock head with pneumatic caissons are elaborated. Subsequently in chapter 9 the construction of the lock head inside a building pit is elaborated shortly.

Part III

ANALYSIS OF CONSTRUCTION METHOD

5

PNEUMATIC CAISSONS

One of the building methods mentioned in the appendix are pneumatic caissons. In this chapter first a short introduction on caissons is given in section 5.1. Subsequently the different components required for the working of a caisson are mentioned in section 5.2. Hereafter in section 5.3 the definition of the construction process and the procedure for designing is given. At last in section 5.4 the method of excavation of the working chamber is discussed

5.1 INTRODUCTION

Pneumatic caissons are not the only existing type of caissons. Caissons are often used in hydraulic engineering and are often hollow boxes constructed out of reinforced concrete used for a variety of functions. Pneumatic caissons do have a lot of similarities with open– and suction caissons which are used for other applications. Some background information about the open– and suction caissons is given in appendix D.1. In the appendices also a historical overview of caisson is given in D.2 and an overview of reference projects is given in section D.3.

The pneumatic caisson method involves a construction of a relative rigid box at ground level that is lowered into the ground by excavating the soil underneath it.

Under the bottom plate of the pneumatic caisson an air-pressurized space, called the working chamber, is present which is made up of tapering walls 2 to 3 m high around the perimeter of the caisson base slab. These tapering walls are called the cutting edges of the caisson. The working chamber is kept dry by an overpressure. A cross section of a pneumatic caisson is given in figure 5.1.

Due to the increased air-pressure, groundwater is not able to enter the working chamber. This method can be compared with the principles of a diving bell. The air pressure in the working chamber balances the pore-water pressure at the level of the cutting edge so there can be excavated in the dry. The deeper the caisson is located under the water table, the higher the air pressure must be. This is limited in practice because the time workers can stay in the working chamber will decrease in order to prevent them from decompression illness. [Bame, 2013]

The soil in the working chamber is loosened with water jets and can be removed hydraulically to a basin outside the caisson. The caisson will "sink" into the ground because soil underneath the cutting edge will fail. In time, when the bottom slab including cutting edges and first parts of the walls are sinking a successive stage of concrete walls is cast on top of the sinking walls, this continues till the caisson reaches its designed depth. Extra ballast weight on top of the bottom slab can be used to increase the weight of the caisson and speed up the subsidence of the caisson. [Nonveiller, 1987]

When the air-pressure is partly released in the excavation chamber, the caisson will subside further. This is done at a speed of 60 cm to 1 m per day, depending on the surface area of the

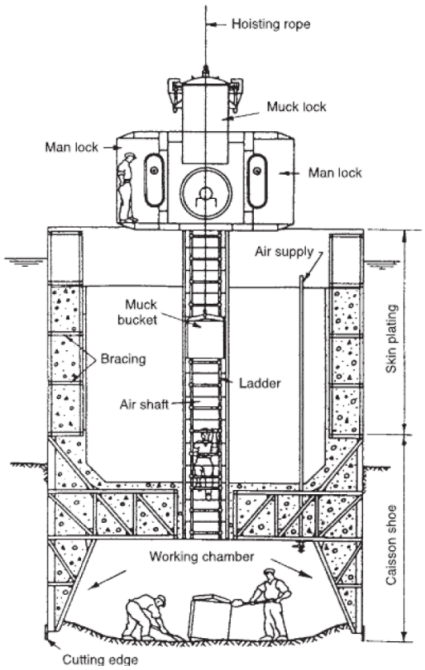

Figure 5.1: *Cross section and components of a pneumatic caisson [Kolymbros, 2005]*

caisson and the presence of obstacles in the ground. [Ministerie van Infrastructuur en Milieu, 2008]

At some distance above the cutting edge a peripheral gap is made in the caisson. With pre-installed grout pipes the wall gap will be filled with bentonite suspension. This reduces the skin friction between the caisson and its surroundings. [Kolymbros, 2005]

After the final depth has been reached, the working chamber will be filled with concrete.

Pneumatic caissons do have a lot of advantages, most important advantages are:

- Obstacles that are present in the subsoil can be inspected and removed easily since the soil that was surrounding it will be removed.
- The subsidence of pneumatic caissons is not accompanied by continuous vibrations, which are often present by traditional building methods. Like for instance the installation of sheet– and combi-walls.
- There is no need to lower the water table around the pneumatic caisson, so there is no impact on buildings in the vicinity of the caisson.
- There is limited space needed around the location of the pneumatic caisson. This building method can be applied in urban areas.
- There is no effect on the water table below and outside the caisson.
- The ability to construct and subside the caisson in different and changing soil conditions.

Apart from the advantages, the disadvantages working under high pressures is expensive and a lot of ballast is needed to continue subsidence.

5.2 COMPONENTS

In order to provide access to the working chamber a system consisting of an air lock and an air shaft is designed. A chamber made out of steel is placed at the upper side of the air shaft and is called a air-lock. In this air-lock, which is situated above the water level, workmen can enter and exit the caisson.

The air-lock has two air-tight doors. One door is connected with the outside air, the other one is connected with the air-shaft. Workmen who are starting with their employment will enter the air-lock and gradually the pressure inside the air-lock will be increased. After the pressure inside the air-lock equals the pressure inside the working chamber, workmen are able to open the second door and can enter the air-shaft which brings them to the working chamber. When workmen want to leave the caisson, the procedure described above will take place in the reverse order.

By opening a valve in the airlock, fresh air is able to circulated inside of the working chamber. On a pneumatic caisson multiple pumps, motors and air compressors are present to provide for enough air-pressure within the different elements. Normally this equipment is placed above the bed level. [Gohil, 2012]. In a pneumatic caisson electrical installations, different pumps, supply pipes for water entry and outflow pipes for the water-sand mixture are present [Bongers and Haterd, 1995]

5.3 CONSTRUCTION OF THE PNEUMATIC CAISSON

A pneumatic caisson can be build and subsided in different ways. The first option is to cast and finish the caisson completely on surface level before subsidence starts. In that case formwork can easily be placed and aligned without changes in the meantime. After completion the caisson is still above surface level and the caisson can be checked. Another option is to start the process of subsidence when the cutting edges and bottom slab are finished. During subsidence the upper part of the caisson will be built synchronously. The pneumatic caissons of the lock heads can be constructed and subsided in five steps as described by [Bongers and Haterd, 1995].

- **Step 1** - Construction of the quay wall. This retaining wall can consist of a sheet pile wall, combi-wall or cofferdam. *(Figure 5.2)* At the location of the lock heads there is less space (15 meter) available for anchors. De retaining wall at this location can be constructed in a (more heavier) way. Soil should be supplemented to a level of NAP +6 meter or the soil on the land abutment should be excavated towards the ground water table to achieve a horizontal surface level.

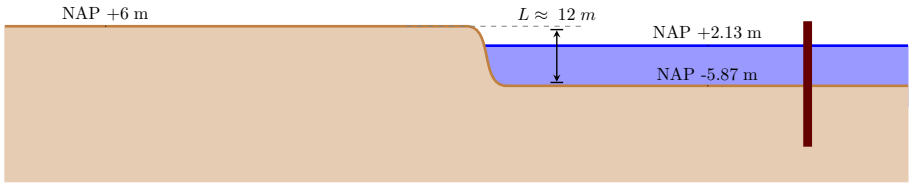

Figure 5.2: *Step 1 - Construction of retaining wall*

- **Step 2** - In common the construction of the pneumatic caissons starts with the construction of a sand terp. This sand terp can be both constructed in a shallow excavation or can be created above surface level. *(Figure 5.3)*

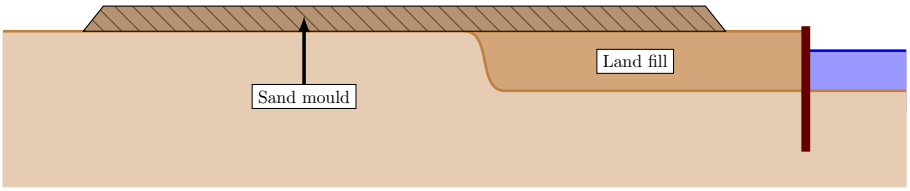

Figure 5.3: *Step 2 - Land fill and placement of sand mould*

- **Step 3** - The lock head can be constructed as one or multiple caissons. This will be elaborated in the next chapters. The cutting edges, bottom slab and caisson wall can be cast after the reinforcement has been placed. This all will be done on surface level. After hardening of the concrete, at both end-sides watertight bulkheads will be installed. For this purpose strutted sheet– or combi-wall profiles can be used or the faces can be closed and made watertight with temporary concrete bulk heads. *(Figure 5.4)*

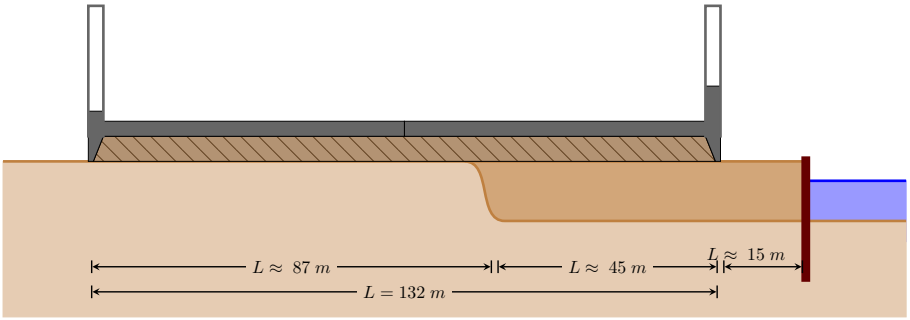

Figure 5.4: *Step 3 - Construction of the caisson*

- **Step 4** - After the completion of the caisson and before the subsidence start, the sand mould under the structure will be removed at atmospheric pressure. After the sand in the working chamber is removed, spray lances and pumps can be installed as well as air shafts, decompression rooms and electricity. After all equipment has installed the excavation can start. After subsidence progresses the air pressure inside the working chamber will be increased in order to prevent inflowing of groundwater. *(Figure 5.5)*

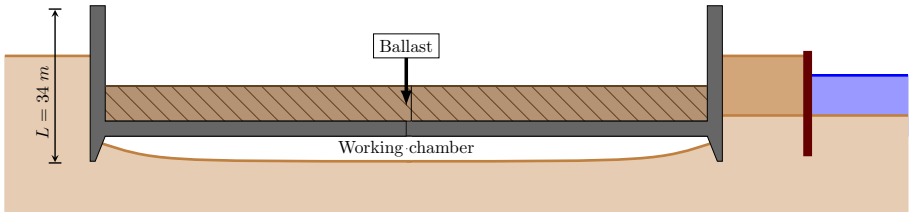

Figure 5.5: *Step 4 - Excavation inside the working chamber and addition of ballast*

- **Step 5** - In order to achieve subsidence the soil below the cutting edge must fail. Soil will be pushed towards the working chamber as can be seen in figure 5.6. In section 5.4 this principle is explained.

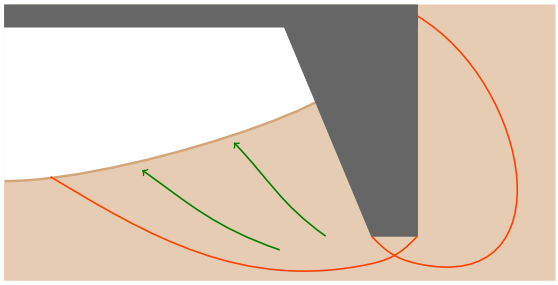

Figure 5.6: *Slip plane of the soil below the cutting edge*

The self weight of the construction together with the weight of all equipment are providing the downward directed force. The counteracting and upward directed forces are consisting out of the friction between soil and concrete and the excess air pressure on the lower side of the bottom slab. To reduce the friction between soil and concrete the caisson floor is just a couple of centimeters wider than the caisson walls. A bentonite slurry is pumped inside this gap between soil and concrete walls. When the downward directed forces are too small to achieve soil collapse below the cutting edge. Extra ballast can be used to increase the downward load of the caisson. After the final depth is reached the working chamber will be filled with concrete to achieve extra bearing capacity. *(Figure 5.7)*

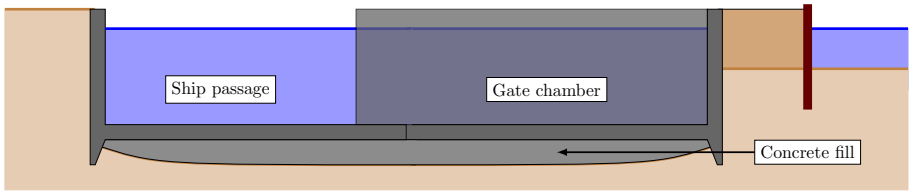

Figure 5.7: *Step 5 - Filling the working chamber with concrete and completion of the lock head*

5.4 EXCAVATION OF SOIL

There are multiple ways to excavate the soil in the working chamber. These excavation methods can be divided in two groups:

- Excavation by workers in the working chamber
- Remote excavation

There are also different techniques to excavate the soil out of the working chamber. softer soils can be excavated by use of water jets. This is called hydraulic mining or hydraulicking. Soil particles are washed out and the sand-water mixture is pumped out to a sedimentation basin. The water-sand mixture exist out of roughly 85% water and 15% soil particles. [LievenseCSO, 2014d] Here the sand can be separated from the water which will be re-used. The extent of the sedimentation basin is dependent on the surface area of the pneumatic caisson and the amount of pumps that are used. As indication a sedimentation basin five times the surface area of the pneumatic caisson can be used. The more stiffer and cohesive soil layers must be excavated by hydraulic grabs or –buckets.

5.4.1 EXCAVATION BY WORKERS IN THE WORKING CHAMBER

Working in the working chamber of a pneumatic caisson is very hard since the working chamber is put under high pressure, has a high temperature and high humidity. Therefore this method requires robust and experienced workers. In figure 5.8 a photo of the inside of the caisson is shown to give insigh into the conditions.

Figure 5.8: *Photo of the inside of the working chamber of a pneumatic caisson [Pepers, 2011]*

Excavation inside the working chamber can take place in different orders. [Nonveiller, 1987]

1. Horizontal cuts are made all along the perimeter of the cutting edge so that the caisson is always in a state of limit equilibrium and sinks in small increments. (*See figure 5.9a*)

2. Starting from the center of the caisson/compartment, vertical cuts to a predefined depth below the cutting edge are made until the moment a critical value l_c is reached whereupon rupture starts. (*See figure 5.9b*)

3. Uniform horizontal cuts are made all along the perimeter of the cutting edge, keeping the width of the resisting wedge l constant until a critical depth is reached where after the rupture occurs on the plane rp. (*See figure 5.9c*)

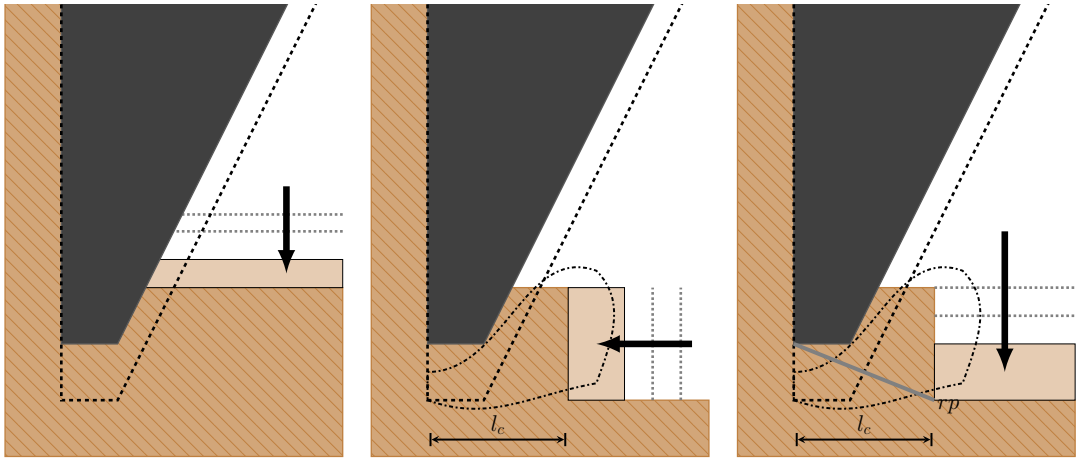

(a) *Horizontal cuts* **(b)** *Vertical cuts to a predefined depth* **(c)** *Horizontal cuts with fixed length of resisting wedge*

Figure 5.9: *Different excavation approaches arround the cutting edge [Nonveiller, 1987]*

Workers in the working chamber are exposed to the danger of caisson disease. This is a disease which is also known as diversd́isease or the bends. During pressurisation gasses like nitrogen are dissolved in the body. When workers are to long under pressurisation or the depressurisation is going to quickly, dissolved gases coming out of solution into bubbles inside the body. Since bubbles can form in or migrate to any part of the body, caisson disease can produce many symptoms, and its effects may vary from joint pain and rashes to paralysis and death. Individual susceptibility on caisson disease can vary from day to day, and different individuals under the same conditions may be affected differently or not at all. The maximum working time is therefore limited and is dependent on the overpressure. According to [Kamerling and van den Boogaard, 1986] it is legally defined that the maximum overpressure is 3.5 atm to reduce the risk on caisson disease. The maximum depth thereby below the groundwater table is 35 meter.

From figure 5.10 it can be seen that from a overpressure of 1.8 atm the maximum allowable working time is decreasing quickly. This means that multiple working shifts which different working men on a single day are required.

5.4.2 REMOTE EXCAVATION

To reduce the above mentioned risks with respect to caisson disease, another possibility is the use of remote excavation equipment. This method can be subdivided in two groups. A situation whereby the equipment is operated manually from a control room above the surface level or a situation whereby the equipment is working automatically without human intervention.

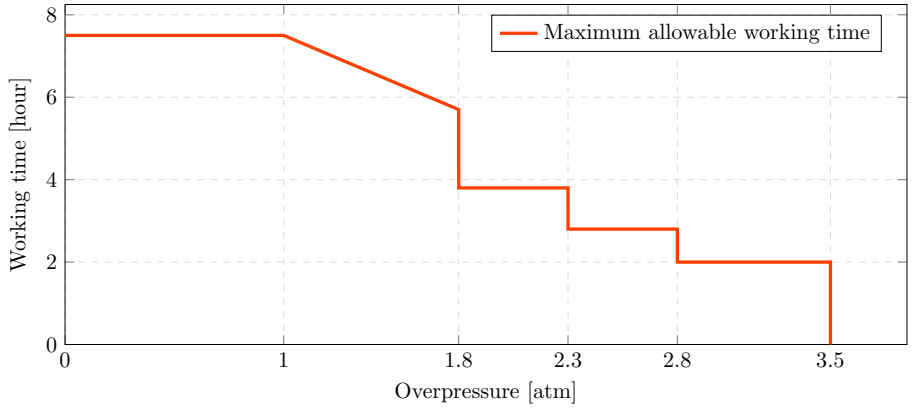

Figure 5.10: *Maximum working time during overpressure [Kamerling and van den Boogaard, 1986]*

A system for remote excavation can be split in globally three components: An excavating system, soil transfer system, and ground conveyor system. The excavator is an overhead traveling type whose wheels are driven by a hydraulic motor to run on two rails installed to the ceiling of the working chamber. The system is driven manually or automatically with help of laser and ultrasonic sounds for the positioning.

The soil transfer system installed in the working chamber automatically puts excavated materials in a soil bucket. It consists mainly of a telescopic clamshell bucket, soil receiving board, chute, and slide gate. The soil conveyor system ensures that the excavated material is transported with help of soil conveyor cranes, soil hoppers and soil buckets outside of the caisson. [Kodaki et al., 1997]. Parts of the Shanghai metro tunnel of line 7 are constructed with pneumatic caissons. Both excavation and discharging of soils were done by the automated excavation and remote controlling systems. [Peng et al., 2010] A photo of the automatic excavator inside the working chamber is given in figure 5.11

Figure 5.11: *Automatic excavator inside the working chamber [Oraukia Tech, 2009]*

Part IV

NEW LOCK TERNEUZEN

6

CONCEPT DEVELOPMENT OF PNEUMATIC CAISSONS

This chapter starts with the general construction planning of the new lock in section 6.1. In section 6.2 two construction alternatives are proposed. To prevent the inflow of water and soil in the caisson during subsidence different possibilities for the design of a bulkhead are given in section 6.3. In the last section of this chapter, section 6.4, the general external forces acting on the caisson are given. The variant-specific loads are elaborated in the next chapters.

6.1 GENERAL CONSTRUCTION PLANNING

From the map as provided in figure 2.2 it can be concluded that about half of the new lock must be built in the current channel. During the construction the western– and eastern lock must remain fully operational. Due to the closure and demolition of the middle lock the total lock capacity for the complex is temporary decreasing until the opening of the new lock. The closure of yet another lock is therefore not desirable. Traffic from the western side of the channel must be able to reach the eastern side of the channel. A road connection between both sides of the lock complex must therefore be maintained. In the enumeration below the different steps of the construction process are described.

- **Step 1** - The most construction details are concentrated at the lock heads. It is therefore important that the construction starts with the lock heads. The southern lock head is located in the entrance channel for both the middle– and eastern lock. To guarantee ship passage to the eastern lock the most eastern peninsular must be removed first to obtain an extended entrance channel to this lock. Around the areas where land reclamation will take place, sheet– or combi-walls can be constructed. The removed soil from the peninsular can be used to create the first land fill at the northern lock head, hereafter the existing quay wall at the eastern side of the western lock can be supplemented with soil from the eastern peninsular.

  In order to obtain a separation between the land fill and the new part of the channel a quay wall is required. This quay wall can be constructed as sheet pile wall in combination with anchors since the retaining heights are small. At the location of the lock head the space between retaining wall and lock head is small. At those location a stiffer combi-wall or cofferdam structure can be constructed. The design of these quay walls is outside the scope of this master thesis.

  When the most eastern peninsular is almost removed and there is enough space for both land fill and ship passage to the eastern lock this third land fill for the southern lock head can be realised. Due to the initial land fill at the location of the new lock the consolidation

process can start in a prior stadium in comparison with the other area's of land fill. The settlement on those locations will thereby be smaller. In figure 6.1 step 1 is given.

- **Step 2** - In the second step the land fill between both lock heads takes places. Besides the quay walls on the southern side of the new lock can be removed and the entrance channel for the lock can be dredged. From this point on there is only one road is use between both sides of the lock complex. The most southern road is taken out of use and will be removed. A schematization is given in figure 6.2.

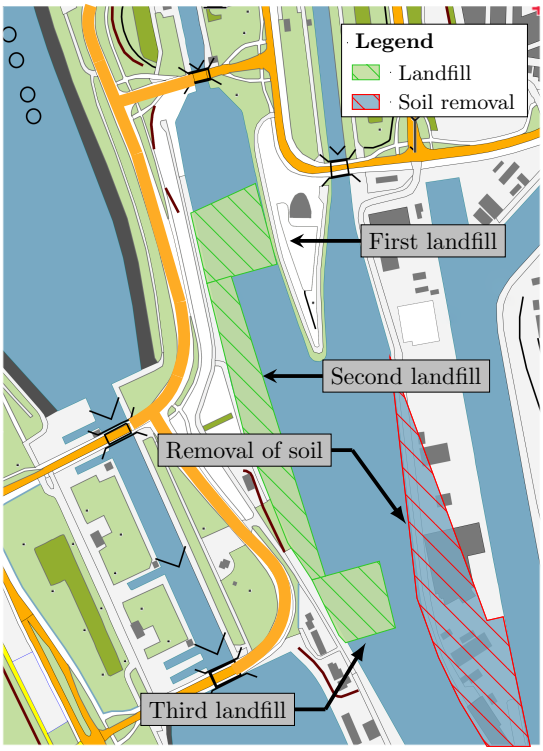

Figure 6.1: *Start land fill and removal of soil*

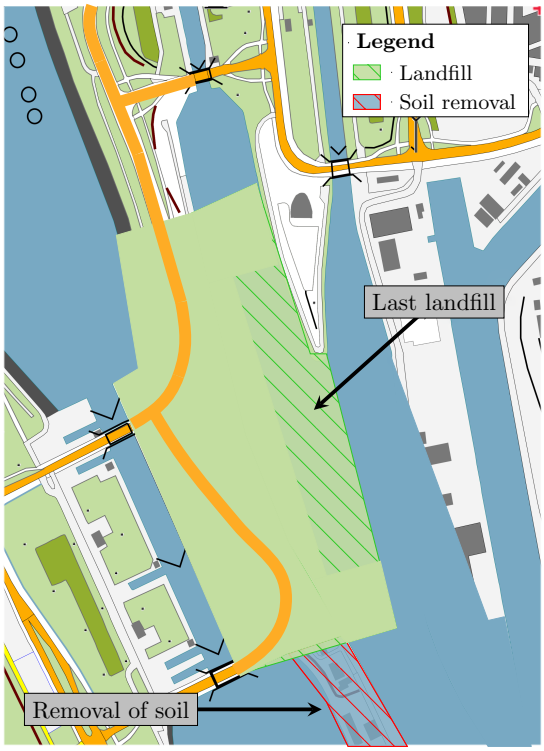

Figure 6.2: *Finishing land fill*

- **Step 3** - In step three of the construction process the road is relocated over the new land fill. This temporary road is schematisated in figure 6.3.
- **Step 4** - In the fourth step the middle lock with adjacent quay walls is removed. On the same time the construction of the lock heads can start. The building method for each method is already described in the previous chapters. The size of the lock heads in not on scale because this is dependend on the lock gate design. A schematisation is given in figure 6.4.

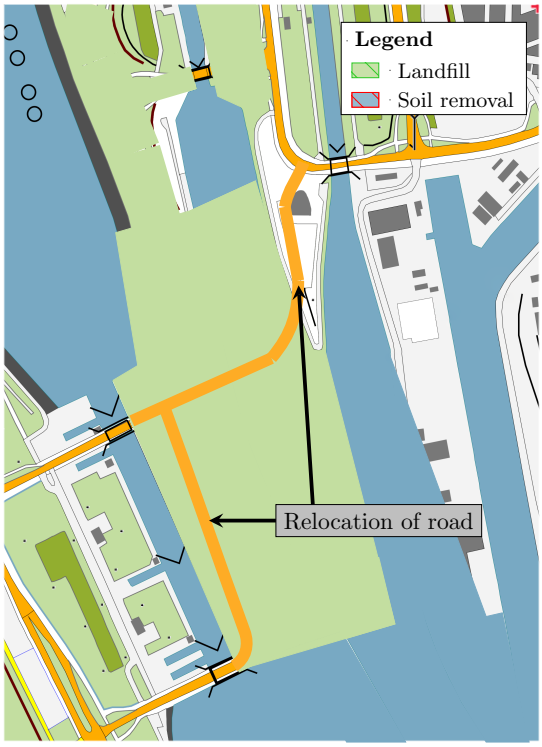

Figure 6.3: *Relocation of road*

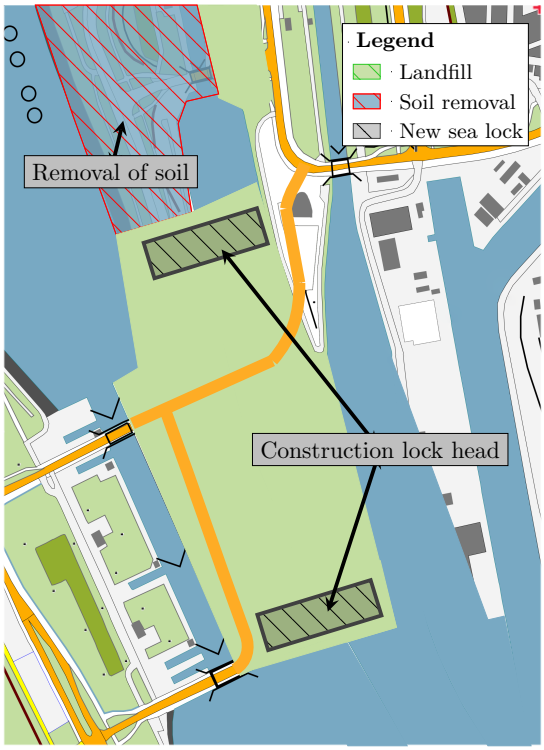

Figure 6.4: *Construction of lock heads*

- **Step 5** - The temporary road is relocated to the final location. This is schematised in figure 6.5.
- **Step 6** - In the last step the lock chamber can be constructed. The caisson of the lock head can be connected to the lock chamber. This is elaborated in appendix F.7. A second road can be constructed which connects the southern lock head of the western lock with the southern lock head of the eastern lock. The traffic can, whatever the status of ship passage is, always find a way to the other side of the lock complex. This is schematised in figure 6.6.

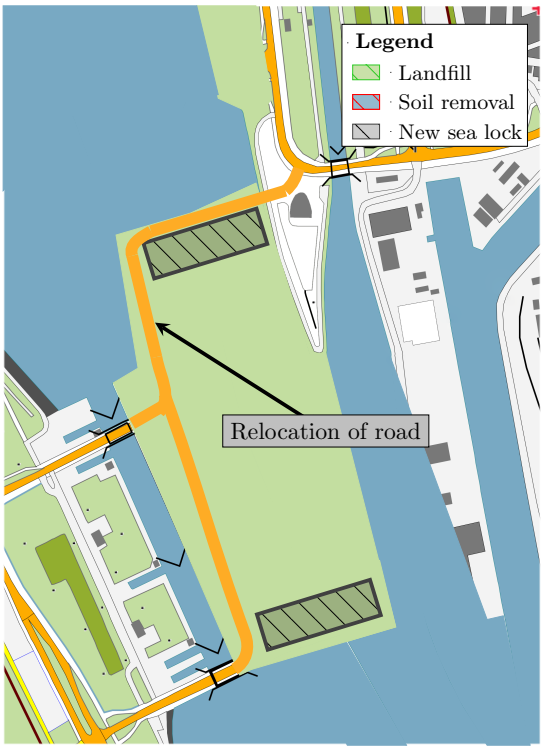

Figure 6.5: *Relocation of road*

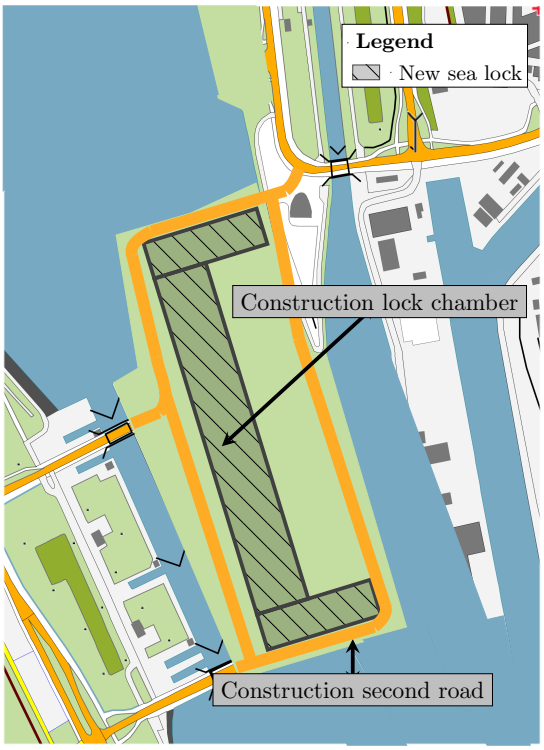

Figure 6.6: *Construction of lock chamber*

A global planning corresponding to the construction phases above is given in appendix E.1. The estimated construction time of the lock heads are given in appendix E.2. The exact location of the pneumatic caissons in relation to the surroundings is given in appendix A.4.

6.2 CONSTRUCTION ALTERNATIVES

According to boundary conditions and requirements the draught of the lock will be situated at NAP -17.26 meter. The gate will consist out of a rolling door requiring guidance rails and rolling equipment below the gate. The design of the gates is outside the scope of this master thesis and therefore a height of 1.74 meter is taken for these equipment so that the top of the bottom slab of the caisson is situated on a level of NAP -19 meter. The dimensions of the gate type design was summarized in section 4.2. Several options and compositions can be considered for the construction of both lock heads.

- **Variant 1** - Construction of one large pneumatic caisson where the working chamber is divided in multiple compartments. Assumed is a maximum span of 20 meter. Compartments with larger dimensions are possible. However, occurring loads and moments are becoming larger by increasing dimensions. Inside the compartment the air pressure can be set independently of the other compartments for different excavation depths. Due to the subdivision of the caisson in multiple compartments also multiple air– and soil discharge shafts are required as well as more equipment to control this pressure. This option is schematized in figure 6.7 where a plan view of the caisson is given.

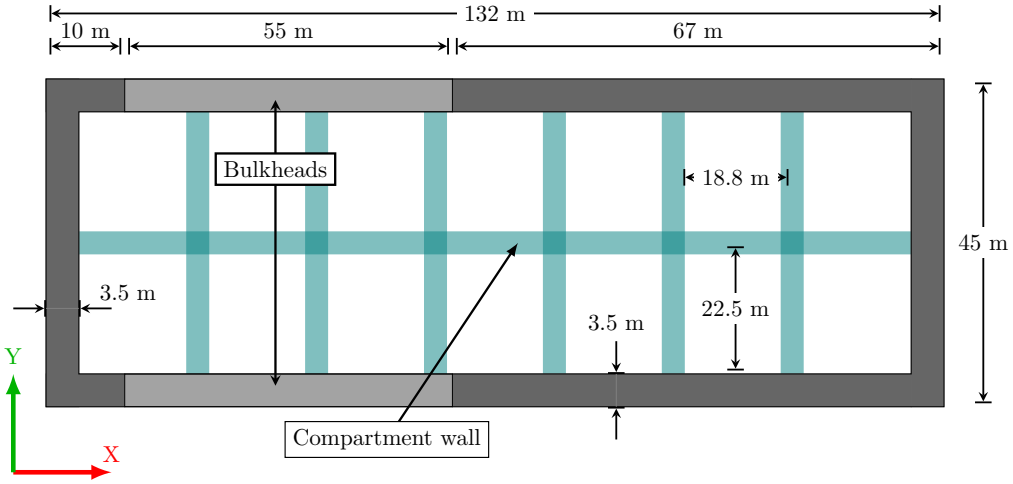

Figure 6.7: *Plan view of one large caisson. The caisson is divided in multiple compartments*

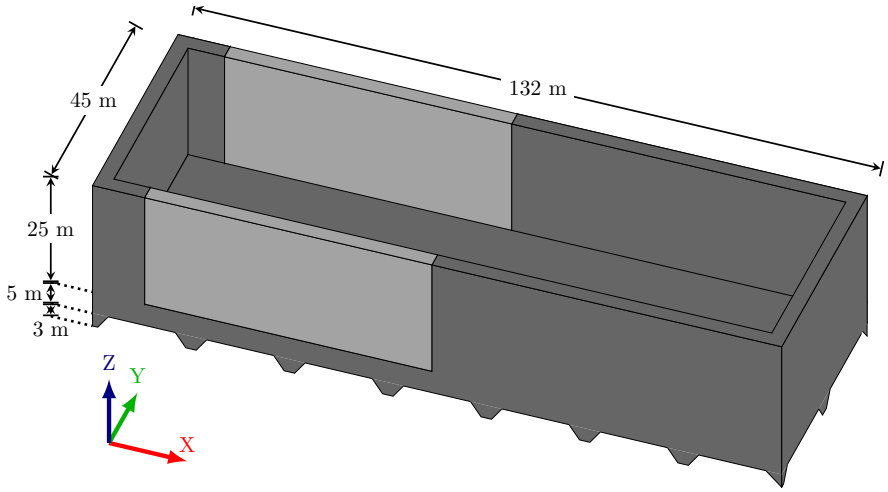

Figure 6.8: *3D schematisation of variant 1. One large caisson is covering the complete lock head*

- **Variant 2** - The construction of two caissons which can be subsided individually. One caisson is covering the gate recess and the other caisson is covering the gate chamber. This option is schematised in figure 6.9

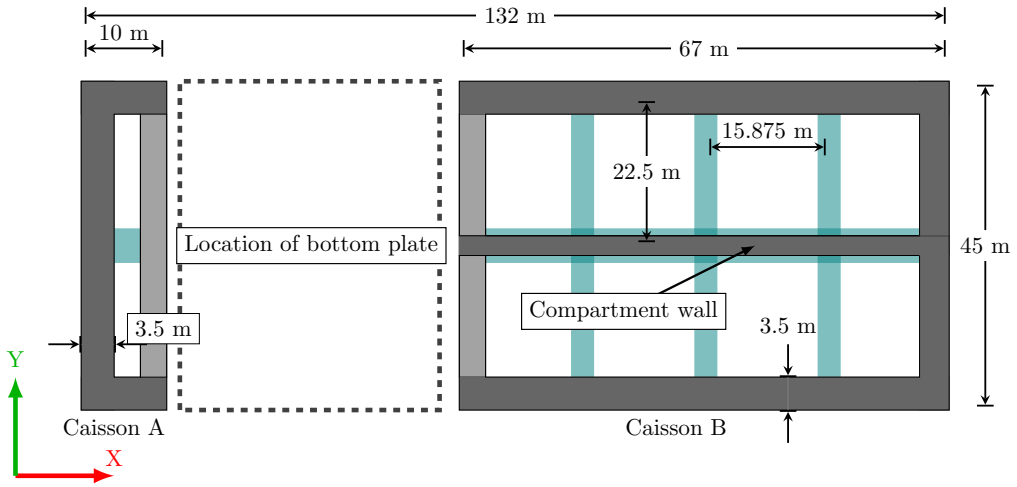

Figure 6.9: *Plan view of one large caisson. The caisson is divided in multiple compartments*

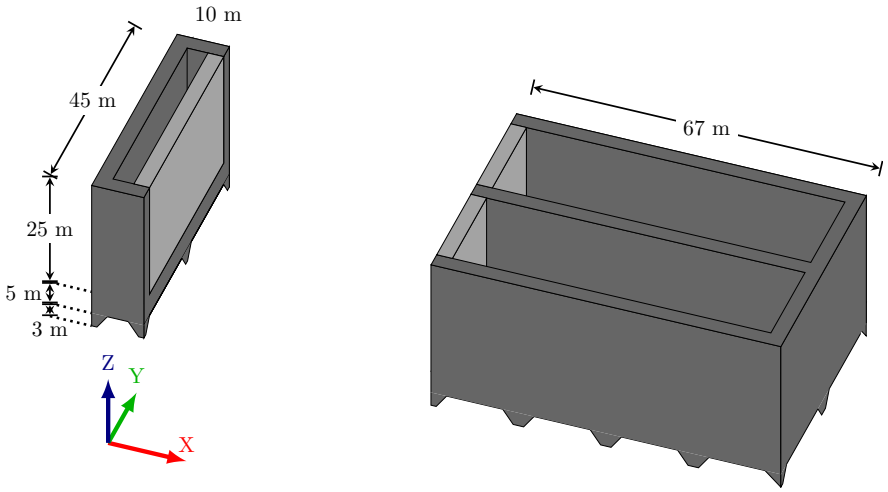

Figure 6.10: *3D schematisation of variant 2. Two smaller caissons are covering the gate recess and gate chamber*

The specific dimensions of the above mentioned variants will be elaborated in the following chapters. Some loads and dimensions are however constant in each design and will therefore be worked out in the next sections of this chapter.

6.3 SELECTION OF BULKHEAD

Due to the function as lock head, large openings in the caisson walls are required for the passage of ships during the lifespan of the construction. During subsidence of the caisson these recesses must be closed to prevent the inflow of soil and water. A bulkheads is used to make the opening water and sand-tight. Bulkheads from different materials and with different shapes are possible.

- **Concrete** - The recess in the caisson wall can be consist out of a temporary concrete wall. It must be ensured that reinforcement is not running over the total length of the caisson. Preferably none, or as less as possible reinforcement must be used in the bulkhead walls. This makes the demolishing of the bulkhead after subsidence, which takes place below the water level, more difficult. In contrast to steel bulkheads do concrete bulkheads have stiffness in the direction of the plane.
- **Steel** - Sheet pile wall elements, combi-walls or tubular piles can be used to ensure a water- and sand tight barrier. At increasing retaining heights elements with larger orthogonal stiffness, EI_z, are required. A disadvantage of sheet pile wall elements is the absence of stiffness in the direction of the plane $EI_x \approx 0$ and $EI_y \approx 0$. Loads in the top of the gate recess can't be transferred to the top of the walls of the gate chamber. To improve stability of the bulkhead struts can be used to stabilize the construction. Another disadvantage is the unequal distribution of the weight of the caisson over the length of the caisson which effects the rotation of the caisson and complicates the subsidence process.

Due to both the absence of stiffness in the direction of the plane when using a steel bulkhead and the unequal distribution of weight over the length of the caisson, a concrete bulkhead is used for the calculations in the next chapters.

6.4 EXTERNAL LOADS ACTING ON CAISSON

During subsidence and in the final situation different kinds of loads are acting on the caissons. These loads have large influences on the deflections of the caisson and on the process of subsidence. In table 6.1 the five most important and dominant loads acting on the caisson-soil interface are summarized. Behind the specific load the dependencies of that specific load are listed.

Table 6.1: *Overview of loads acting on the caisson*

Load case	Dependent on
Self-weight (§ 6.4.1)	• Volume of concrete
Wall Friction (§ 6.4.2)	• Soil properties • Perimeter caisson • Height of bentonite trench
Air pressure (§ 6.4.3)	• Hydraulic head
Bearing capacity (§ 6.4.5)	• Depth • Soil composition and properties • Foundation surface
Ballast	• Self-weight • Wall friction • Air pressure • Bearing capacity of cutting edge

In the design special attention is required for the following three issues during excavation. [Bowles, 1988]

- The quantity of air pressure inside the working chamber to prevent the inflow of groundwater.
- The self-weight of the structure
- The amount of ballast weight required to achieve a smooth subsidence.

The above mentioned loads are important for the vertical equilibrium of the caisson. During subsidence of the caissons the downward directed forces must be slightly larger than the resisting upward directed forces. In formula terms the following situation must be satisfied:

$$F_{selfweight} + F_{ballast} > F_{friction} + F_{air} + F_{bearing} \tag{6.1}$$

In the final phase both upward and downward directed forces must be equal:

$$F_{selfweight} + F_{ballast} = F_{friction} + F_{air} + F_{bearing} \tag{6.2}$$

After reaching the design depth the working chamber with an overpressure is filled with concrete. The vertical bearing capacity is thereby enlarged. After finishing the interior of the lock head, the bulkheads can be removed and the caisson can be filled with water. Also during the lifetime of the construction both upward and downward directed forces must be equal.

$$F_{selfweight} + F_{components} + F_{water} = F_{bearing} \tag{6.3}$$

All loads described acting on the caisson are schematized in figure 6.11.

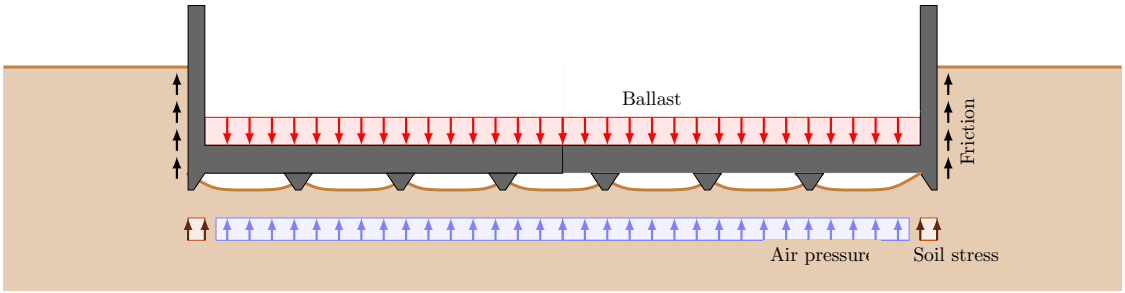

Figure 6.11: *Loads acting on the pneumatic caisson*

During subsidence of the caisson and in the final situation different loads are applying on the caisson. The loads mentioned in the previous section will be elaborated in the next sections.

6.4.1 SELF-WEIGHT OF THE CAISSON

One of the largest loads is caused by the self weight of the caisson. The value of the downward directed load caused by the self-weight is direct proportional to the dimensions of the structure and thereby the amount of concrete and steel that is used. Above the groundwater table the volumetric weight of concrete is $\gamma_{concrete} = 25\ kN/m^3$ and below the groundwater table the effective weight is $\gamma_{concrete;sub} = 15\ kN/m^3$. The corresponding internal dimensions of the lock heads are based on the project of the Deurganckdoksluice nearby Antwerp. (*See appendix D.3*). This assumption can be justified because the lock head of the Deurganckdoksluice has similar dimensions. However, it should be observed that this lock head is built in an open

excavation and therefore, there is no phase of subsidence. The global dimensions of the caissons equal for all variants are given in figure 6.12.

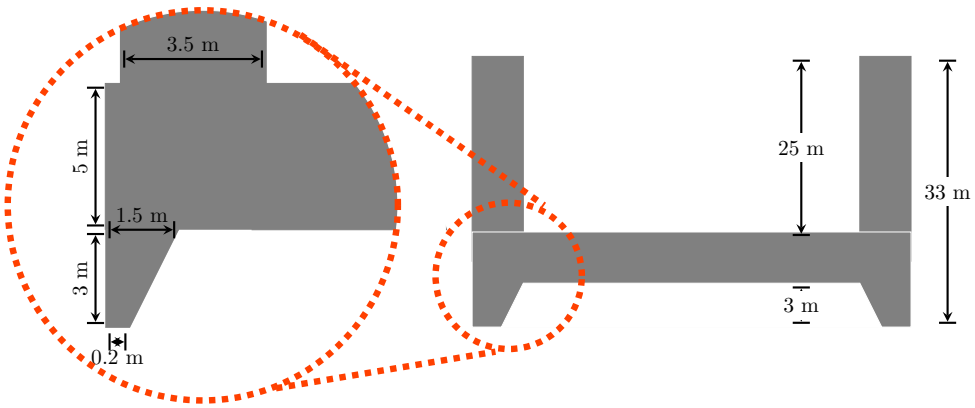

Figure 6.12: *Global internal dimensions of the pneumatic caisson (not on scale)*

6.4.2 WALL FRICTION

During subsidence of the structure, the caisson experience friction resistance between the concrete surface of the caisson and the surrounding soil. To decrease this resistance between soil and concrete a gap above the cutting edge is kept filled with a bentonite-water suspension. Stabilization of the soil face by this bentonite based suspension prevents friction through ground collapse. A rubber apron fitted around the upper portion of the cutting edge prevents inward flowing of the bentonite lubrication.

In appendix B.3 different methods to estimate the wall friction are proposed. There are multiple ways to calculate the wall friction on the caisson. Burland suggested a formula based on the horizontal earth pressure and the wall friction angle. This method assumes that the excess pore water pressures caused by volume displacement dissipates in time. With this formula the skin friction, f_s, in both cohesion and cohesion less soil can be calculated:

$$f_s = K_n \cdot \sigma'_{eff} \cdot \tan(\delta) \tag{6.4}$$

Where K_n is defined as the coefficient of neutral soil pressure and σ'_{eff} is defined as the effective stress. The wall friction angle δ at the concrete-soil interface can be assumed equal to $\frac{3}{4} \cdot \theta$ and at the bentonite-concrete interface equal to $\delta = 5°$. [Banjac, 1996] The wall shear stress can also be assumed equal to $f_s = 5$ a 10 kN/m^2 at the bentonite-soil interface. In the following calculations the average value for the wall friction at the location of the bentonite lubricant of $f_s = 7.5$ kN/m^2 will be assumed. For the concrete-soil interface at the lower part of the construction the formula of Burland is used. The neutral earth pressure coefficient depends on the angle of internal friction and can be calculated according to equation 6.5.

$$K_n = 1 - \sin(\theta) \tag{6.5}$$

The vertical effective stress in the soil can be calculated easily by summing up the effective weight of all soil layers above. [D-Sheet Piling Manual]. In figure 6.13 the water pressure (u), total soil stress (σ_{tot}) and effective stress (σ_{eff}) are plotted over depth.

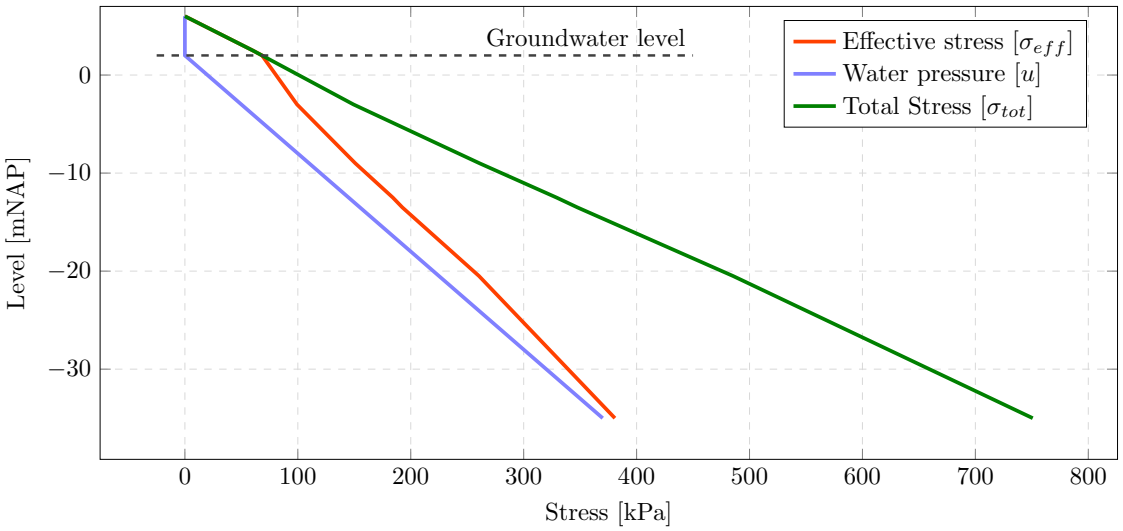

Figure 6.13: *Values for water–, total–, and effective soil stress*

The total resisting force can be calculated by multiplying the wall shear stress coefficient (f_s), perimeter of the caisson (P) and submerged height of the caisson (h_s).

$$F_{friction} = \sum (f_s) \cdot P \cdot h = P \cdot \sum_{z=0}^{z=h_s} [K_a^n \cdot \sigma_{eff}^n \cdot \tan(3/4 \cdot \theta^n) \cdot h_s] \tag{6.6}$$

Because the friction force is reduced by the introduction of the bentonite lubricant equation 6.6 is adjusted. Equation 6.7 gives the total friction force over depth.

$$\begin{aligned} F_{friction;including\ bentonite} &= \sum (f_s) \cdot P \cdot h \\ &= P \cdot \sum_{z=0}^{z=h_s} [K_a^n \cdot \sigma_{eff}^n \cdot \tan(3/4 \cdot \theta^n) \cdot h_{ce}^n] + [(h_s - h_{ce}) \cdot 7.5] \end{aligned} \tag{6.7}$$

Where h_{ce} is the height of the cutting edge. The equation is schematized in figure 6.14.

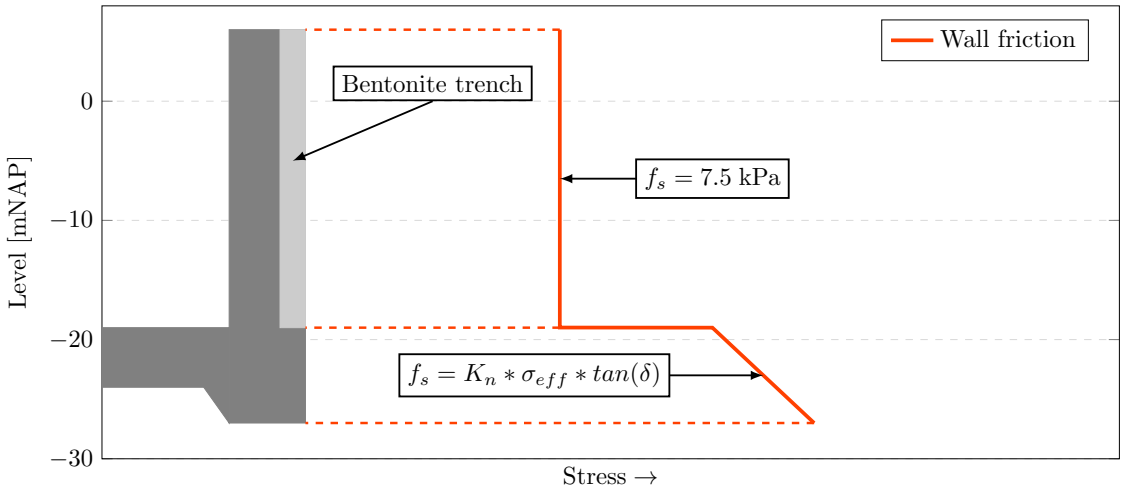

Figure 6.14: *Schematization of different zones of wall friction*

The value for $F_{friction}$ is calculated for all stage during the process of subsidence. The calculations can be found in appendix G.4. The value of $F_{friction}$ for both the situation with and without bentonite trench and divided by the perimeter are plotted in figure 6.15.

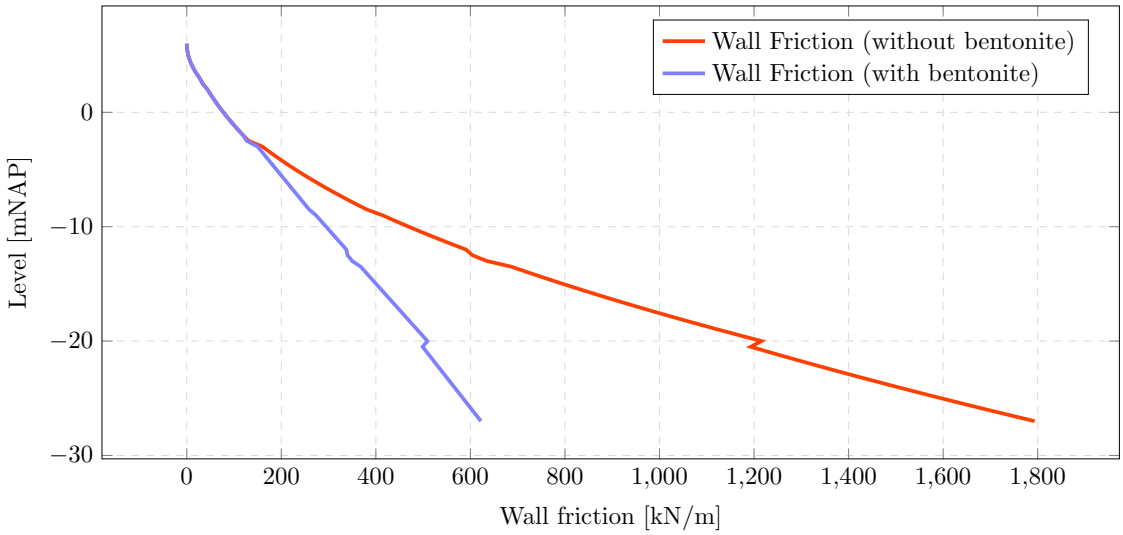

Figure 6.15: *Wall friction with and without bentonite slurry over depth per running meter circumference*

As can be seen from the figure the wall friction in the absence of a bentonite-water suspension is considerably higher at larger depths.

6.4.3 AIR PRESSURE

To prevent the inflow of groundwater during excavation below the groundwater table an overpressure must be present inside the working chamber. The air pressure should be automatically

adjusted to the increasing water-pressure over depth in order to maintaining the water stress in the soil below the working chamber and stabilize the surrounding groundwater table. Consequently by the use of an overpressure the disturbances to the environment will be minimalized. The groundwater table is located at a height of NAP +2 meter. The total upward force which is caused by the (increased) air pressure and is defined at the value of the air pressure multiplied with the surface area of the bottom slab. The upward force can be calculated according to equation 6.8.

$$F_{air} = A_{bottomslab} \cdot u \tag{6.8}$$

Where u is the hydraulic water pressure and $A_{bottom\,slab}$ the surface area of the bottom slab where the air pressure is acting on. The force per square meter is given in figure 6.16. The calculations can be found in appendix G.4.

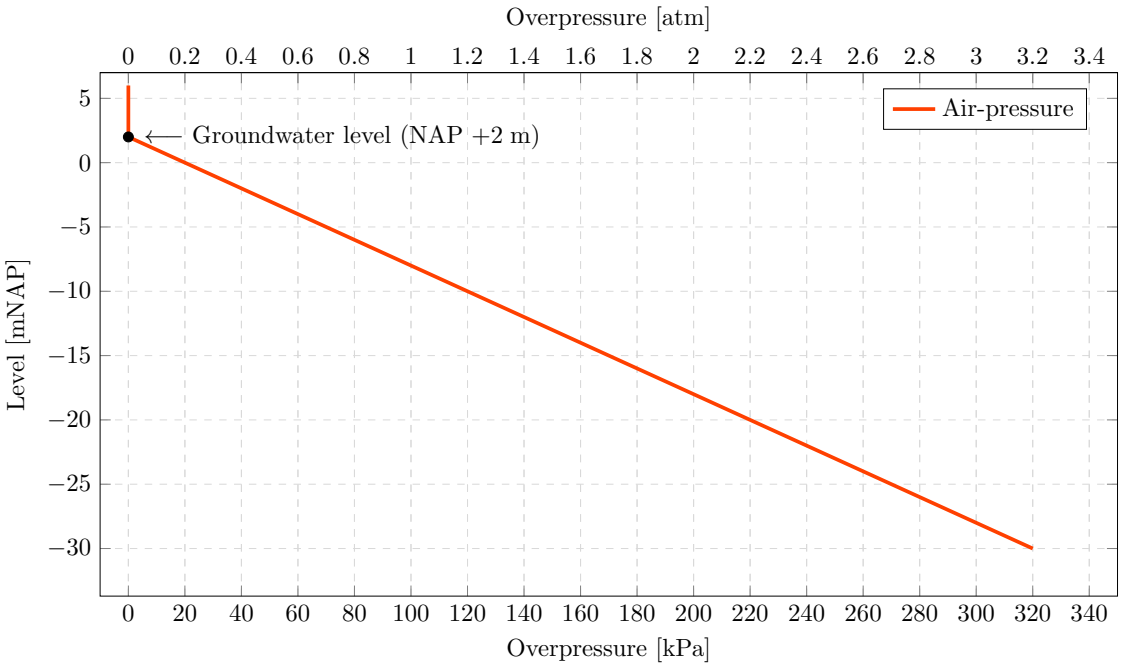

Figure 6.16: *Air pressure over depth*

6.4.4 HORIZONTAL SOIL PRESSURE

The horizontal soil and water stresses on the caisson walls can be determined by equation 6.9.

$$\underbrace{\sigma_h'}_{\text{Total horizontal stress}} = \underbrace{K \cdot \sigma_v' - 2 \cdot c \cdot \sqrt{(K)}}_{\text{Horizontal soil stress}} + \underbrace{u}_{\text{Water stress}} \tag{6.9}$$

Where σ_v is the effective vertical soil stress, c the cohesion and K the ground pressure coefficient, this is the active– or neutral ground pressure coefficient or a value in between dependent on the deflection of the caisson wall. Because the caisson is a very stiff construction with small deflections the neutral coefficient of horizontal soil pressure should been used according to [NEN 9997-1+C1:2012].

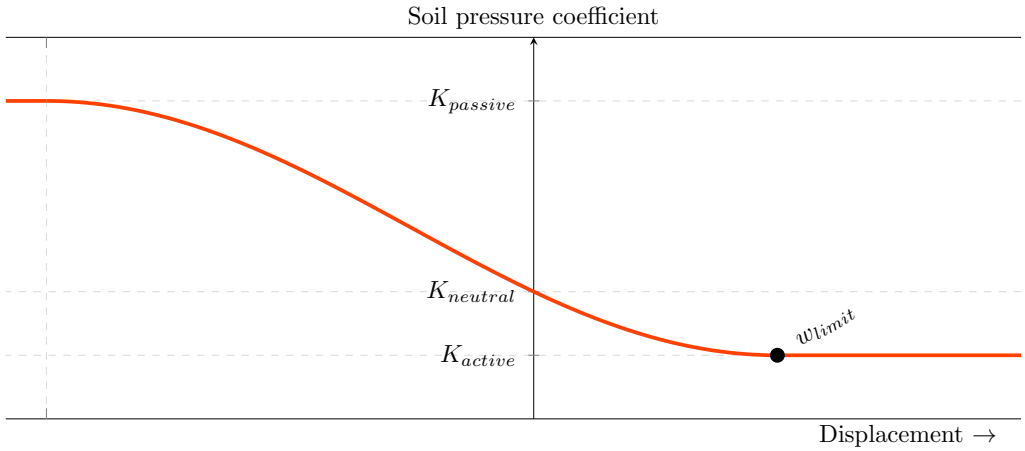

Figure 6.17: *Soil pressure coefficient as function of deflection of caisson wall (Deflection in the direction of the soil stress is taken positive)*

6.4.5 BEARING CAPACITY DURING SUBSIDENCE

One of the most important forces for equilibrium of the pneumatic caisson is the vertical bearing capacity. The bearing capacity of the caisson during subsidence is dependent on multiple parameters. The most important parameter is the total surface area of the foundation. The foundation in this case consist out of the horizontal surface area of the cutting edge and compartment wall which are in contact with the soil. By varying the depth of the excavation and thereby the width of the cutting edge the total bearing capacity can be adjusted.

The state just before failure of the soil is called a limit state and the function that describes this situation is the so-called reliability function. To guarantee a certain safety margin, the capacity of the soil is tested against the load of the caisson, according to: [NEN 9997-1+C1:2012]

$$R_d > S_d \qquad \Leftrightarrow \qquad \frac{R_{rep}}{\gamma_r} > S_{rep} \cdot \gamma_s \tag{6.10}$$

Where R_{rep} and R_d are respectively the characteristic– and design value for the soil capacity and S_{rep} and S_d are respectively the characteristic– and design value for the load. In normal situations the characteristic values should be derived in such a way that the calculated probability of a unfavourable value for the considered limit state is not more than 5%. In the calculations for the bearing capacity therefore the 5% upper limit (95% probability of undershoot) of the load is used and the 5% lower limit (95% probability of exceedance) of the soil capacity. In that case the total failure probability is then extremely small.

To achieve subsidence of the caisson the bearing capacity should be decreased. This can be done by reducing the foundation surface of the caisson which is equivalent to excavating the working chamber and thereby decreasing the width, w_{ce}, of the cutting edges. At some point the capacity of the soil will become smaller than the acting load as schematized in figure 6.18. The soil below the cutting edge will fail locally and as a result the caisson will subside. Due tot the trapezoidal shape of the cutting edge the foundation surface will increase until a new equilibrium is reached.

Two cases for the determination of the soil capacity are distinguished. First the lower limit of the bearing capacity is of importance for the calculations. When the actual soil capacity is

less than the theoretical lower limit value, the caisson may subside further than expected and workmen can come in tribulation between soil and bottom slab. Second, the upper limit of the soil capacity is of less importance. When the soil does not fail after the theoretical capacity has been reached there simply can be excavated further in the working chamber until the actual capacity of the soil has been reached and subsidence still occurs.

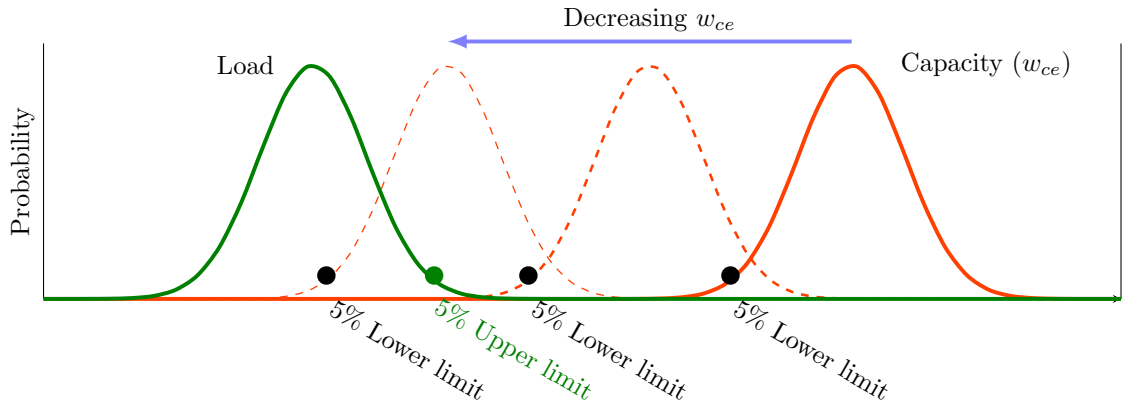

Figure 6.18: *Schematization of load and capacity interaction*

The bearing capacity is not only depending on the width of the cutting edge but also on mechanical properties of the soil such as density, shearing strength and deformation characteristics, on the original stresses in the subsoil and on the water conditions in the ground and on physical characteristics of the foundation. For example size, depth, shape and roughness and on the way in which the foundation is installed. In view of mathematical difficulties the problem can at present only be solved by simplified methods. [Meyerhof, 1951] Therefore a strip foundation will be assumed. There are six different scenario's in which drained and undrained soil layers are located below the foundation. The theoretical background, the determination of the soil capacity and the check on basal stability are given in appendix B.4.

The result of the calculations from the appendix are given in figure 6.19 where the different colors are standing for the different scenario's elaborated. In the final stage the working chamber will be filled with concrete and therefore the foundation surface will increased to prevent further subsidence of the caisson during the lifespan.

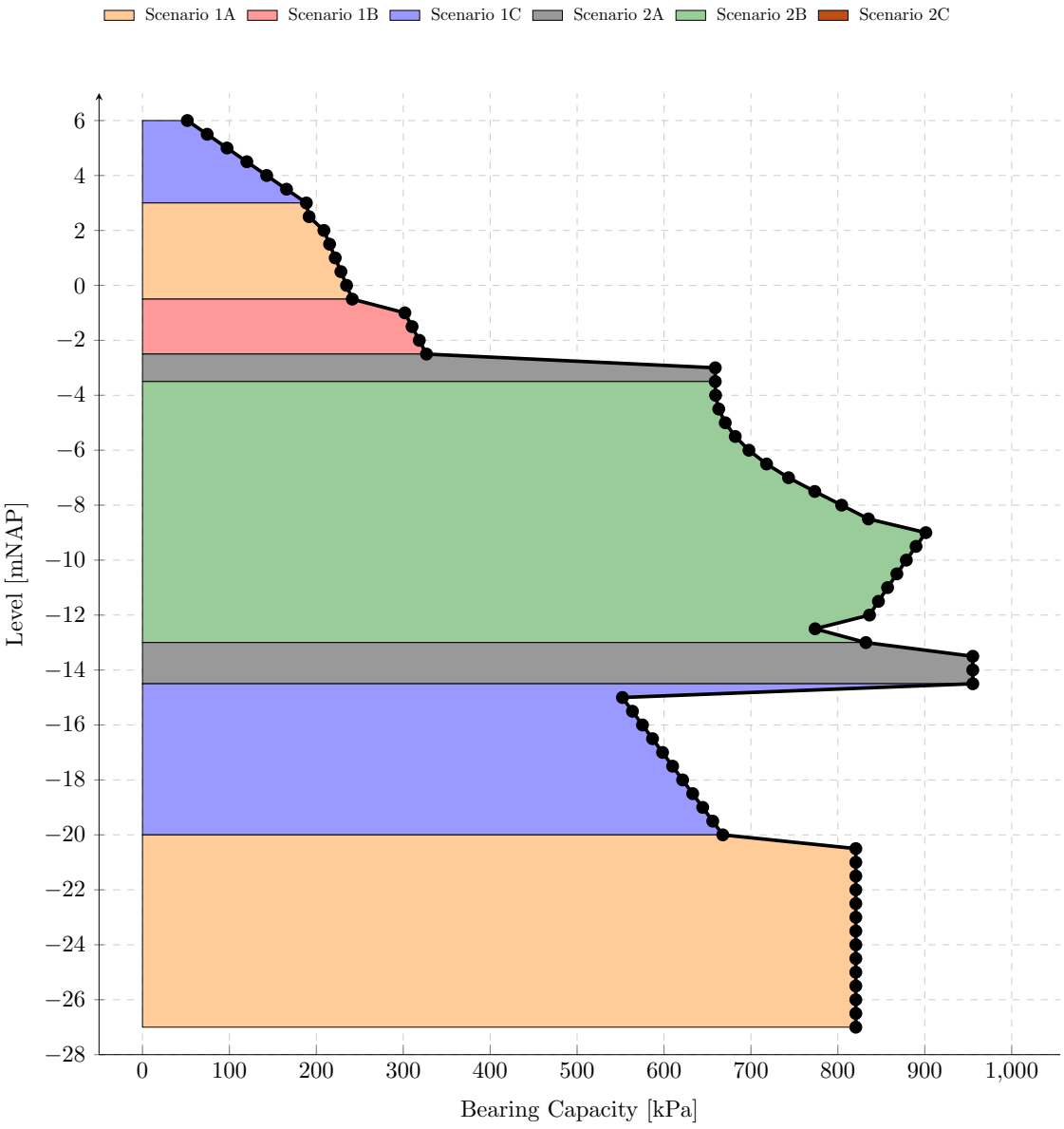

Figure 6.19: *Bearing capacity per square meter over depth*

7

VARIANT 1 - ONE LARGE CAISSON DIVIDED INTO SEVERAL COMPARTMENTS

The first variant elaborated consists out of the construction of one large pneumatic caisson covering the complete lock head. The working chamber is divided into several compartments. Therefore multiple air– and soil discharge shafts are required as well as more equipment to control the air pressure in working chamber.

This chapter starts with an explanation of all internal– and external dimensions in section 7.1. In the previous chapter all global loads are already elaborated. In section 7.2 these loads are worked out further to provide insight in the process of subsidence. Thereafter in section 7.3 the structural schematization of the design with all corresponding assumptions is given. Subsequently with help of SCIA Engineer[1] the feasibility of the caisson will be analyzed and worked out in section 7.4. In section 7.5 at the end the potential undesirable unequal subsidence of the caisson is elaborated.

7.1 DIMENSIONS OF THE CAISSON

In figure 6.8 a three dimensional schematization of the caisson was given as well as the direction of the coordinate system. The dimensions are further defined in this section. In figures 7.1–7.3 the dimensions of the 3D schematization are given for respectively the x–, y– and z-direction.

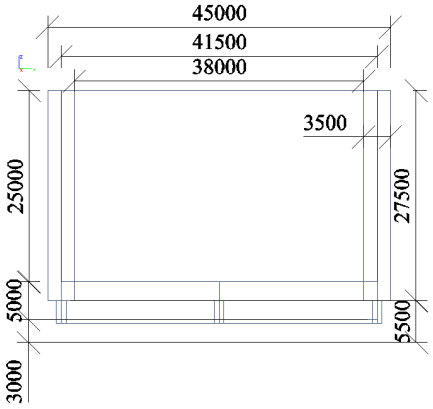

Figure 7.1: *Dimensions in yz-plane*

1 SCIA Engineer - Finite elements software for structural calculations, structural design and structural constructions

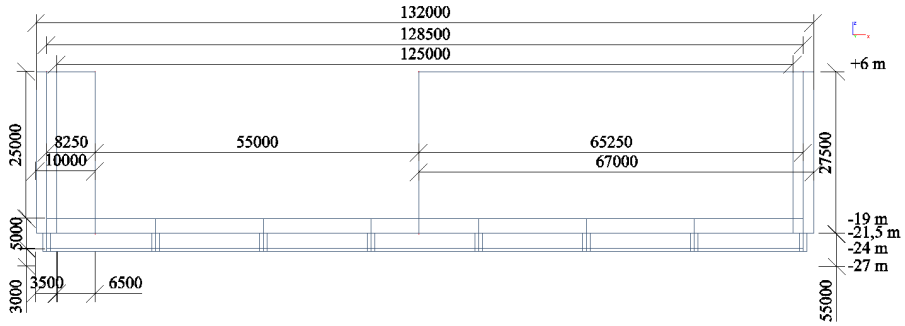

Figure 7.2: *Dimensions in xz-plane*

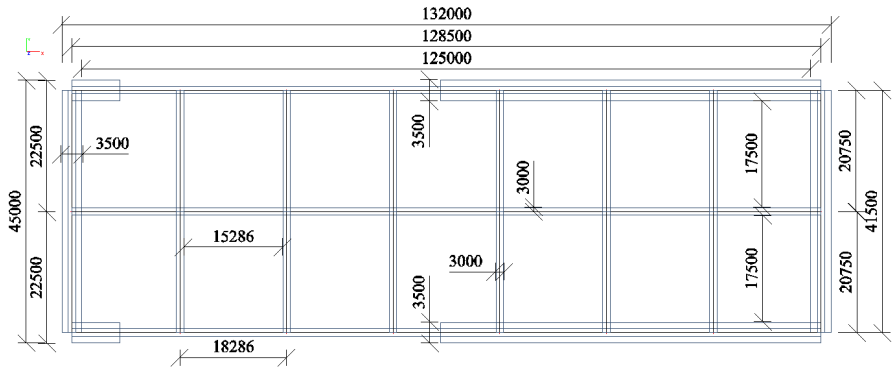

Figure 7.3: *Dimensions in xy-plane*

7.2 PROCESS OF SUBSIDENCE

7.2.1 ANALYSIS OF FORCES

With help of the following equation the net-force on the caisson which is dependent on the width of the cutting edge can be calculated.

$$F_{net}(w_{ce}) = F_{selfweight} - [F_{friction} + F_{air}(w_{ce}) + F_{bearing}(w_{ce})] \tag{7.1}$$

Where $F_{friction}$ and F_{air} are elaborated in the previous chapter. The self-weight of the caisson at surface level is calculated in appendix F.1. The effective value of the self-weight was depending on the depth of the caisson below the groundwater table because of the hydraulic head. The submerged weight of the caisson over depth is given in figure 7.4.

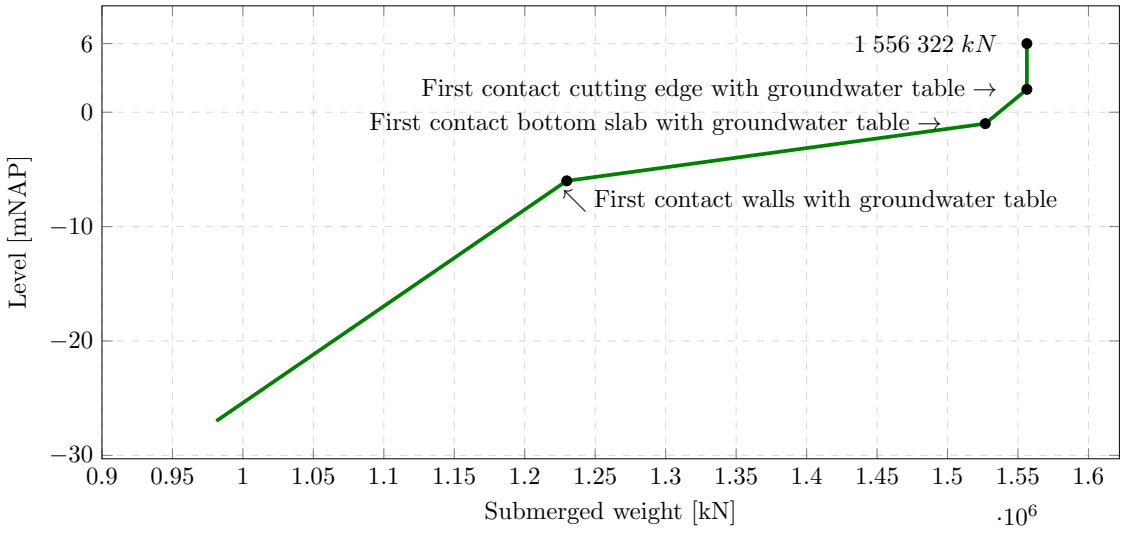

Figure 7.4: *Submerged weight of the caisson*

The resisting bearing force, $F_{bearing}(w_{ce})$, is defined by the maximum stress ($\sigma_{max,z}$), multiplied by the horizontal foundation surface of the concrete-soil interface ($A_{foundation}$) at the cutting edges at a depth z. The surface area of the bottom slab where air pressure is acting on is depending on the width of the cutting edge.

$$\begin{aligned} F_{bearing}(w_{ce}) &= A_{foundation} \times \sigma_{max,z} \\ F_{air}(w_{ce}) &= (A_{bottom\ slab} - A_{foundation}) \times \sigma_{air,z} \end{aligned} \tag{7.2}$$

Where:

$$A_{foundation} = L \times W - (L - (2 + x_L) \cdot w_{ce}) \cdot (W - (2 + x_w) \cdot w_{ce}) \tag{7.3}$$

In the formula above, L and W are the length and width of the caisson and x_L and x_W are respectively the number of compartment walls in the length and width. The width of the cutting edges at both sides of the caisson and the compartment walls are assumed equal. The required width to achieve equilibrium can be found easily by requiring equilibrium of equation 7.1. In the equation, w_{ce} is the only unknown variable and the formula can thereby be solved. The result is given in figure 7.10 where the width of the cutting edge, w_{ce}, is plotted as orange line. The calculations are given in figure F.2. According to the figure a number of conclusions can be drawn.

1. At the first meters of subsidence there is no vertical equilibrium. Even without the cutting edges the bearing capacity of the soil is less than the weight of the caisson. Without any additional measures the fully excavation of the working chamber is not possible. In that case the caisson will start penetrating in to the subsoil from the start without any manual excavation below the caisson. Multiple solutions are possible:
    - *Option 1* - Limit the weight of the caisson by constructing the caisson in multiple phases.
    - *Option 2* - Enlarge the foundation surface by broadening the width of the cutting edges and compartment walls.

- *Option 3* - Increase the foundation surface by the addition of extra compartment walls.

The decrease of weight of the caissons by construction the caisson walls in a later stadium does not have enough effect to achieve equilibrium between soil and caisson at the start of subsidence. The cutting edge must enlarged to a very large extent to obtain equilibrium which moreover complicates the process of subsidence in a later stadium. This also increases the weight of the caisson which causes a vicious circle because due the increase in weight wider cutting edges are required. This explains also why the addition of extra compartments walls has little effect because also in that case extra weight will be introduced.

The second conclusion that can be drawn is:

2. From a certain moment the upward forces are too large to achieve any further subsidence of the caisson. The width of the cutting edges becomes negative in order to achieve equilibrium what is obviously not possible. Even without contact between the cutting edge and underlying soil the caisson will not subside further because of the resisting air and friction forces. Potential solutions are:
   - *Option 1* - Addition of extra weight in the form of ballast.
   - *Option 2* - Temporary decrease of the air pressure. When the time span is short enough water does not have the time to flow in the working chamber.

Both conclusions described above are contradictory. On one hand the downward directed loads must be as small as possible to achieve a workable space within the working chamber and to be able to excavate the soil. On the other hand the downward direct load must be increased to achieve any further subsidence of the caisson during the last stadium of subsidence.

7.2.2 STRATEGY OF SUBSIDENCE

The challenges during the process of subsidence is to obtain a net resultant force at all times which is nearby the point of equilibrium ($F_{net} = 0$). Two steps as described in the previous section have to be taken.

1. Decrease the weight of the caisson during the first part of the process of subsidence.
2. Increase the weight of the caisson during the last part of the process of subsidence.

DECREASE THE WEIGHT OF CAISSON

The construction of the caisson can take place in two different phases. The operation mode as described in section 5.3 must therefore be adjusted. In the first phase the cutting edges and compartment walls are constructed at a level of NAP +2 meter. This is at the level of the groundwater table and hence no dewatering of the building site are required. This part of the caisson has a weight of only 816 323 kN and has thereby a share of $\frac{816\,323}{1\,556\,322} = 52\%$. After sufficient hardening of the concrete this part of the caisson is subsided over a vertical distance of 5 meter towards a level of NAP -3 m. Hereafter the caissons walls are constructed and the process of subsidence can be continued until a depth of NAP -10 meter. From this point on ballast will be applied to achieve further subsidence and simultaneously the area around the caisson will be supplemented with sand towards a level of NAP +6 meter.

INCREASE THE WEIGHT OF CAISSON

To increase the weight of the caisson ballast can be used. When water is used as ballast material it will accumulate during a inclined subsidence of the caisson, causing an extra external moment and aggravates the inclination. The use of sand as ballast material is therefore a more applicable solution because first a limit value must be exceed before sand particles starts to move. In the design every meter the caisson subsides after reaching a depth of NAP -10 meter, 80 centimeters of ballast sand must been applied. In figure 7.5 the total weight, submerged weight and amount of ballast sand is plotted as function of the depth.

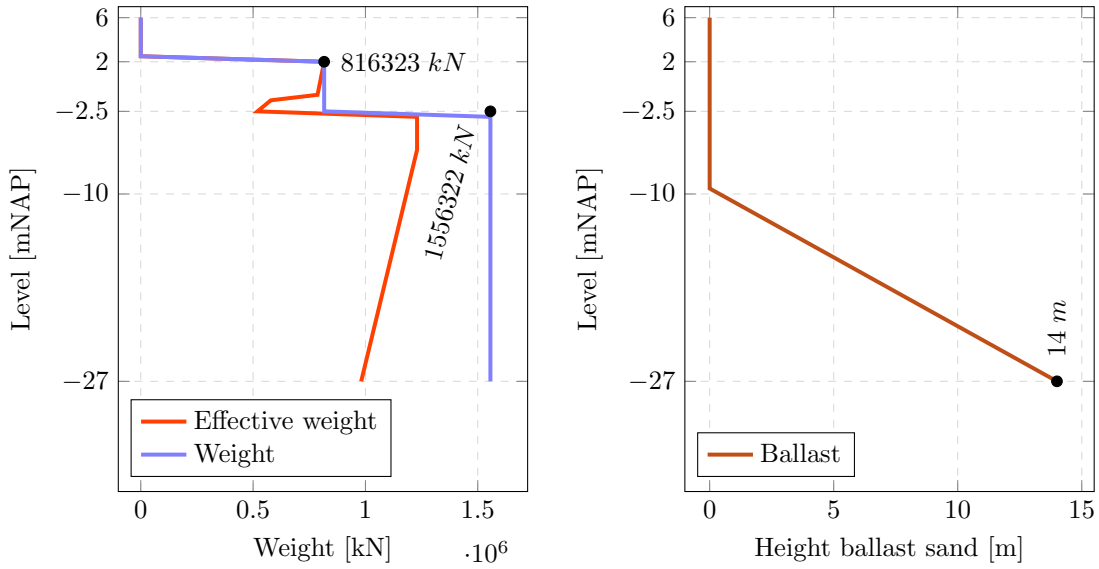

Figure 7.5: *Weight of the caisson (left) and quantity of ballast (right)*

The different phases are schematised in figures 7.6–7.9.

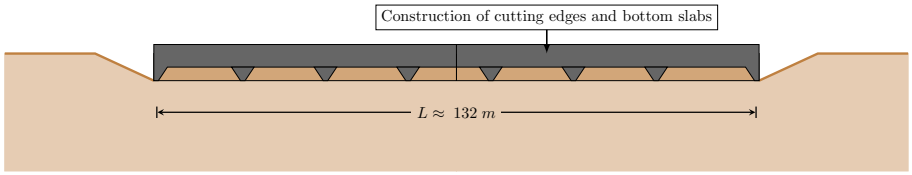

Figure 7.6: *Construction of bottom slab and cutting edges on sand mould at a level of NAP +2m*

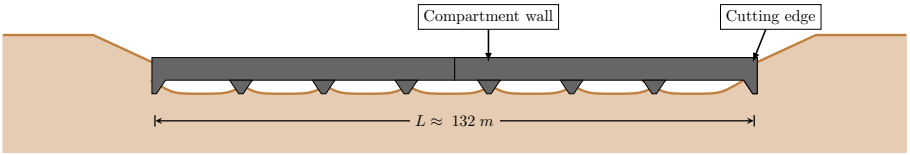

Figure 7.7: *Subsidence of lower part caisson until a level of NAP -3m*

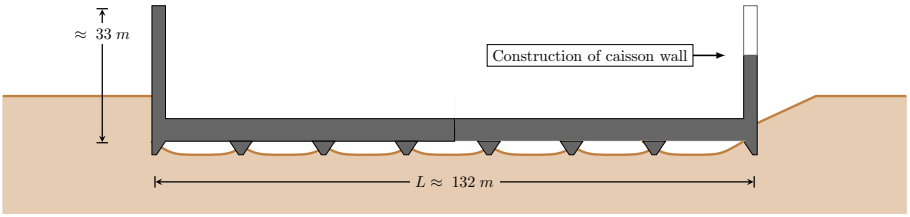

Figure 7.8: *Construction of remaining part of caisson*

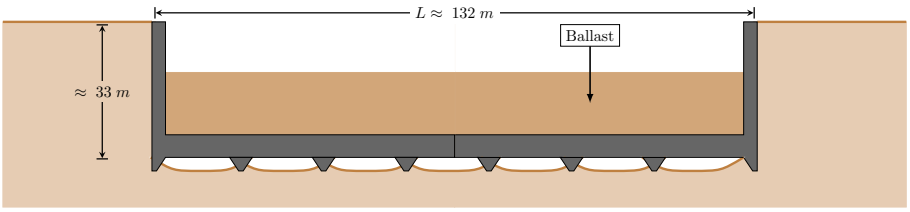

Figure 7.9: *Continuation of subsidence and applying of ballast*

In figure 7.10 the original width determined with equation 7.1 as well as the new derived cutting edge width are given.

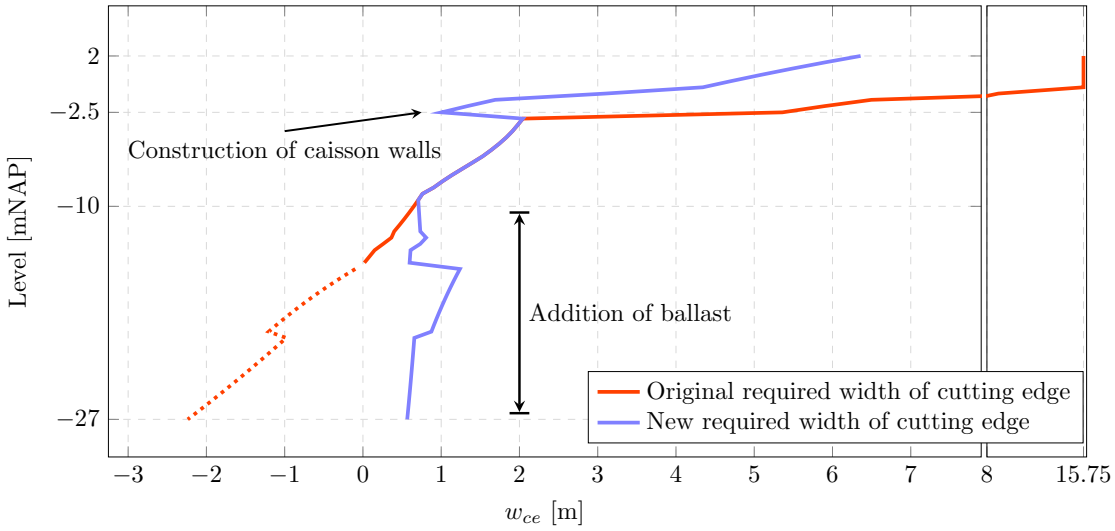

Figure 7.10: *Calculated width of the cutting edge*

In figure 7.11 all external forces on the caisson are plotted. It can be concluded that the friction force has by the use of bentonite a minor role.

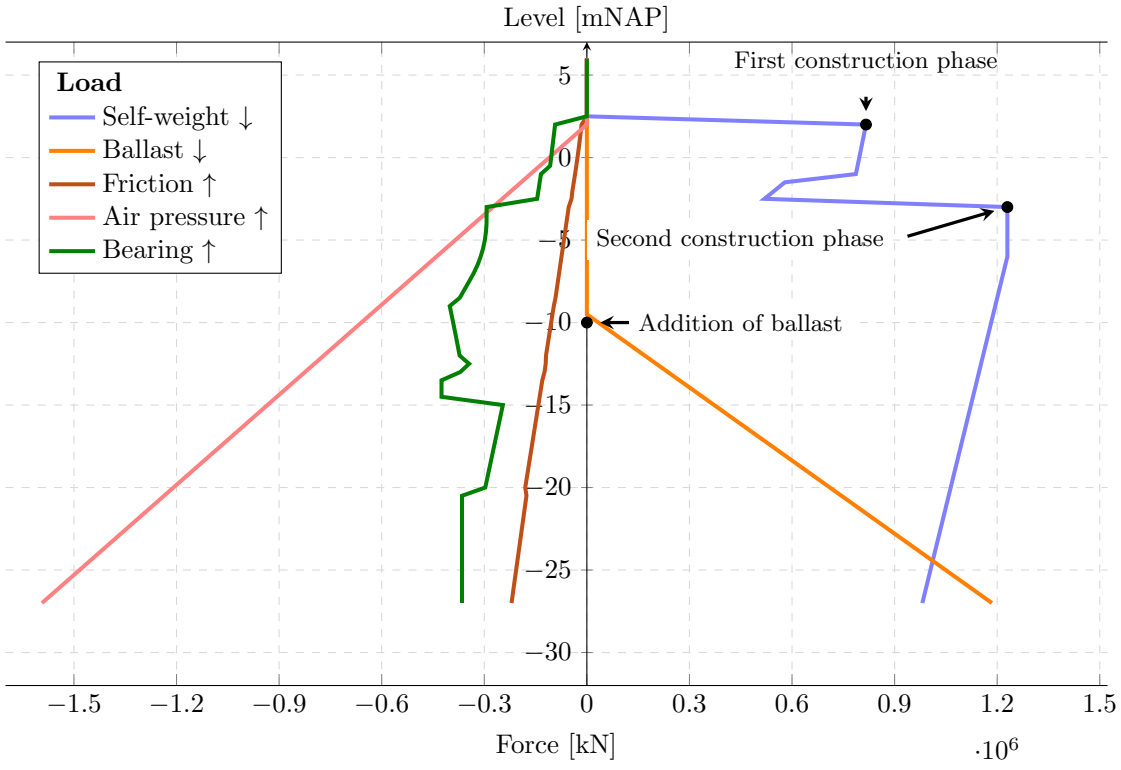

Figure 7.11: *Overview of the different forces acting on the caisson*

SETTLEMENT DURING LIFETIME

Due to the compressibility of the soil the caisson will settle during its lifetime. The order of magnitude of the settlements can be calculated according to the formula of Koppejan:

$$\Delta H = H \cdot \left(\left(\frac{U}{C_p'} + \frac{1}{C_s'} \log(t) \right) \cdot \ln\left(\frac{\sigma_{v;i}' + \Delta\sigma_v'}{\sigma_{v;i}'} \right) \right) \tag{7.4}$$

The settlement at the end of the lifetime ($\pm$ 50 years, $t = 365 \times 50$ days) will be calculated. At that moment the soil is completely consolidated, hence $U = 1$. According to [Fugro, 2014] the primary– and secondary compression coefficients of the Boom clay which is situated between NAP -20.5 and NAP -38 m are respectively $C_p' = 33.2$ and $C_s' = 156.8$. The underside of the construction is situated on NAP -27 m. In the middle of this layer (NAP -32.5 m) the initial effective stress is $\sigma_{v;i}' = 360.05$ kPa. Due to the construction of the caisson the vertical stress in the soil will increase. The load of the caisson will be distributed under an angle of $\theta = 30°$ in both directions. The effective surface area of the foundation is thereby:

$$\begin{aligned} A_{eff} &= (132 + 2 \cdot \tan(\theta) \cdot h) \times (45 + 2 \cdot \tan(\theta) \cdot h) \\ &= (132 + 2 \cdot \tan(30°) \cdot (32.5 - 27)) \times (45 + 2 \cdot \tan(30°) \cdot (32.5 - 27)) \\ &= 7104 \text{ m}^2 \end{aligned} \tag{7.5}$$

The total additional stress in the soil layer is originating from the (submerged) weight of the caisson. The total submerged weight of the caisson can be found in appendix F.1, $F_{caisson;sub} = 981156$.

The total increase of stress is:

$$\Delta\sigma_v' = \sigma_{v;caisson}' - \sigma_{v;soil}' \tag{7.6}$$

Where the total decrease of effective vertical (soil) stress is $\sigma_{v;soil}' = 314.4$ kPa according to G.4 and the total stress by the presence of the caisson $\sigma_{v;caisson}'$ on NAP -32.5 m is:

$$\begin{aligned} \sigma_{v;caisson}' &= (F_{caisson;sub} + F_{workchamber})/A_{eff} \\ &= \frac{(981156 + 15 \cdot ((132 - 2 \times 0.85 - 6 \times 1.7) \cdot (45 - 2 \times 0.85 - 1 \times 1.7))}{7104} \\ &= 148 \text{ kPa} \end{aligned} \tag{7.7}$$

The total settlement ΔH is calculated according equation 7.4, $\Delta H = 0.217$ m. This is an acceptable value. The walls of the lock chamber will also settle, although the settlement will be smaller because of the smaller weight.

7.3 STRUCTURAL SCHEMATISATION OF THE CAISSON

In the previous section the vertical force equilibrium was elaborated. In the current section the effect of the loads and supports on the structure itself will be elaborated. First the soil will be elaborated as distributed linear spring, thereafter the different kinds of loads acting on the caisson are worked out. This section will be completed with the results of the displacements and force equilibrium.

7.3.1 STRUCTURAL SOIL SCHEMATISATION

The load on the cutting edge is not uniformly distributed over the circumference of the caisson. This has two causes. First cause is the irregularities in the soil composition. The type of soil used for the land fill and the associated properties are dependent on the design. The largest part of the soil below the future lock head is undisturbed but also here disturbances are possible. When on one side of the caisson a stiffer soil layer is present in comparison with the other side of the caisson, loads will not be transmitted uniformly. Second cause is the difference in excavation approaches which are present in order to control the sinking process of the caisson. Due to an excavation on one side of the working chamber the effective width of the cutting edge will decrease and the caisson is not equally supported. The influence of the soil on the structure and the difference in excavation approaches can be determined on two ways:

1. Schematising the soil as a spring
2. Impose deformations on the structure

Schematising the soil as a linear spring has some disadvantages: [Vrijling, 2011]

- The stiffness of the soil is not linear.
- The spread of stress in the subsoil is not schematised.
- The springs are not linked and therefore shear stresses are not taken into account.
- The soil is not a spring and does not behave as one.

Despite of the disadvantages, schematising the soil as a spring gives in an easy way reasonable good results. The soil will be schematised as linear spring in order to calculate the forces in the construction.

Following Hooke's Law the elongation of a spring is proportional to the force being applied on the spring. The key concept is in this context, the so-called spring constant indicates how stiff or rigid the spring is, or anything else formulated: how big the deformation of the spring if a certain force acts on the spring. In formula form:

$$F = k \cdot u \tag{7.8}$$

Where F is the force acting on the spring, u is the deformation of the spring or soil and k is the spring constant. In soil mechanics the spring constant is called the modulus of subgrade reaction. The modulus of subgrade reaction can be determined by field tests or by correlation with other tests. There is no direct laboratory procedure for determining k-value. The modulus of subgrade reaction is not only dependent on the soil properties but also on the geometry of the foundation.

An average value of $k = 27.4\ MN/m^3$ [LievenseCSO, 2014e] is used for the modulus of subgrade reaction. The depth of the different layers is not equally distributed in space. Therefore at the interfaces between soil and cutting edges the caisson is on one side supported by a stiffer soil layers while in the meantime the other side of the caisson is supported by a more weaker soil layer or vice versa. Therefore the modulus of subgrade reaction varies over distance. Because it is difficult to determine the exact value, it is assumed that the values are varying between $\frac{k}{\sqrt{\lambda}}$ and $k \cdot \sqrt{\lambda}$. In the literature [Limbergen, 1988] a factor of $\lambda = 2$ is used. Because of the large differences in properties between the different soil layers in Terneuzen $\lambda = 5$ is used for the calculations. This assumption will be verified later.

7.3.2 LOADS AND LOAD COMBINATIONS

In the previous chapter and sections the different loads acting on the caisson were already introduced. The loads acting on the caisson are determining the required dimensions of the caisson. During subside of the caisson the horizontal soil and water pressure will increase as well as loads from soil friction and ballast. For the calculations the air pressure is not taken into account because of the possible absence during accidence of these. Two normative situations or load combinations are distinguished and will be worked out further.

- **Load combination 1** - After subsidence of the caisson to its final depth the downward directed loads from the ballast and self-weight of the bottom slab are at their maximum value. Because in this governing situation the working chamber is still not filled with concrete at this time. Also the forces originating from horizontal soil and water loads and friction are at their maximum value. At this moment the bulkhead is still present. Due to the stiffness of concrete bulkheads in the direction of the plane the deflection of the gate recess should be smaller in comparison with steel bulkheads. A $t_{wall} = 3000$ mm thick concrete wall is used as bulkhead. Preferably there is no reinforcement present inside the bulkhead. This complicates the removal of the bulkhead after final subsidence. A control of this will be performed later on.
- **Load combination 2** - After filling of the working chamber the bulkhead will be removed. During the lifetime of the caisson also the water pressure is acting on the inside of the working chamber. The total horizontal surface at the bottom of the caisson is in contact with the soil.

Not all loads are acting on the same moment with the same magnitudes on the caisson. In the enumeration below the different loads with corresponding order of magnitude are described.

- **Self-weight** - The self-weight of the construction is meanly dependent on the amount of concrete that is used for the different components of the structure. The self-weight influences directly the amount of ballast that is required for a smooth subsidence of the caisson. Concrete class C35/45 with an unit weight of $\gamma_{concrete} = 25$ kN/m^3 is assumed. The Young's modulus, which is a measure of the stiffness, can not be given unambiguously because concrete shows behavior of creep. In addition concrete can also crack. A cracked cross-section shows less resistance to deflection. The calculation of the Young's modulus is very complex and, in practice therefore, a value of $E_{concrete;crack} = 13 \times 10^3$ MPa is used in which all effects of creep and rupture of the concrete are converted.
- **Friction** - At the largest part of the caisson bentonite is situated between the concrete and soil resulting in a shear force on the outer walls of the caisson of 7.5 kPa. At the cutting edge where the bentonite trench is absent the shear force has a value of 50 kPa. (*See figure 6.14*)
- **Air pressure** - The increased air pressure in the working chamber forms a gradient with the outer air pressure. Acting as a upward directed load on the bottom slab. However, in emergency cases, a loss of the over-pressure can occur. Therefore in the calculations the absence of air pressure is assumed.
- **Ballast** - Ballast is used in the last stage of subsidence. The ballast is acting on both the bottom slab of the caisson. For calculations it is assumed that the ballast is not acting on

the inner side of the outer walls because that loads is not present in all situations. The ballast has a maximum height of 14 meter. The total distributed load by an unit weight of $\gamma_{ballast} = 18$ kN/m^3 is $q_{ballast} = 14 \cdot 18 = 252$ kN/m

- **Horizontal soil pressure** - The soil surrounding the caisson is acting on the outer walls of the caisson. The caisson is acting as retaining wall. The horizontal soil stress increases from 0 kPa at the top of the caisson walls towards 374 kPa at the lowest point of the cutting edges. (*See figure 6.13*)
- **Water pressure (outside)** - Groundwater is acting hydro-statically on the caisson walls. The ground water pressure increases from zero at NAP +2 meter towards 290 kPa at NAP -27 m.
- **Water pressure (inside)** - A minimum water level of NAP 0m is assumed. The water inside the caisson is acting both on the caissons walls as well as on the bottom slab of the caisson which is in direct contact with the subsoil. The water pressure increases hydrostatically to a level of 210 kPa at a depth of NAP -19 m.

In table 7.1 the used safety factors for the calculations are given.

Table 7.1: *Safety factors for the calculation*

Load	Load combination 1	Load combination 2
Self weight	1.2	1.2
Wall friction	1.2	1.2
Air pressure	0	0
Ballast	1.2	0
(Horizontal) soil forces	1.2	1.2
Water pressure (outside)	1.2	1.2
Water pressure (inside)	0	0.9

7.3.3 2D ANALYSIS

In first instance the pneumatic caisson, with the given dimensions of figure 6.9, is elaborated as elongated prismatic beam. In the remaining of this chapter the caisson will be elaborated further. In order to obtain an order of magnitude for displacements and internal force and moment distribution a two dimensional analysis is made. The caisson is seen as thin walled two dimensional structure. The two dimensional analysis is elaborated further in appendix F.3.

Although the calculations presented in the previous section do give an indication for the actual moments and forces on the caisson, they are based on a simplified two-dimensional concept with corresponding boundary conditions. In reality the moment distribution in the caisson is dependent on three-dimensional effects. By this is referred to the fact that the wall of the caisson is not a simply wide beam, clamped in at one side and with a free edge at the other side, but is connected with the adjacent side-walls which retain any deformation at the edges of those walls. In two-way spanning slabs bending moments as well as torsional moments occur. Loads will be transferred in both x– and y direction to the cutting edges which are the supports. Both load combinations are elaborated in the next paragraphs.

7.3.4 STRUCTURAL SOIL SCHEMATIZATION IN 3D

In the 2D schematization the influence of the soil on the structure and the difference in excavation approaches were determined by the use of linear soil springs with different properties over the length of the caisson. These effect occurs also in the three-dimensional schematization. According to [Kraneveld et al., 2004] a threesome normative scenarios are given. These scenarios which are given in figures 7.12 – 7.14 are reflecting the maximum unfavourable expected conditions during subsidence and during the final situation. A more unfavorable situation does not occur because before that situation can exist the caisson has already subsided further into the soil which adjust the load distribution not later than one of the limit cases.

In the three-dimensional calculations four cases are distinguished:

- **Soil schematisation 1** - Caisson is supported on a homogeneous layer of soil, this is the zero alternative.
- **Soil schematisation 2** - The edges of the caisson are supported on a firmer and stronger layer of soil in comparison with the soil located below the center part of the caisson. A sagging moment in the construction will occur. (*See figure 7.12*)

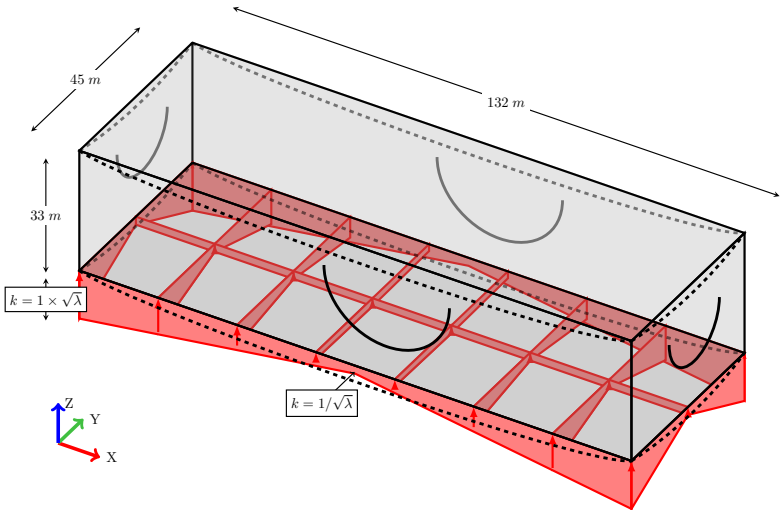

Figure 7.12: *Soil situation 1 - Sagging moment due to load distribution*

- **Soil schematisation 3** - The edges of the caisson are supported on a weaker layer of soil with less bearing capacity in comparison with the soil located below the center part of the caisson. A hogging moment in the construction will occur. (*See figure 7.13*)

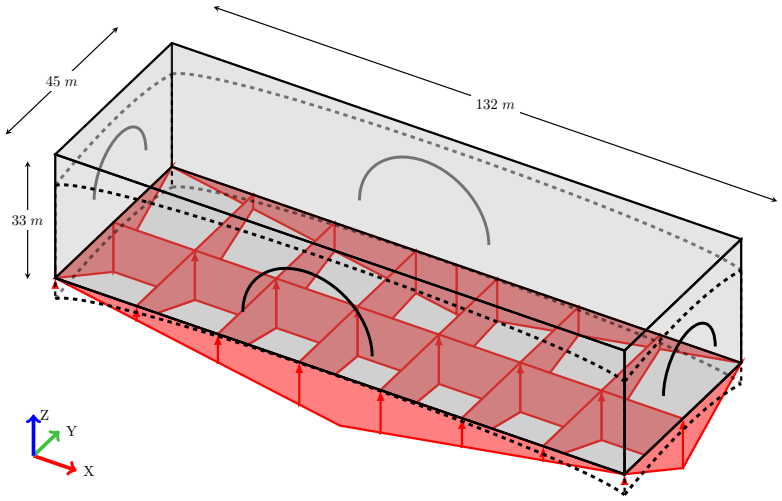

Figure 7.13: *Soil situation 2 - Hogging moment due to load distribution*

- **Soil schematisation 4** - The caisson is supported diagonally on a stiff soil layer. Torsion in the structure will occur in a larger extent. This results in extra shear stresses in the bottom plate and adjacent walls. (*See figure 7.14*)

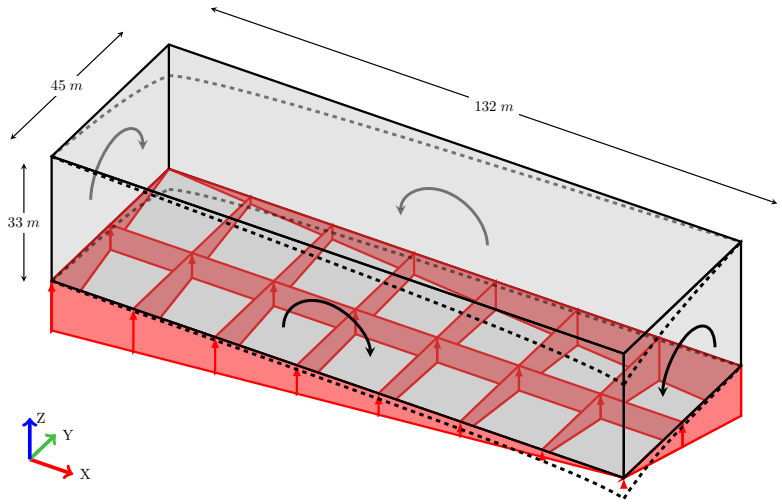

Figure 7.14: *Saging moment in diagonal due to load distribution*

Due to the limitations of the SCIA Engineer software package the linear increasing stiffness of the soil over the length and width of the cutting edges will be inserted as uniform stiffness over a specific width. The width of one compartment is chosen in x-direction an the length of a half compartment in y-direction. The values for the soil stiffness below the cutting edges are given in appendix F.4.

7.4 FEASIBILITY OF THE CAISSON

In SCIA Engineer a plurality of forces, moments and stresses in the construction can be calculated. In this section a check on the feasibility of the caisson will take place. This is done with reference to the normal forces as well as the design moments M_{xd+}, M_{xd-}, M_{yd+} and M_{yd-} in the caisson. The design moments are defined as the sum of the bending moments m_x and m_y and torsional moment m_{xy}. In formula form:

$$\begin{aligned} mxD- &= -m_x + |m_{xy}| \\ myD- &= -m_y + |m_{xy}| \\ mxD+ &= m_x + |m_{xy}| \\ myD+ &= m_y + |m_{xy}| \end{aligned} \tag{7.9}$$

The bending moment has often the largest value at the middle of the plates. The torsional moment has usually the largest value at the plate edges. The design normal forces n_{xD} and n_{yD} are defined as respectively the normal forces n_x and n_y summed up with n_{xy}, a shear force.

The design moments and –normal forces should be calculated and analyzed for the different structural parts, load cases and supports conditions. A flowchart wherein the different calculations are listed is given in figure 7.15

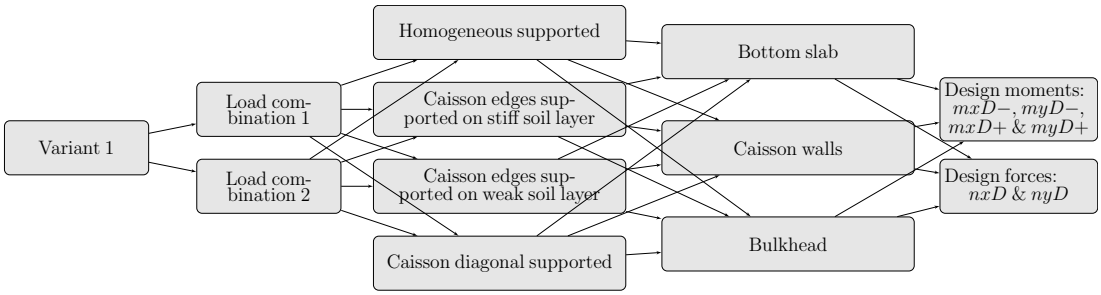

Figure 7.15: *Schematisation of the different calculations*

The resistance against failure is determined by the height of the concrete compressive zone and the amount and location of reinforcement. When tension forces are acting on the different structural parts of the caisson the resistance against failure will decrease. For that reason the structure has to be checked on the presence and combination of both the acting tension force as well as the resistance against bending moment.

In contrast to tension forces, compression forces do increase the bending moment capacity of the structure. The largest part of the axial forces are caused by the soil pressure and due to deflections. At the start of the process of subsidence, there are no soil stresses acting on the caisson and the deflections are limited to the deflections caused by the self-weight. Therefore, compressive forces are not taken in to account. In table 7.2 the maximum design moments occurring in the caisson are presented.

Table 7.2: *Maximum design moments in caisson*

Part	**mxD-** [kNm/m]	**mxD+** [kNm/m]	**myD-** [kNm/m]	**myD+** [kNm/m]
Bottom slab	30712	14005	52961	10880
Wall slab	33548	16701	41568	14134
Bulkhead	19515	13986	27413	11864

The maximal occurring design moment ($mxD-$, $myD-$, $mxD+$ and $myD+$) should be smaller than the total maximum moment resistance $M_{Rd}(N)$, which is dependent on the acting normal forces. Both positive and negative moments are acting on the caisson. Apart from the bending moments and axial forces in the caisson the structure should also be checked on the maximal occurring shear forces. In the following section the caisson bottom slab will be elaborated, subsequently in the following sections the caisson walls and bulkhead are elaborated. The individual results are given in appendix G.

7.4.1 ACTING MOMENT ON CAISSON BOTTOM SLAB

The thickness of the caisson bottom slab was assumed to be 5 meters in height. The moments on the lower side of the bottom slab are schematised in figure 7.16 and 7.17 for respectively the x– and y-direction during homogeneous supported conditions. The dark blue surface area indicates that at that location the bending moment is nil. Therefore when looking at the caisson bottom slab it can be seen that the design moments on the lower side of the bottom slab are almost present over the total surface area. Therefore reinforcement should be added on the total surface area of the underside of the bottom plate.

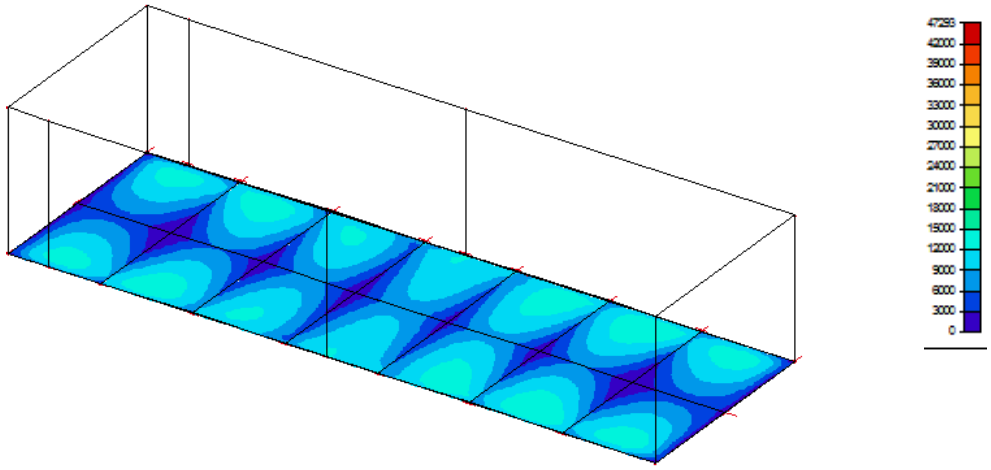

Figure 7.16: *Design moments in lower side of bottom plate for homogeneous supported caisson in x-direction*

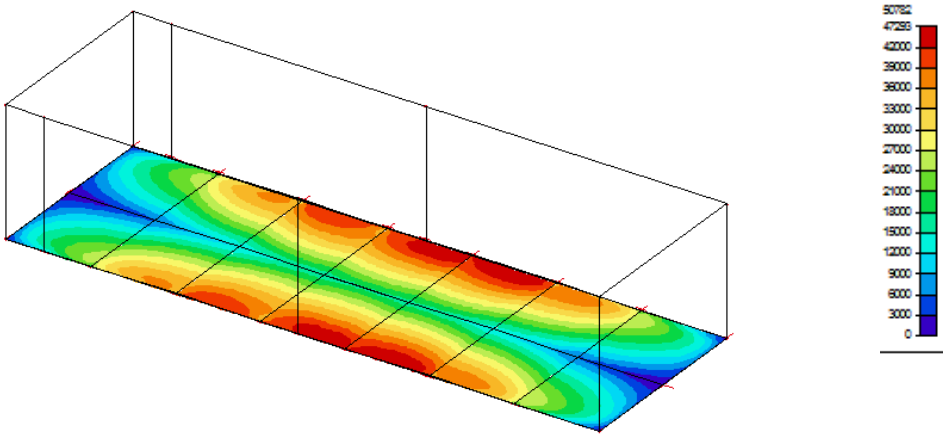

Figure 7.17: *Design moments in lower side of bottom plate for homogeneous supported caisson in y-direction*

On top of the bottom slab positive moments in x-direction are only occurring at the corners of the caisson and at some intersections of the bottom slab with the different compartment walls as can be seen in figure 7.18 and 7.19 for the moments in x– and y-direction. The non-blue color in the figure indicates the area where a positive moment on the upper side of the bottom slab is acting and were thus reinforcement on the upper side of the bottom slab is necessary.

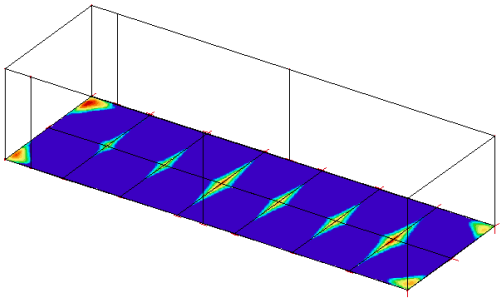

Figure 7.18: *Location of reinforcement in caisson bottom slab for x-direction*

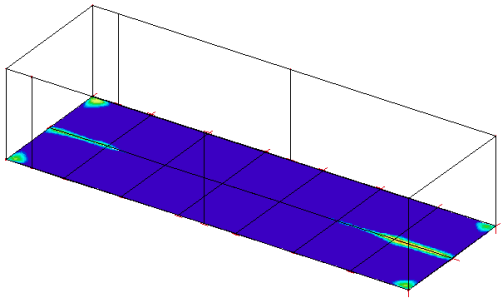

Figure 7.19: *Location of reinforcement in caisson bottom slab for y-direction*

In figures 7.20 and 7.21 the normal forces inside the bottom slab are schematised. In about half of the bottom slab tension forces are occurring. These tension forces reduce the resistance against bending moments.

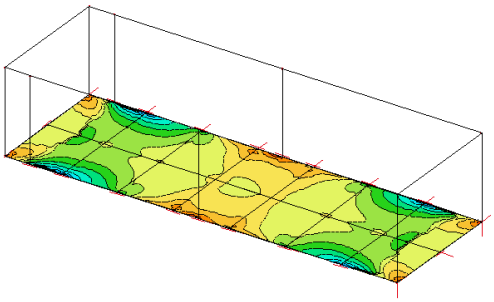

Figure 7.20: *Normal forces in x-direction*

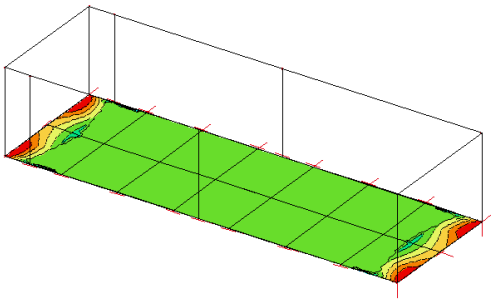

Figure 7.21: *Normal forces in y-direction*

7.4.2 DESIGN OF CAISSON BOTTOM SLAB

The occurring design moments and tension forces are calculated and the results are given in appendix G.2. In appendix F.5.1 the resistance of the reinforced concrete bottom slab against normal– and bending forces is calculated. In table 7.3 a summary of the occurring design moments and tension forces is given as well as a proposed reinforcement plan.

Table 7.3: *Required reinforcement by a bottom slab thickness of 5000 mm*

	Unit	x-	y-	x+	y+
$M_{ed;max}$	kNm/m	30712	52961	14005	10880
$N_{ed;max}$	kNm/m	1588	3676	1588	3676
Location	-	Bottom	Bottom	Top	Top
Reinforcement	-	⌀32-150	⌀32-150	⌀32-150	⌀32-150
# of reinforcement rows	-	4	7	2	2
A_s	mm^2/m	21447	37532	10723	10723
M_{rd}	kNm/m	37909	59854	18267	13526

With the proposed reinforcement plan of table 7.3 a total of $\frac{\sum A_s \cdot 1000}{10^9} \cdot 7850/5 = 126\ kg/m^3$ of reinforcement steel is required. This is more than the $70\ kg/m^3$ that was used for the construction of the Deurganckdok lock. The calculations are based on the assumption that the maximal design moment is acting on the same location as the maximum tensile force. In reality, the two maximums are acting on different locations. The maximum design moment is acting in the center of the span while the maximum tensile force is acting at the intersection with the cutting edges and compartment walls. Although the maximum of the tensile force and bending moment does not occur at the same location, they are located close to each other. By means of the anchorage length of the different reinforcement bars the proposed reinforcement plan must be present over the major part of the bottom slab.

SHEAR FORCES

The maximum shear force can be determined from the SCIA model. The design shear force is determined by the function of $q_{max,b}$ which has been defined as:

$$q_{max,b} = \sqrt{q_x^2 + q_y^2} \tag{7.10}$$

In figure 7.22 it can be seen that large shear forces are occurring. The maximum shear resistance of the concrete without the use of stirrups is calculated in appendix F.5.2. The maximum resistance is $V_{Rd;c} = 1477$ kN/m in x-direction. The occurring shear forces in the structure are higher then the maximum capacity of the concrete. In figure 7.22 the location where the maximum shear force is exceeded is filled in red. This means that about 50% of the bottom slab must be reinforced against shear.

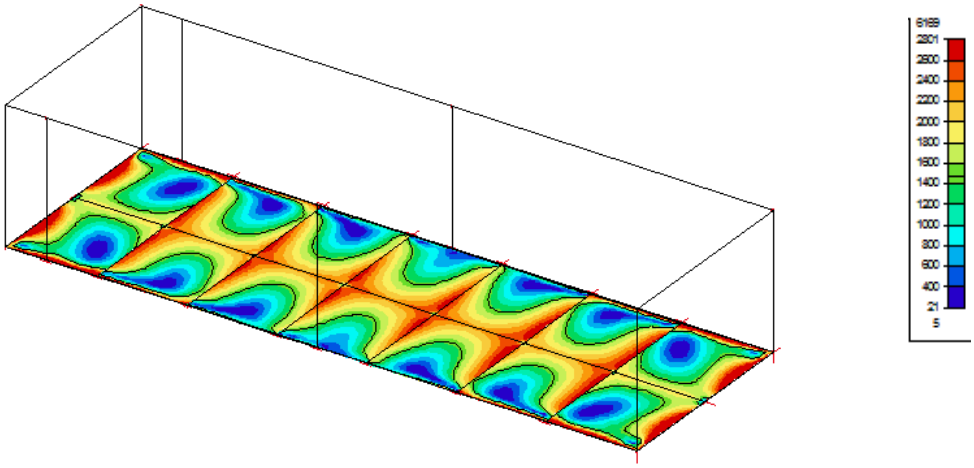

Figure 7.22: *Maximum shear force in the plane of caisson bottom slab*

An important comment has to be made about the maximum shear resistance of concrete. According to the Eurocode concrete has a resistance of $V_{Rd;c} = 1477$ kN/m, the shear resistance per unit width is dependent on the height of the concrete slab. In previous engineering codes the shear resistance of concrete was independent on the height of the concrete. A maximum shear stress of $\tau_c = 0.56$ N/mm^2 could then be used. For a 5000 mm thick slab the maximum resistance was $V_{Rd;c} = 0.56 \cdot 5000 = 2800$ kN/m. This is almost twice as much. In this scenario only 10– to 20% must be reinforced against shear forces.

7.4.3 ACTING MOMENT ON THE CAISSON WALLS

In table 7.2 the maximum design moments on the caisson walls are given. The x-direction of the walls is defined as the horizontal direction in the extension of the wall and the y-direction is defined as the vertical direction in the extension of the wall. The distribution of the design moments are schematised in figure 7.23 and 7.24 for respectively the x– and y-direction during homogeneous supported conditions. For a distinct view only the half of the results are drawn on the caisson walls. Due reasons of symmetry in the homogeneous supported situation, the results are equal.

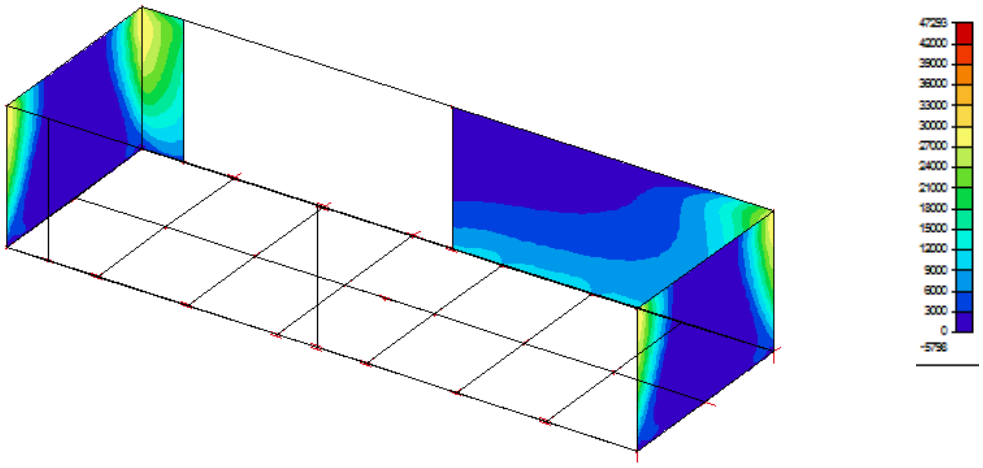

Figure 7.23: *Design moments on the outside of caisson wall for a homogeneous supported caisson in x-direction*

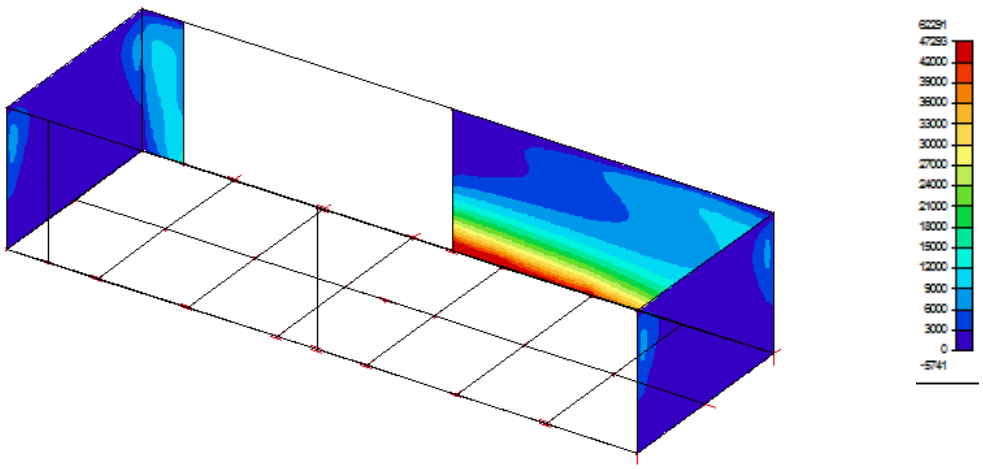

Figure 7.24: *Design moments on the outside of caisson wall for a homogeneous supported caisson in y-direction*

It can be seen that the design moment in horizontal (x–) direction has the largest magnitude at the corners of the caisson. The adjacent walls will prevent any rotation of the wall and ensures that the caisson wall is clamped in between the other walls. This causes a large moment at the supports. In the vertical (y–) direction the wall is clamped in at one side. The presence of the head walls is reducing the rotation and deformation at the upper side of the walls. When the comparison is made with a clamped beam, then it is also apparent from this that the largest moment is present at the supports or lower side of the caisson wall.

7.4.4 DESIGN OF CAISSON WALLS

The thickness of the caisson walls was defined at 3500 millimeter. In table G.3 of the appendix the occurring design moments and tension forces are given for the different scenarios and parts

of the caisson. In table 7.4 a summary of these forces and the proposed reinforcement plan is given.

Table 7.4: *Required reinforcement for a caisson wall with a thickness of 3500 mm*

	Unit	x-	y-	x+	y+
$M_{ed;max}$	kNm/m	33548	41568	16701	14134
$N_{ed;max}$	kNm/m	7887	7534	7887	7534
Location	-	Bottom	Bottom	Top	Top
Reinforcement	-	⌀32-150	⌀40-125	⌀32-150	⌀32-125
# of reinforcement rows	-	8	5	5	3
A_s	mm^2/m	42893	50265	26808	19302
M_{rd}	kNm/m	37993	48755	22803	14707

With the proposed reinforcement plan of table above a total of $\frac{\sum A_s \cdot 1000}{10^9} \cdot 7850/3.5 = 219\ kg/m^3$ of reinforcement steel is required. This is a very large amount of reinforcement. These amount of reinforcement can be explained by the used assumptions.

In figures 7.25 and 7.26 the location of reinforcement is given for respectively the horizontal and vertical direction. The area's of the wall where a positive bending or torsional moment is acting and therefore reinforcement is required are filled in red. A blue color indicates an area where on the given side of the wall in the specified direction no reinforcement is required because only compressive forces are present.

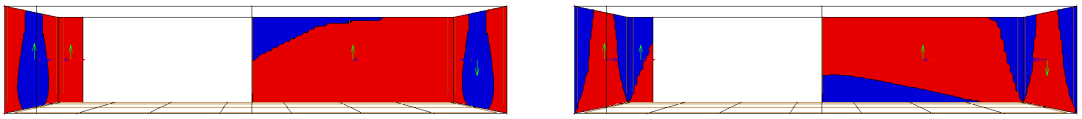

(a) *Outside* **(b)** *Inside*

Figure 7.25: *Location of required reinforcement in horizontal (x–) direction, view in global y-direction)*

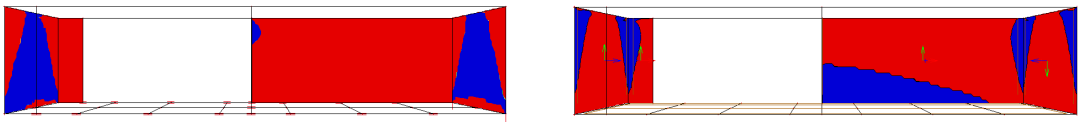

(a) *Outside* **(b)** *Inside*

Figure 7.26: *Location of required reinforcement in vertical (y–) direction, view in global y-direction)*

From the figure it can be concluded that almost all walls must be reinforced on both sides and in both directions. In a normal design assignment, the amount and location of the reinforcement can be optimized and a more specific reinforcement plan can be established. However it is expected that the material profits are low. In the different load cases and scenario's, moments are acting on different places. Therefore larger parts of the structure have to be reinforced.

The caisson walls have to be checked in accordance with the bottom slab on shear resistance. The maximum shear stress the concrete wall can handle is $V_{Rd;c} = 1016$ kN/m according to appendix F.5.2. The locations where this shear force is exceeded are filled in red in figure 7.27. It can be concluded that major part of the caissons must be reinforced against shear forces. These locations are situated around corners, edges or intersections with other structural elements. It is cost efficient to determine the exact location of shear reinforcement further so that no unnecessary reinforcement is used.

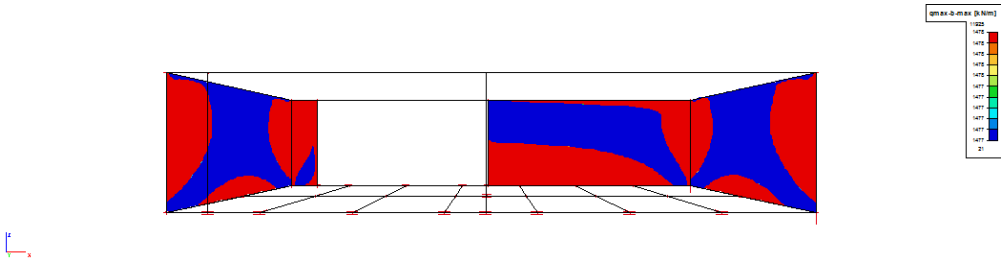

Figure 7.27: *Location were shear reinforcement is required in caisson walls.*

7.4.5 ACTING MOMENT ON THE CAISSONS BULKHEAD

The moments on the outer side of the bulkhead are schematised in figure 7.28 and 7.29 for respectively the x– and y-direction during homogeneous supported conditions.

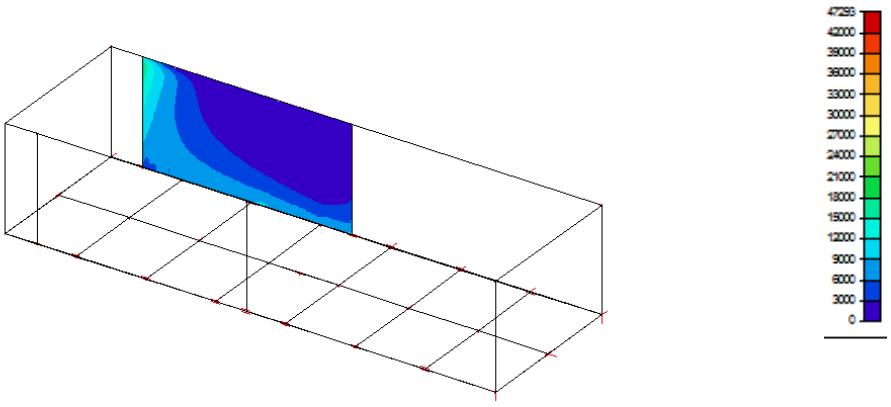

Figure 7.28: *Design moments in bottom plate in x-direction for a homogeneous supported caisson*

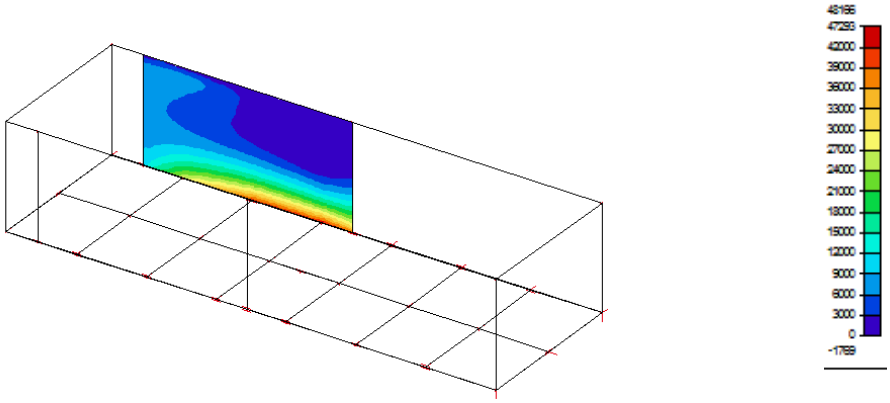

Figure 7.29: *Design moments in bottom plate in y-direction for a homogeneous supported caisson*

The acting moments are showing large similarities with the moments occurring in the caisson walls. Because all specific moments in the bulkheads are smaller than then in the caisson walls the same kind of reinforcement can be used. More important are the specific stresses between the caissons walls and bulkhead and between the caissons bottom slab and concrete. As less as possible reinforcement must been applied between both elements as it makes it difficult to removed the bulkhead afterwards. In figure 7.30 the stresses between caisson wall and –bulkhead are given.

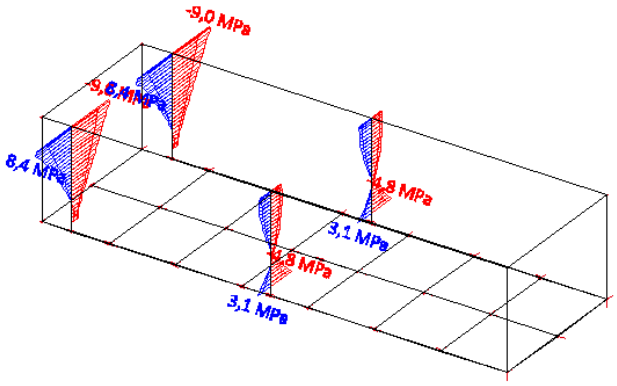

Figure 7.30: *Stresses between caisson wall and –bulkhead*

It can be seen that the tension stresses, up to values of 8.4 N/mm^2, are larger then the tensile force concrete can handle, $f_{ctm} = 3.2$ N/mm^2 for C35/45. Reinforcement is therefore required in the connection between bulkhead and caisson wall.

7.4.6 COMPARISON WITH TWO-DIMENSIONAL RESULTS

Primarily the deflection of the different parts of the caisson are checked for all individual load cases, load combinations and soil schematisations. In the symmetrical soil schematisations the

moment distribution and deflections are showing also symmetrical behavior. The results from the three-dimensional calculations given in table 7.2 can be compared with the results achieved from the simplified two-dimensional calculations from appendix F.3. The differences between the moments are compared according to:

$$\frac{M_{3d}}{M_{2d}} \times 100\% \tag{7.11}$$

The (maximum) moment in the caisson wall has a value between $M_{3d,wall,inside} = -16701$ kNm and $M_{3d,wall,outside} = 33548$ kNm. In the simplified calculations a bending moment of $M_{2d,wall} = 52227$ kNm was calculated which was independent of the soil schematisation. The calculated moment in three dimensions is just only 63% of the moment calculated in the simplified situation. This is explicable because in reality the moment distribution in the caisson is dependent on three-dimensional effects. In the three dimensional model also moments are occurring in the caisson wall in the horizontal direction. This is also explainable because the walls are clamped in between the other walls, this effect was not taken into account in the simplified calculations.

In the moment distribution of the caisson bottom slab is more variation. In x-direction the moments calculated in the three dimensional case are in the range of 80% – 105% of the moments calculated in the simplified two-dimensional case. In y-direction the differences are something larger but still in the range 50%–155% which are plausible because of the large simplifications in the two-dimensional calculations.

7.4.7 INFLUENCE OF SUPPOSED SOIL SUPPORTS

In the previous section an assumption is used to schematize the influence of the different soil layers on the caisson. A maximum difference in soil stiffness of $\lambda = 5$ was used for the calculations. In figure 7.31 the influence of λ on the moment distribution in the caisson bottom slab is given. The dashed line indicates the maximum design moment from table 7.2 derived with $\lambda = 5$ which is used in the calculations. From the figure it can be concluded that in the case of a sagging moment in the caisson, a higher differential stiffness of the soil does increase all design moments on both sides of the bottom slab and in both directions for an additional 17%–30%. By a larger hogging moment, the moments are increased to a much lesser extent.

In appendix G.3 new calculations are performed with the adjusted occurring design moment. It turns out that on the underside of the bottom slab extra layers of reinforcement are required. It can be concluded that by placing extra reinforcement it is possible to enlarge the resistance of the concrete in that extent that the total acting forces and moments can be resisted by the cross-section without modification of the (internal-) dimensions of the caisson. In figure 7.32 the results for the caisson wall are plotted. From the figure it can be concluded that the distribution of soil stiffness below the caisson has far less influence to the moment distribution in the caisson walls. An increase in stiffness difference can only increase the design moments by an additional 4%–6%.

7.4.8 INFLUENCE OF INTERNAL DIMENSIONS

For the design of the lock head the same internal dimensions are applied as used for the lock head of the Deurganckdok lock. In this section the influence of the internal dimensions on the moment distribution is elaborated.

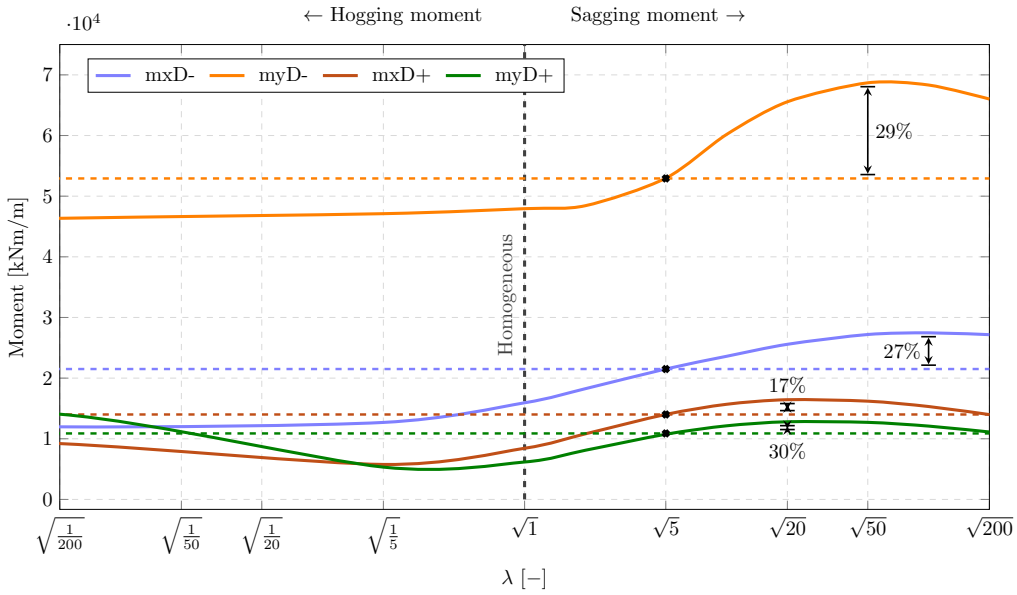

Figure 7.31: *Influence of λ on moment distribution of caisson bottom slab. On the left side of λ = 1 a hogging moment is present, on the right side of λ = 1 a sagging moment is present (Logarithmic scale)*

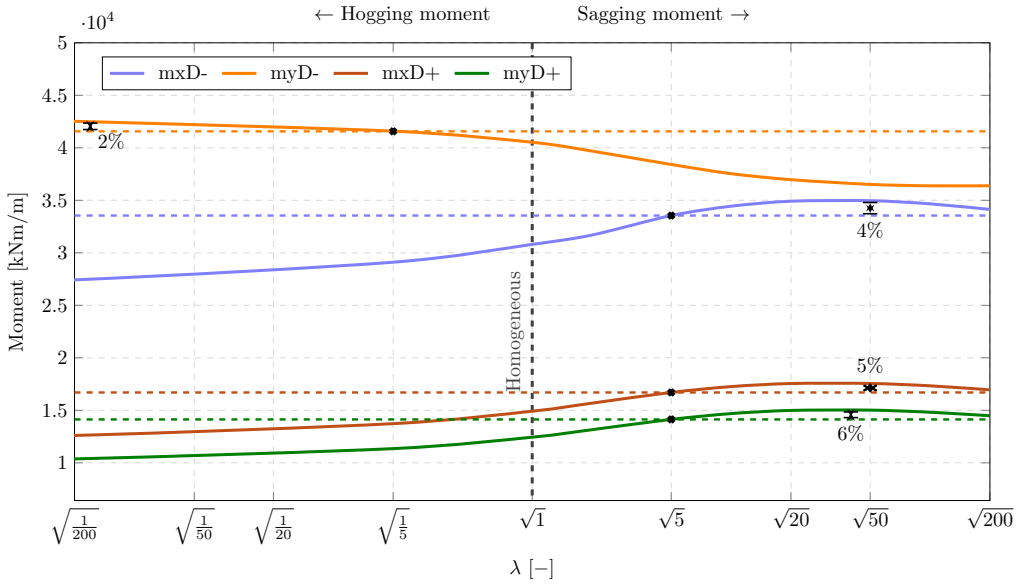

Figure 7.32: *Influence of λ on moment distribution of caisson walls. On the left side of λ = 1 a hogging moment is present, on the right side of λ = 1 a sagging moment is present (Logarithmic scale)*

The caisson is a statically indeterminate structure. This means that the moment distribution in the caisson is dependent on the stiffness of the different structural elements. Hereby it is not possible to modify the internal dimensions of the elements without a complete analysis of the structure on the renewed moment distribution and the altered resistance of the concrete against

tension forces and bending moments. A reduction in height in, for example, the caisson bottom slab can increase the design moments in the caisson wall.

In figure 7.33 the effect of a reduction of the wall thickness is plotted. The maximum occurring moment in both the x– and y-direction from table 7.4 are plotted. The design moment is decreasing by a smaller wall thickness, which is explainable by the decrease in stiffness. The maximum design moment is located at the intersections of the caisson wall with the other adjacent walls and the bottom slab. These intersections are acting as clamped supports. Due to the decreasing stiffness in the structure larger deformation are possible and thereby causes a decrease in the occurring moment.

Due to a decrease of the wall thickness the resisting moment, M_{rd}, of the reinforced concrete element will also decrease. The figure shows that the resisting moment decreases faster than the occurring design moment. The maximum resistance moment is based on the thickness of the caisson wall, height of the concrete compressive zone, reinforcement distribution and maximum reinforcement ratio. Due to the dependency of the effective depth, d, and thereby the dependency in x– and y-direction another maximum resistance moment can be found. The maximum resistance moment for the original cross-section can be found in table 7.4. The resisting moment and reinforcement plan for the reduced structural parts are given in the figure. It appears that a wall thickness of 3000 mm with the current used assumptions and boundary conditions is not possible. A minimal wall thickness of $\pm$ 3400 mm is required. To be sure, the bulkhead and bottom slab have to be analysed when a wall thickness of 3400 mm is used.

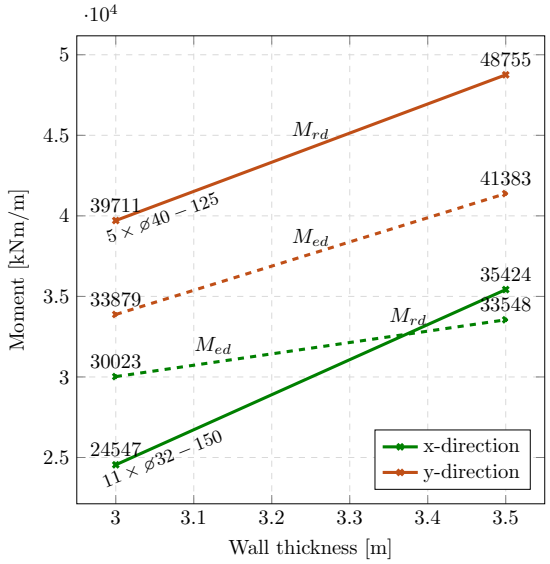

Figure 7.33: *Influence on the moment distribution as result of a reduction of the thickness of the caisson walls*

In figure 7.34a the effect of a reduction in height on the caisson bottom slab is plotted. In this situation the self-weight of the bottom slabs reduces. However, in order to achieve subsidence of the caisson extra ballast is required. Thereby the total load is equal and must be transmitted by a smaller cross-section. In the same manner as described above the stiffness of the structure is reduced. Due to this reduction larger deflections are possible which caused indirectly a reduction of the fixed moment at the intersections between the bottom slab and the caisson walls. In figure 7.34 the effect of a reduction on the height of the bottom slab are plotted for both the caisson

bottom slab itselfs as well as for the caisson walls. Due to a constant cross-section of the wall, the resistance moment $M_{rd;wall}$ remains equal. From figure 7.34 it can be concluded that the height of the bottom slab can be reduced to 4.3 m. Only in that case $M_{ed;wall} \leqslant M_{rd;wall}$. When for a specific reason the height of the bottom slab must be reduced further, the thickness of the walls must be increased in order to resist the design moments and tension forces. However, this will result in shifting concrete volume to other structural parts instead of a decrease in concrete volume.

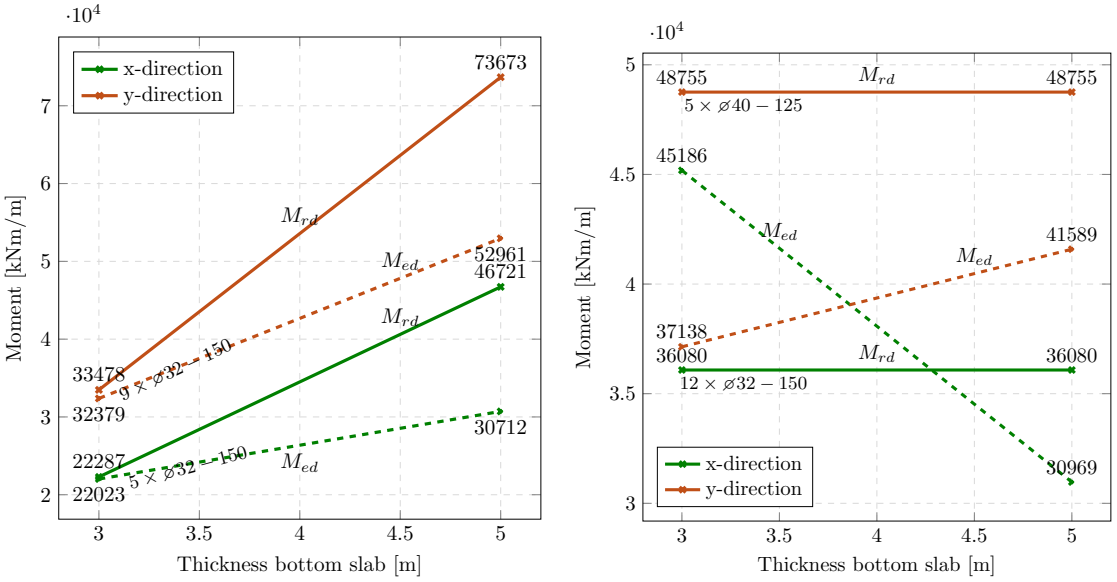

(a) *Moment distribution in caisson bottom slab*

(b) *Moment distribution in caisson wall*

Figure 7.34: *Influence on the moment distribution as result of the reduction in height of caisson bottom slab*

When a further reduction of the internal dimensions is desired, pre-stressed concrete can be used in order to increase the moment resistance.

7.4.9 MEASURES TO REDUCE AMOUNT OF REINFORCEMENT

In tables 7.3 and 7.4 a reinforcement plan for respectively the bottom slab and walls was proposed. Multiple layers of reinforcement bars in different directions are required. The reinforcement bars are placed close to each other to obtain a feasible design. This complicates the flow of concrete during the casting process. In practice this reinforcement design causes problems. Not only the casting process is inconvenient. Due to the large number of reinforcements bars and stirrups intensive handling of these reinforcement components are needed on the building site. This handling require many cranes and other heavy equipment. Also on top of the bottom slab at a height of 4–5 meter many reinforcement bars and stirrups are required. Many rebar spacers and frames are required to put and hold these elements into position. This is technically feasible but not desirable. It should be examined whether the amount of reinforcement can be reduced. This can be establish in different ways.

- The use of prestressed concrete

- Increasing the thickness of the concrete elements

PRESTRESSED CONCRETE

In conventional reinforced concrete the tensile strength of reinforcement steel is combined with the compressive strength of concrete to obtain a strong building material in both compression and tension.

The principle behind prestressed concrete is that compressive stresses induced by high strength steel tendons in a concrete member before loads are applied will balance the tensile stresses imposed in the member during service. [Manufacturers, 2015] By the introduction of prestressed tendons inside the concrete the amount of reinforcement can be reduced.

INCREASING THE THICKNESS OF THE CONCRETE ELEMENTS

A second option is to increase the height of the concrete elements. Due to the increase in height the internal lever arm from the center of the cross-section towards the reinforcing steel increases. As a result less reinforcement is required. Because the resistance moment is quadratically dependent on the height of the concrete element. The increase of self-weight will not be a limiting factor.

7.5 ROTATION OF THE CAISSON AND THE RESULTING INCREASED HORIZONTAL PRESSURE.

The caisson can rotate due irregularities in the soil composition or the load distribution of the caisson. The caisson can rotate on either the x, y and z-direction. By means of the large quantity of soil that has to be displaced the rotation in z-direction is negligible small. In figure 7.35a and 7.35b the rotation in the different directions is given.

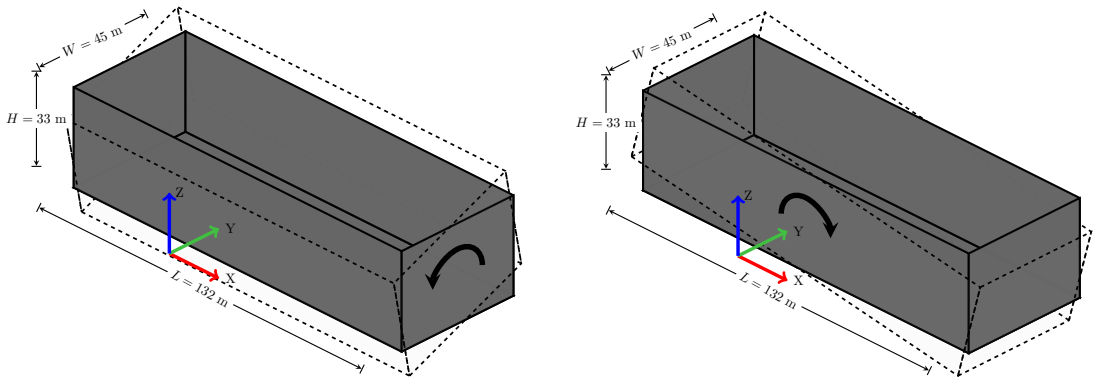

(a) *Rotation of the caisson over the short side (x-direction)*

(b) *Rotation of the caisson over the long side (y-direction)*

Figure 7.35: *Rotation of the caisson in different directions*

De rotation in x– and y direction will be elaborated. During the construction of the cutting edges and bottom slab of the caisson at surface level all outer forces are in equilibrium and hence the external moment is zero: $M_{caisson} = 0$ and there is no rotation. During subsidence of

the caisson a rotation of the caisson may occur due to the uneven bearing capacity of the cutting edges or an unequal excavation of the working chamber as schematised in figure 7.36.

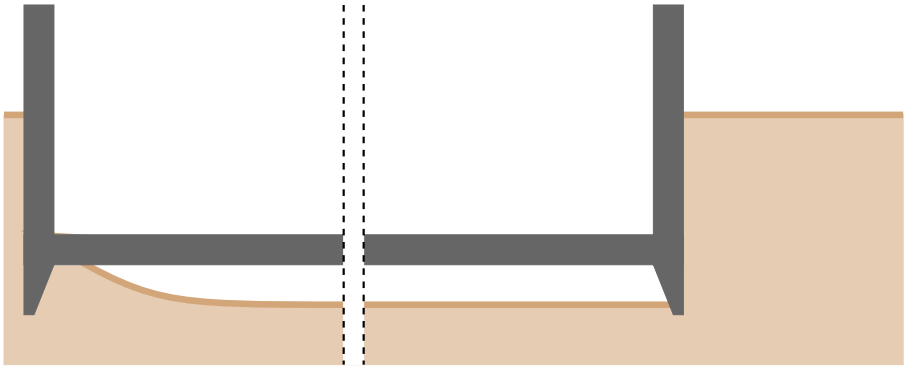

Figure 7.36: *Unequal excavation of the working chamber*

When the bearing capacity on one side in not sufficient to resist the caisson, this can be caused by the irregularities in the soil composition or the excavation on one side of the caisson, a rotation will occur. On that moment not all external forces are in equilibrium, $M_{caisson} \neq 0$, the caisson will come in a tilted position and will lean against the soil as schematised in figure 7.37. Due to the rotation a horizontal displacement will occur. The largest displacement occurs at the top of the construction. At the cutting edges of the caisson the horizontal displacement is zero.

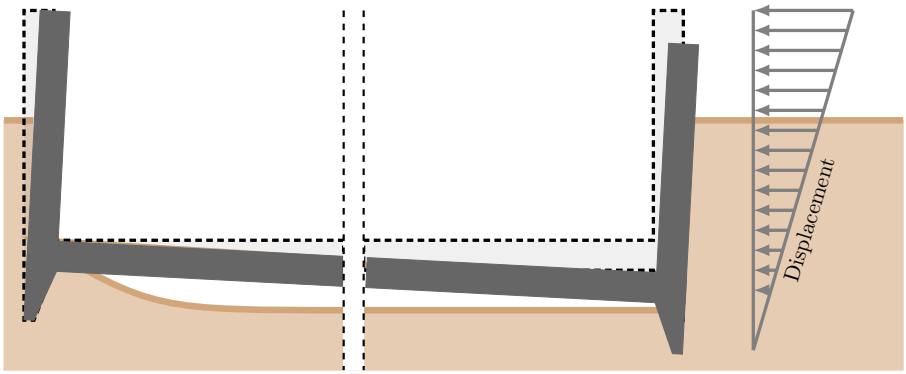

Figure 7.37: *Inclination of the caisson*

Due to the compression of the soil body an extra horizontal force will act on the caissons wall. This horizontal soil pressure is locally higher than the neutral ground pressure and may even be passive. It is assumed that the soil pressure is directly proportional to the horizontal displacement, limited by the maximum passive soil stress. Due to this increase in soil stress a new equilibrium $M_{caisson} = 0$ occurs. The requirement on a differential settlement is set at 1:300 with the horizontal [NEN 6740][2].

The most unfavourable conditions which can cause a rotation of the caisson arise when: [Bongers and Haterd, 1995].

2 The norm of an uneven settlement of 1:300 is officially intended for residential environments but in this case also assumed for the pneumatic caissons because of the small tolerances required due to the water retaining function.

- During the first stage of subsidence of the caisson. When soil in the working chamber is increasingly removed from the center of the caisson towards the cutting edges. At that moment there is no increased air pressure and the total weight of the caisson is resting on the cutting edges.
- In the last stadium when the caisson is at its final depth and the pressure in the working chamber is removed. The weight of the caisson and ballast is then quite suddenly transferred from the air pocket to the cutting edges. When the bearing capacity at one side of the caisson is significantly different on the other side an inclination can appear.

In the next case the situation is analysed when half of the caisson is subsided into the ground. The situation has been analyzed for the cross-section in y-direction. The caisson has a total height of 33 meter. During the moment halfway the subsidence process, the caisson is at a depth of $\frac{1}{2} \cdot 33 = 16.5$ m. At the lowest point of the caisson, at the cutting edge, the neutral earth pressure predominates. Halfway the subsided part there is a kink in the stress diagram of figure 7.38. Above this point the maximum passive soil stress predominates, below this point the maximum soil stress is restricted by the displacement of the caisson. The situation halfway the subsidence process is analysed because below this point settlements are not expected anymore because the caisson is already clamped in for the largest part. In this case a vertical differential settlement of $1:300 = \frac{45}{300} = 0.15$ m is used to perform the calculations. The horizontal displacement $w(z)$ is thereby:

$$w(z) = \underbrace{15}_{\text{Differential settlement}} / \underbrace{45}_{\text{Width caisson}} \times \underbrace{\frac{1}{2} \cdot 33}_{\text{Height caisson}} = 5.5 \text{ cm} \tag{7.12}$$

The neutral soil stress at a depth z is defined according to equation 7.13.

$$\sigma_{neutral}(z) = K_n(z) \times \sigma_{eff}(z) = (1 - \sin(\theta(z))) \times \sigma_{eff}(z) \tag{7.13}$$

The passive soil stress at depth z is defined following equation 7.14.

$$\sigma_{passive}(z) = K_p(z) \times \sigma_{eff}(z) = \frac{(1 + \sin(\theta(z)))}{(1 - \sin(\theta(z)))} \times \sigma_{eff}(z) \tag{7.14}$$

The unrestricted maximum force as result of the rotation is defined as:

$$\sigma_{rotation}(z) = \sigma_a(z) + k_h \times w(z) \tag{7.15}$$

Where k_h is the modulus of subgrade reaction. A value of $k_h = 5000$ kN/m^3 is used. The maximum force is restricted by the passive soil stress. The maximum force as result of rotating of the caisson can not be larger than the passive soil stress.

$$\sigma_{horizontal} = \begin{cases} \sigma_{passive} & \text{if } \sigma_{rotation} > \sigma_{passive} \\ \sigma_{neutral} & \text{if } \sigma_{neutral} > \sigma_{rotation} \\ \sigma_{rotation} & \end{cases} \tag{7.16}$$

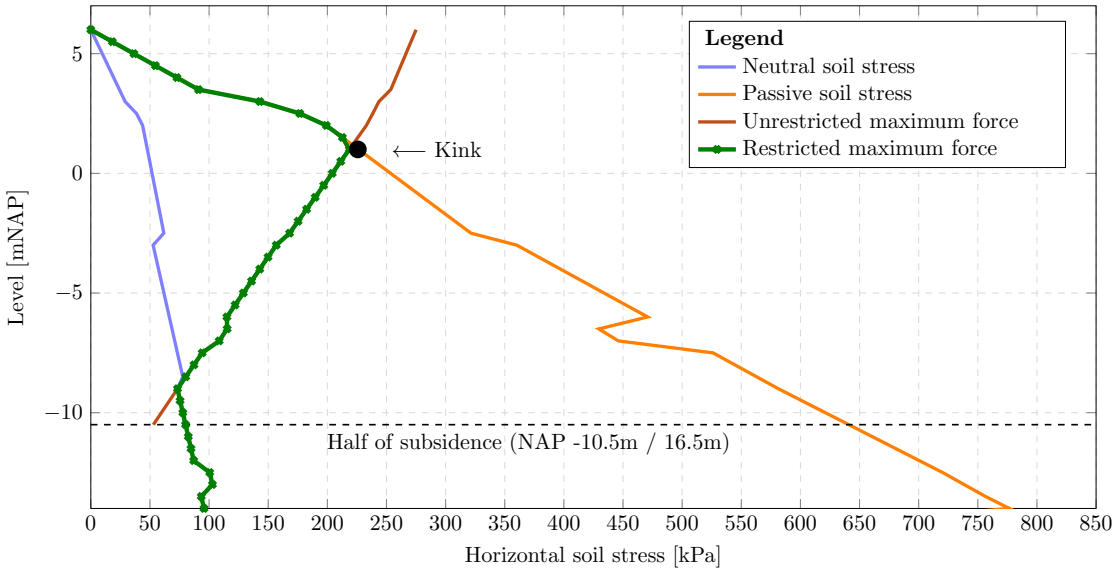

Figure 7.38: *Horizontal soil stress on caisson due to rotation*

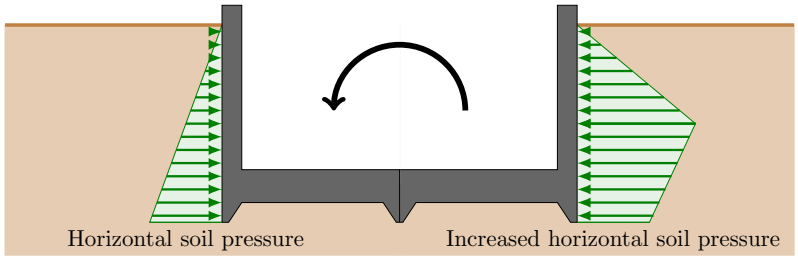

Figure 7.39: *Inclination of caisson with associated extra horizontal load*

COUNTERACTING ROTATING OF THE CAISSON

A rotation of the caisson must be prevented. The following options are used to counteract the rotation or inclination of the caisson:

- Permanent and predetermined options, for example increasing the number of compartment walls, hereby the effect of unequal excavations in the working chamber will be decreased. Another option is relocating the ballast when instead of sand, fixed units of ballast are used which are easy to displace.
- The most common solution is the excavation on the other side from the caisson as seen from the place with the largest subsidence.

The effect of an unequal excavation of the working chamber is elaborated in appendix F.6.

8

VARIANT 2 - TWO CAISSONS WHICH ARE SUBSIDED INDIVIDUALLY AND DIVIDED INTO SEVERAL COMPARTMENTS

The second variant concerns the construction of two separate caissons. One large caisson is containing the gate chamber and another smaller caisson is covering the gate recess. Both caissons are connected with a large bottom slab or normal caisson whereupon the guiding equipment for the lock gates can be connected. Due to the subdivision of the caisson in multiple compartments also each caisson requires it's own air– and soil discharge shafts as well as more equipment to control the air-pressure.

This chapter starts with an explanation of all internal and external dimensions in section 8.1. Subsequently in section 8.2 the process of subsidence and all corresponding forces are elaborated. In section 8.3 the structural assumptions for this design are elaborated and in section 8.4 calculations are performed to get insights in the order of magnitude of occurring forces and moments. Then, in section 8.6 the horizontal and rotational stability of both caissons is considered. The chapter concludes with section 8.5 where the connection between both pneumatic caissons is elaborated.

8.1 DIMENSIONS OF THE CAISSON

In figures 8.1–8.3 the dimensions of the 3D schematisation are given for respectively the x–, y– and z-direction. In figure 6.10 a three dimensional schematisation of the caisson was given as well as the direction of the coordinate system.

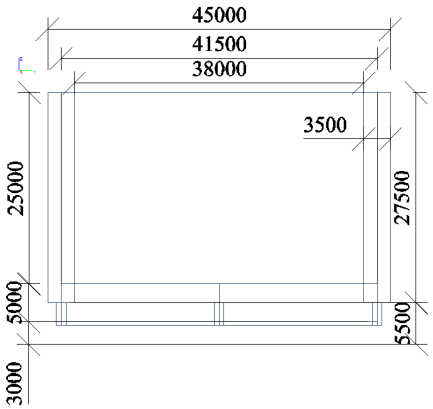

Figure 8.1: *Dimensions in the yz-plane*

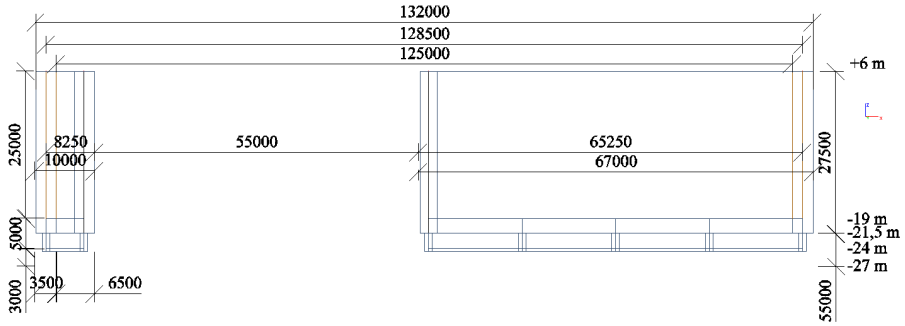

Figure 8.2: *Dimensions in the xz-plane*

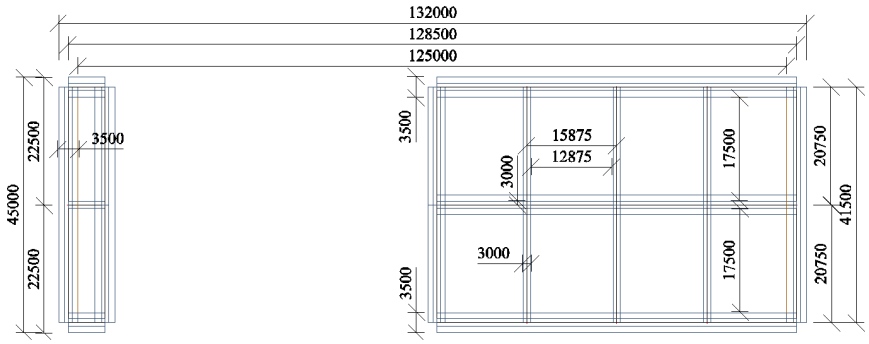

Figure 8.3: *Dimensions in the xy-plane*

8.2 PROCESS OF SUBSIDENCE

In section 7.2 the subsidence of the pneumatic caisson from the first construction alternative was described. In the same way the subsidence of the two caissons for the second variant can be elaborated. The equation for the net force on the caisson was given as:

$$F_{net}(w_{ce}) = F_{selfweight} - [F_{friction} + F_{air}(w_{ce}) + F_{bearing}(w_{ce})] \tag{8.1}$$

The self-weight of the caissons at surface level are calculated in appendix F.1. Due to the presence of groundwater the submerged weight of the caisson will decrease over depth because larger parts of the construction are situated below the groundwater table. The submerged weight of both caissons from the second variant are given in figure 8.4

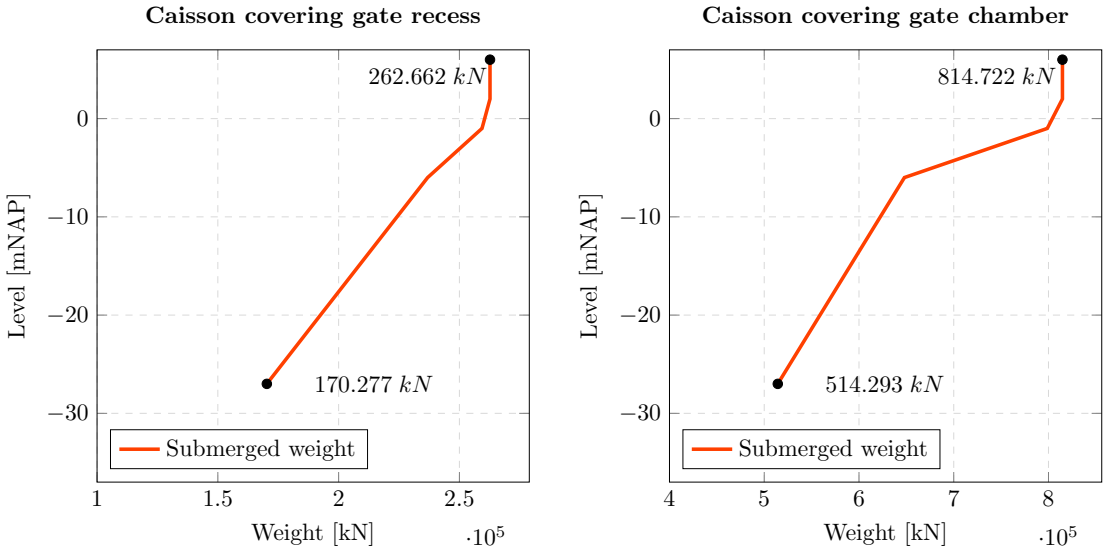

Figure 8.4: *Submerged weight of the caissons*

As can be expected from the results from the previous chapter for the calculations of the first construction alternative it is not possible to construct the caissons at surface level and subside them to the desired depth without additional measures. At the begin of the process of subsidence the downward directed loads are too large and in the meantime the downward directed loads are too small at the end of the process of subsidence. Therefore for both caissons the same measures as taken in the previous chapter are taken:

- Constructing the caisson in different phases.
- Use of ballast weight.

SMALL CAISSON COVERING GATE RECESS

The bottom slab, compartment walls and cutting edges are constructed and submerged to a depth of NAP -3 meter. After the lowest point of the cutting edge has reached this depth the walls of the caissons as well as the bulkhead can be constructed. At a depth of NAP -22 m the potential upward directed forces are larger than the downward directed loads and ballast is required to achieve further subsidence of the caisson. Every meter the caisson has to be subsided below this level 30 centimeters of ballast sand is required.

LARGE CAISSON COVERING GATE CHAMBER

The second caisson of this construction alternative is larger than the first caisson. Because the weight of the caisson walls is better divided over the total surface area the acting stress from the caisson on the soil is smaller. Therefore the walls and bulkhead can be constructed when the other parts of the caisson have reached a level of NAP -1 meter. From a level of NAP -13 m, 100 centimeter of ballast-sand is required to achieve an additional meter of subsidence. This is schematised in figure 8.5.

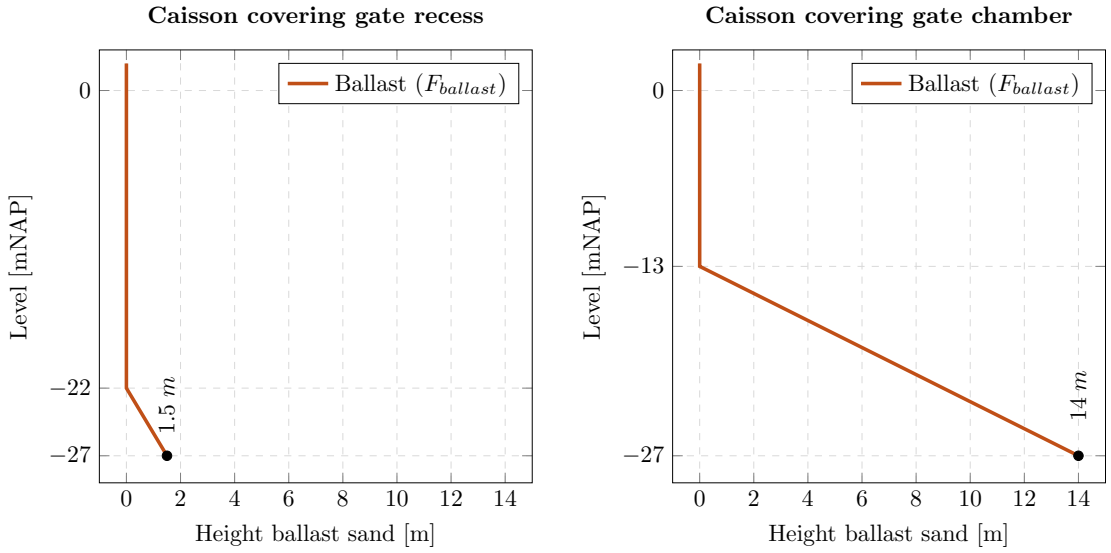

Figure 8.5: *Required amount of ballast sand*

All loads during every stage of subsidence are all known. The friction forces and upward directed load from the air pressure in the working chamber are all elaborated in section 6.4. In the previous paragraph the quantity of the self-weight and ballast are elaborated. Only unknown force is the bearing capacity of the soil which was dependent on the surface area of the foundation, which was in turn dependent on the width of the cutting edge. In figure 8.6 and 8.7 the original width of the cutting edges without any measures as well as the new width of the cutting edge are given for respectively the smaller and larger caisson. The calculations are given in appendix F.2.

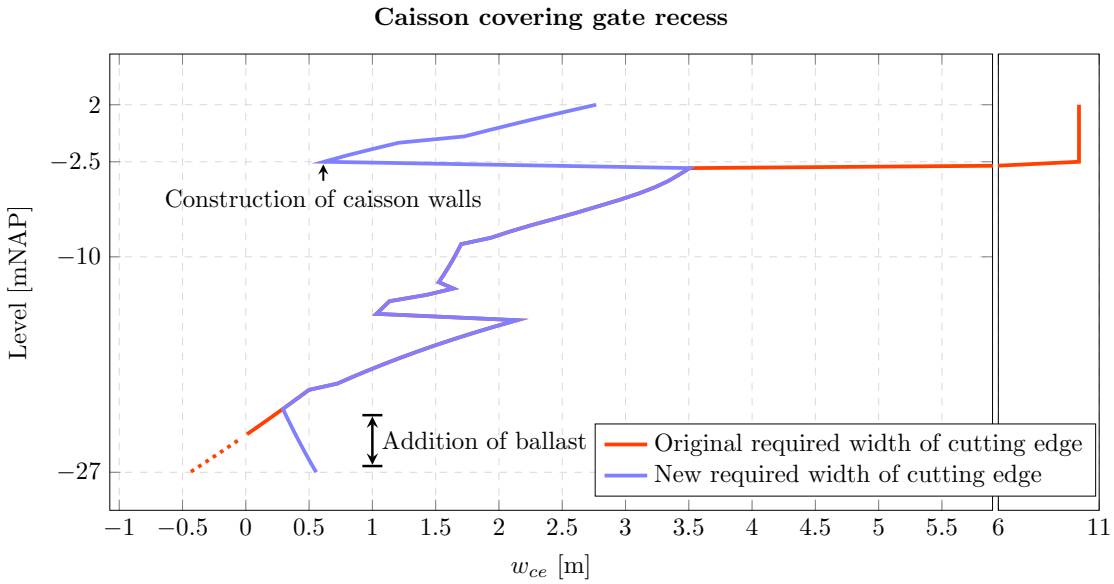

Figure 8.6: *Calculated width of the cutting edge for caisson covering the gate chamber*

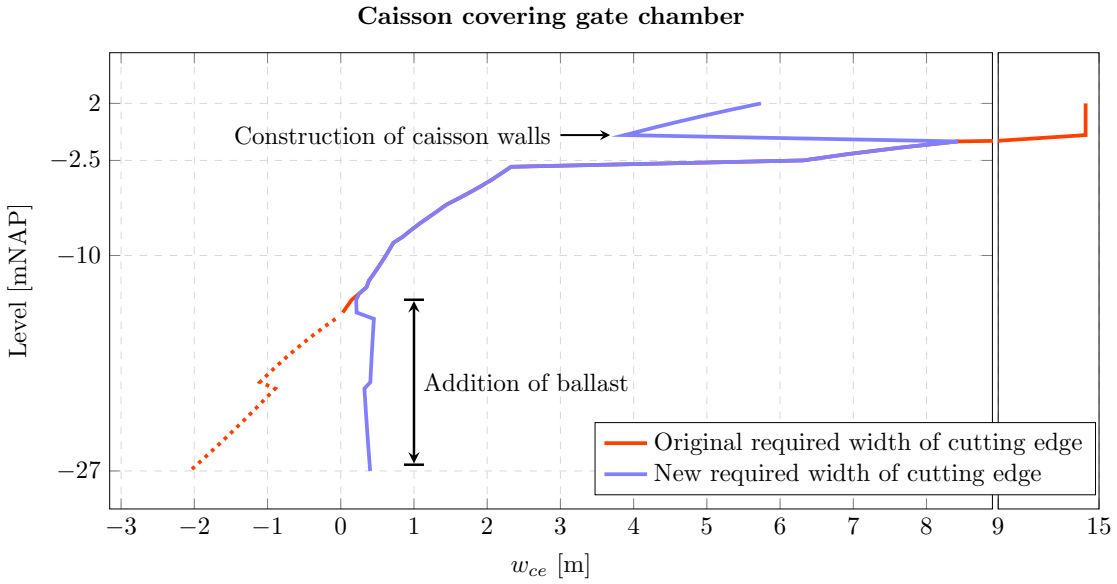

Figure 8.7: *Calculated width of the cutting edge for caisson covering the gate recess*

8.3 STRUCTURAL DESIGN OF THE CAISSON

The construction of this variant has a lot of similarities with the previous variant. The caissons will be built on the same location and hence the same soil conditions are applying. The construction will be supported on the same linear soil springs with an average stiffness of $k_{gem} = 27.4\ MN/m^3$ as explained in section 7.3.1. The modulus of subgrade reaction is varying over distance. Because it was difficult to determine the exact value, it was assumed that the values are varying between $\frac{k}{\sqrt{5}}$ and $k \cdot \sqrt{5}$. The difference between the lowest value and the highest value was thereby defined by a factor 5. Therefore the same spring support distribution as in the previous chapter will be used. The distribution of the springs is given in appendix F.4.

This variant will be analysed on the two governing load combinations as explained in section 7.3.2. The first load combination with maximum soil and ballast loads in combination with the presence of a bulkhead and a second load combination which represents the situation during the lifetime of the caisson. Possible influences from the lock chamber and/or ship passages (for example collision forces) are not taken in to account.

8.4 FEASIBILITY OF THE CAISSON

The four moments elaborated in the previous section for the first variant are also elaborated for the second variant. The results are given in table 8.1.

Table 8.1: *Maximum design moments in caisson*

Part	**mxD-** [kNm/m]	**mxD+** [kNm/m]	**myD-** [kNm/m]	**myD+** [kNm/m]
Gate recess				
Bottom slab	30135	17483	11501	20205
Wall slab	11834	8927	12308	6814
Bulkhead	8153	6805	8252	9700
Gate chamber				
Bottom slab	11292	25403	8022	6186
Wall slab	24501	23882	13886	11486
Bulkhead	20602	4221	9259	5081

will be elaborated, starting with the caisson bottom slab, followed by the caisson walls and bulkhead.

8.4.1 DESIGN OF CAISSON BOTTOM SLAB

The values for the different kind of soil reactions are given in table G.6 for the caisson corresponding to the gate recess and table G.7 for the caisson corresponding to the gate chamber. The moments on the lower side of the bottom slab are schematised in figure 8.8 and 8.9 for respectively the x– and y-direction during homogeneous supported conditions.

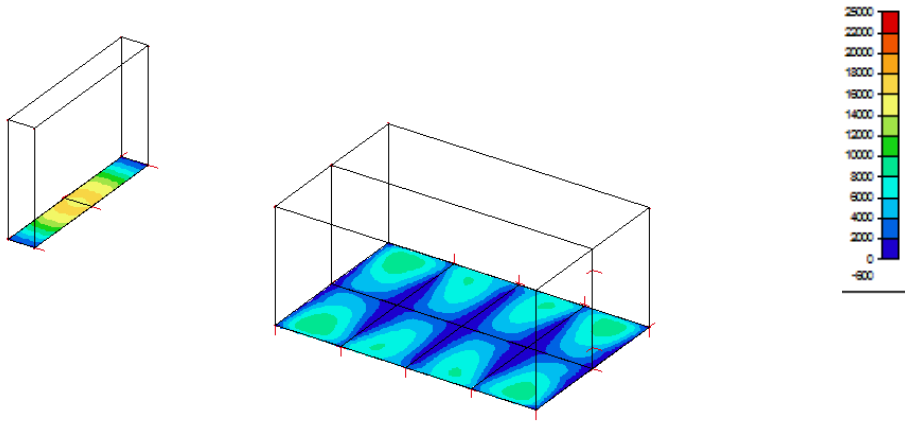

Figure 8.8: *Reinforcement moments in bottom plate in x-direction for a homogeneous supported caisson*

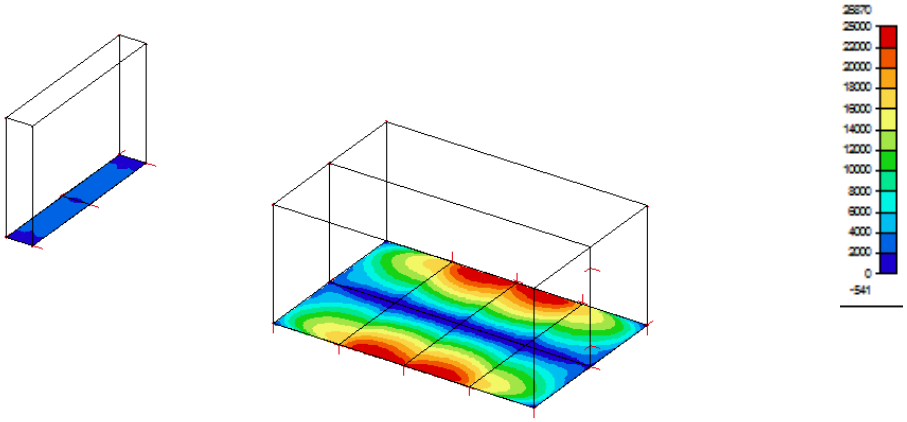

Figure 8.9: *Reinforcement moments in bottom plate in y-direction for a homogeneous supported caisson*

As can be seen in the appendix the occurring moments in this second variant are considerably smaller than the occurring moments in the first variant as seen in 7.3. In table 8.2 a summary of the used reinforcement is given. The proposed reinforcement plan has been derived from the maximal occurring moment. As result of the smaller moments in the bottom slab also less reinforcement is required.

Table 8.2: *Required reinforcement by a bottom slab thickness of 5000 mm*

	Unit	**mxD-**	**myD-**	**mxD-**	**myD+**
$M_{ed;max}$	kNm/m	11299	25403	6096	6186
$N_{ed;max}$	kNm/m	3372	8069	3372	8069
Location	-	Bottom	Bottom	Top	Top
Reinforcement	-	⌀32-150	⌀32-150	⌀32-150	⌀32-150
# of reinforcement rows	-	2	5	2	3
A_s	mm^2/m	10723	26808	10723	16085
M_{rd}	kNm/m	14110	34341	14110	13540

A total of $\frac{\sum A_s \cdot 1000}{10^9} \cdot 7850/5 = 101\ kg/m^3$ reinforcement steel is required.

SHEAR FORCES

In the caisson bottom slab large shear forces are occurring. The maximum shear resistance of the concrete without the use of stirrups was calculated in appendix F.5.2. The maximum resistance was 1477 kN/m in the x-direction. The occurring shear forces in the structure are higher then the maximum capacity of the concrete. In figure 8.10 the part where the maximum shear forces are exceeded are filled in red.

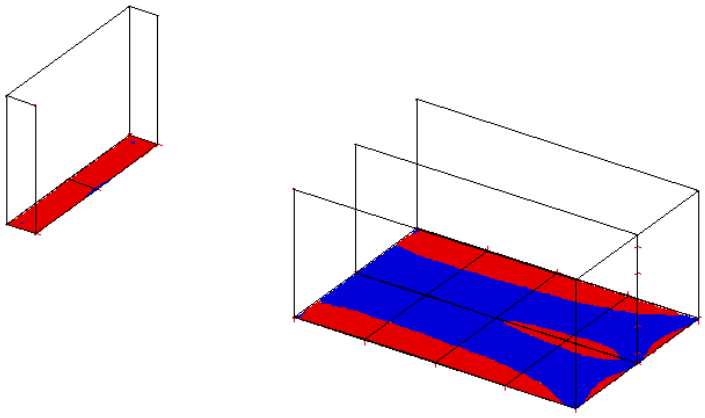

Figure 8.10: *Shear forces in caisson bottom slab*

In comparison with the first variant the shear forces and places where shear reinforcement must been applied are smaller.

8.4.2 DESIGN OF CAISSON WALLS

The values for the different kind of soil reactions are given in table G.9 for the caisson corresponding to the gate recess and table G.10 for the caisson corresponding to the gate chamber. The moments on the outer side of the caisson walls are schematised in figure 8.11 and 8.12 for respectively the x– and y-direction during homogeneous supported conditions.

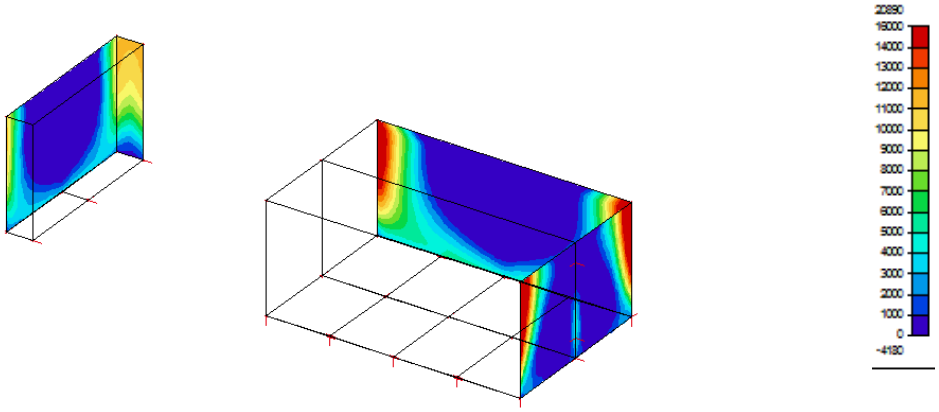

Figure 8.11: *Reinforcement moments in caisson wall for both caissons in x-direction for a homogeneous supported caisson*

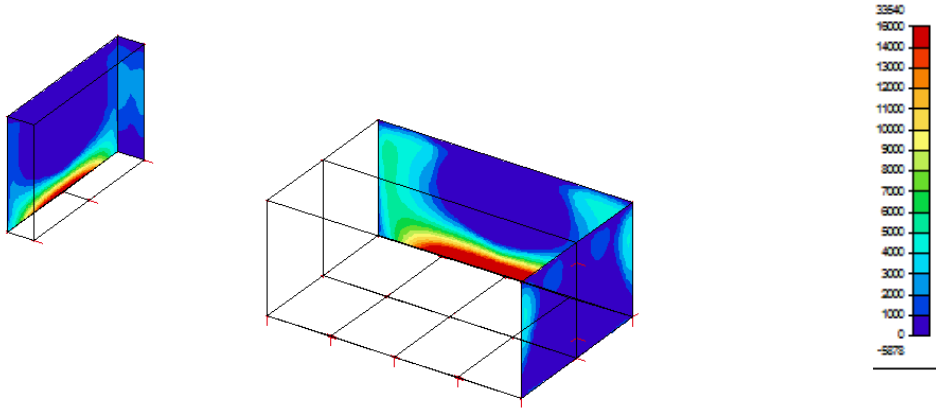

Figure 8.12: *Reinforcement moments in caisson wall for both caissons in y-direction for a homogeneous supported caisson*

In table 8.3 a summary of the used reinforcement is given. The underlying calculations and assumptions were already given in appendix F.5.1.

Table 8.3: *Required reinforcement for a caisson wall with a thickness of 3500 mm*

	Unit	**mxD-**	**myD-**	**mxD-**	**myD+**
$M_{ed;max}$	kNm/m	29968	52922	14005	10880
$N_{ed;max}$	kNm/m	4517	6598	4517	6598
Location	-	Bottom	Bottom	Top	Top
Reinforcement	-	⌀32-150	⌀40-125	⌀32-150	⌀32-150
# of reinforcement rows	-	6	6	3	3
A_s	mm^2/m	32170	60319	16085	16085
M_{rd}	kNm/m	32329	55848	14900	11715

A total of $\frac{\sum A_s \cdot 1000}{10^9} \cdot 7850/3.5 = 196$ kg/m^3 reinforcement steel is required.

SHEAR FORCES

There is a large difference in the way forces are transmitted inside the structure for the case there is a bulkhead or there is no bulkhead present. In figure 8.13 for the two different load scenario's the shear forces are given. The red color indicates that the maximum allowable shear force the concrete can resist is exceeded.

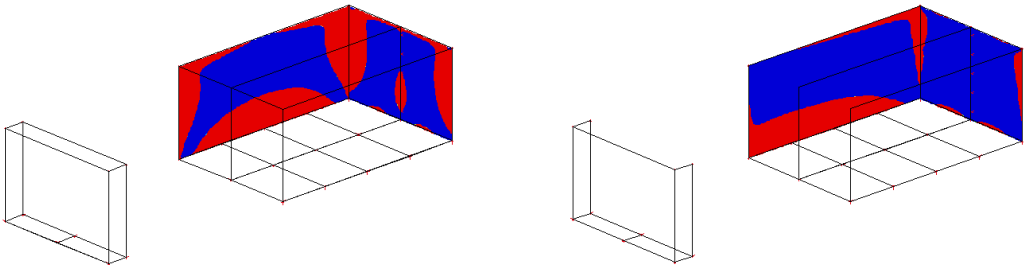

(a) *Shear forces inside caisson wall for load combination 1* **(b)** *Shear forces inside caisson wall for load combination 2*

Figure 8.13: *Shear forces inside caisson wall*

In the figure it can be seen that in the edges and corners the shear capacity of the concrete is exceeded, in the center part of the different sections the shear force is below the shear capacity of the concrete.

8.4.3 DESIGN OF CAISSON BULKHEAD

The values for the different kind of soil reactions for the bulkhead are given in table G.12 for the caisson corresponding to the gate recess and table G.13 for the caisson corresponding to the gate chamber. The moments on the outer side of the bulkhead are schematised in figure 8.14 and 8.15 for respectively the x– and y-direction during homogeneous supported conditions.

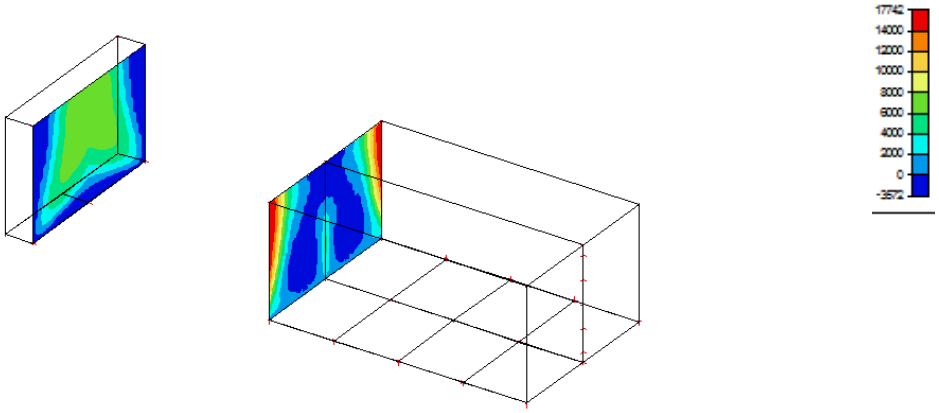

Figure 8.14: *Reinforcement moments in bulkhead in x-direction for a homogeneous supported caisson*

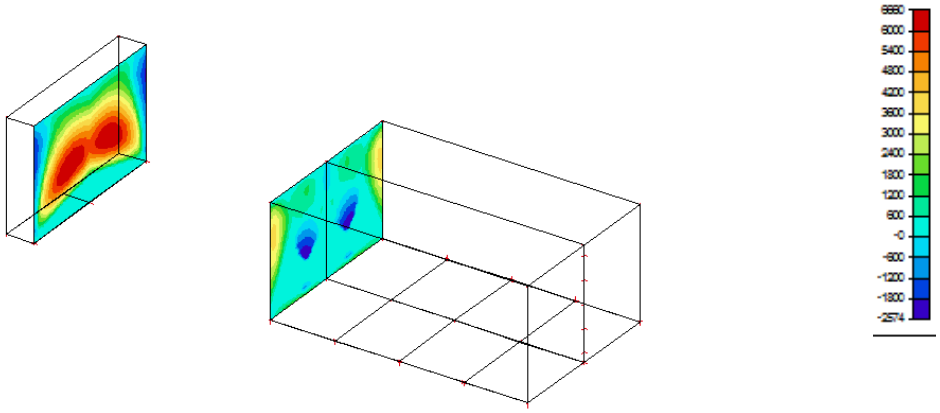

Figure 8.15: *Reinforcement moments in bulkhead in x-direction for a homogeneous supported caisson*

Also in this variant it is important that there is used as less reinforcement as possible as an increase of reinforcement at the corners of the bulkhead does increase the difficulty of removing these. The stresses in the concrete at the intersection caisson wall and –bulkhead are given in figure 8.16.

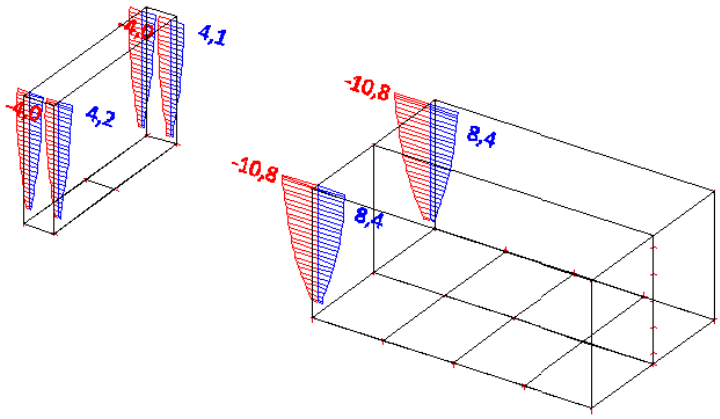

Figure 8.16: *Stresses at intersection caisson wall and –bulkhead (in* N/mm^2*)*

Also here the tension stresses in the concrete are larger than the tensile capacity of the concrete $f_{ctm} = 3.2\ N/mm^2$ for C35/45 so reinforcement is required.

8.4.4 VERIFICATION OF THE RESULTS

In the same way as described in variant 1 the influence of the different soil layers on the caisson will be checked. Also in this case a difference in soil stiffness of $\lambda = 5$ was used for the calculations. In figure 8.17 the influence of λ on the moment distribution in the caisson bottom slab was given. From the figure it can be concluded that the moments in the underside of the bottom slab are reaching it limit value when the caisson is supported on stiff edges and sagging moment acts on the caisson. The increase of moment is in the order of 6%–11%. The moments at the upper

side of the bottom slab are reaching its limit value when the edges of caisson are supported on a weak soil layer. The increase in design moment is in this case in the order 30%–40%.

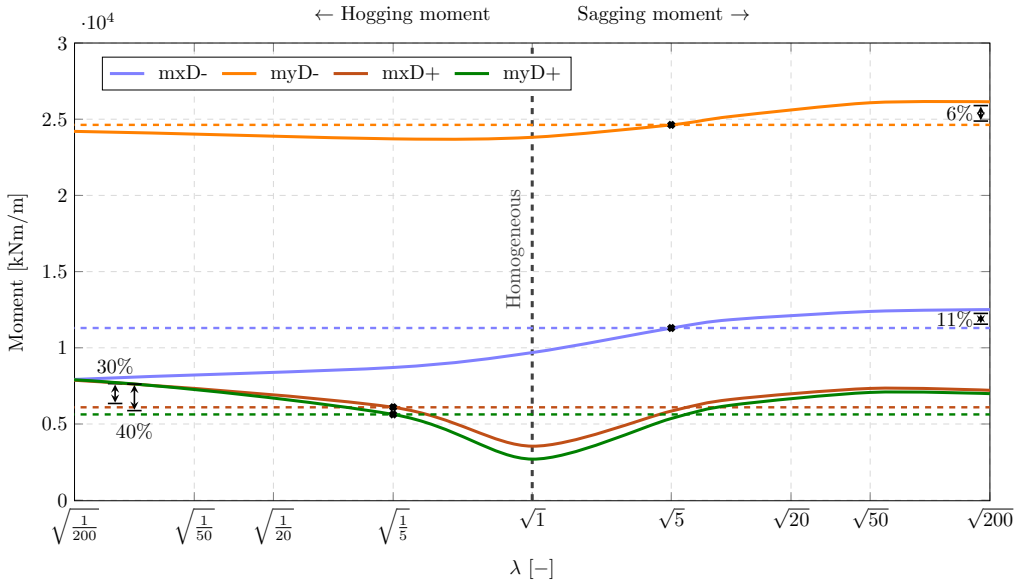

Figure 8.17: *Influence of λ on moment distribution of caisson bottom slab. On the left side of λ = 1 a hogging moment is present, on the right side of λ = 1 a sagging moment is present*

In figure 8.18 the results for the caisson wall are plotted. Also in this case it can be concluded that in a normative situation where the stiffness of the soil is distributed in the most unfavourable way the moment in the caisson can increase further to an extent of approximately 4%–5%.

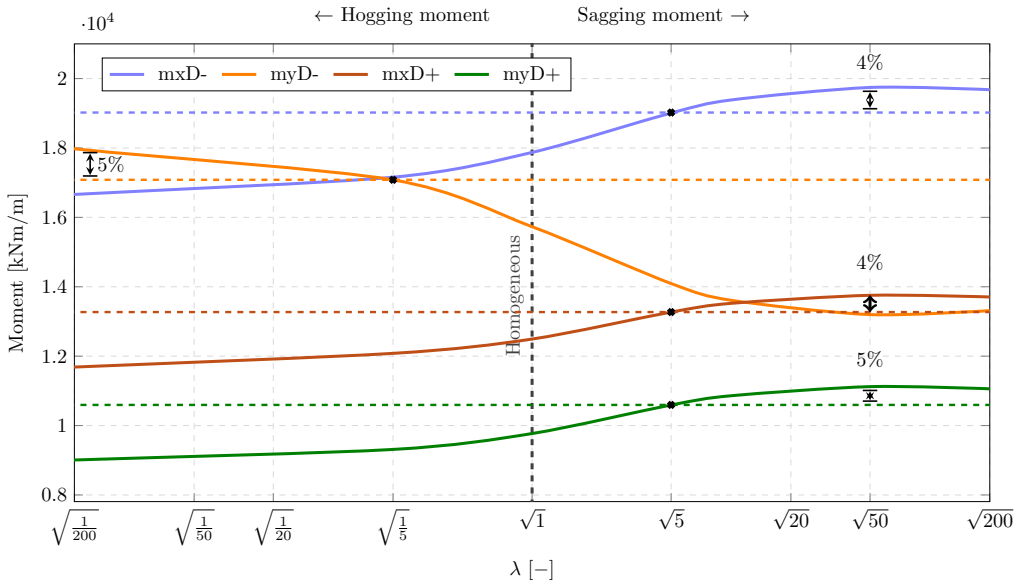

Figure 8.18: *Influence of λ on moment distribution of caisson walls. On the left side of λ = 1 a hogging moment is present, on the right side of λ = 1 a sagging moment is present*

In appendix G.3 new calculations are performed with the adjusted occurring design moment. It turns out that only at the underside of the caisson bottom slab an extra layer of reinforcement is required in x-direction.

In table 8.2 and 8.3 the reinforcement plan was given. Just as with the first variant, also in this construction alternative large quantities of reinforcement are required. The same possibilities as mentioned in the previous chapter could be considered. The use of prestressed steel to increase the compressive forces in the concrete or the enlargement of the cross-section to increase the internal lever arm to the resultant of the reinforcement bars.

8.5 CONNECTION BETWEEN CAISSONS

After removing of the soil between the caissons the construction of the bottom plate can start. These acts as foundation for the guiding rail and moving equipment and prevents the effects of piping below the lock gates. There are multiple ways to construct this foundation .

- Underwater concrete
- An immersed caisson

8.5.1 UNDERWATER CONCRETE

After the desired depth is reached the space between the bottom slabs and cutting edges of both caissons will be filled with under water concrete. The difficulties in this option are concentrated in achieving an exact horizontal level of the underwater concrete floor. The floor must be exact horizontal since no cracks and chinks may exist between the gate and the concrete floor. In figure 8.19 the location of the underwater concrete floor is schematised. After casting of the concrete both caissons are fixed to each other.

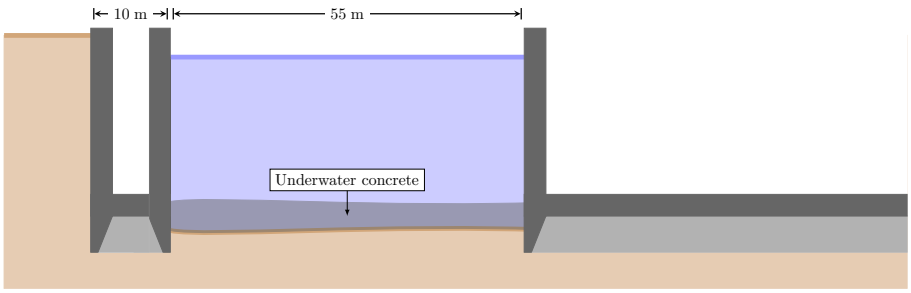

Figure 8.19: *Casting of the underwater concrete floor*

After excavating of the intermediate soil the bulkheads can be removed. Subsequently after hardening of the concrete the guiding rails and moving equipment of the lock gates can be installed. Because there is always a layer of water on top of the concrete floor there is no risk on upheaval of the floor and hence no tension piles are required.

8.5.2 CONNECTION WITH A CAISSON

The alternative for the use of underwater concrete is the use of a caisson. The advantage of a separate caisson is the possibility to construct the caisson at a different location and asses the caisson before installation.

After subsidence of the pneumatic caissons, the enclosed soil body can be removed as well as the excavation of the entrance channel to the lock heads. At this moment the lock chamber is not finished yet, ensuring the watershed between the Westerscheld and the land behind it. When the caisson is constructed it can be transported over water to the lock complex. This is schematised in figure 8.20.

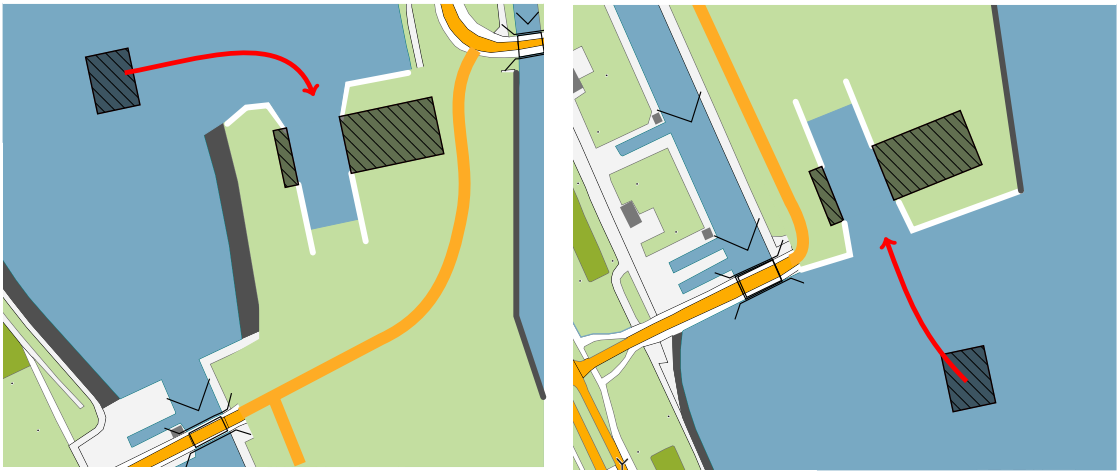

(a) *Northern lock head* **(b)** *Southern lock head*

Figure 8.20: *Floating in of the caisson, the pneumatic caissons are finished and subsided. The entrance channel is not ready, ensuring the separation between the Westerscheld and the channel*

Due to the large dimensions of the caisson it can not be transported through the western lock. This means that one caisson have to be constructed on the interior side of the lock and the other caisson elsewhere, these can be transported through the Westerscheld towards the lock complex.

Due to the enclosure of air, the caisson can float from itself. After reaching it final position the caisson can be immersed. Air inside the caisson can be released gradually and with help of anchors and cables the caisson can be placed in position.

When a caisson is used to support the guiding rail and lock gates, an entrance channel must be present wherein the caisson could be floated in. When the caisson is placed in position it can be immersed and connect both pneumatic caissons. Due to the shape of the caisson and the presence of multiple hydraulic jacks the exact horizontal position can be achieved. Possible settlements of the structure can be counteract later on. The connection between the immersed– and pneumatic caisson is schematised in figure 8.21.

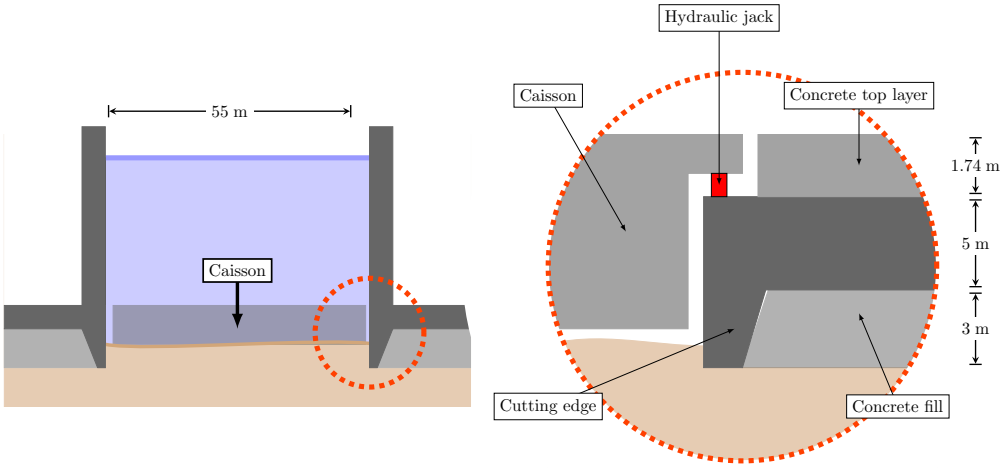

Figure 8.21: *Embedding of the caisson between both pneumatic caissons (not on scale)*

For a feasibility test a caisson with outer dimensions $l \times w \times h = 55 \times 45 \times 6$ is assumed. The caisson is split in 4 compartments and all the walls have a thickness of 1 meter.

The total weight of the caisson per unit length is thereby:

$$W_{caisson} = [(45 \times 6) - (2 \times (\frac{45 - 3 \times 1}{2}) \times (6 - 2 \times 1))] \times 25 \text{kN/m}^3 = 2550 \text{ kN/m} \tag{8.2}$$

Requiring equilibrium during transport, when the space inside the caisson is filled with air, the draft of the caisson can be calculated:

$$\frac{W_{caisson}}{l \times \gamma_{water}} = \frac{2550}{45 \times 10 \text{kN/m}^3} = 5.66 \text{ m} \tag{8.3}$$

This is less than the height of the caisson and thereby plausible. In figure 8.22 the forces acting during floating conditions are given. In this case only the water pressure andself-weightt are acting on the caisson. The maximum moment is occurring in y-direction in the top of the caisson and amounts $M_{ed;max} \approx 1500$ kNm/m.

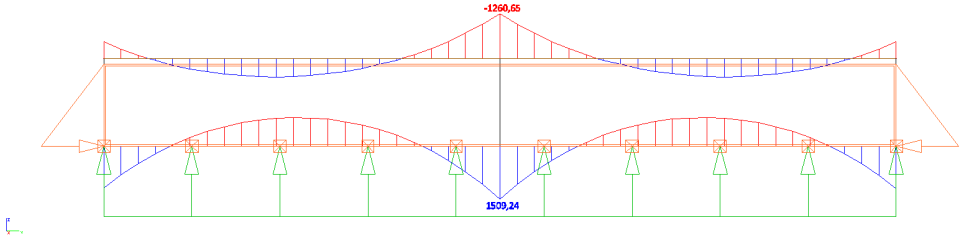

Figure 8.22: *2D schematisation of the immersed caisson in cross section during floating conditions*

In [LievenseCSO, 2014a] a weight of $W_{gate} = 2616 \times 10^3$ kg for the lock gates is calculated. It is assumed that the weight of the 9 meter thick lock gates is transmitted through three guiding rails, schematised as line loads, on the caisson. ($n = 3$) The value of the line load in a closed position (on top of the caisson) is:

$$\frac{W \times g}{l \times n} = \frac{2616 \times 10^3 \cdot 9.81}{55 \times 3} = 155 \text{ kN/m} \tag{8.4}$$

In figure 8.23 the acting line loads as well as the moment distribution from self-weight, forces from the guiding rail as well as the water pressure are given for the cross section.

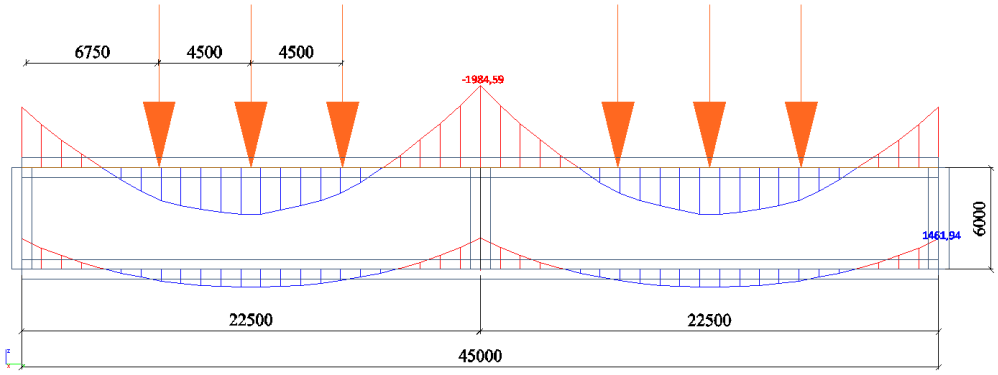

Figure 8.23: *2D schematisation of the immersed caisson in cross section*

The maximum moment in the caisson is $M_{ed;max} \approx 2260$ kNm/m. With two rows of $\varnothing - 32 - 150$ in both direction this moment can be resisted. ($M_{rd;x} = 2610$ kNm/m & $M_{rd;y} = 3258$ kNm/m)

The caisson will be supported on both the by the edges on hydraulic jacks, ensuring an exact horizontal level. The top of the pneumatic caissons bottom slab was situated on NAP -19 meter. The minimal draft in the lock is set at NAP -17.26 meter according to section 4.1. In the intervening space the guiding rails for the lock gates can be installed.

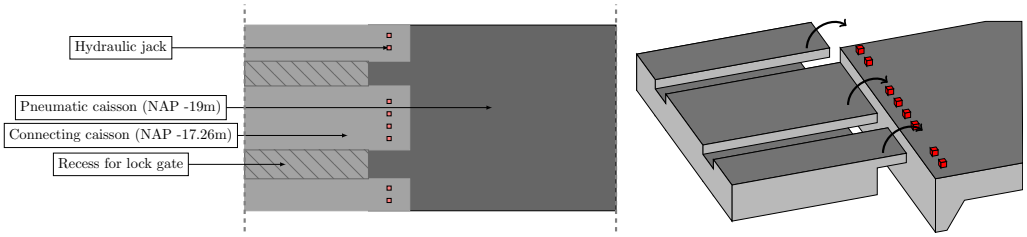

Figure 8.24: *Top view and three dimensional view of the connection between caisson and pneumatic caisson*

Due to the presence of the Boom Clay below the caissons the connection between immersed– and pneumatic caisson does not have to be watertight. The seepage of small quantities of water is not a major issue. Eventually the gaps between the caissons can be filled up with small amounts of for example underwater concrete to achieve a water-tight connection.

8.6 EXTERNAL STABILITY OF THE CAISSON

When both pneumatic caissons are subsided and the working chamber is filled with concrete the completion of the lock head can start. The soil between both caissons must be removed. This will be done for a major part below the groundwater table. This is schematised in figure 8.25. The most critical moment occurs at the time the intermediate soil is removed and on one side the ground pressure is completely absent. The caisson must be checked on horizontal and rotational stability which is schematised in figure 8.26.

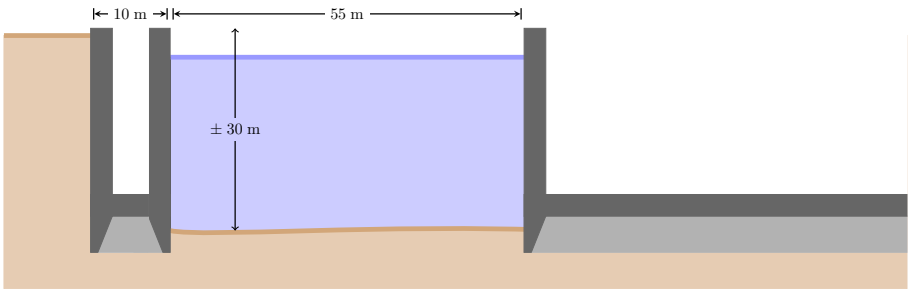

Figure 8.25: *Excavation between both pneumatic caissons to a level equal to the lower side of the designed underwater concrete floor*

8.6.1 HORIZONTAL STABILITY

The horizontal force on the caisson exists out of the effective horizontal soil stress and the water pressure. The water pressure is present on both sides of the caisson and has therefore no effect on the stability. The horizontal force, $\sum H$, must be transferred to the subsoil. The friction force on the underside must be larger than the horizontal load acting against the caisson wall to prevent the caisson from sliding which is schematised in figure 8.26a.

The maximum friction capacity is defined as the total vertical load, $\sum V$, multiplied by a dimensionless friction coefficient f.

$$\sum H \leqslant \sum V \times f \tag{8.5}$$

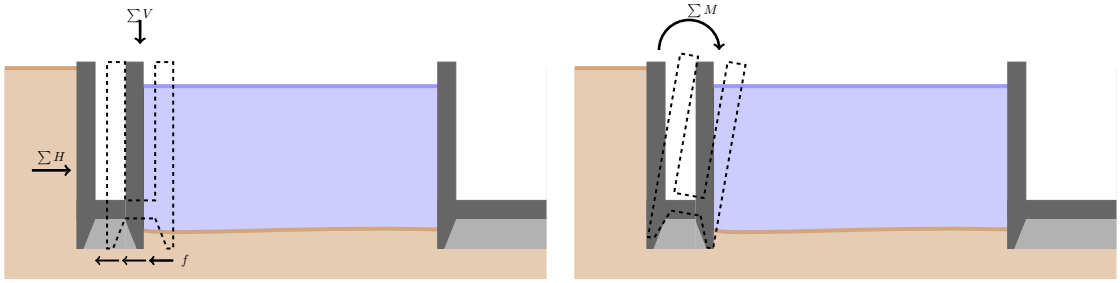

(a) *Horizontal stability* **(b)** *Rotational stability*

Figure 8.26: *Stability of the caisson*

Where f, the friction coefficient, is defined as $f = \tan(\delta)$. The friction angle δ at the concrete-soil interface can be assumed equal to $\frac{3}{4} \cdot \theta_{\text{boom clay}} \Rightarrow f = \tan(\frac{3}{4} \cdot 25) = 0.34$.

The net horizontal force $\sum H$ caused by the effective horizontal soil stress is calculated by:

$$\sigma_{\text{horizontal}}|_z = K_N|_z \cdot \sigma_{\text{eff}}|_z \tag{8.6}$$

$$H = \underbrace{w}_{\text{Width of caisson}} \cdot \sum_{z=6}^{z=-27} \sigma_{\text{horizontal}}|_z \tag{8.7}$$

The total horizontal force as well as the moment caused thereby is calculated in appendix G.5 and amounts $\sum H = 136333$ kN. The total vertical (submerged-) weight of the caisson was given in figure 8.4 and amounted $V_{\text{caisson}} = 170277$ kN.

The weight of the concrete fill in the working chamber is defined by:

$$\begin{aligned} V_{\text{working chamber}} &= \underbrace{(10 - 2 \cdot 0.5 \cdot (1.5 + 0.2))}_{\text{Avg.Length}} \times \underbrace{(45 - 2 \cdot 0.5 \cdot (1.5 + 0.2))}_{\text{Avg.Width}} \times \underbrace{3}_{\text{Height}} \times \underbrace{25 - 10}_{\text{Volumetric Weight}} \\ &= 16172 \text{ kN} \end{aligned}$$

The caisson is filled with ballast. The weight of the ballast is:

$$\begin{aligned} V_{\text{ballast}} &= \underbrace{(10 - 3.5 - 3)}_{\text{Length}} \times \underbrace{(45 - 2 \cdot 3.5)}_{\text{Width}} \times \underbrace{(6 - -19)}_{\text{Height}} \times \underbrace{(18 - 10)}_{\text{Effective volumetric weight}} \\ &= 26600 \text{ kN} \end{aligned}$$

$$\sum H \leqslant \sum V \times f \quad \Rightarrow \quad \sum H \leqslant (V_{\text{caisson}} + V_{\text{concrete fill}} + V_{\text{ballast}}) \times f$$

$$136333 \leqslant \underbrace{(170277 + 16172 + 26600)}_{\sum V = 213049} \times 0.34 = 72436$$

Equation 8.6.1 does not fulfill the requirements and it can be concluded that there is no horizontal stability during the construction of the lock head. During the lifetime of the construction, horizontal compressive forces can be transferred by the immersed caisson as elaborated in section 8.5.

The following options can be considered to achieve horizontal equilibrium during the construction:

- The use of struts between both caissons to prevent displacements.
- The use of anchors to transfer horizontal forces to the subsoil.

8.6.2 ROTATIONAL STABILITY

The other possibility of instability is the rotation of a caisson caused by the horizontal soil pressure on one side of the caisson. The eccentricity, e, of the caisson can be calculated with the following equation:

$$e = \frac{\sum M}{\sum V} \tag{8.8}$$

Seen from the center of the caisson, the moment, M, is defined by the horizontal load multiplied by the lever-arm. The lever-arm, a, is defined by $\frac{1}{3}$ times the height of the caisson because of the triangular shape of the horizontal soil pressure:

$$\begin{aligned} \sum M &= \sum H \times a \\ &= 136333 \times (\frac{1}{3} \cdot 33) = 1499670 \text{ kNm} \end{aligned} \tag{8.9}$$

The vertical load was defined in the previous paragraph, $\sum V = 213049$ kN

$$e = \frac{\sum M}{\sum V} = \frac{1499670}{213049} = 7.04 \text{ m} \tag{8.10}$$

The distance from the moment center to the intersection point of the resulting force and the bottom line of the structure amounts 7.04 meter. This point is situated outside the caisson and therefore rotation of the caisson will occur as schematised in figure 8.26b.

Different options can be taken in to consideration to prevent rotation of the caisson. It is a difficult to impossible exercise to create a moment resisting connection between the pneumatic– and immersed caisson. The solution must prevent instability during both the construction phase as well as during the lifetime of the construction. The installation of struts between both caisson is therefore not a feasible option.

The use of anchors

In the same way as anchors are used for the construction of sheet–, combi– and diaphragm walls, anchors can also be applied to prevent any rotation of displacement of the caisson. See figure 8.27a.

Increase of caisson height

By increasing the height of the caisson, by increasing the height of the working chamber or by introducing an extra vertical compartment, the caisson will be fixed by the surrounding soil preventing any rotation. See figure 8.27b. In this case the working chamber is situated on a larger depth. This means that during the process of subsidence larger air pressures are required inside the working chamber to prevent the inflow of water. This means that in all probability the maximum working time in overpressure wherein people may work will be exceeded. The excavation process must then be remotely controlled so that there are no people in the working chamber

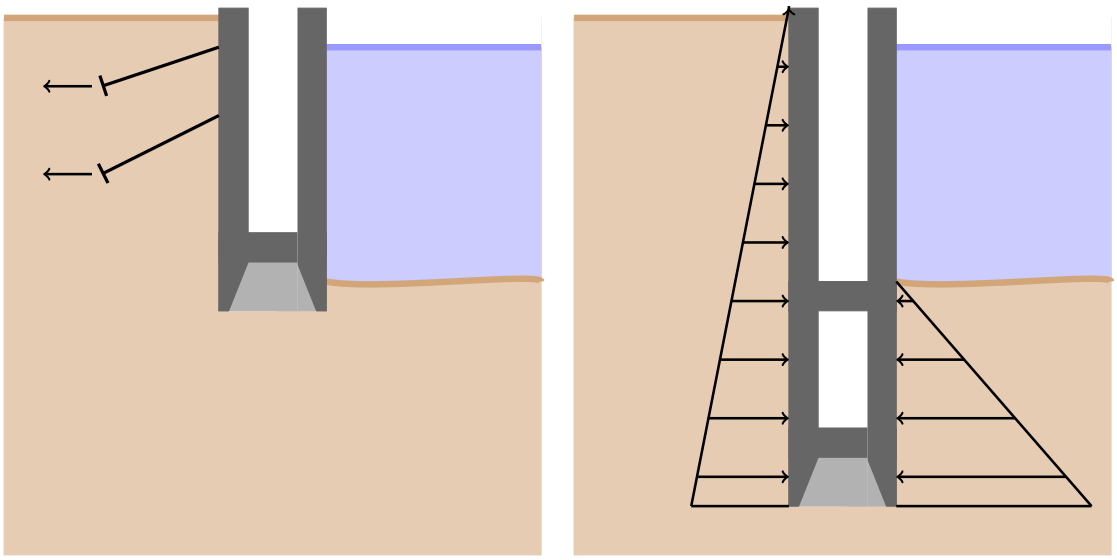

(a) *Anchors providing stability* **(b)** *Deepened caisson*

Figure 8.27: *Stability of the caisson*

Widening of caisson

The caisson must be widened in such extent that the resultant of the forces will be situated within the caisson. Besides this the vertical load will become larger by the increase of the self-weight. The horizontal soil load however will remain equal. Due to the widening of the caissons more soil has to be excavated below the caisson and more building materials are required.

Widening of the working chamber of the caisson

Because the only function of the enlarged caisson is maintaining the stability, another option is to increase the width of the working chamber of the caisson in a manner as can be seen in figure 8.28a.

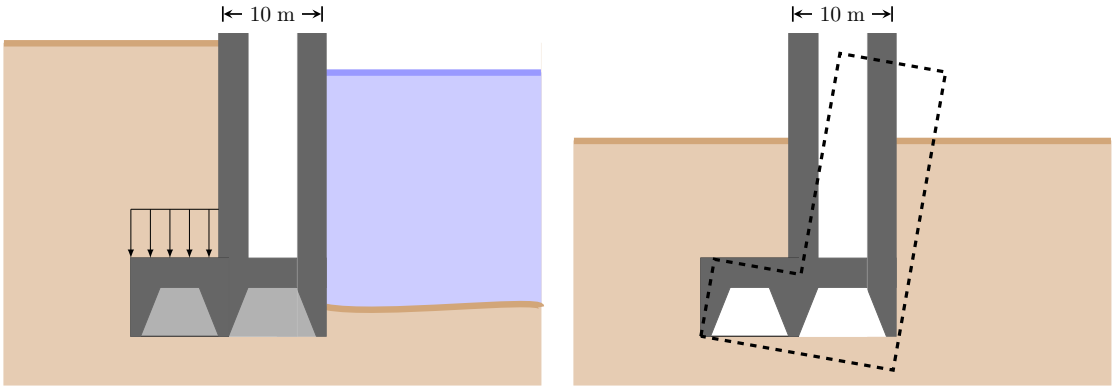

(a) *Caisson with enlarged working chamber*

(b) *Rotating caisson due to the eccentricity in the downward load during subsidence*

Figure 8.28: *Stability of the caisson*

By extending the working chamber to the left in reference to figure 8.28a the weight of the soil on top of it has a positive effect. The disadvantage of this solution is the eccentricity of the vertical load caused by the self-weight. Therefore without additional measure rotation of the caisson will occur during subsidence as schematised in figure 8.28b unless additional measures are foreseen. To prevent any rotation the basis of the caisson can be enlarged on both sides to prevent any eccentricity in the vertical load. Another solution to counteract the eccentricity is placing ballast on top of the left working chamber of figure 8.28a. To achieve any effect this should be heavy material like steel for example.

9

REFERENCE DESIGN - TRADITIONAL BUILDING PIT

As alternative for the construction of the lock head with pneumatic caissons a traditional building pit can be used to construct the lock heads. The majority of locks that have been built in the past are constructed with help of a building pit. The construction of a building pit is therefore a proven method. The diversity of building pit types were already mentioned in appendix C. In this chapter a design which satisfies the requirements will be made for the lock head. This starts with the description of the building pit in section 9.1 and continuous with the water tightness of the building pit in section 9.2. This chapter ends with an elaboration of the chooses building pit design in section 9.3.

9.1 CONSTRUCTION SEQUENCE

The exact building sequence of the building pit is depending on the type of retaining structure, type of closure of the bottom of the building pit and usage of struts and anchors. The construction covers the following steps:

- **Removal of obstacles** - Different cables and lines, for example potable water supply, sewer and telephone lines.
- **Construction of the retaining wall** - Different types of retaining walls can be considered as explained in appendix C.1.
- **Initial excavation** - This step is schematised in figure 9.1.

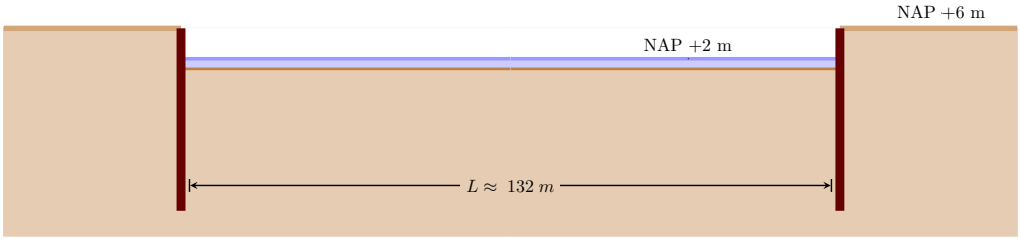

Figure 9.1: *Initial excavation inside the building pit*

- **Placing of anchors and/or struts** - When a combi-wall, cofferdam or a combination of these with a relieving platform is used the second step of the construction consist out of installing of the layers of anchors and/or struts. Because the groundwater level is at a level of NAP +2m and the anchors or struts must be installed on a lower level than

the groundwater table. There are two options to mount the anchors and/or struts to the retaining wall. First option is to lower the groundwater table inside the building pit for a short amount of time. Due to the low permeability of the Boom Clay it takes quite some time before the groundwater is flowing in to the building pit. When lowering the ground water table inside the building pit the effect of bursting open of the soil must be considered. This will be done in the next subsection. In figure 9.2 a retaining wall with a layer of struts (left) and anchors (right) is schematised.

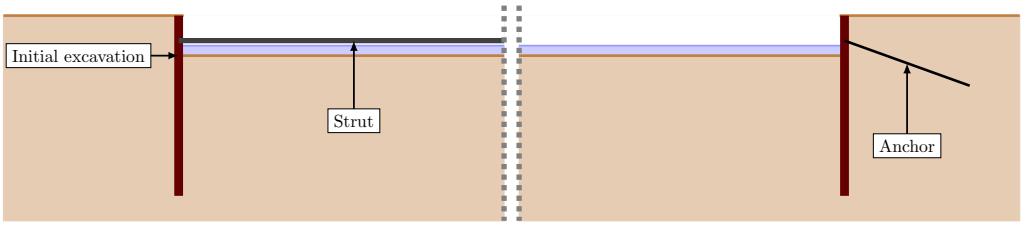

Figure 9.2: *Placing of struts (left) or anchors (right)*

- **Continuation of excavation** - After the struts and/or anchors are placed in position the excavation of the building pit can be continued.
  - In certain cases, including this one, multiple layers of struts and/or anchors are required. However from a certain the depth the water level can not be lowered further because of the present hydraulic head below the clay layer and the risk on bursting open of the soil layers below. Therefore another option is to mount the anchors and/or struts below the water surface with help of divers. This is more costly and time consuming. This step is shown in figure 9.3.

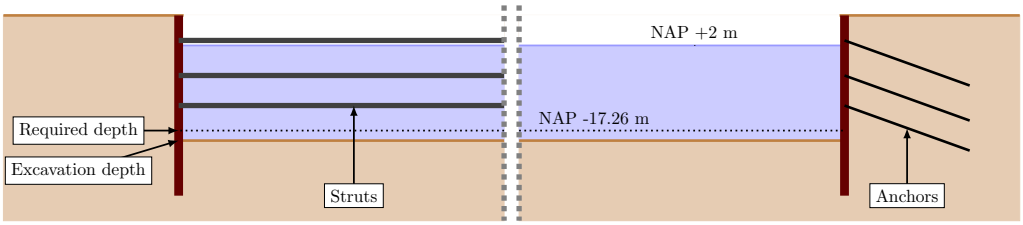

Figure 9.3: *Further excavation of the building pit and installation of extra layers of struts (left) or anchors (right)*

- **Installation of tension piles** - After the building pit is fully excavated, tension piles or anchors can be placed at the bottom of the building pit to prevent uplifting of the subsequently to construct underwater concrete floor. This can be done with equipment above the water table. This step is schematised in figure 9.4.

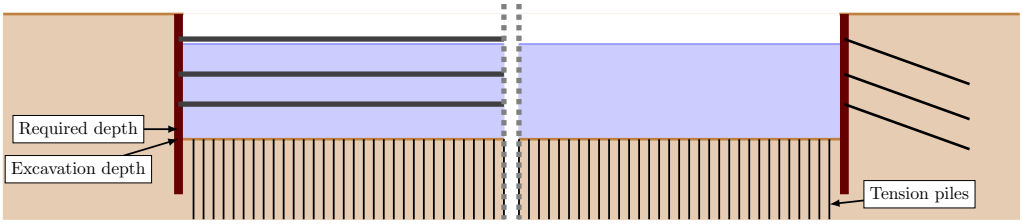

Figure 9.4: *Installing of tension piles*

- **Construction of underwater concrete floor** - When the anchors or tension piles are installed the construction of the underwater concrete floor can start.
- **Dewatering** - When the concrete floor is cast and is sufficient hardened, the remaining water inside the building pit can be pumped out. This step is schematised in figure 9.5.

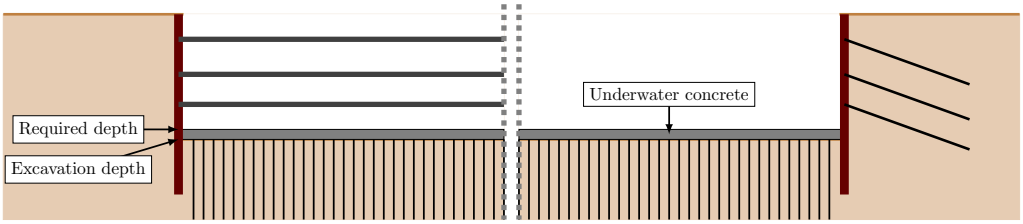

Figure 9.5: *Casting of underwater concrete floor and dewatering of the building pit*

- **Completion** - When the building pit is completed the lock head can be constructed within the building pit. After completion of the lock head the combi-walls can be removed. This step is shown in figure 9.6.

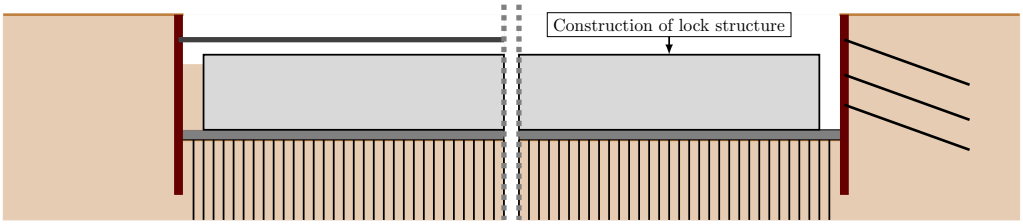

Figure 9.6: *Construction of lock within building pit*

9.2 WATER TIGHTNESS OF THE BUILDING PIT

There are different options to achieve a dry construction environment.

- **Normal excavation** - In case there is an impermeable layer present in the subsoil only the water above this impermeable layer has to be removed. Because of the impermeable layer

water from deeper located soil layers is not able to flow upwards in to the building pit. The risk on hydraulic burst must be determined.

- **Excavation with drainage** - When the hydraulic head below the building pit is decreased by means of drainage the risk on hydraulic burst will decrease and when permeable layers are present less water will flow in to the building pit. The amount of water to be drained must be calculated.
- **Excavation with underwater concrete** - The last established option is the use of underwater concrete. In this case the building pit will be excavated in the wet after which an underwater concrete floor will be constructed. Subsequently the water will be pumped out. The underwater concrete floor can be designed in two ways: When the weight of the concrete is high enough to compensate the upward water pressure tension piles are not required. This occurs in situations of a shallow building pit or when the groundwater table is located very deep. The thickness of the concrete layer can not be increased infinite. In the other case the tension piles are used to reduce the height of the concrete layer. Reducing the thickness can be done with piles or anchors.

In the case of the new lock in Terneuzen an impermeable clay layer is present between NAP -20.5 and -38 meter. It can be used possibly as barrier between the building pit and the underlying water table.

9.2.1 HYDRAULIC BURST

According to [NEN 6740] the check on bursting open of the soil can be performed with equation 9.1. The total weight of the soil above the impermeable layer must be larger than the total upward groundwater pressure u_z below the layer of Boom Clay.

$$u_z \leqslant \sum_{j=1}^{j=n} d_{j,d} \times \gamma_{j,d} \tag{9.1}$$

$$u_z = H_d \times \gamma_w \quad \Rightarrow \quad u_z = (2-(-38)) \times 10 = 400 \text{ kPa}$$

When a excavation depth of NAP -19 is assumed the total downward force is equal to the weight of the sand layer between NAP -19 and -20.5 meter and the Boom Clay layer between NAP -20.5 and -38 meter:

$$\sum_{j=1}^{j=n} d_{j,d} \times \gamma_{j,d} = (-19-(-20.5)) \times 19.1 + (-19-(-38)) \times 19 = 361.2 \text{ kPa}$$

Because the upward force (400 kPa) is larger than the downward force from the clay layer (361.2 kPa) the clay layer will burst open without additional measures. The hydraulic head must be lowered with $(400-361.2)/10 = 3.8$ meter to make a safe construction towards NAP -19 meter possible. This is to much for water pressure dewatering. In the wide surroundings the groundwater table will decrease considerably and existing construction will settle.

9.2.2 UNDERWATER CONCRETE

The use of a underwater concrete floor will prevent the inflow of water or upheaval of the clay. When using an underwater concrete floor the building pit will be excavated in the wet and after the desired level is reached an concrete floor will be installed. After hardening of the concrete the building pit will be de-watered and the concrete will counteract the water pressure. Without tension piles a larger concrete floor is required. The height of the concrete floor can in that case be calculated according to equation 9.2.

$$u_z \leqslant \sum_{j=1}^{j=n} d_{j,concrete} \times \gamma_{j,concrete} \tag{9.2}$$

Where the upward water pressure (u_z) and downward directed load of the concrete floor are equal to:

$$u_z = H_d \times \gamma_w \quad \Rightarrow \quad u_z = (2 - (-19 - d_{j,concrete})) \times 10 = 210 + d_{j,concrete} \times 10 \text{ kPa} \tag{9.3}$$

$$\sum_{j=1}^{j=n} d_{j,concrete} \times \gamma_{j,concrete} = d_{j,concrete} \times 25 \tag{9.4}$$

A floor thickness of $d_{j,concrete} \approx 14$ m is required. Which implies that for a building pit with the groundwater level at NAP +2 meter and a depth of NAP -19 meter there must be excavated towards a depth of NAP $-19 - 14 = -34$ meter. Eventual a concrete with a higher volumetric weight can be used to decrease the concrete height. Basalt, barite and magnetite can be used as heavily aggregate. But even when heavy concrete is used this is either not common and therefore tension piles are required.

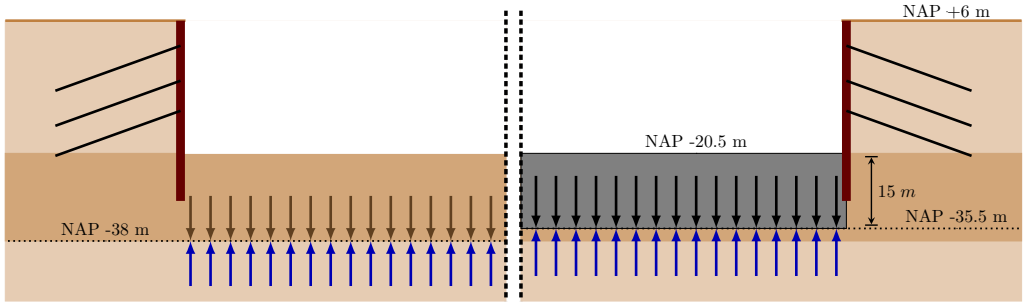

Figure 9.7: *Forces on the Boom Clay layer (left) and underwater concrete floor (right)*

9.2.3 TENSION PILES

In the design of an underwater concrete floor combined with tension piles there are several design possibilities. Most important design choices are the height of the underwater concrete floor, length of the anchors and there mutual distance. The ratio between these parameters depends on local circumstances such as the availability of standardize tension piles on the market, the availability of equipment and the local soil properties. The safety on hydraulic burst of the underwater concrete floor depends on two mechanisms:

- Friction along the pile shaft of the individual tension pile (friction mechanism)
- The mobilized ground soil weight by the friction along the pile shaft around the pile foundation that acts as a counterweight to the tensile load (clump weight mechanism).

There are different types of tension piles which can be divided in two groups, soil displacing and non-soil displacing. GEWI anchors are often used in combination with underwater concrete floors. In appendix C.2 the dimensioning and verification of the used tension piles are given.

9.3 DESIGN OF BUILDING PIT

As elaborated in the previous sections there are different methods to construct the lock head with help of a building pit. The most important design choices are the type of retaining construction and the occlusion between building pit and the underlying soil. The available space is limited, therefore an open excavation is not considered as feasible option. Due to the function of the lock-head as water retaining structure, where lock gates, turning points, recesses and guiding rails must be placed within very small tolerances, strict requirements are demanded for the final position of those elements. Because of this reason a construction below the water surface is not considered as feasible option and only the design of a dry building pits is taken into consideration. In this design, as an alternative to the pneumatic caissons, a design is proposed consisting out of a building pit from combi-walls wherein the lock head is constructed. An underwater concrete floor in combination with tension piles is ensuring a watertight closure with the ground below. The combi-walls can be used for two purposes.

- First option is to create a building pit out of combi-walls. In this temporary building pit the lock head can be constructed. After finishing of the lock heads the combi-walls are removed.
- In the second option the combi-wall are part of the final structure. Because in this case there are high requirements on stiffness, deformation and lifetime this option is not further considered.

The occurring moment in the combi-walls are dependent on the stiffness of the combi-wall elements. A medium to heavy profile is used to check the feasibility of combi-walls. In a final design the combi-wall can be optimised to prevent the construction of an over dimensioned combi-wall. This also decreases the costs. The parameters of the combi-wall are shown in table 9.1 and the layout of the combi-wall with the given dimensions is schematised in figure 9.8..

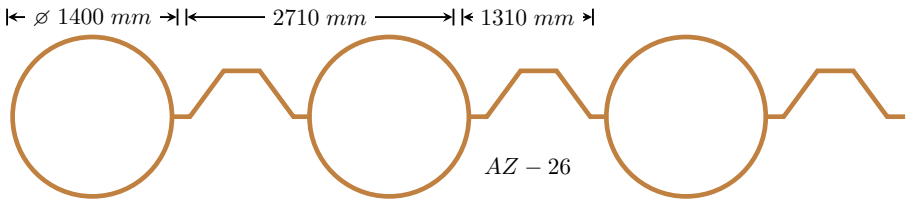

Figure 9.8: *Layout of the combi-wall*

With help of the following formulas the section modulus, moment of inertia and the maximum resisting moment of the combi-wall can be calculated.

Table 9.1: *Properties of the combi-wall*

Steel properties			
E	210000	kPa	Youngs-modulus
f_γ	235	mm	Minimum yield strength
Tube properties			
L	40	m	Length
$\varnothing$	1400	mm	Outer diameter
t	20	mm	Wall thickness
I_{tube}	2.60×10^6	cm^4/m	Moment of inertia
Sheet pile properties (2xAZ-26)			
L	35	m	Length
w_{AZ-26}	1310	mm	Width of double profile
W_{AZ-26}	55510	cm^3/m	Section modulus
Combi-wall properties			
$w_{combi-wall}$	2710	cm/m	Total width

$$\begin{aligned} W_{combined} &= (\frac{\pi \cdot (\varnothing^4 - (\varnothing - 2 \cdot t)^4}{32 \cdot \varnothing} \cdot 10^{-3} + W_{AZ-26} \cdot \frac{w_{combi} - \varnothing}{w_{combi}}) / w_{combi} \cdot 1000 \\ &= (\frac{\pi \cdot (1400^4 - (1400 - 2 \cdot 20)^4}{32 \cdot 1400} \cdot 10^{-3} + 55510 \cdot \frac{2710 - 1400}{2710}) / 2710 \cdot 1000 \\ &= 11251 \text{ cm}^3/\text{m} \end{aligned} \tag{9.5}$$

With the given dimensions of the tubular piles the moment of inertia is calculated:

$$\begin{aligned} I_{tube} &= \frac{\pi(\varnothing^4 - (\varnothing - 2 \cdot t)^4)}{64} \times 10^{-3} \\ I_{tube} &= \frac{\pi(1400^4 - (1400 - 2 \cdot 20)^4)}{64} \cdot 10^{-3} = 2.06 \times 10^6 \text{ cm}^4 \end{aligned} \tag{9.6}$$

The moment of inertia of the tubular piles can be combined with the moment of inertia of the sheet pile walls.

$$\begin{aligned} I_{combined} &= \frac{I_{AZ-26} \cdot w_{AZ-26} + I_{tube} \cdot 1000}{w_{combi}} \\ I_{combined} &= \frac{2600 \cdot 1310 + 2.6 \times 10^6 \cdot 1000}{2710} = 7.8 \times 10^6 \text{ cm}^4 \\ EI_{combined} &= 7.8 \times 10^6 \cdot 2.1 \cdot 10^5 = 1.65 \cdot 10^6 \text{ kNm}^2/\text{m} \end{aligned} \tag{9.7}$$

With the section modulus known the maximum allowable moment can be calculated:

$$M_{max} = W_{combined} \cdot f_\gamma = 11251 \cdot 235 = 2644 \text{ kNm} \tag{9.8}$$

The underwater concrete floor is modelled as strut with a surface area of $A_{concrete} = 3\ m^2/m$ and stiffness modulus of 30 GPa a buckling length of half the span. $L_{buckling} = \frac{1}{2} \cdot L_{span} = \frac{1}{2} \cdot 45 = 22.5\ m$. The construction of the building pit is subdivided in four phases:

- **Step 1** - Excavation towards a level of NAP -6m.
- **Step 2** - Installing of anchor at NAP -5m followed by an excavation towards a level of NAP -14m.
- **Step 3** - Installing of anchor at NAP -13m followed by an excavation towards a level of NAP -21m.
- **Step 4** - Casting of underwater concrete floor and pumping of the building pit.

Two layers of anchors are required to achieve a stable design. The properties of the anchors used are given in table 9.2.

Table 9.2: *Properties of GEWI anchor*

⌀	63.5	mm
A	3167	mm^2
E	210	GPa
Center to center distance	1	m

The calculations will be performed with use of D-Sheet Piling. The results are given in table 9.3.

Table 9.3: *Results from D-Sheet for a lock head constructed out of combi-walls*

Stage	**Moment** [kNm]	**Shear force** [kN]	**Displacement** [mm]
Step 1	-7292	-845	483
Step 2	-5575	-1046	462
Step 3	-6802	1414	458
Step 4	-6810	-2168	453

It can be seen that the maximum force occurs in step 3 and is $M_{Ed} = 7292$ kNm. The maximum resisting moment is $M_{Rd} = 2901 \times 2.71 = 7861$ kNm. So the combi-wall fulfills the requirements because $M_{Ed} \leqslant M_{Rd}$.

10

CONSIDERATION BETWEEN THE VARIANTS

In this chapter a comparison will be made between the different elaborated variants in this thesis. The elaborated variants are:

- **Variant 1** - One large caisson divided into several compartments *(Chapter 7)*
- **Variant 2** - Two caissons which are subsided individually and divided into several compartments *(Chapter 8)*
- **Variant 3** - Reference design, Traditional building pit *(Chapter 9)*

In the first section the advantages and disadvantages of the different variants are enumerated. In the second section a trade-off matrix is composed to come to the best solution.

10.1 ADVANTAGES AND DISADVANTAGES

VARIANT 1 - ONE LARGE CAISSON DIVIDED INTO SEVERAL COMPARTMENTS

The advantage of using one large caisson is that there are no temporary structures necessary. Therefore this option is less expansive in comparison with a traditional building pit. For the construction of the caissons can start an initial landfill on the eastern side of the western lock is required. Because the concrete is cast at surface level it saves costs and it can be inspected afterwards. By the absence of large temporary structures the building time is shorter. However, there is less experience in subsiding pneumatic caissons in stiff layers of Boom clay.

Due to the use of one large caisson there are no differential settlements between the caissons and afterwards no connection between the caissons has to be realized.

VARIANT 2 - TWO CAISSONS WHICH ARE SUBSIDED INDIVIDUALLY AND DIVIDED INTO SEVERAL COMPARTMENTS

As just described, the construction with pneumatic caissons, has some advantages over a traditional building pit design. The use of two caissons has some benefits over the use of one caisson. The used caissons are more rigid then in the first variant. Besides that, the caissons can be designed more slender.

VARIANT 3 - REFERENCE DESIGN, TRADITIONAL BUILDING PIT

The use of a traditional building pit has however some advantages over the use of pneumatic caissons. Due to the absence of a desanding plant and bentonite installation there is a limited

requirement on the working space. There is no risk of pressure related accidents, however, in this variant tension piles as well as anchors have to be installed below the water level. Due to the temporary facilities like combi-walls and anchors the expenses are larger. Therefore this is the most expensive option.

10.2 COMPARISON

The three variants above are compared in a trade-off matrix which is given on the next page. The building times where calculated in appendix E.2 and the global costs are estimated roughly in appendix E.3. In table 10.1 a summary is given.

Table 10.1: *Summary of the building time and estimated costs*

	Variant 1	**Variant 2**	**Variant 3**
Building time	22 months	22 months	30 months
Estimated costs	€ 48.3 million	€ 37.7 million	€ 52.6 million

It should be clear that these numbers are rough estimates wherein only the order of magnitude is of importance.

The comparison between the different alternatives is made on basis of six aspects. *Feasibility, Safety, Risk, Required materials, Building time* and *Costs* . For each variant one, two or three points are given where one point stands for moderate properties with respect to the given aspect, two points stands for average properties with respect to the given aspect and three points stands for the best possible properties with respect to the given aspects. All points are summed up. On basis of the points mentioned above, the reference design consisting out of the building pit comes as winner out of the comparison.

Trade-off table		Variant 1 One large caisson divided into several compartments	Variant 2 Two caissons which are subsided individually and divided into several compartments	Variant 3 Reference design, Traditional building pit
evaluation criteria				
Feasibility	Rating	1	2	2
	Reason:	- Considerably requirement on working space (sedimentation basin and bentonite desanding installation) - Initial landfill requirement - Less stiff construction compared with option 2 - Large amounts of shear reinforcement are required.	- Considerably requirement on working space (sedimentation basin and bentonite desanding installation) - Initial landfill requirement - Stiff construction compared to option 1	- Limited requirement on working space - Installing of anchors below the water table - Vibration and noise during construction of combi-wall
Safety	Rating	2	2	3
	Reason:	- Risk at working at increased air pressure	- Risk at working at increased air pressure	- Risk at working below the surface table
Risks	Rating	1	1	3
	Reason:	- Less experience of pneumatic caissons in practice - Unequal settlements during subsidence - Risks for working men at increased air pressure - Application of pneumatic caissons in Boom Clay	- Less experience of pneumatic caissons in practice - Unequal settlements during subsidence - Risks for working men at increased air pressure - Application of pneumatic caissons in Boom Clay	- Hydraulic burst of building pit - Soil retaining elements not on depth - Tension piles have insufficient capacity - Removing elements of temporary building pit - However, it is a proven method
Materials	Rating	1	2	3
	Reason:	- The continuing bottom slab of the caisson increases the amount of concrete	- Due to the more slender design of the caisson less concrete is required	- Temporary combi-walls are required for the building pit - More slender design of the lock head
Building time	Rating	3	3	2
		- 22 months	- 22 months	- 30 months
Costs	Rating	3	3	1
	Reason:	- Relatively inexpensive to lock head, no temporary facilities necessary - Concrete can be cast at surface level (saves costs) - Concrete fill of the working chamber (increase costs)	- Relatively inexpensive to lock head, no temporary facilities necessary - Concrete can be cast at surface level (saves costs) - Caissons must be connected below the water table which increases the costs - Concrete fill of the working chamber (increase costs)	- Higher expenses due to temporary facilities - Smaller margin required for unexpected costs
	Costs	- Estimated costs of 48.200.000 euro	- Estimated costs of 37.700.000 euro	- Estimated cost of 52.600.000 euro

Total points:	**11**	**13**	**14**

Part V

CONCLUSIONS AND RECOMMENDATIONS

11

CONCLUSIONS AND RECOMMENDATIONS

11.1 CONCLUSIONS

The conclusion of this thesis is presented by the construction alternatives which are given in: *Part IV - New lock Terneuzen*. This is done because the determination that a pneumatic caisson can be used for the construction of the new lock in Terneuzen, while fulfilling the local conditions and requirement, cannot be answered by a single answer. In this thesis only the construction of a lock head is taken in to consideration because, in contrast to the lock chamber, it is assumed that these should be constructed in a dry environment.

Two variants for the construction of the lock heads with pneumatic caissons are elaborated:

1. The construction of one large pneumatic caisson with a length of 132 meter, width of 45 meter and a height of 33 meter containing the complete lock head including the gate chamber and gate recess. The working chamber is divided into 14 compartments.
2. The construction of two (compartmentalized–) pneumatic caissons which can be subsided independently. One caisson with a length of 10 meter, width of 45 meter and a height of 33 meter is covering the gate recess and the other caisson with a length of 67 meter, width of 45 meter and a height of 33 meter is covering the gate chamber. The enclosed space between both caissons, where ships will sail through, is sealed off by an immersed caisson or underwater concrete floor.

SUBSIDENCE OF THE CAISSON

The calculations shows that, independent of the chosen construction variant, it is impossible to subside a pneumatic caisson from surface level to design depth without additional measures. In the first phase of the construction the downward directed loads must be reduced. This can be done by constructing the pneumatic caisson in two different stages. By increasing depth the resisting upward forces are becoming larger. Therefore ballast can be used to increase the weight of the caisson. Besides that, the friction forces are decreased by the application of a bentonite slurry trench over the height of the caisson walls.

FEASIBILITY OF THE CAISSONS

With help of SCIA Engineer software two construction alternatives are calculated and analysed on their internal force– and moment distribution. The dimensions of the caissons are sufficient for the required amount of reinforcement and can resist the bending– and torsional moments. Multiple layers of reinforcement are required in multiple directions and on both sides of the

walls and slabs. The resistance of the concrete against shear forces is too low and therefore about 50% of the bottom slab and walls have to be reinforced against these forces. An amount of 101 kg/m^3 – 219 kg/m^3 of reinforcement is required. This large amount of reinforcement complicates the construction of the caisson and therefore increases the building costs.

If the first construction alternative, consisting out of one large caisson, is compared with the second construction alternative, consisting out of two separate caisson, it can be concluded that the occurring moments and shear forces inside the caisson of the second variant are considerable smaller. In a subsequent design step, smaller dimensions may be used for the design which saves costs.

COMPARISON WITH TRADITIONAL BUILDING PITS

The use of pneumatic caissons to construct the lock head has some advantages over the use of a traditional building pit. The fact that (1) the building time of the lock head with help of pneumatic caissons is shorter, (2) the costs are smaller, (3) pneumatic caissons can be constructed in controlled conditions above the surface level, (4) pneumatic caissons have a minimal influence to the surroundings and finally, (5) it is in a structural perspective a feasible option, makes the construction of the lock heads with pneumatic caissons at first sight an appropriate option.

In favor of the shorter building time and lower building costs the construction method has some important disadvantages that can not be neglected.

It should be noted that the adopted outer dimensions of the caisson in the calculations propose a caisson which is not stable in reality. Most of the given solutions propose a different shape of the caisson. For these alternative shapes more materials are required. Therefore, the actual price will be higher than the price given in the report and the given building time will be shorter than the actual required building time. Because of these reasons there will be less points given in the trade off matrix to the pneumatic caisson options which improves the choice of a traditional building pit.

During the subsidence of the pneumatic caissons a considerably working space is required for the sedimentation basin and bentonite de-sanding installation. By the lack of experience, the possibility of an uneven subsidence and working under overpressure the associated risks are higher and the risk of cost overrun becomes larger. Thereby it must taken into account that a very large amount of both shear– and bending reinforcement is required. The reinforcement bars are placed close to each other in order to obtain a feasible design. This complicates the flow of concrete during the casting process. Due to the large number of reinforcements bars and stirrups intensive handlings of reinforcement components are required on the building site. This handlings require many cranes and other heavy equipment. Overall it can be concluded that the design is technical feasible but not desirable. In order to obtain a feasible design the amount of reinforcement should been reduced.

A part of the loads and internal forces are only present during the process of subsidence. Therefore some parts of the construction are over-dimensioned during the lifetime.

Different conclusions are drawn up. Some conclusions are in favor of the construction of the lock head with pneumatic caisson, others are in detriment of the used method. In chapter 10 a comparison is made between a lock head conducted in a single caisson, two caissons and in a traditional building pit. The variants are compared on basis of six aspects. *Feasibility, Safety, Risk, Required materials, Building time* and *Costs* . The comparison shows that the reference design, the use of a traditional building pit to construct the lock head, is the best conceivable option. This is

primarily caused by the high degree of safety, the lower risk and limited requirement of working space.

The main objective as stated in the introduction was:

Are there possibilities to use pneumatic caissons for the new lock at Terneuzen?

The conclusion, that is made on basis of the introduction, boundary conditions and requirements, is that the use of pneumatic caissons for the construction of the lock heads is indeed technical possible. However it has not the preference by the large number of above mentioned disadvantages and limitations.

11.2 RECOMMENDATIONS

In this report a number of assumptions and simplifications are made which can be reviewed during further research. The following points have to be taken into consideration:

- The proposed dimensions of the smaller caisson covering the gate recess in the second construction variant provides a non-stable caisson. One of the given solutions for this problem should been chosen and elaborated further. This should also been done for the associated building costs and construction time.
- The proposed reinforcement scheme is difficult to implement. The design must be adjusted so that the amount of reinforcement can be reduced.
- This study does not take into account the effect of stiffness of the structure on the occurring soil stresses. However both are related with each other only a predefined load on the caisson walls is used.
- The calculation of the bearing capacity of the soil is calculated with the formulas of Brinch Hansen. The cutting edges of the caisson are seen as (multiple) strips which form a grid. However the theory is only valid for single strips and the corresponding boundary conditions for the application of this theory are not met. During further research the behaviour of soil around the cutting edge should be elaborated further.
- Due to the presence of both layers of sand and stiff clay layers different excavation equipment is necessary. In a follow-up study more research to the excavation process and the precise method of excavation of the Boom Clay can be examined.
- A more detailed elaboration of the pneumatic caisson will provide more insight in the risks, duration of the work and associated costs which play a decisive role.
- For the internal-dimensions of the different construction parts global dimensions are chosen based on reference projects. The effect of modified dimensions is only elaborated globally. In a follow-up study the exact effect on the force– and moment distribution can be examined.

Part VI

REFERENCES

LIST OF FIGURES

LIST OF TABLES

BIBLIOGRAPHY

AHN. Actueel hoogtebestand nederland, 2014. URL http://www.ahn.nl. visited on: 2014-07-02.

Douglas Allenby, Giles Waley, and David Kilburn. Examples of open caisson sinking in scotland. *Proceedings of the ICE-Geotechnical Engineering*, 162(1):59–70, 2009. ISSN 1751-8563.

Menard Bachy. Jet grouting, 2010. URL http://menardbachy.com.au/jet_grouting.php. visited on: 2014-10-07.

Abda Berisso Bame. New method of sinking caisson tunnel in soft soil, October 2013. URL http://urn.kb.se/resolve?urn=urn:nbn:no:ntnu:diva-23298.

Robert Banjac. Bearing capcity, 1996. URL http://environment.uwe.ac.uk/geocal/foundations/founbear.htm. Faculty of Environment and Technology, University of West-England, visited on: 2014-11-03.

Frederic Bernier, Xiang Ling Li, and Wim Bastiaens. Twenty-five years' geotechnical observation and testing in the tertiary boom clay formation. *Geotechnique*, 57(2):229–237, 2007. ISSN 1751-7656.

Laurits Bjerrum and Ove Eide. Stability of strutted excavations in clay. *Geotechnique*, 6(1):32–47, 1956. ISSN 1751-7656.

ing.R.P. Bongers and ing.G.W.J. van de Haterd. Pneumatisch afzinken van sluishoofden. *Cement Online*, 1995(5), 1995.

Boorsma B.V. Concept of the bascule rolling gate, December 2013.

Joseph E. Bowles. *Foundation analysis and design*. McGraw-Hill, 1988. ISBN 0070067767.

B. Braun, J. Shuster, and E. Burnham. Ground freezing for support of open excavations. *Engineering Geology*, 13(1-4):429–453, 1979. ISSN 0013-7952. doi: http://dx.doi.org/10.1016/0013-79527990048-6. URL http://www.sciencedirect.com/science/article/pii/0013795279900486. Ground Freezing.

Drs. J.V.M. Brugge and B.J. Vrouwe. Project car fase 1 - kartering slecht doorlatende laagpakketten van tertiaire formaties, 1996.

J. B. Burland. Shaft friction of piles foundation in clay - a simple fundamental approach. *Ground Engineering*, 6(3):30–42, 1973.

CUR 2001-4. *Ontwerpregels voor trekpalen*, 2001.

CUR 236. *Richtlijn Ankerpalen*, 2011.

D-Sheet Piling Manual. *D-Sheet Piling Manual*, July 2014.

J.G. de Gijt. *A History of Quay Walls*. PhD thesis, TU Delft, September 2010.

Eric DeLony. Context for world heritage bridges, 1996. URL http://www.icomos.org/en/home-doc/116-english-categories/resources/publications?start=100. visited on: 2014-06-23.

Engineers Australia. Gustave eiffel, 2014. URL https://www.engineersaustralia.org.au/queensland-division/gustave-eiffel. visited on: 2014-06-23.

Fugro. Rapportage laboratorium onderzoek. Lab report, May 2014.

Prof. P. D. Gohil. Caissons - module iii, 2012. URL http://www.gtucampus.com/uploads/studymaterials/Degree%20Engineeringgaurav.tandonCaissons%20Module%203.pdf.

Karen Hill. Description of the eiffel tower, August 2011. URL http://www.thaiengineering.com/project-in-world/730-description-of-the-eiffel-tower-the-1st.html.

Won-Pyo Hong, Geu-Gewen Yea, Tae-Hyung Kim, and Jung-Man Nam. Evaluation of unit skin friction to large size pneumatic caisson during the process of sinking. In *The Fifteenth International Offshore and Polar Engineering Conference*. International Society of Offshore and Polar Engineers, 2005.

WP Hong and AJ Sung. Estimation method of skin friction of pile. *Proc. of Korean Society of Civil Engineers (I)*, pages 427–443, 1987.

ST. Horseman, M.G. Winter, and D.C. Entwistle. *Geotechnical characterization of boom clay in relation to the disposal of radioactive waste*. Commission of the European communities, Nottingham, United Kingdom, 1987.

ing. Kees Huisman. Bijzondere belastingen op onderwaterbeton, 2013.

M.W. Kamerling and W.J. van den Boogaard. Caissonmethode voor diepe kelders in de utiliteitsbouw. *Cement Online*, 1986(2), 1986.

G.J. Kleefmann. *Inleiding ondergronds bouwen*. COB, 2002.

Katsumi Kodaki, Masanori Nakano, and Satoshi Maeda. Development of the automatic system for pneumatic caisson. *Automation in Construction*, 6(3):241–255, 1997. ISSN 0926-5805. doi: http://dx.doi.org/10.1016/S0926-5805(97)00007-1. URL http://www.sciencedirect.com/science/article/pii/S0926580597000071.

Dimitrios Kolymbros. *Tunnelling and Tunnel Mechanics*, book section 10, pages 203–209. Springer Berlin Heidelberg, 2005. ISBN 978-3-540-25196-5. doi: 10.1007/3-540-28500-8_10. URL http://dx.doi.org/10.1007/3-540-28500-8_10.

Korea Highway Corporation. Yeong jong bridge, 2002. URL http://www.yeongjongbridge.com/english/young/habugon/03-new17.asp. visited on: 2014-06-27.

ir. M.R. Kraneveld, dr.ir. R.A. Vonk, and ir. J.C.W.M. de Wit. Uitvoering in pneumatische caissons. *Cement Online*, 2004(2), 2004.

LievenseCSO. Systeemontwerp bijlage 4; analyse rapport type deuren dossier c-d. Internal report, January 2014a.

LievenseCSO. Bijlage 3 - uitwerking bouwmethodes. Internal report, August 2014b.

LievenseCSO. Systeemontwerp (systeemdocumentatie). Systeemontwerp dummy dossier D, 2014c.

LievenseCSO. Ontwerp sluisconstructie en kademuren. Internal report, August 2014d.

LievenseCSO. Fugro grondeigenschappen. Data file, December 2014e.

LievenseCSO. Notitie rijkwijdte en detailniveau, 2014f. URL http://zeesluisterneuzen.nl/sites/default/files/downloads/Notitie%20Reikwijdte%20en%20Detailniveau.pdf. VNZT-R-020-3-NRD.

LievenseCSO. Grondwaterstanden en stijghoogtes tbv ontwerp civiele constructie sluis. Internal report, July 2014g.

ir.R. van Limbergen. Cad-techniek bij ontwerp waterkrachtcentrale linne. *Cement Online*, 1988 (9), 1988.

Americas Cement Manufacturers. Prestressed concrete, 2015. URL http://www.cement.org/cement-concrete-basics/products/prestressed-concrete. visited on: 2014-26-02.

GG Meyerhof. The ultimate bearing capacity of foundatons. *Geotechnique*, 2(4):301–332, December 1951.

Dale Miller. Construction methods. In *2nd International Workshop*. PIANC, September 2011. URL http://docs.pianc.us/smart11/docs/PIANC-LOCKS-WORKSHOP_SEPT_2011_(ABSTRACTS).pdf.

Ministerie van Infrastructuur en Milieu. The amsterdam metro, 2008. URL http://publicaties.minienm.nl/download-bijlage/13287/c5815-deel-7.pdf. visited on: 2014-06-23.

G Modoni, P Croce, and L Mongiovi. Theoretical modelling of jet grouting. *Geotechnique*, 56(5): 335–347, 2006.

W.F. Molenaar. *Locks, Hydraulic Structures*. TU Delft, March 2011.

NEN 6740. *Geotechniek - Basiseisen en belastingen*, September 2006. URL http://www.nen.nl/NEN-Shop/Norm/NEN-67402006-nl.htm.

NEN 6745-1. *Geotechniek - Berekeningsmethode voor funderingen op palen*, December 2006. URL http://www.nen.nl/NEN-Shop/Norm/NEN-674312006-nl.htm.

NEN 9997-1+C1:2012. *Geotechnisch ontwerp van constructies - Deel 1: Algemene regels*, April 2012. URL http://www.nen.nl/NEN-Shop/Norm/NEN-99971C12012-nl.htm.

NEN-EN 1992-1-1. *Eurocode 2: Ontwerp en berekening van betonconstructies*, November 2011. URL http://www.nen.nl/NEN-Shop/Norm/NENEN-199211C22011-nl.htm.

Ervin Nonveiller. Open caissons for deep foundations. *Journal of geotechnical engineering*, 113(5): 424–439, 1987. ISSN 0733-9410.

NV Westerscheldetunnel. De westerscheldetunnel: Megaproject met grensverleggende boortechniek, April 2001.

Omran Ista. Foundation technology - diaphragm wall, 2014. URL http://www.omranista.com/eng/tech5.php. visited on: 2014-08-13.

Oraukia Tech. Pneumatic caisson unmanned operation excavator, 2009. URL http://www.oraukia.com/en/pro_info.asp?bid=133&id=44. visited on: 2015-02-09.

Cees Ouwendijk. Een metro in amsterdam, Oktober 1977.

Fang-Le Peng, Hai-Lin Wang, Yong Tan, Zheng-Liang Xu, and Yao-Liang Li. Field measurements and finite-element method simulation of a tunnel shaft constructed by pneumatic caisson method in shanghai soft ground. *Journal of Geotechnical and Geoenvironmental Engineering*, 137 (5):516–524, 2010.

Ir R. Pepers. Pneumatische caissons noord zuidlijn amsterdam. In *Koersief*. Heijmans Civiel, October 2011.

Zsolt Rémai. Correlation of undrained shear strength and cpt resistance. *Civil Engineering*, 57(1): 39–44, 2013.

Rijkswaterstaat. Waterstanden terneuzen, 2011. URL http://www.rws.nl/images/TERNZN_tcm174-335725.pdf. visited on: 2014-07-02.

A. W. Skempton. The bearing capacity of clays. 1951.

Bart Stam. De metro die nooit afkwam, August 2005. URL http://www.technischweekblad.nl/de-metro-die-nooit-afkwam.74521.lynkx. visited on: 2014-09-22.

Jaap Steketee. Zware metalen, July 2007.

Karl Terzaghi. *Soil mechanics in engineering practice*. John Wiley and Sons, 1996. ISBN 0471086584.

TNO. Het effect van een vries-dooi cyclus op het mechanische gedrag van de klei van boom bij de westerscheldetunnel, June 1998.

Michael John Tomlinson. *Foundation design and construction*. Pearson Education, 2001. ISBN 0130311804. URL http://www.scribd.com/doc/129581419/tomlinson-foundation-design-and-construction.

Tung Feng. Diaphragm walls and rectangular piles, 2009. URL http://www.tungfeng.com/contruction/diaphragm-walls-and-rectangular-piles/. visited on: 2014-10-31.

Gauthier van Alboom, Jan Maertens, Hilde Dupont, and Koen Haelterma. Glauconiethoudende zanden. *Vakblad Geotechniek*, april 2012.

VN Vijayvergiya and JA Focht. A new way to predict the capacity of piles in clay. In *Fourth Annual Offshore Technology Conference, Houston*, volume 2, pages 865–874, 1972.

dr.ir. A. Vrijburcht. *Design of locks*. Ministry of Transport, Public Works and Water Management, June 2000. ISBN 90-369-3305-6.

prof.ir.drs. J.K. Vrijling. *Manual Hydraulic Structures*. TU Delft, February 2011.

VSF. Open caissons, 2014. URL http://www.vsf.nl/nl/funderingen/overige-funderingstechnieken/open-caissons-afzinken. visited on: 2014-09-19.

prof.dr.ir. J.C. Walraven. *Reinforced Concrete*. TU Delft, January 2011.

Zhenliang Xu, Fangle Peng, Yong Tan, and Hailin Wang. Parametric studies of ground deformation induced by pneumatic caisson construction in soft soils. In *Geoenvironmental Engineering and Geotechnics*, pages 63–70, 2010.

Geu-Guwen Yea and Tae-Hyung Kim. Vertical cutting edge forces measured during the sinking of pneumatic caisson. *Marine Georesources and Geotechnology*, 30(2):103–121, 2012. ISSN 1064-1190.

Yeo-Won Yoon. *Static and dynamic behavior of crushable and non-crushable sands : validation of stress-dilatancy theory*. Rijks Universiteit Groningen, Faculteit Toegepaste Wetenschappen, 1991.

APPENDICES

A

BOUNDARY CONDITIONS

A.1 SURFACE ELEVATION

In section 3.1 the surface elevation was given. On the map of figure 3.1 three profiles were indicated. The first cross section, C1 is located 200 meters south of the middle lock. The second cross section, C2, is located at the same height of the western lock. The last cross section, C3, is located at the inner head of the western lock. The cross sections are presented in respectively figure A.1, A.2 and A.3

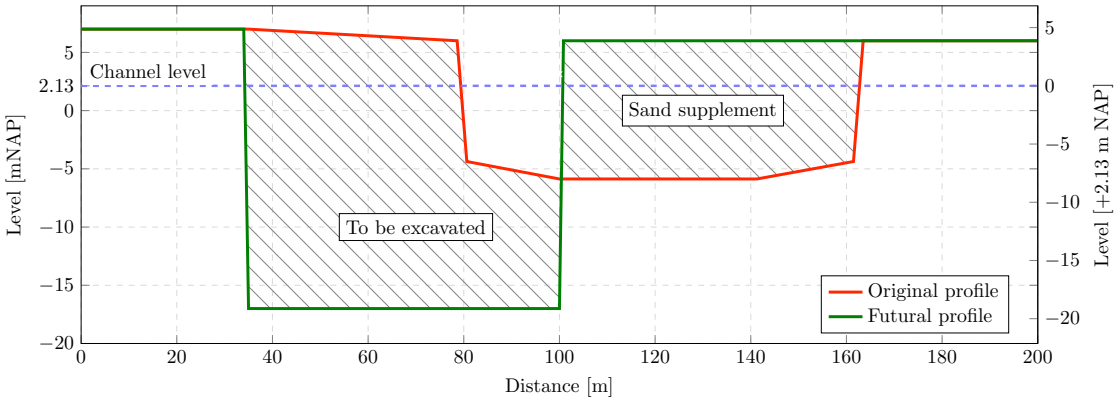

Figure A.1: *Cross section C1*

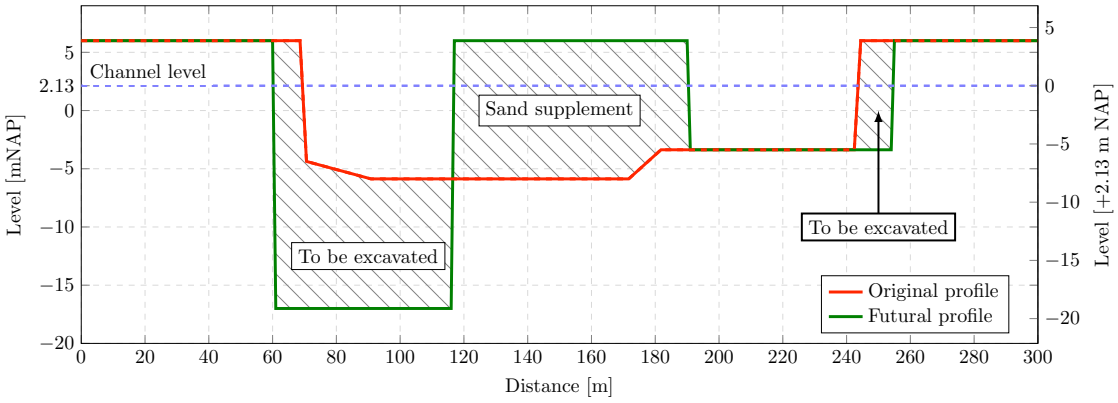

Figure A.2: *Cross section C2*

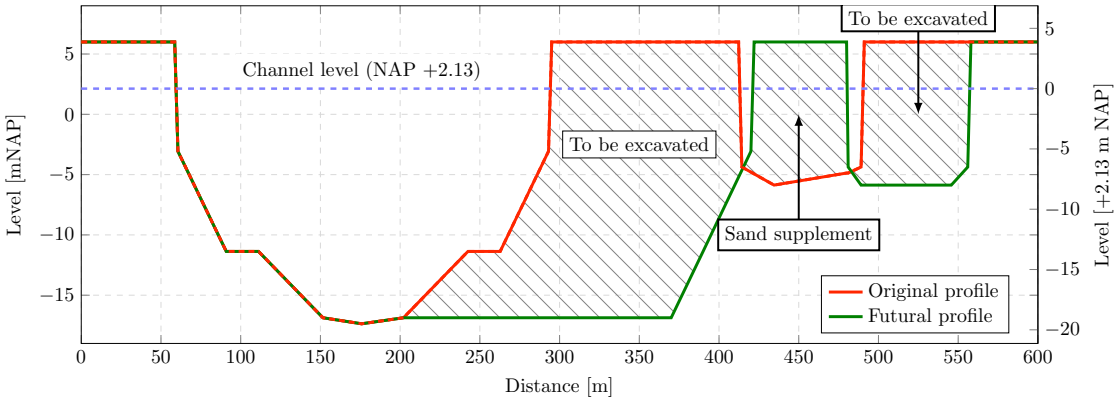

Figure A.3: *Cross section C3*

The normative depth of the channel is NAP -11.37 meter.

A.2 SOIL PROPERTIES

A.2.1 DINOLOKET

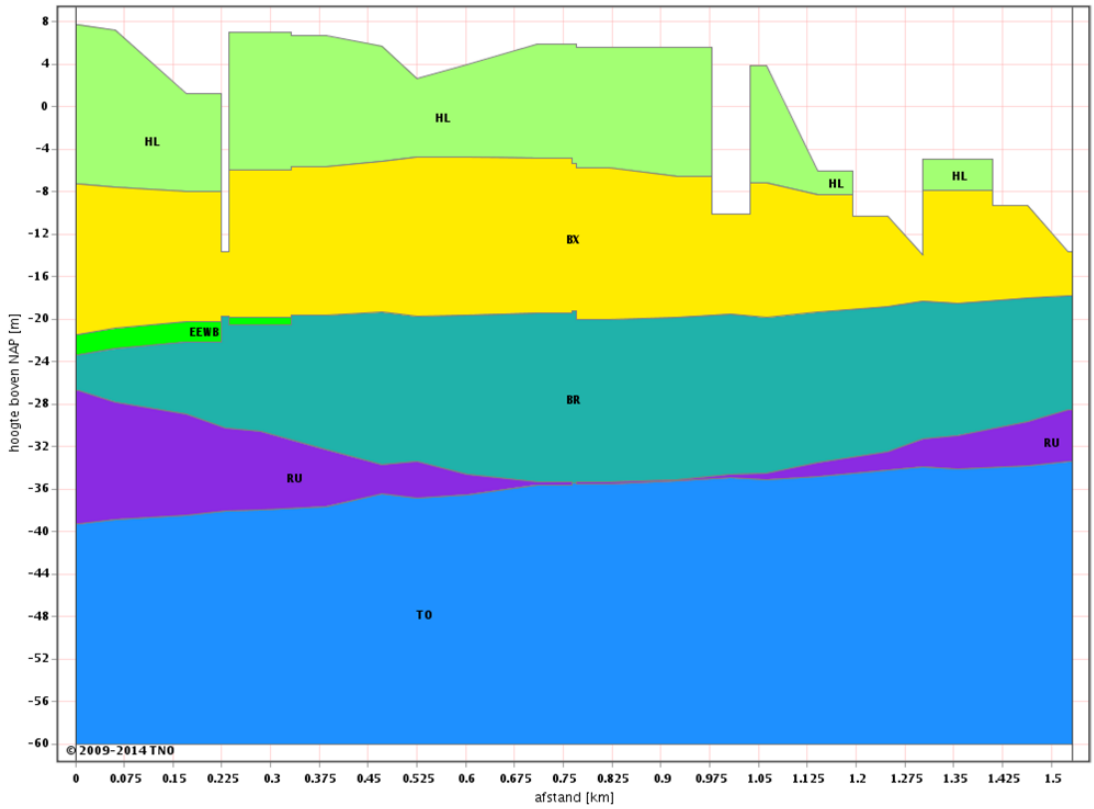

Figure A.4: *Cross section of the soil profile at the location of the new lock*

A.2.2 CPT

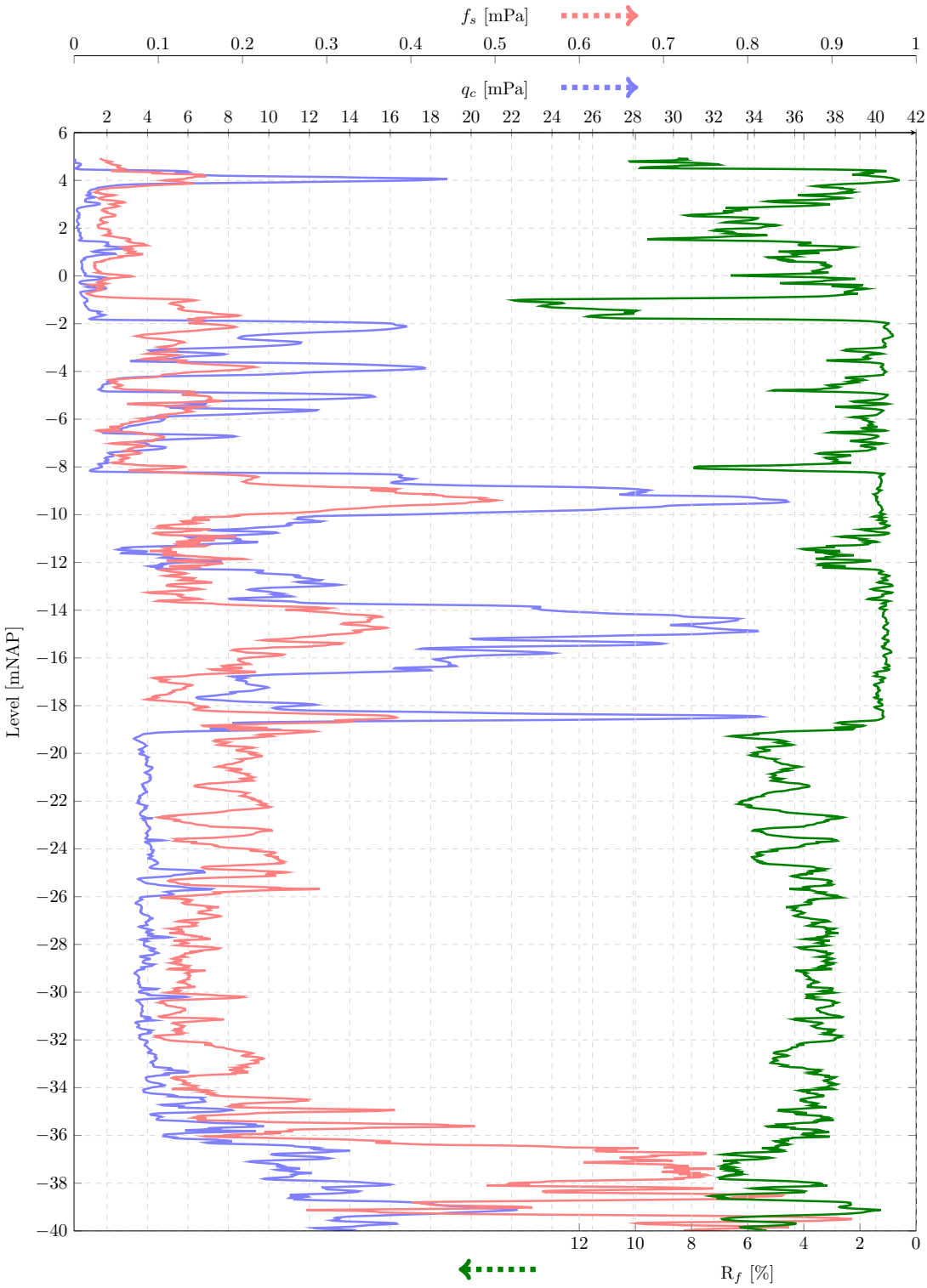

Figure A.5: *Results of cone penetration test [LievenseCSO, 2014c]*

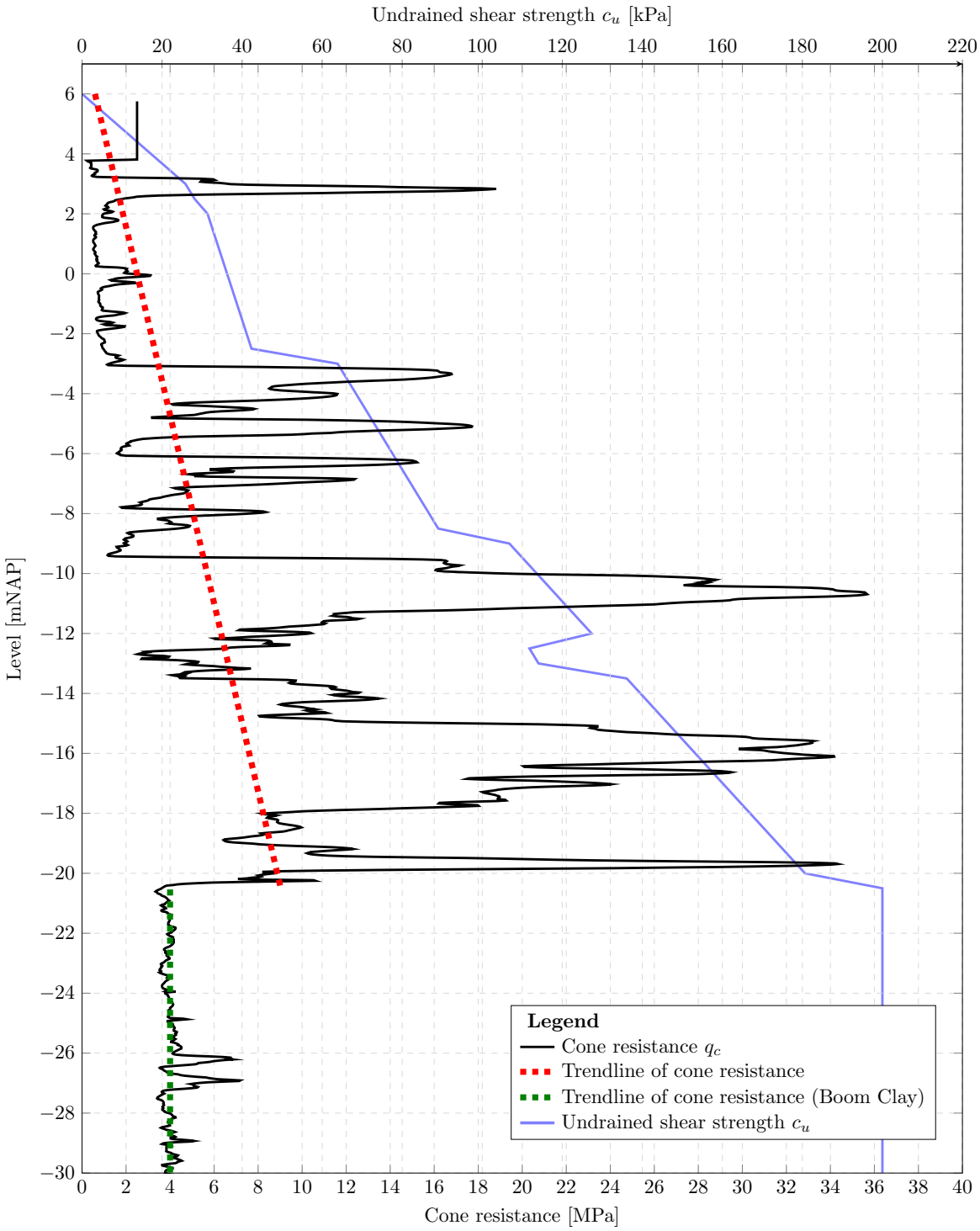

Figure A.6: *Results of cone penetration test [LievenseCSO, 2014c]*

A.2.3 SOIL PARAMETERS

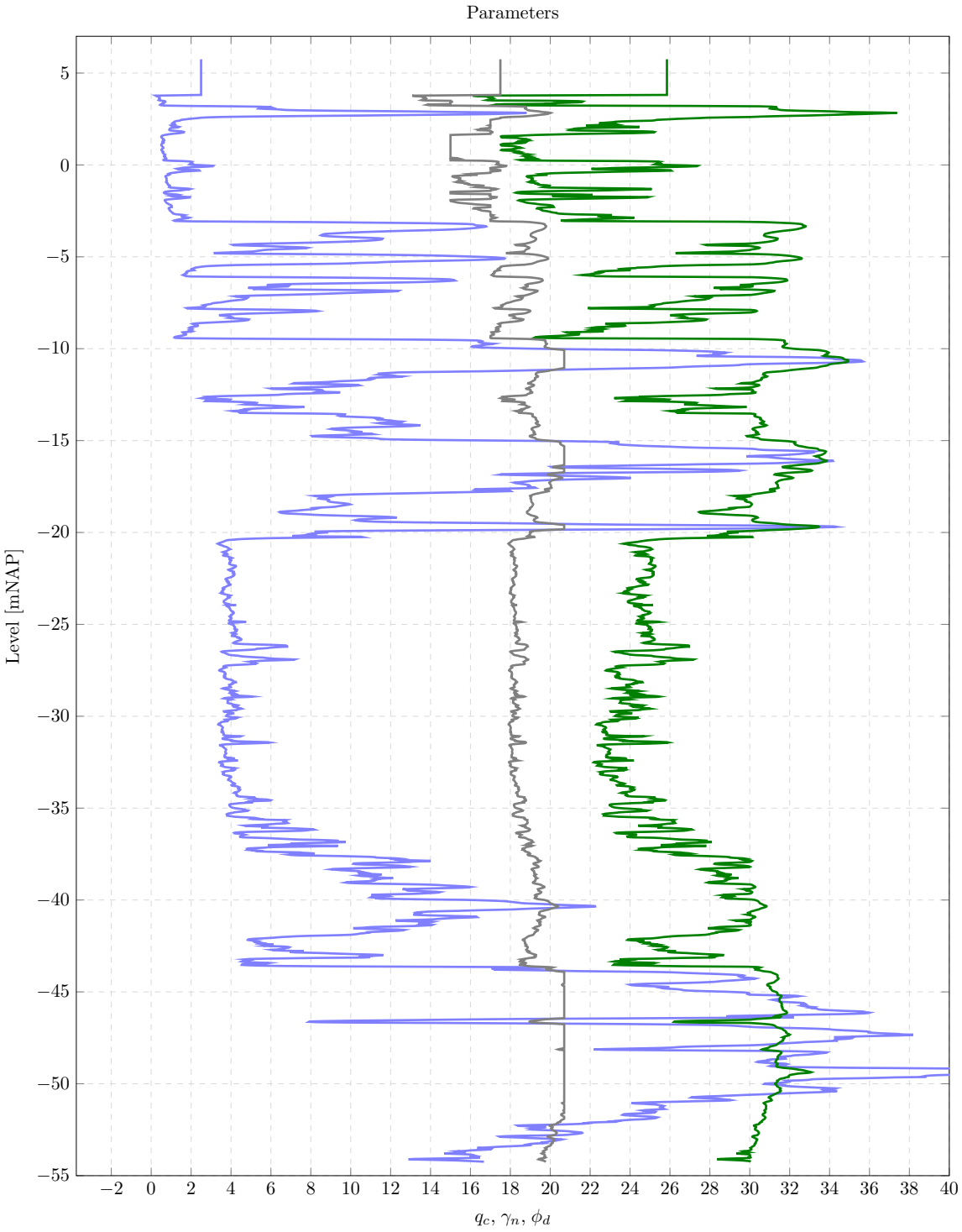

Figure A.7: *Soil properties at proposed location southern lock head [LievenseCSO, 2014c]*

A.3 LOCK GATES

There are three types of gates that are considered for the construction of the new lock, each with its own dimensions. The gate types considered are:

- Rolling doors
- Bascule rolling doors
- Curved rolling doors

In the following sections these gates are elaborated further.

A.3.1 ROLLING DOOR

A rolling door is a flat upright door construction that closes perpendicularly to the water flow direction. The hydraustatic loads on the gate are transferred to the chamber walls. Rolling gates can retain the water in two directions. An adjacent compartment is present at one side of the lock head, called the gate chamber. On the other side a gate recess is present. The gate rests on two or multiple roller carriages. The carriages are guided along rails. The gate is guided along the rails with sliding guides while the horizontal guiding wheels at the top keep the gate in vertical position during movement. Usually the gate is equipped with float control chambers, which result in decreased load on the roller carriages. Advantages of this type of gate are the light operating mechanism and the little required amount of space required in the length of the lock. Disadvantages are the required space in the width of the lock head. When the gate is open it must be completely stored in an adjacent compartment. In a previous design proposal it has been established that two gates per lock head are required. This design choice will not be elaborated further. A gate 10 meter thick and 60 meter in length is assumed. In a closed position on both sides 2.5 meter is present to transfer the hydraulic forces on the lock gate. The walls are assumed 3.5 meter in width. In the gate compartment a clearance of 1 meter is present to store the guiding equipment. A schematisation of this type of gate and all dimensions are given in figure A.8, A.9 and A.10

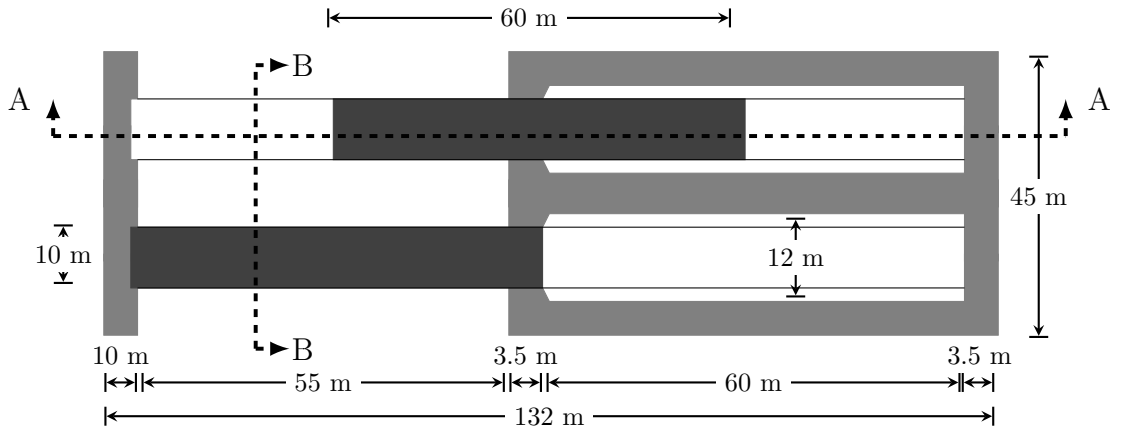

Figure A.8: *Plan view of the rolling door concept with corresponding dimensions*

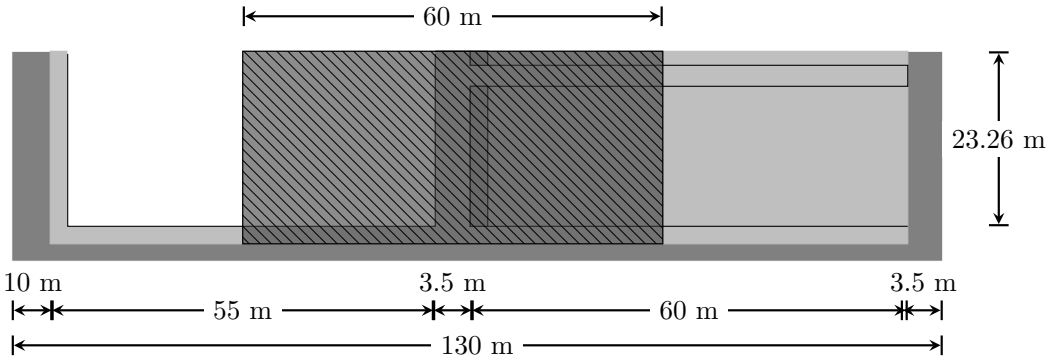

Figure A.9: *Longitudinal cross-section A-A of the rolling door*

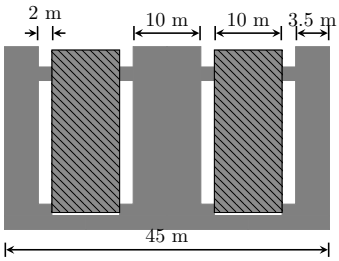

Figure A.10: *Longitudinal cross-section B-B of the rolling door*

A.3.2 BASCULE ROLLING DOOR

The bascule rolling gate is a new type of lock gate which combines a conventional rolling gate with the mechanical principle of a rolling bridge. In this case the lock gate is suspended above to a constructive cantilevered girder which can be moved by means of two rolling tracks. The constructive girder is being integrated in the lock gate design. Contrary to a conventional rolling gate, a rolling bascule bridge has no rolling tracks on the bottom of the lock, but these are situated in position on top of the lock above the waterline. Therefore the revision, accessibility and maintenance of the rolling tracks is better and can be much easier. The door is solid fixed to the trolley-structure. For this type of door a larger adjacent area is required because in this case not only the door but also the mounted trolley structure should be completely stored in an adjacent compartment when the door is opened. The width of the compartment were the door is stored remains the same. There is little to no difference between the two above described types of gates. Both needs a rectangular building pit. Only the length and thereby the ratio length divided by width is different. [Boorsma B.V.] The trolley-structure is assumed to be equal to half the length of the gates. A schematisation of the bascule rolling door and all dimensions are given in figure A.11, A.12 and A.13. Where in the last figure the forces at the supports are schematised as red arrows.

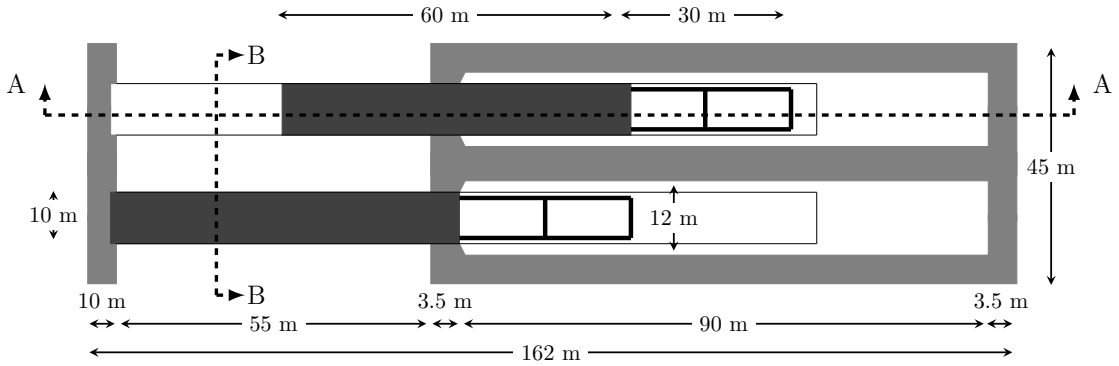

Figure A.11: *Plan view of the bascule rolling door concept with corresponding dimensions*

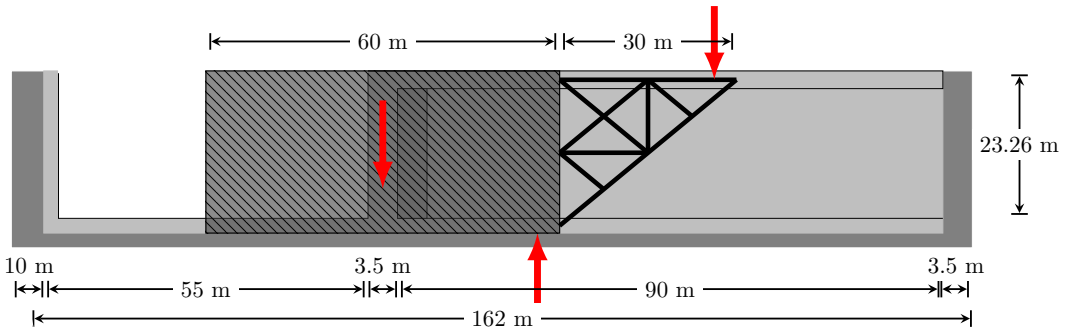

Figure A.12: *Longitudinal cross-section A-A of the bascule rolling door*

Pneumatic caissons with (a partly) inclined bottom plate are not previously constructed. Therefore also the variant of figure A.13 can be used. However a large unused space is created

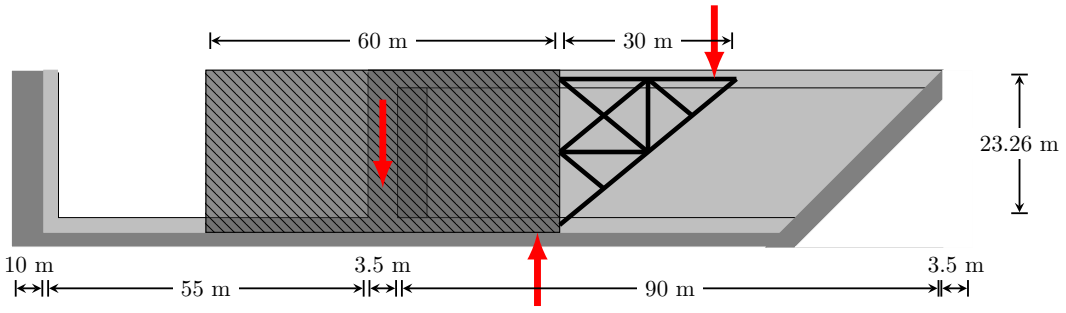

Figure A.13: *Longitudinal cross-section A-A of the bascule rolling door (straight bottom plate)*

A.3.3 CURVED ROLLING DOOR

The third and last option for a gate design in the new lock of Terneuzen is a curved rolling door. The idea behind this option is the same as in the first gate design. Only when using a curved variant less space adjacent to the lock is needed because of the smaller dimensions. However

the length of the compartment is smaller, the width of the compartment is larger because of the curved shape. Thereby the ratio length over width is different, the shape of the compartment is more like a square instead of a rectangular as in the previous two gate designs. In figure A.14 a schematisation of the gate design is given.

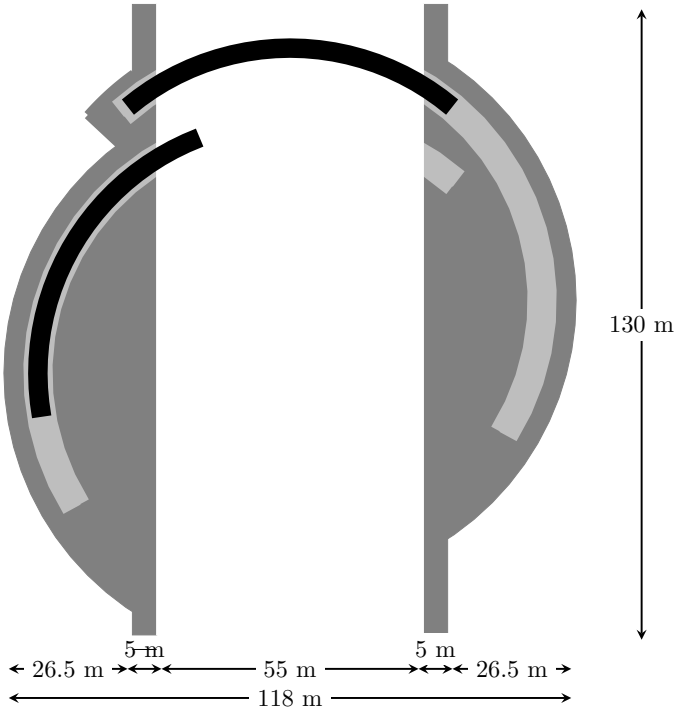

Figure A.14: *Dimensions of the curved rolling door concept*

A.4 LOCATION OF THE CAISSONS

The location of the caisson is given in figure A.15 a cross section at the location of the lock head is given in figure A.16.

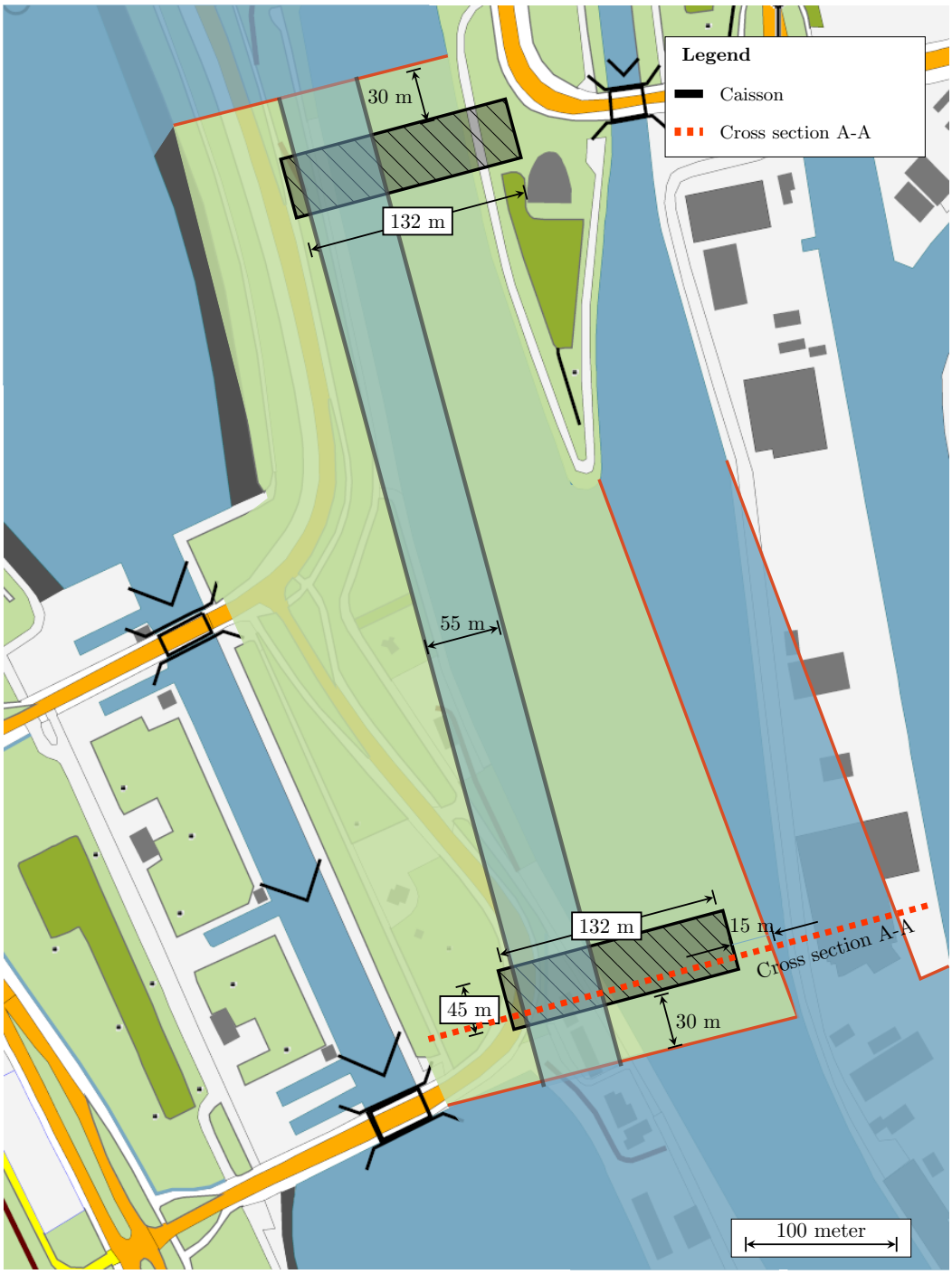

Figure A.15: *Location of the caissons*

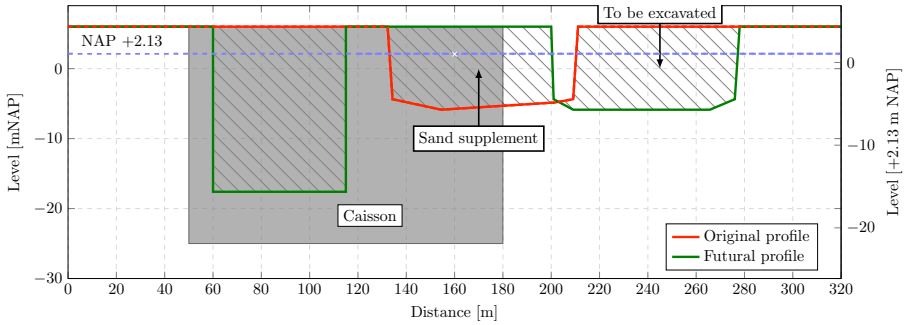

Figure A.16: *Cross section A-A*

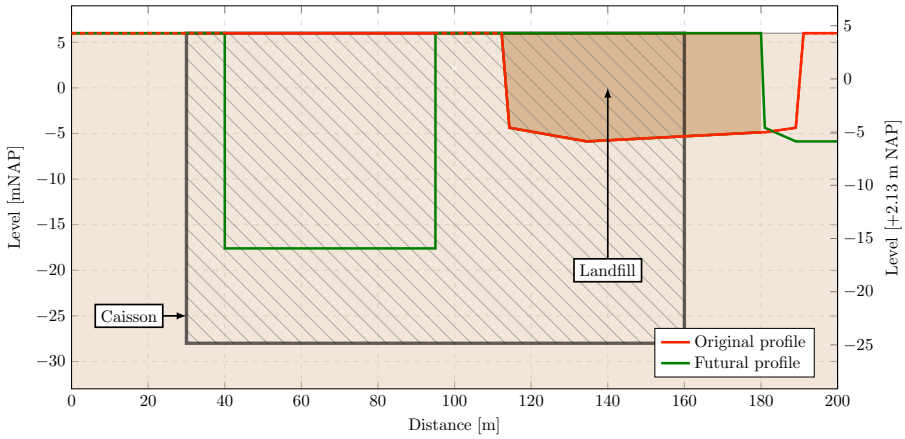

Figure A.17: *Difference in soil composition cross section A-A*

B

SOIL

B.1 SOIL TYPES

B.1.1 GLAUCONITE SANDS

The term glauconite was originally derived from the Greek word of Glaucos, which means blueish or green. The characteristic green color of glauconite is caused by the content of iron. [van Alboom et al., 2012]

Glauconite is a small, dark-green colored, clay-mineral and can be found on a lot of different places and can be compared with a mineral called Mica. [NV Westerscheldetunnel, 2001] Glauconite indicates that the sand body has been formed in a marine environment. Glauconite grains do have the same dimensions as the parts of the quartz grains. Through an sieve analysis, sands containing glauconites will be classified as sands. When comparing glauconite sands with sands only consisting out of silica the same granulometric properties can be bound. Due to the presence of glauconite grains in sand, The inner-sand will behave differently because the glauconite grains. The pores of the sand will influence the grain skeleton as soon as deformation takes place. The sand will behave due to the presence of glauconite grains more plastic and shows a different deformation behaviour. In some cases the sand will reacts as clay.

According to Mohs hardness rating, glauconite has a relatively low hardness of 2, The mineral silica has with a relative hardness value of 7 a much larger resistance to mechanical deformation than the glauconite grains have. [Yoon, 1991] When some force is acting on glauconite containing sands, the grains can be deformed and crushed easily. This has a major impact on the geotechnical properties of sand which contains high values of glauconite.

The behavior of soil containing glauconite is evolving from sandy to clayey. Also remnants from shells and fine gravel are common in glauconite sands. The pore water in this kind of sands contains always iron.

B.1.2 BOOM CLAY

The Boom clay which is part of the Formation of Rupel. This formation is deposited in the Early and Middle Oligocene, approximately 35-30 million years ago. The Boom clay layer can be characterised as very stiff to hard. The thickness of the Formation of Rupel was originally larger than the current thickness. Erosion during the Oligocene (23 to 34 million years ago) and over-consolidation are both the cause of this high stiffness. [Brugge and Vrouwe, 1996] It is important to note that the Boom Clay behaviour is characterised by a highly non-linear stress-strain response. [Bernier et al., 2007]

The Boom clay is a typical clay soil which can be determined easily from a CPT. It will be characterised by a almost constant cone tip resistance of 4 MPa and a friction number of 3 – 5 %. Boom clay has an OCR (Over Consolidation Ratio) of 2.4. [Horseman et al., 1987]

B.2 TOXICITY OF SANDS CONTAINING GLAUCONITE

From the soil layer composition and parameters of table 3.1 on page 14 and the calculations in the report it can be concluded that the bottom of the building pit and bottom of the caisson structure does not come in contact with the sands containing glauconite. It was assumed that these soil parameters were uniform over the total length of the lock. Actually the depth of the sand containing glauconite is not uniform distributed over the length of the lock and on the location of the northern lock head this layer is located much shallower.

The general chemical formula of the mineral glauconite is:
$(K \cdot Na)(Fe \cdot Mg \cdot Al)_2(Si \cdot Al)_4O_{10}(OH)_2$. In the general formula, we find the most important elements from which the glauconite mineral is composed. However, glauconite shows also a large *cation exchange capacity*. This is the capacity of the subsoil to exchange positive ions with the soil. This results in a high adsorption capacity for various heavy metals like arsenic, lead, nickel, zinc and chromium. [van Alboom et al., 2012]. Without any construction activities there is no risk on, for example, released arsenic because the environment is anaerobic. (without oxygen). However when operations in the subsoil are performed, the subsidence of a caisson, the risk on released arsenic and other heavy metals must be examined. The risk on poisoning can be divided in two groups. Direct poisoning of working men which can inhale the air which is contaminated with heavy metals in the working chamber. Metals are uncommon as volatile compounds, but if they are present, they represent a risk because the absorption via the lungs is much larger than through the gastrointestinal tract. This is the organ system responsible for consuming and digesting foodstuffs, absorbing nutrients, and expelling of waste. Another risk of poisoning with heavy metals is the consumption of contaminated water. This is only imaginable if the drinking water is drawn from a well in a contaminated area and the quality of the water is not checked. In addition, another indirect recording possibility is the consumption of crops which are sprayed with contaminated groundwater. [Steketee, 2007]

B.3 SKIN FRICTION

The downward movement of pneumatic caissons that are subsided into the ground are retaining by skin friction. Therefore concrete caissons are designed in such a way that the self-weight of the caisson exceeds the skin friction at every stage during submersion. To obtain smooth sinking of a caisson the ratio between the total self-weight of the caisson and the total amount of skin friction should have at least a factor of 2 following [Nonveiller, 1987]. Else a smooth sinking process of the caisson could be difficult. To fulfill both requirements the skin friction that could be expected by the submersion of a new caisson must be known.

In [Hong et al., 2005] different methods to evaluate the skin friction of a pneumatic caisson are treated. Discussed are the α -method, β- method, λ -method and K_0 -method. The α -method is originally proposed by [Tomlinson, 2001] to calculate the frictional resistance of piles in stiff clay layers. The skin friction is computed using the un-drained shear strength and an empirical adhesion factor which incorporates the ground condition, the embedded pile's diameter and

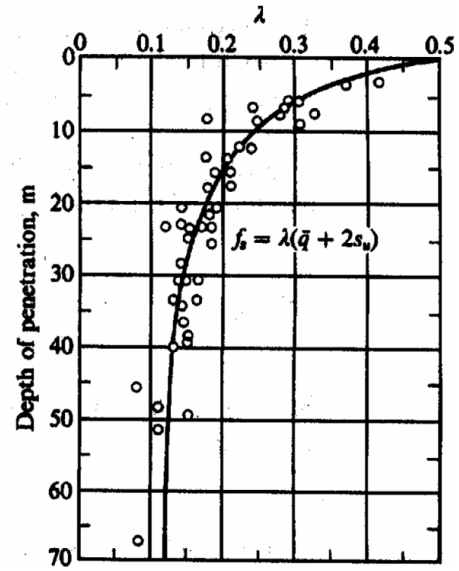

Figure B.1: *Values of the λ -coefficient.*

length of pile. To calculate the frictional resistance both two factors are multiplied with each other:

$$f_s = \alpha * c_u \quad \text{(Eq. 1)}$$

Following [Hong et al., 2005] some organizations concluded from existing data and new executed test that a better correlation of load test and computed pile capacity can be obtained using effective stress parameters. The soils near pile are over-consolidated and the un-drained shear strength is changed. Therefore, skin frictional resistance should deal with the effective vertical stresses. [Burland, 1973] suggested the following formula to calculate skin friction along piles in both cohesion and cohesion less soils:

$$f_s = K_s * q' * \tan(\delta) \quad \text{(Eq. 2)}$$

In this method it is assumed that the excess pore water pressures caused by volume displacement are essentially dissipated in time. Another method proposed by [Vijayvergiya and Focht, 1972] is based on the effective vertical stress and cohesion strength. Apart from this a dimensionless coefficient is introduced which is related to the penetration depth of a pile into marine clay.

$$f_s = \lambda(\bar{q} + 2 \cdot c_u) \quad \text{(Eq. 3)}$$

Values of the λ -coefficient can be found in figure B.1 Last method following [Hong et al., 2005] is the method of [Hong and Sung, 1987]. This method is also based on test with pile foundations and is based on the effective vertical stress (σ') and the undrained shear strength (c_u)

$$f_s = K_n * \sqrt{(\delta' * c_u)} \quad \text{(Eq. 4)}$$

Where $K_n$is a dimensionless skin friction coefficient which is dependent on effective vertical stress and undrained shear strength of soils. On basis of field tests the conclusion can be drawn that the skin friction is reduced in depth in a parabolic way. This is explicable because the

skin friction mainly depends on the soil-caisson interface and only at the bottom of the caisson there is contact between the soil and the caisson. Above the bottom a bentonite suspension decreases the skin friction significantly. Apart from this it can be concluded that the skin friction parameters predicted by the K_n-method are more in comparison with the measurement data obtained from a field test with a large size pneumatic caisson having a wide base than the skin friction parameters obtained by the λ-method. The α-method and β-method are in this research not compared with field measurements. In contrast to the theory and field test, due [Terzaghi, 1996], experience in the past has demonstrated that methods for evaluating the skin friction on the basis of soil tests are unreliable. The principal source of information for this statement are the forces measured during the start of subsidence of caissons that had become stuck in the ground. Following this records of forces below 8 meters of depth the values of skin friction measured per unit of contact area reached a constant value. Values that are measured during the sinking process of caissons are in line with the values obtained from labatorial tests but are not always equal. This is because the magnitude of the skin friction factor f_s is not only dependent on the soil properties but is also related with the shape of the lowest part of the caisson, the method of excavation and the size of the caisson. In table B.1 values for skin friction during the sinking of pneumatic caissons in practice are given.

Table B.1: *Skin friction values at different soils*

Type of soil	**Skin friction** f_s [kPa]
Silt and soft clay	8-30
Very stiff clay	50-100
Loose sand	13-35
Dense sand	13-35
Dense gravel	50-100

In fine grained soils, like silt and clay, friction between the soil and caisson can be reduced by using a smooth coating on the outside of the caisson. Test at the San Francisco Oakland Bay have showed that friction on the soil-caisson interface can be reduced up to 40% when a smooth coating was used.

In literature [Allenby et al., 2009] observed skin friction values achieved from real situations are given. These are shown in table B.2

Table B.2: *Observed skin friction in comparison with data from Terzaghi*

Site	**Dimensions** [m]	**Soil Conditions**	**Skin Friction**	
			Observed [kPa]	**Terzaghi** [kPa]
Lower Zambezi	11 × 6 × 38	Mainly sand	23	13-70
Howrah	55 × 25 × 32	Soft clay and sand	29	8-35
Kafr-el-Zayat	15.5 × 5.5 × 25	Sand and silt	19-26	8-35

When the last two columns are compared it can be seen that the observed skin friction values are in agreement with the practical range given by [Terzaghi, 1996]. Tests with finite-element software has indicated the importance of small skin friction forces on the interface soil - caisson

during subsidence of a pneumatic caisson. [Xu et al., 2010] conducted a research towards the settlement of the surface level outside the caisson and upheaval of soil inside the caisson in the working chamber. Settlements at surface level must be strongly reduced in area's in vicinity to buildings. To measure the relation between skin friction and settlements multiple scenarios were tested each with a different unit skin friction. For the reference scenario a skin friction of $f_s = 20$ kPa was used. To compare this value with other cases also test with $f_s = 0$, 10, 30 and 40kPa were performed.

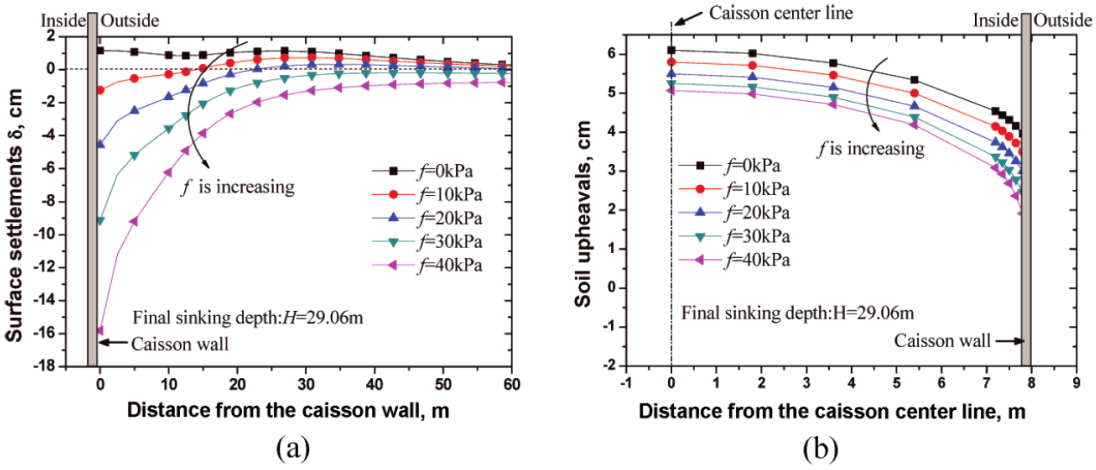

Figure B.2: *Measured settlements and upheaval with FEM-software.*

From figure B.2 it can be concluded that skin friction has an effect on the surface settlements. First analyzing the results of the settlements at surface level at the outer side of the caisson. It can be seen that the higher the skin friction is the higher the settlements will be. In this specific case when a uniform distributed skin friction of $f_s = 40$ kPa was applied a settlement of 16 centimeter was measured. On the other side, in a fictitious case where there exists no skin friction, the opposite happens and a upheaval of the soil of 1 centimeter is measured. The subsidence of a caisson influences the settlements at the surface level to approximately 2-3 times the underground height of the caisson. Second it can be concluded that skin friction do also cause soil upheaval inside the working chamber of the caisson. This would occur due to unloading. Although differences are small, they are actually there. Upheaval located in the center line of the caisson were more significant than the upheaval of soil at the caisson walls. It can be concluded in this case that the higher the skin friction values are the smaller soil upheaval is. In case of zero skin friction ($f_s = 0$ kPa) the soil upheaval in the center of the working chamber is approximately 6 centimeter. In the performed case where the skin friction was $f_s = 40$ kPa a soil upheaval of 5 centimeter in the center was measured. It can be seen that upheaval of soil beneath the caisson decreased in a linear way with the increase of f_s, but in a relatively gradual rate.

B.3.1 COMPARISON BETWEEN WALL FRICTION ACCORDING TO TERAGHI AND BURLAND

In addition to the calculations made in section 6.4.2 a comparison will be made between the wall friction calculations methods of Terzaghi and Burland in the case of Terneuzen. In this section, instead of the used formula of Burland, the skin friction will be calculated according to the

coefficients proposed by Terzaghi [Terzaghi, 1996]. He proposed different kinds of coefficients for different kinds of soils. The table with coefficients is given in table B.1. These factor are applied on the soil conditions at Terneuzen in table B.3

Table B.3: *Upper and lower bound values for skin friction according to Terzaghi [Terzaghi, 1996]*

Top level of layer	Description	Skin Friction	
		Lower bound [kPa]	Upper bound [kPa]
NAP +6	Top layer	8	30
NAP +2.5	Clay	8	30
NAP -3	Sand including clay	13	35
NAP -9	Sand	13	35
NAP -12.5	Sand including clay	13	35
NAP -13.5	Sand	13	35
NAP -20.5	Boom Clay	50	100

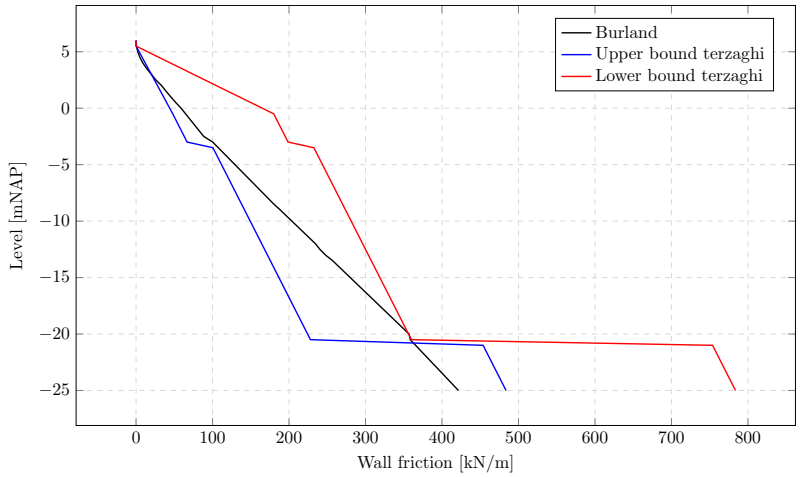

Figure B.3: *Wall friction over depth per running meter*

From figure B.3 it can be seen that the upward directed friction force is located between the upper and lower bound of the formula proposed by Terzaghi until a level of approximately NAP -20 meter. From this point on the Boom Clay layer begins and there is a major difference between the wall friction coefficients (f_s) in both methods.

B.4 BEARING CAPACITY OF FOUNDATIONS

As explained in the main part of this study the bearing capacity calculated according to [NEN 9997-1+C1:2012] is only a 5% lower limit of the bearing capacity. By decreasing the width of

the cutting edge and thereby the foundation surface at some point the load is larger than the capacity of the soil.

Before the bearing capacity can be calculated the influence depth must be known. The influence depth is the depth below the strip foundation or in this case cutting edge where the loads on the foundation do influence the soil conditions. The influence depth is dependent on the effective angle of internal friction (θ'_k) and the width of the foundation. The influence depth (z_e) can be calculated using table B.4 and is schematised in figure B.4.

Table B.4: *Influence factors [NEN 9997-1+C1:2012]*

θ'_k	z_e/b
5	0.77
10	0.88
15	1
20	1.16
25	1.35
30	1.59
35	1.9
40	2.33
45	2.95

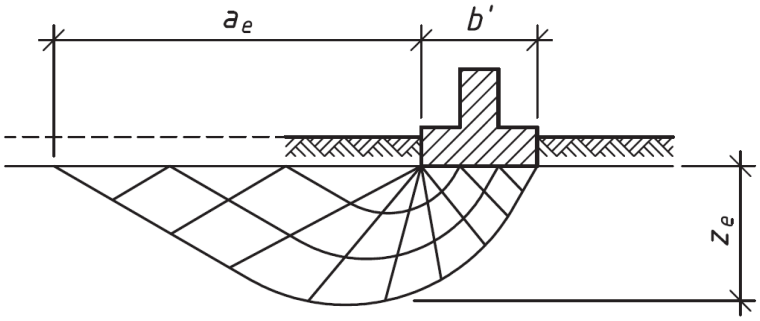

Figure B.4: *Schematisation of the influence depth and width [NEN 9997-1+C1:2012]*

For a cutting edge with around 4 meter wide the influence depth is situated between 4.5 and 6.5 meters. Because the influence depth depends on the angle of internal friction this also depends on the depth because the angle of internal friction depends on the depth. The depth of influence h_e is situated on a level z_e below the foundation depth d:

$$h_e = d + z_e \qquad \text{(Eq. 5)}$$

According to [NEN 9997-1+C1:2012] there are six different cases in which drained and undrained soil layers are located below the foundation. All possibilities are explicated in figure B.5.

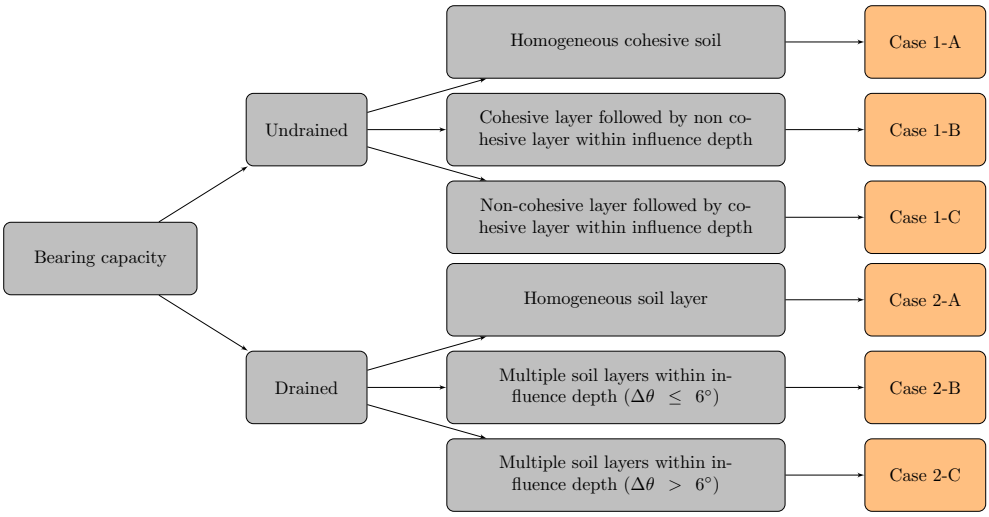

Figure B.5: *Different situations of cohesive and non-cohesive soils below the foundation and within the influence depth.*

Case 1-A

The soil between the surface of the foundation and the depth of in influence consist out of a homogeneous layer of cohesive soils. The maximum bearing capacity of the soil can be calculated according to formula Eq. 6.

$$\sigma_{max;d} = (\pi + 2) \cdot c_{u;d} \cdot s_c \cdot i_c + \sigma'_{v;z;d} \tag{Eq. 6}$$

Where $\sigma_{max;d}$ is the design value of the maximum foundation stress on the effective foundation surface. The undrained shear strength can be found in two different ways. From surface level towards the Boom clay layer the soil is normally consolidated and the undrained shear strength can be found according:

$$c_u = c \cdot \frac{\cos(\theta)}{1 - \frac{1}{3} \cdot \sin(\theta)} + \sigma_{eff} \cdot \frac{\sin(\theta)}{1 - \frac{1}{3} \cdot \sin(\theta)} \tag{Eq. 7}$$

Because the Boom Clay between NAP -20.5 and -38 meter is an overconsolidated soil the undrained shear strength can be determined using an empirical formula: [Rémai, 2013]

$$c_u = \frac{q_c}{20} \tag{Eq. 8}$$

The value of the cone resistance and the value of the undrained shear strength over depth can be found in section A.2.2. s_c is the shape factor for the influence of cohesion:

$$s_c = 1 + 0.2 \cdot \frac{w_{ce}}{L}$$

It is assumed that the load from the caisson is acting vertically on the soil. Therefore the reduction factor for the influence of cohesion obtained from an oblique force $i_c = 1$.

$\sigma'_{v;z;d}$ is the design value for the effective vertical soil stress caused by the ground cover at the construction level. These has a value between 0, absence of soil on the inner side of the working

chamber and the effective weight of 3 meter soil when the cutting edge is surrounded by soil as can be seen in figure B.6.

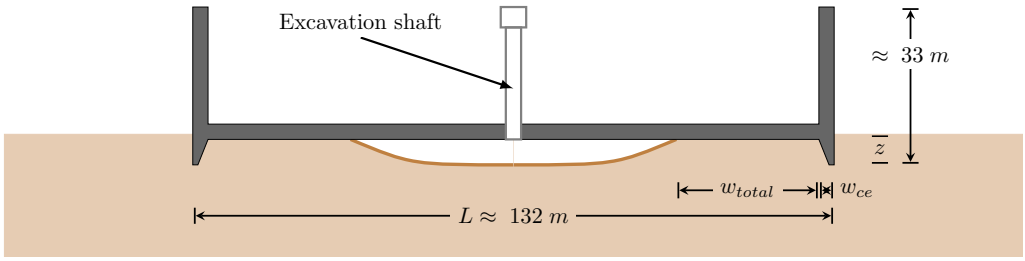

Figure B.6: *Schematisation of the caisson when the bottom slab is partly supported by the soil*

Case 1-B

Directly below the surface of the foundation a cohesive soil layer is present which is followed by a non-cohesive soil layer within the influence depth. This non-cohesive soil layer must be ignored and the cohesive soil layer with all its properties must be extended virtually to the depth of influence. The bearing capacity of the cohesive layer can be calculated according to formula Eq. 9.

$$\sigma_{max;d} = ((\pi + 2) + \frac{w_{ce}}{h_{sq}}) \cdot c_{u;d} + \sigma'_{v;z;d} \qquad \text{(Eq. 9)}$$

Where w_ce is the width of the foundation strip and h_{sq} is the height of the cohesive layer.

Case 1-C

Directly below the surface of the foundation a non-cohesive soil layer is present which is followed by a cohesive soil layer within the influence depth. The foundation must thereby be placed virtually at the top of the cohesive layer. During the check on punching, the width of the foundation surface must be spread with an angle of 8° with the vertical to ensure a load distribution on the upper side of the less stronger layer. Non-cohesive soil layers below this cohesive layer must be ignored and the cohesive soil layer with all its properties must be extended virtually to the depth of influence. The enlarged foundations surface on the virtually new depth is schematised in figure B.7

$$\sigma_{max;d} = (\pi + 2) \cdot c_{u;d} \cdot s_c \cdot i_c + \sigma'_{v;z;d} \cdot \frac{(\tan(8) \cdot d_{virt} \cdot 2 + w_{ce})}{w_{ce}} \qquad \text{(Eq. 10)}$$

Where d_{virt} is the distance between the actual depth of the cutting edge and the virtual depth of the cutting edge.

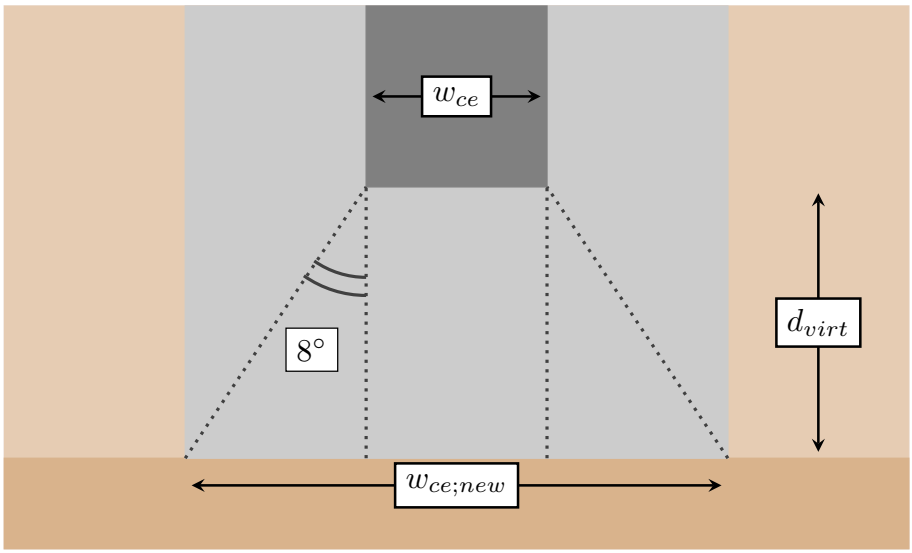

Figure B.7: *Location of the virtually deepened and widened foundation*

Case 2

The soil between the surface of the foundation and the depth of in influence consist out of a layer of non-cohesive soils. The maximum bearing capacity of the soil can be calculated according to formula Eq. 11.

$$\sigma_{max;d} = (c_{gem;d} \cdot N_c \cdot s_c \cdot b_c \cdot i_c) + (\sigma'_{v;z;d} \cdot N_q \cdot s_q \cdot b_q \cdot i_q) + (\frac{1}{2} \cdot \gamma'_{gem;d} \cdot w_{ce} \cdot N_\gamma \cdot s_\gamma \cdot b_\gamma \cdot i_\gamma) \quad \text{(Eq. 11)}$$

The parameters in the drained situation must be determined as weighted average between the foundation surface and the normative depth of influence. This applies to the factor of internal friction, cohesion and the effective unit weight of the soil. When the soil between the foundation level and the surface level consist out of a layer of homogenoeus soil the weighted average consist out of only the actual parameter.

$$\theta'_{gem} = \frac{\sum_{j=1}^{j=n} h_j \cdot \theta'_{j;d} \cdot X_j}{\sum_{j=1}^{j=n} h_j \cdot X_j} \quad \Rightarrow \quad \theta'_{gem;d} = \frac{\theta'_{gem}}{\underbrace{\gamma_\theta}_{\gamma_\theta = 1.15}} \quad \text{(Eq. 12)}$$

$$c'_{gem} = \frac{\sum_{j=1}^{j=n} h_j \cdot c'_{j;d} \cdot X_j}{\sum_{j=1}^{j=n} h_j \cdot X_j} \quad \Rightarrow \quad c'_{gem;d} = \frac{c'_{gem}}{\underbrace{\gamma_c}_{\gamma_c = 1.6}} \quad \text{(Eq. 13)}$$

$$\gamma'_{gem} = \frac{\sum_{j=1}^{j=n} h_j \cdot \gamma'_{j;d} \cdot X_j}{\sum_{j=1}^{j=n} h_j \cdot X_j} \quad \Rightarrow \quad \gamma'_{gem;d} = \frac{\gamma'_{gem}}{\underbrace{\gamma_\gamma}_{\gamma_\gamma = 1.1}} \quad \text{(Eq. 14)}$$

Where:

X_j	Distance between the center of the layer to the influence depth h_e	[m]
$\theta'_{gem;d}$	Design value for the weighted average of the angle of internal friction	[°]
h_j	Height of layer j	[m]
$\theta'_{j;d}$	Design value of the effective angle of internal friction for layer j	[°]
n	Number of layers between the bottom and the influence depth	[-]
$\theta'_{gem;d}$	Design value for the weighted average of the effective cohesion	[kPa]
$c'_{j;d}$	Design value of the effective cohesion for layer j	[kPa]
$\gamma'_{gem;d}$	Design value for the weighted average of the effective unit weight	[kN/m^3]
$\gamma'_{j;d}$	Design value of the effective unit weight for layer j	[kN/m^3]

In figure B.8 a schematisation of the parameters is given.

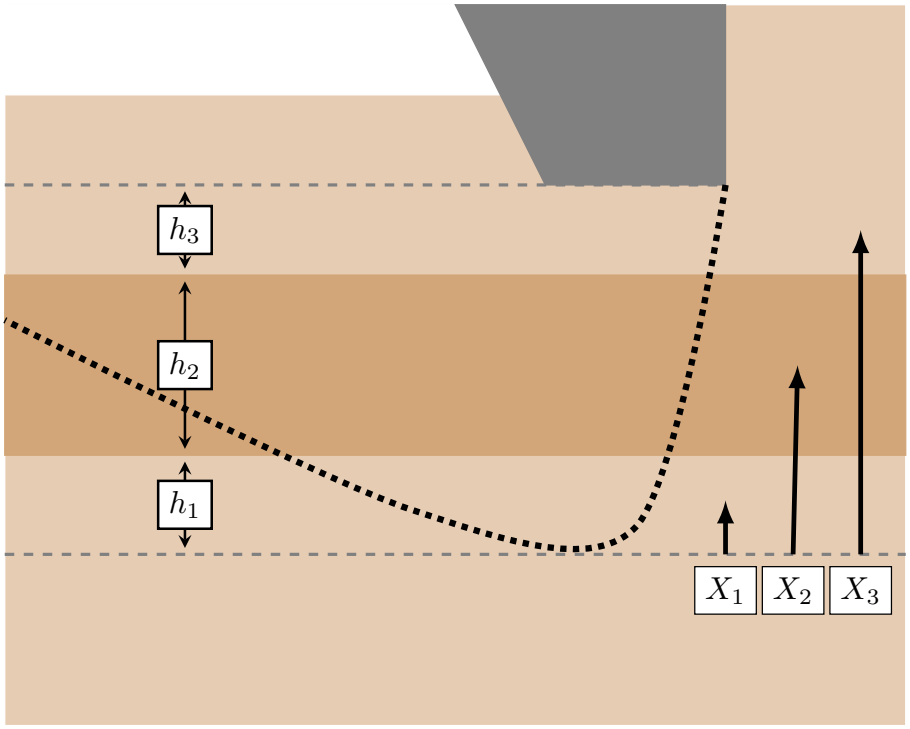

Figure B.8: *Schematisation of the parameters to calculate the weighted average*

Where N_c, N_q and N_γ are bearing capacity factors for respectively the cohesion, ground cover and effective unit weight of the soil below the foundation surface. These factors only vary on

the weighted average of the effective angle of internal friction. The bearing capacity factors can be calculated with formula Eq. 15.

$$\begin{aligned} N_c &= \frac{\cos(\theta'_{gem;d}}{\sin(\theta'_{gem;d})} \cdot (N_q - 1) \\ N_q &= e^{\pi \cdot \tan(\theta'_{gem;d})} \cdot \tan(45 + \theta'_{gem;d}/2)^2 \\ N_\gamma &= \tan(\theta'_{gem;d}) \cdot 2 \cdot (N_q - 1) \end{aligned} \tag{Eq. 15}$$

s_c, s_q and s_γ are shape factors also for respectively the cohesion, ground cover and effective unit weight of the soil below the foundation surface. These factors depend on the shape of the strip foundation, width (w_{ce}) and length (B) and angle of internal friction. These shape factors can be calculated using formula Eq. 16.

$$\begin{aligned} s_c &= 1 + 0.2 \cdot \frac{w_{ce}}{B} \\ s_q &= 1 + \frac{w_{ce}}{B} \cdot \sin(\theta'_{gem;d}) \\ s_\gamma &= 1 - 0.3 \cdot \frac{w_{ce}}{B} \end{aligned} \tag{Eq. 16}$$

b_c, b_q and b_γ are reduction factors for an inclined ground surface. However in this case a straight ground surface is supposed. The reduction factors i_c, i_q and i_γ must be applied in the presence of a horizontal load. In the case of the pneumatic caisson we suppose only vertical directed forces. Therefore these reduction factors do not apply and $b_c = b_q = b_\gamma = i_c = i_q = i_\gamma = 1$ (no reduction).

B.4.1 CHECK ON BASAL STABILITY

Apart from the calculations of the bearing capacity the caisson must be checked on basal stability. The downward directed force of figure B.9 my not exceed the resistance force caused by soil shear strength. Else undrained shear failure will occur.

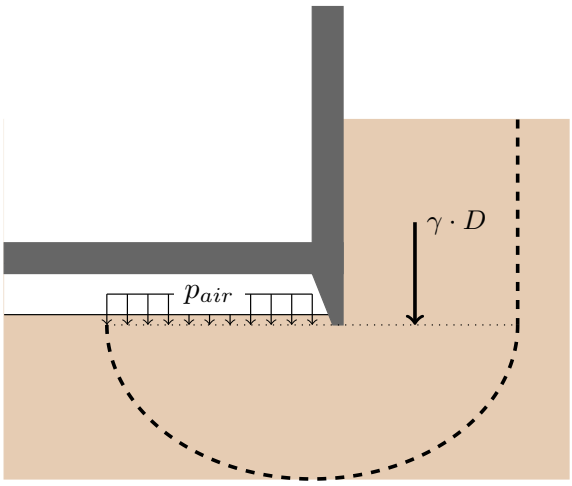

Figure B.9: *Schematisation of the forces causing an instability of the excavation*

The factor of safety for undrained shear failure can be calculated by dividing the resting forces on the inner side of the caisson by the driving forces from outside the caisson. [Bjerrum and Eide, 1956] proposed an equation for computing the factor of safety in cohesive soils based on the reverse bearing capacity problem. The formula includes the undrained bearing capacity equation of [Skempton, 1951]. Where the minimum value of the design pneumatic chamber pressure is equal to the hydrostatic water pressure at the level of the cutting edge.

$$N_c \cdot c_u + p_{air} \geqslant \gamma \cdot D = \sigma_{tot} \qquad \Rightarrow \qquad \frac{N_c \cdot c_u + p_{air}}{\sigma_{tot}} \geqslant 1 \qquad \text{(Eq. 17)}$$

The result is given in figure B.10.

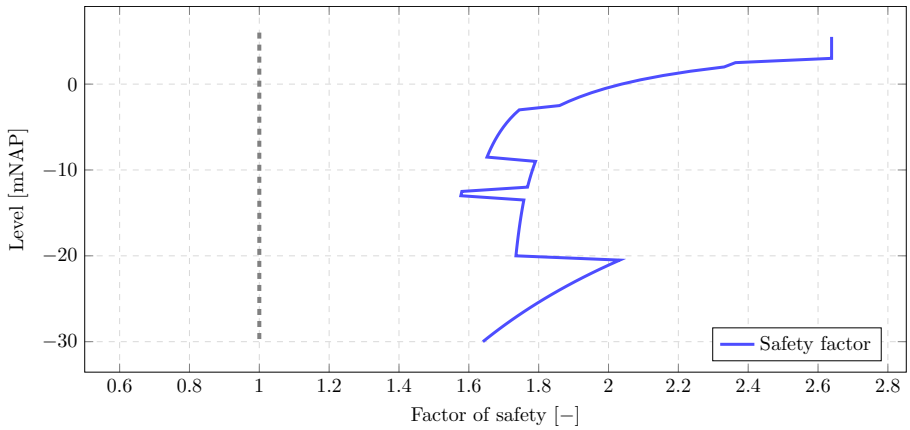

Figure B.10: *Safety factor for stability of excavation*

C

ALTERNATIVE CONSTRUCTION METHODS

C.1 CONSTRUCTION METHODS IN GENERAL

The lock head and –chamber must be able to absorb and transmit the ground and water loads as well as the forces that are caused by navigation. There are several possibilities and associated construction methods for the lock head and –chamber. Depending on local conditions some construction methods are more suitable than others. For this reason, a selection is made according to situations in which certain alternatives are suitable to a greater or lesser degree. These are in succession:

- Dimensions of the lock
- Waterlevels
  - Inside the lock chamber
  - Groundwater table
  - Hydraulic head
- Soil conditions
  - Strength
  - Permeability
- Presence of nearby structures
  - Possible settlements of those nearby structures
  - Available space for anchors
- Available construction materials and equipment
- Possible limitations to pumping
- Possibility of working below the water level

In the overview below, different construction methods for both the lock head and –chamber are given. Multiple designs are possible, depending on the conditions mentioned at the beginning of this section. Solutions can be divided in two groups. First group consist of options with an impermeable floor or seepage barrier. Water is not able to flow through the construction. This option can be considered when the soil is very permeable and (ground)water from outside the lock can otherwise easily flow under the retaining walls into the lock chamber. Also the opposite can occur when the groundwater table is relatively low and there is high water inside the lock.

Water from inside can easily flow out of the lock chamber. To prevent this an impermeable floor must be designed. An impermeable floor can consist of concrete elements which supports the lock chamber walls or consist off an impermeable geo-textile.

The other group consist of the permeable floors. When previous problems don't take any significant role. Bed protection is required to prevent erosion inside the lock and prevent collapse of the retaining walls by absence of the passive soil pressure. Permeable floors can exist out of a bed protection, or a concrete floor where holes are made in and are filled with gravel to get an equal water pressures under and above the floor.

C.1.1 SEPARATE CONSTRUCTIONS

In this section the options are listed where a temporary structure is used to construct the lock which is not a part of the final structure.

Slope combined width a seepage screen

Assumed that a deep impermeable layer is present which prevent a vertical flow of groundwater. A natural slope is combined with a seepage screen. This option can only be used when there is enough space to create a natural slope. Because of the available impermeable layer it is possible to de-water the construction pit between the seepage screens. This option is schematised in figure C.1

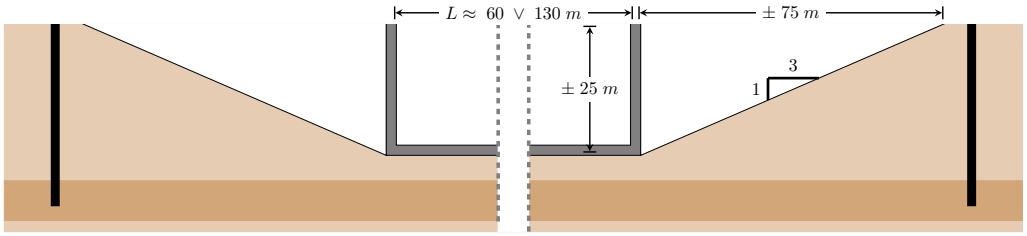

Figure C.1: *Schematisation of an open building pit*

Building pit in combination with an impermeable layer

In this case there is also a deep impermeable layer present. When there is a lack of space for a natural slope, a construction pit with help of sheet pile walls, combi-walls or diaphragms walls can be used. All methods do have their own benefits and disadvantages. For a diaphragm wall a large surface area is required for storage of reinforcement bars, desanding plant for bentonite etc. In this option there is no vertical flow of water by presence of the impermeable layer. This option is schematised in figure C.2

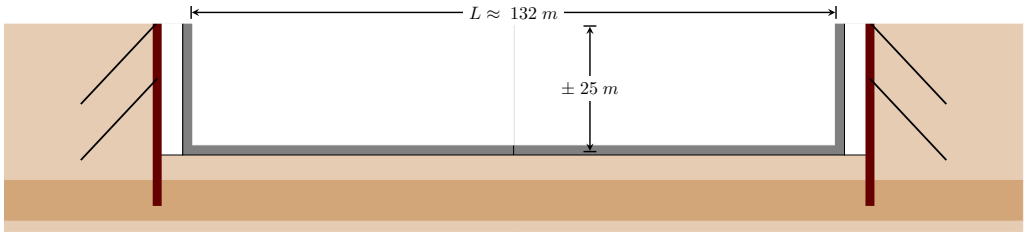

Figure C.2: *Schematisation of a building pit with an existing impermeable layer*

Building pit in combination with an underwater concrete floor

When there doesn't exists an impermeable layer as in the previous cases, an underwater concrete floor can be used to prevent groundwater flow. In this case the weight of the underwater concrete floor resists the upward water pressure. The retaining wall can be constructed as sheet pile–, combi– or diaphragm wall. This option is schematised in figure C.3

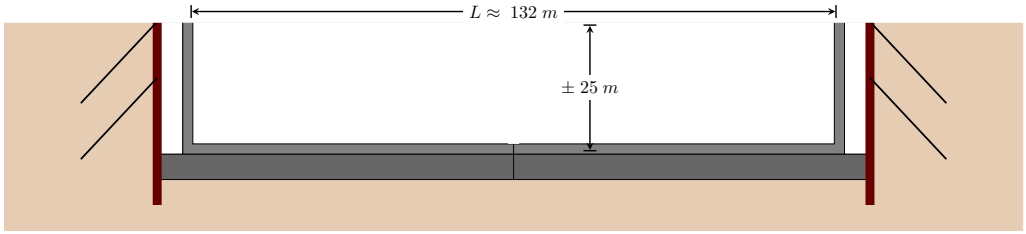

Figure C.3: *Schematisation of a building pit with an underwater concrete floor*

Building pit in combination with an underwater concrete floor (with tension piles)

This case is similar to the previous scenario, only here the underwater concrete floor is not able to prevent the upward water pressure. Therefore tension piles and/or anchors are helping to resist the upward soil and water pressure. This option is schematised in figure C.4

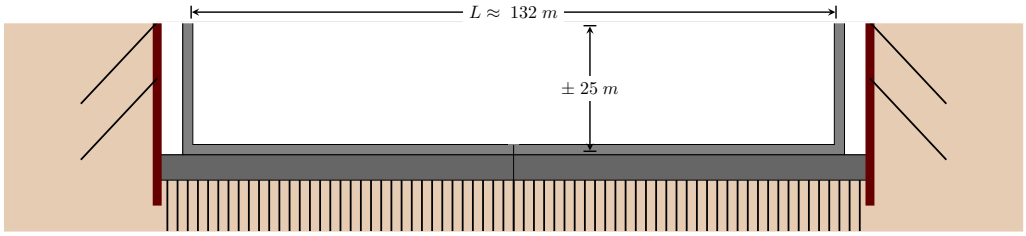

Figure C.4: *Schematisation of a building pit with an underwater concrete floor and tension piles*

C.1.2 BUILDING PIT/METHOD AS PART OF THE FINAL CONSTRUCTION

In continuation of the previous subsection in the following subsection the options are considered where the first initial structure is immediately part of the final structure.

Cofferdam

Another possibility to design the lock is with help of a cofferdam. Actually these are two sheet pile walls or combi-walls combined to each other. Because of the limited retaining height of a sheet pile wall only a cofferdam existing out of 2 combi-walls may be considered. The two combi-walls can be connected with help of struts or anchors to each other. This option is schematised in figure C.5

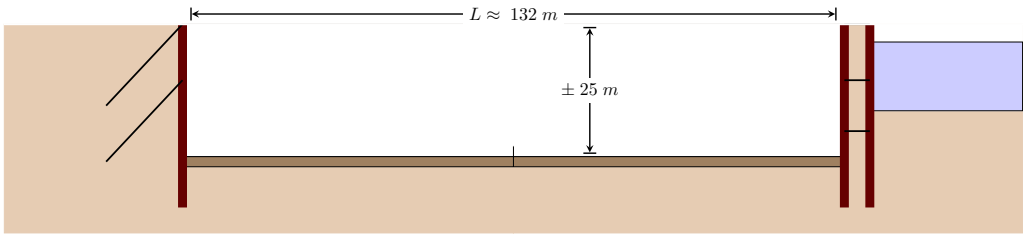

Figure C.5: *Schematisation of a cofferdam on the right side*

Sheet pile– or combi-wall (With underwater concrete)

Most of the times a sheet pile wall is used for construction with small retaining heights. When a sheet pile wall is not able to resist the occurring forces anchors and struts can be used to provide extra resistance against deformations and collapsing. The required stiffness of the retaining wall determines the amount of struts and anchors required. Another possibility is the use combi-walls. Combi-walls are commonly used by large retaining heights and to limit (unequal) subsidence of nearby structures. A combi-wall is a combination between a traditional sheet pile wall and circular steel tubes. Tubes are separated with two or three sheet pile walls. In this option the wall is thereby also part of the final construction. In this scenario the floor of the lock is constructed with help of an underwater concrete floor but it can also be constructed with help of a bed protection which is described in option 7. Special attention is needed for the lock heads. These requires a high stiffness. Due to corrosion the stiffness of the combi-wall degrades. When a lifetime of 100 years is required a very large combi-wall profile is required. This option is schematised in figure C.6

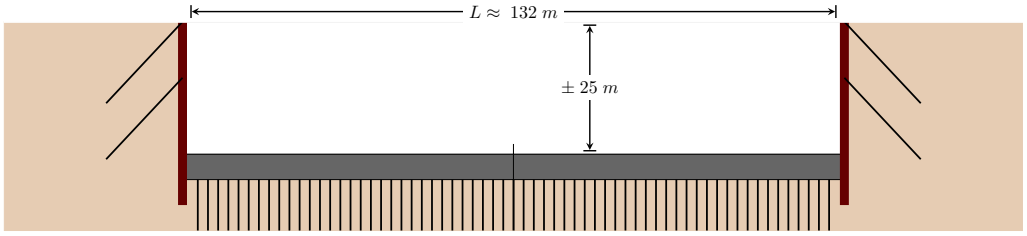

Figure C.6: *Schematisation of a combined structure of sheet pile– or combi-walls with an underwater concrete floor*

Sheet pile– or combi-wall (With bed protection)

Similar case, only here the bottom exists out of an open bed protection where water can flow through. This option is schematised in figure C.7

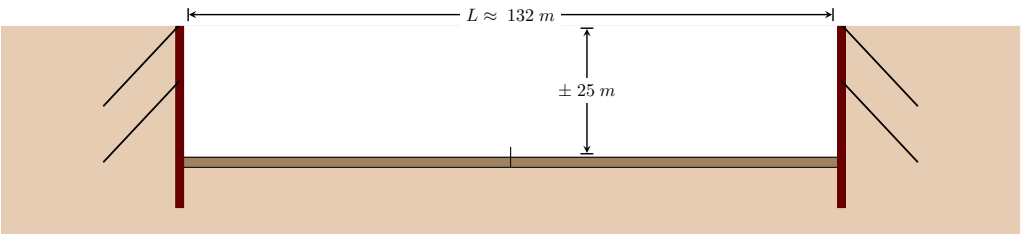

Figure C.7: *Schematisation of a combined structure of sheet pile– or combi-walls with a bed protection*

Diaphragm wall (With underwater concrete)

Diaphragm walls are used for larger retaining heights or to limit subsidence to nearby structures. A diaphragm wall is a reinforced concrete wall formed below surface level. Diaphragm walls can reach lengths up to 50 meters below surface level and have an average thickness between 50– and 150 centimeter. The first step for a diaphragm wall is to construct a guiding wall for the hydraulic grab or hydrofraise. Guide walls provide a template for wall excavation and panel layout, support the top of the trench, restrain the end-stops between the different panels, serve as a platform to hang the reinforcement, provide a reference elevation for inserts of anchors etc., support the tremie pipes and hold down the cage during concreting. [Omran Ista, 2014]. After completion of the guiding wall the actual excavation can start. Simultaneously with the excavation of the soil a mix of bentonite is pumped in the excavation to prevent soil collapsing. After excavation finishes a reinforcement cage can be placed inside the excavation trench. Concrete can be cast starting from the bottom moving up above. Bentonite slurry is collected at the top and will be de-sanding at a slurry plant. This slurry plant includes a slurry mixer, storage tanks, and de-sanding units. Sufficient storage tanks must be used for bentonite slurry hydration. It is important that there is sufficient work area to set up the slurry plants. The construction process of a diaphragm wall is schematised in figure C.8

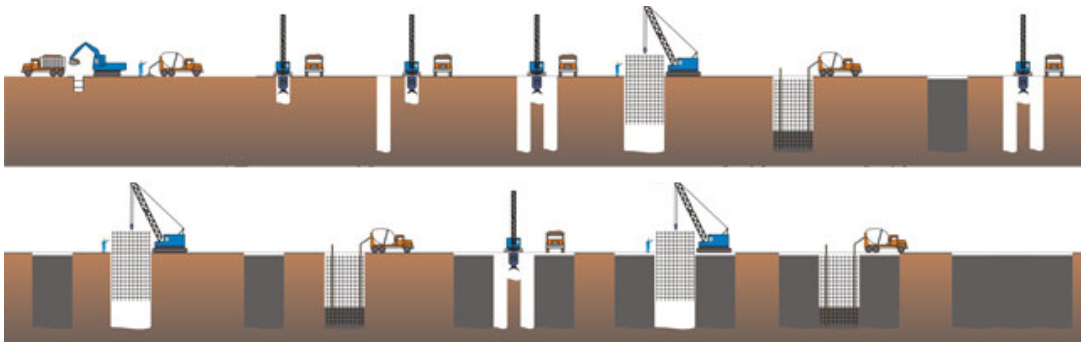

Figure C.8: *Construction Process of diaphragm wall [Tung Feng, 2009]*

In this option a diaphragm wall is combined with a concrete underwater floor. This option is schematised in figure C.9

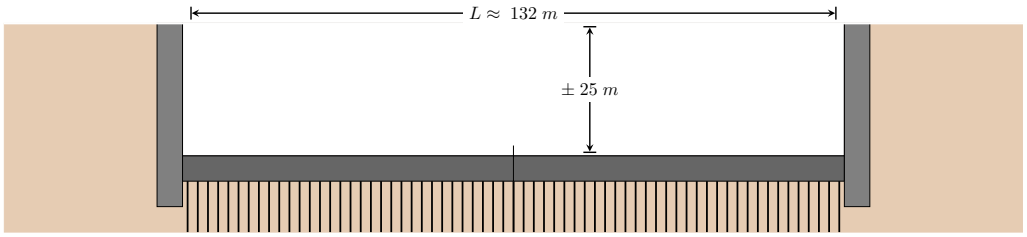

Figure C.9: *Schematisation of a combined structure out of diaphragm walls and an underwater concrete floor*

Diaphragm wall (With bed protection)

Similar case, only here the bottom exists out of an open bed protection where water can flow through. This option is schematised in figure C.10

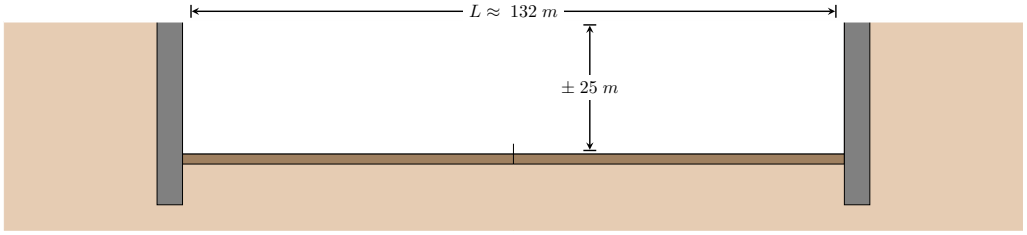

Figure C.10: *Schematisation of a combined structure out of diaphragm walls and a bed protection*

Relieving platform (With underwater concrete floor)

When large retaining height are present the effective soil stress on the active side of the retaining wall are very high. Therefore, it can be economically interesting to make use of a relieving platform in order to decrease the soil stress acting on the retaining wall. A relieving platform can be constructed on top of a, smaller dimensioned sheet pile wall or combi-wall. The soil pressure above the platform and the weight of the platform itself are transmitted to the foundation piles. Therefore the horizontal and vertical soil pressure at the bottom of the relieving platform are equal to zero. In this option the bottom is designed as underwater concrete floor, either with or without tension piles. This option is schematised in figure C.11

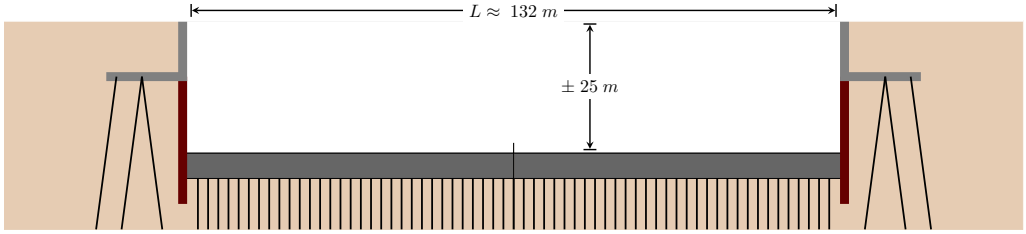

Figure C.11: *Schematisation of a combined structure with a relieving platform and an underwater concrete floor*

Relieving platform (With bed protection)

Similar to the previous option, only now the bottom is designed without underwater concrete but with a bed protection. This option is schematised in figure C.12

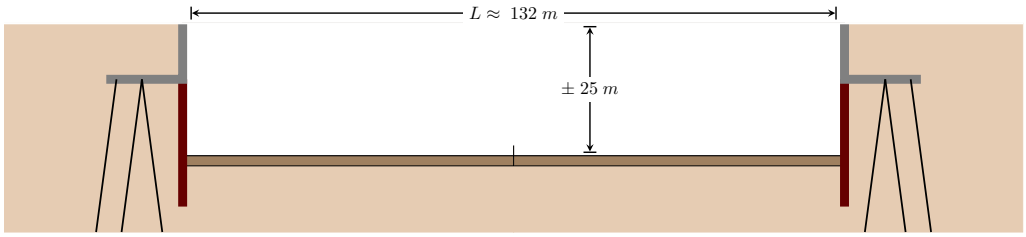

Figure C.12: *Schematisation of a combined structure with a relieving platform and a bed protection*

Pneumatic Caisson

In the case of a pneumatic caisson the structure is constructed at surface level at subsided to the desired depth afterwards. The working of a pneumatic caisson will be explained in chapter 5 and a schematisation is given in figure C.13.

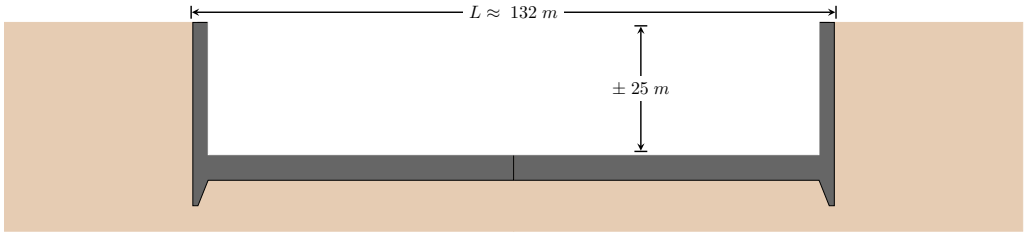

Figure C.13: *Schematisation of a pneumatic caisson*

To increase the capacity of the retaining wall only anchors could be used because of the passage of ships through the lock.

C.2 TENSION PILES

In the next section a design with GEWI anchors will be made, afterwards a check on clump weight will be performed.

C.2.1 FRICTION ALONG PILE SHAFT

From NAP -20.5 meter until a level of NAP -32 meter a cone resistance varying between 4 mPa and 5 mPa is present. Below the boundary of NAP -32 meter the cone resistance will increase. In order to get insight in the order of magnitude off the dimensions, a safe lower limit of the cone resistance is assumed as maximum. ($q_{c,z,max} = 4.5$ mPa) An underwater concrete bottom slab height of $h_c = 2$ meter will be assumed. An higher height would only increase the costs and does not contribute significantly to a larger resistance against the upward directed force. When a lower value is chosen, the shear forces between tension pile and concrete floor would be to high. This means that a total excavation depth from NAP +6 meter towards NAP -23.5 meter is required.

The net value of the upward water pressure below the concrete floor is:

$$\begin{aligned} q_{water} &= FS \cdot (\Delta h_e + h_c) \cdot \gamma_{water} - h_c \cdot \gamma_{concrete} \\ q_{water} &= 1.2 \cdot (22.5 + 3) \cdot 10 - 2 \cdot 25 \\ q_{water} &= 244 \text{ kPa} \end{aligned} \quad \text{(Eq. 1)}$$

This upward pressure of 244 kPa must be retained by the tension piles. The resistance force of the tension piles can be calculated with the following equation: [CUR 2001-4]

$$F_{r,tension,d} = \int_0^{L_{anchor}} q_{c,z,d} \cdot f_1 \cdot f_2 \cdot O_{p,mean} \cdot \alpha_t \cdot dz \quad \text{(Eq. 2)}$$

Where:

$F_{r,tension,d}$	=	design value for the tensile strength of the soil	[kN]
$q_{c,z,d}$	=	design value of the cone resistance at depth z	[kN/m^2]
f_1	=	pile installation factor	[-]
f_2	=	cone resistance reduction factor	[-]
$O_{p,mean}$	=	average circumference of the pile shaft	[m]
α_t	=	pile class factor	[-]
L_{anchor}	=	length of pile	[-]
z	=	depth	[-]

To solve equation Eq. 2, first the representative value for the cone resistance will be calculated. Normally this would be done for each section independently. Because in this case the soil has uniform properties only one calculation will be made. The maximum value of the cone resistance should be multiplied by a factor (ξ) dependent on the number of performed soundings, the number of piles and the stiffness of the construction. A table with the value for M and N can be seen in figure C.14.

M	N						
	1	2	3	4	5	10	>10
1	0,75	0,78	0,79	0,80	0,81	0,82	0,83
2	0,78	0,81	0,83	0,83	0,84	0,86	0,87
3-10	0,81	0,84	0,86	0,87	0,87	0,89	0,90
>10	0,82	0,86	0,87	0,88	0,89	0,91	0,92

Figure C.14: *Values for M, Number of tension piles in the building pit and N, number of performed Standard Penetration Tests (SPT) according to NEN 6740:1991*

In this case the soil parameters are based on just one CPT and multiple ($M \geqslant 10$) tension piles are needed. Therefore $\xi = 0.82$.

$$\begin{aligned} q_{c,z,rep} &= \xi \cdot q_{c,z,max} \\ &= 0.82 \cdot 4.52 \\ &= 3.71 \text{ mPa} \\ q_{c,z,rep,below} &= \xi \cdot q_{c,z,max,below} \\ &= 0.82 \cdot 22 \\ &= 18 \text{ mPa} \end{aligned} \tag{Eq. 3}$$

The design value for the cone resistance can be calculated by dividing the representative value for the cone resistance by the material factor for tension piles ($\gamma_{m,b4} = 1.4$).

$$\begin{aligned} q_{c,z,design,swell} &= \frac{q_{c,z,rep,swell}}{\gamma_{m,b4}} \\ &= \frac{3.71}{1.4} \\ &= 2.65 \text{ mPa} \ = 2650 \text{ kPa} \end{aligned} \tag{Eq. 4}$$

$$\begin{aligned} q_{c,z,design,belowswell} &= \frac{q_{c,z,rep,belowswell}}{\gamma_{m,b4}} \\ &= \frac{18.04}{1.4} \\ &= 12.89 \text{ mPa} \ = 12890 \text{ kPa} \end{aligned} \tag{Eq. 5}$$

A gewi ground anchor $\varnothing = 114$ mm is used. According to [CUR 236] the design diameter is thereby $\varnothing_d = 114 + 20 = 134$ mm

$$O_{p,mean} = \pi \cdot \varnothing = \pi \cdot 0.134 \ = 0.42\text{m} \tag{Eq. 6}$$

According to [CUR 2001-4], for clayey soils f_1 and f_2 can be assumed to be 1. Because the Boom Clay is an over consolidated clay, with an OCR of 5 [TNO, 1998] the cone resistance must be corrected using the following equation:

$$\begin{aligned} q_{c,z,design,ocr} &= q_{c,z,design} \cdot \sqrt{1/OCR} = 2650 \cdot \sqrt{1/5} \\ &= 1185 \text{ kPa} \end{aligned} \tag{Eq. 7}$$

The maximum upward directed swell force can be calculated according [NEN 6745-1].

$$\begin{aligned} F_{swell,rep} &= O_{p,mean} \cdot h_{swell} \cdot \alpha_{z1} \cdot q_{c,z,design,ocr} \\ &= 0.42 \cdot (38 - 20.5) \cdot 0.05 \cdot 1185 \\ &= 435.5 \text{ kN} \end{aligned} \tag{Eq. 8}$$

Where:

h_{swell}	=	Height of swell layer	[m]
α_{z1}	=	Factor whereby the mean cone resisting for swelled layer must be multiplied to determine the shaft frictional resistance.	[-]

At last the pile class factor α must be declared. In figure C.15 the maximum values for the pile class factor in clay and silt can be found.

grondsoort	relatieve diepte z / D_{eq}	α_t
klei/silt $q_c \leq 1$ MPa	$0 < z / D_{eq} < 20$	0,02
klei/silt $q_c \leq 1$ MPa	$z / D_{eq} > 20$	0,025
klei/silt $q_c > 1$ MPa	-	0,025

Figure C.15: *Maximum values for the pile class factor in clay and silt*

In this case the cone resistance of the Boom Clay is above the 1 mPa. An α-factor of 0.025 is used. When picking a mutual distance of 2 meter in both directions, one tension pile must be able to resist an upward pressure F_{upward} of 244 kPa $\cdot$ 1.5 $\cdot$ 1.5 = 549 kPa

Boom Clay is hardly compressible, The displaced soil will swell and the tension resistance will decrease largely.

All factors are known and with help of equation Eq. 2 the length of the anchor (L_{anchor}) can be solved.

$$\begin{aligned} F_{upward} + F_{swell} &= F_{r,tension,d} \\ 549 + 435.5 &= \int_0^{L_{anchor}} (q_{c,z,d} \cdot f_1 \cdot f_2 \cdot O_{p,mean} \cdot \alpha_t) \cdot dz \\ 984.5 &= 1185 \cdot 1 \cdot 1 \cdot 0.42 \cdot 0.025 \cdot L_{anchor} \\ \Rightarrow L_{anchor} &= 79.1 \text{ meter} \end{aligned} \tag{Eq. 9}$$

A anchor length of 79.1 m is obviously too large. The tension pile reaches from the bottom of the concrete floor, NAP -23.50, towards NAP -101.1. A larger surface area for a single tension pile does enlarge the tension piles. A next step can optimize the amount of tension piles. The availability of tension piles and the exact soil conditions determine the final design choice. A schematisation of the underwater concrete floor is given in figure C.16.

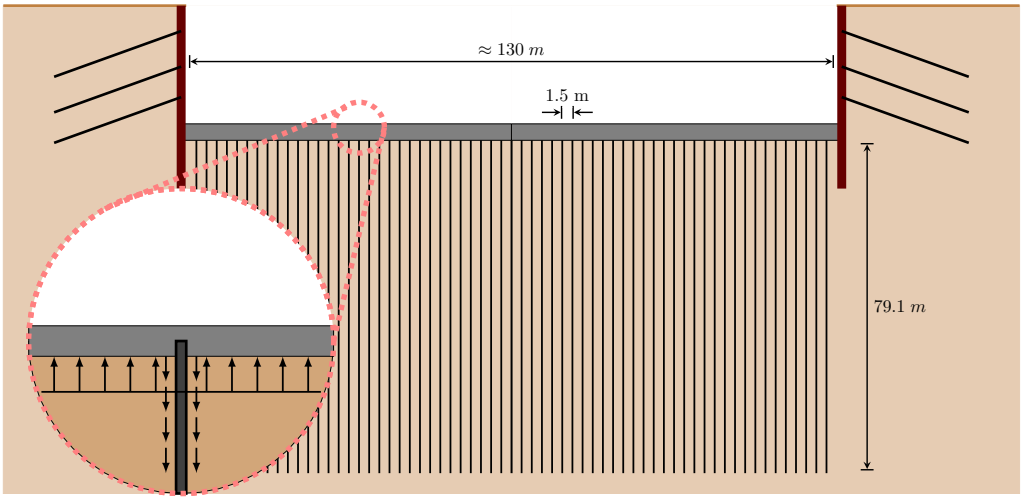

Figure C.16: *Schematisation of the underwater concrete floor*

C.2.2 CLUMP WEIGHT

The upper limit of the tensile capacity is found with the geometry in which case the entire ground volume which is enclosed between the piles is pulled up. The maximum tension force for a single pile is calculated in equation Eq. 10

$$\begin{aligned} F_{clump} &= A \cdot L_{anchor} \cdot \gamma_{boomclay} \\ &= (1.5 \cdot 1.5) \cdot 79.1 \cdot 18.5 = 3292 \text{ kN} \end{aligned} \tag{Eq. 10}$$

The tensile force to pull up the complete ground volume $F_{clump} = 3292$ kN is larger than the maximum occurring tensile force of $F_{r,tension,d} = 984.5$ kN.

C.2.3 SWELL OF UNDERWATER CONCRETE

According to [Huisman, 2013], as a result of the excavation the effective stresses in the subsoil will decrease. In particular cohesive soils, such as the deeper Boom Clay layer will swell as a result of the decrease of effective stress. This can be seen as a kind of reverse consolidation and in dependent on the thickness of the Boom Clay layer, the difference in effective stress before and after excavation and the soil characteristics.

The swell can be calculated according equation Eq. 11

$$\Delta h = \frac{h \cdot C_s}{(1 + e_0)} \cdot \log\left(\frac{\sigma_1' - \Delta p}{\sigma_1'}\right) \tag{Eq. 11}$$

Where:

Δ_h	=	Occurring swell
h	=	Layer thickness
C_s	=	Swell index (0.028)
e_0	=	Initial void ratio (0.7)
σ_1'	=	Initial effective stress in the Boom Clay layer
Δ_p	=	Difference in initial stress before and after excavation

The effective stress, in the initial situation and after excavation is plotted in figure C.17. A point in the middle of the layer (NAP -30 m) is used for the calculation of swell.

$$\Delta h = \frac{(-23.5 - -38) \cdot 0.028}{(1 + 0.7)} \cdot \log\left(\frac{348 - (348 - 63.75)}{348}\right) = -0.188 \text{ m} \tag{Eq. 12}$$

This swell can cause deformation and forces in the concrete floor. The hydrodynamic period where the consolidation process reach a 99% completion level can be calculated according to equation Eq. 13:

$$t_e = \frac{2 \cdot (a \cdot h)^2}{c_v} \tag{Eq. 13}$$

Where:

t_e	=	Time until 99% consolidated [s]
a	=	Constant; when two sided runoff $a = 0.5$ [-]
c_v	=	Average vertical consolidationcoefficient during relieving $(1 \cdot 10^6)$ [m^2/s]

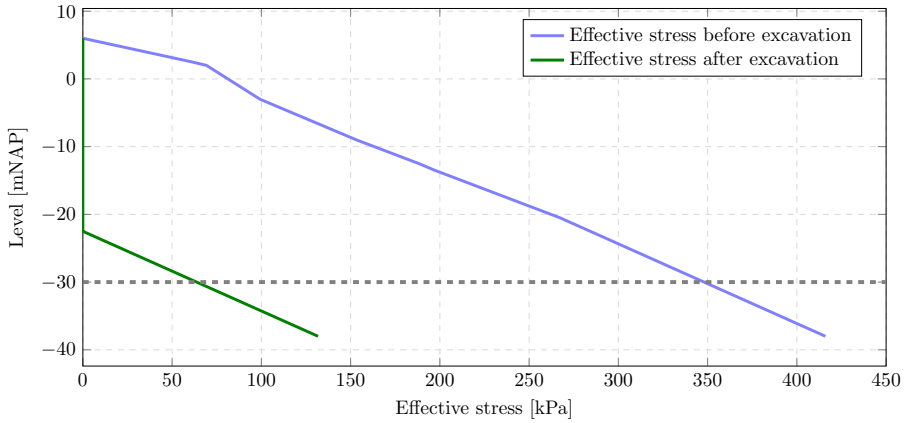

Figure C.17: *Effective stress before and after excavation*

$$t_e = \frac{2 \cdot (0.5 \cdot (-23.5 - -38))^2}{1 \cdot 10^6} = 2.8 \cdot 10^7 \text{ s} = 325 \text{ days} \qquad \text{(Eq. 14)}$$

When the concrete floor is made before full consolidation is reached, this introduces forces on the concrete floor and piles. A percentage of the swell force has to be taken in to account.

D

CAISSONS IN GENERAL

D.1 OPEN– AND SUCTION CAISSONS

D.1.1 OPEN CAISSONS

In history, open caissons have been used for bridge foundations. The caissons were sunk through excavation by hand. The maximum depth of historical excavations was limited to 6 meters below the water table and was carried out by divers. Later it became possible to excavate to greater depths by the introduction of sand pumps and the use of freezing techniques up to hundred meters and more. This caissons where used for mine shafts.

The open caisson excavation method is the oldest of the above three methods of foundations. Precast concrete ring segments constitute a closed ring where in at the bottom of the formed caisson soil is excavated. Due to its own weight the caisson will sink into the ground.

In the case the bottom level of the caisson is above water level the soil can be excavated by mechanical excavators in the dry. In the other case where the bottom level inside the caisson is situated below water level soil can be dredged.

The water above the lowered ground level inside the caisson will prevent uplifting of the underlying soil layers. The pressure from the volume of water above the bottom will be in equilibrium with the hydraulic head. After the caisson has reached its designed final depth a bottom plate will be constructed from underwater concrete. After hardening of the concrete the remaining water volume above this bottom slab will be pumped out of the caisson.

Nowadays open caissons are used in a variety of geo-technical engineering applications such as for deep foundation elements which are bypassing weak soils to tip in firm deeper strata, foundations in clay layers that behave plastically, for the foundation of bridge foundations, in rivers and maritime constructions to reduce the risk of scour or for collecting sewage water through a system of gravity sewer pipe networks. In figure D.1 an open caisson is shown.

Figure D.1: *Photo of the inside of an open caisson [VSF, 2014]*

D.1.2 SUCTION CAISSONS

Suction caissons were first used as anchors for floating structures in the offshore oil and gas industry. The use of suction caissons is also proposed for offshore wind turbines.

Basic principle of the suction caisson is that the caisson will be placed on the bottom of the ocean. Due to its own-weight the caisson will partly penetrate in to the soil. Later the enclosed water body will be pumped out of the caisson. Due to the under-pressure in the caisson the caisson will penetrate deeper and deeper into the soil. Suction caissons are now used extensively worldwide for anchoring large offshore installations to the seafloor at great depths. Without the existence of suction caissons this will become very difficult. In practice it has been shown that suction caissons have been applied to depths of more than 2000 meter.

There has changed a lot between the first use of a suction caissons by Shell in the North-Sea in 1981 and the suctions caissons installed nowadays.

The concept of suction technology was developed for projects where gravity loading is not sufficient for pressing foundation elements into the ground. The technology was also developed for anchors subjected to large tension forces due to waves and stormy weather. The suction caisson technology functions very well in a seabed with soft clays or other low strength sediments. The suction caissons are in many cases easier to install than piles, because it is difficult to drive piles in to the ground at large depths.

D.2 HISTORY

Caissons are used in construction method for long times. There is literature available showing that floating watertight caissons are used to transport a mortar block, part of a quay wall in 250 before Christ. In the described case a wooden mould was constructed first. Subsequently the mortar blocks where cast in the wooden mould. After casting the mould the caisson was transported to the required location of the quay wall. In figure D.2 the floating caisson which is used to transport a mortar block can be seen.

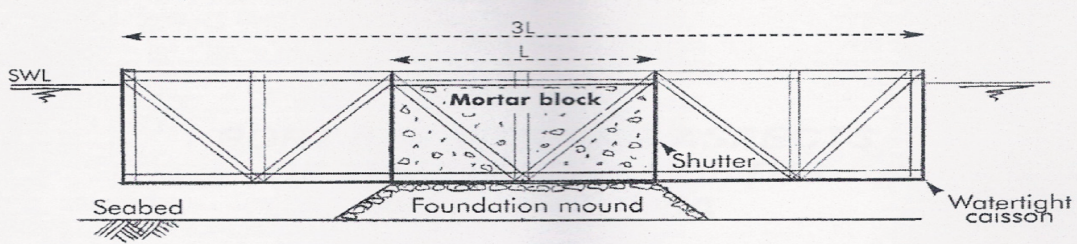

Figure D.2: *Floating caisson used to transport a mortar block [de Gijt, 2010]*

In 100 BC, caissons where also used as part of a quay wall itself. The quay wall was constructed as follows: A wooden framework was made which was filled with pozzolanic mortar with a very light specific weight. This allowed the caisson to be floated and towed into the chosen position by a vessel. When the caisson arrived at the right place and was correctly aligned, the mortar was allowed to harden further. During this process the specific weight of the mortar block increased which ensured that the caisson would remain in place. Multiple caissons were connected using ropes and mortar. In figure D.3 the building of a caisson can be seen.

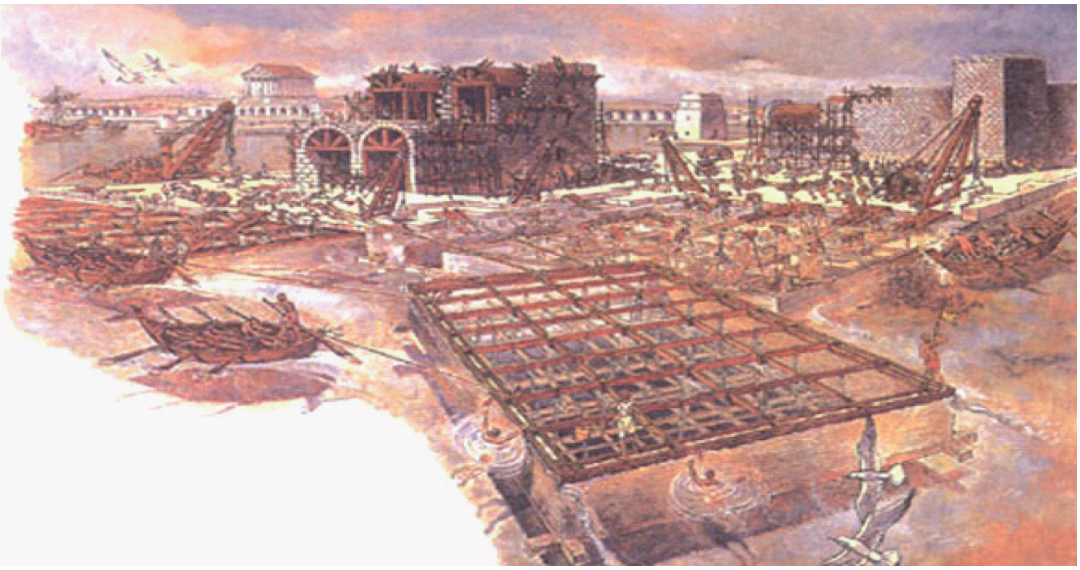

Figure D.3: *Construction of a caisson around 100 BC [de Gijt, 2010]*

However the caisson construction technique was already used for long times, the method of construction was reinvented during the mid-19th. The literature in here is contradictory but it is a fact that the construction method is applied in several projects.

Up until the 19th. century coffer dams and crude caissons were the only means by which foundations could be constructed in water. Their use was limited by the length of wooden piles and by soils that were unsuitable for pile driving because they were either too soft or too hard. William Cubitt and John Wright developed the first pneumatic caisson in 1851 by the construction of a bridge over the River Medway at Rochester (UK). It was similar to the caisson developed by Labelye, who used huge timber boxes which were constructed on shore, were floated into position, and slowly sunk to the bottom of the. Different to the new method was that the chamber of the caisson, which was resting on the river's bottom, was airtight and required workmen to enter by means of airlocks after the water had been driven out by pneumatic pressure.

The invention of this construction method permitted the construction of bridges of unprecedented scale, overcoming the impediment of deep, broad rivers. Isambard Kingdom Brunel used the technique for sinking the piers of his bridge at Chepstow, Wales (UK) and, on a much grander scale, on the Royal Albert Bridge (1859) over the Tamar at Saltash in Cornwall. [DeLony, 1996] In 1886 the foundation of the Brooklyn Bridge in New York was constructed by the use of steel caissons. When four years later Portland cement concrete came available, is was from then on possible to build reinforced concrete caissons as construction element. [de Gijt, 2010]

The experience with the founding of bridge piers on caissons nevertheless was positive, so the French structural engineer Gustave Eiffel selected this same method to found his prestigious tower for the World's Fair of 1889 in Paris. [Engineers Australia, 2014] The northern and western pilar of the Eiffel tower are founded on pneumatic caissons which were subsided to a depth of approximately 20 meter. [Hill, 2011] In the Netherlands, pneumatic caissons have been used for the construction of locks in Lith and Almere. [Miller, 2011]

D.3 REFERENCE PROJECTS

As mentioned before, in section D.2, pneumatic caissons have been used for many times as construction method in the last decades. In this section four reference cases will be treated. The first case-study concerns a pneumatic caisson that is installed as a substructure of the main tower of the Youngjong Grand Bridge, which is connecting the Incheon International Airport with the city of Seoul in South-Korea. The second case-study involves the North-South metro-line in Amsterdam which is currently under construction. The third reference project evaluates another metro-line in Amsterdam, the Oostlijn. This metro-line connects the Nieuwmarkt with Amsterdam Amstel. The last case elaborates the dimensions of the Deurganckdoksluis nearby Antwerp.

D.3.1 FOUNDATION OF YOUNGJONG GRAND BRIDGE IN SEOUL

The Incheon International Airport, which is currently the largest airport in South-Korea and one of the major airports in Asia, is build on an artificial island. The Youngjong Grand Bridge connects the airport with the city of Seoul on the mainland. the construction of the bridge took two years and was completed in August 1998. Pneumatic caissons are installed as a substructure for the two main tower of this suspension bridge. The dimension of the caisson that was used are summarised in table D.2. It must be observed that in this case not the complete caisson will

be subsided into the ground. The caisson will be subsided for only 19 meters. A cross-section of the caisson is given in figure D.4.

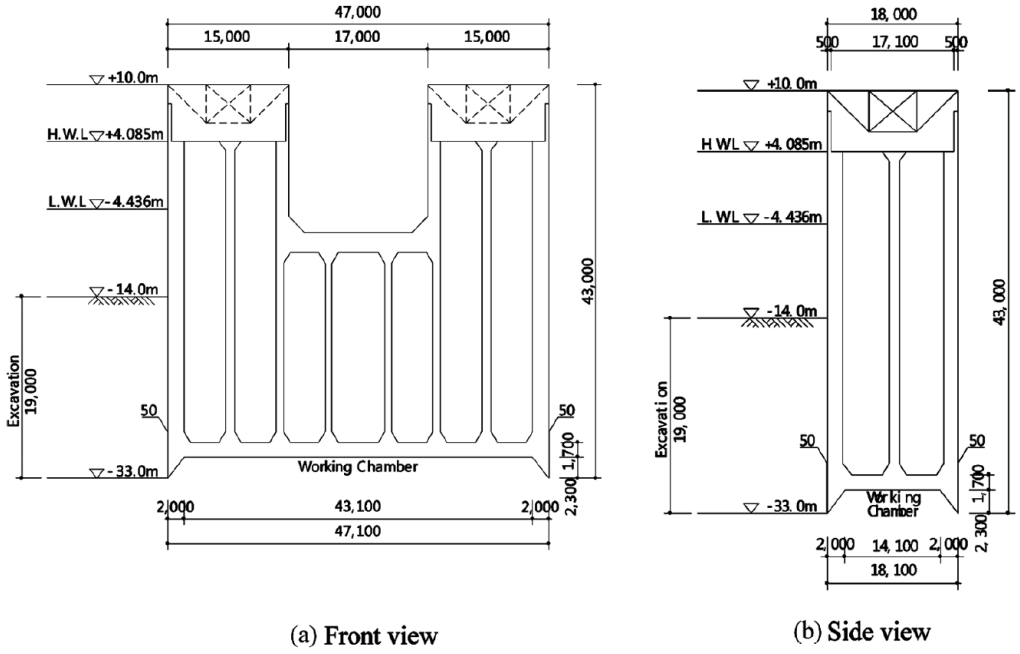

Figure D.4: *Dimensions of the pneumatic caisson used in the eastern tower of the Youngjong Grand Bridge.*

The work-chamber of the caisson exists out of only one compartment. The caisson itself is divided into 13 separate parts. [Korea Highway Corporation, 2002] Water was used to compensate for the required sinking weight and balance the caisson during the process of sinking. Rock mass was blasted and excavated inside the working chamber with help of explosives while soft rocks were broken by pneumatic breakers. [Yea and Kim, 2012]. In the South China Sea at the position of the tower structure, different layers of soil can be found. In table D.1 the different soil parameters can be found.

Table D.1: *Soil properties at the location of the Youngjong Grand Bridge [Hong et al., 2005]*

Ground type	**Height layer** [m]	**Unit weight** γ [kN/m^3]	**Internal friction angle** θ [°]	**Cohesion** c [kN/m^2]
Marine sediment	12.4	17.6	30	112
Weathered rock	2	19.6	30	112
Soft bed rock	1.6	20.6	35	119
Hard bed rock	1.3	21.5	40	500

D.3.2 NORTH-SOUTH METROLINE IN AMSTERDAM

The new North - South metro-line in Amsterdam is at this moment under construction. The 9km long metro-line runs from the northern ring road to the southern ring road and passes the historic and vulnerable city centre. For a small part of the metro-line in the vicinity of the Amsterdam Central station the pneumatic caisson method is applied. This method was the most preferred option because of the construction costs compared with other options and lowest impact to adjacent and old buildings.

In order to protect adjacent buildings, around the perimeter of the site location sheet piles were put in place which were extended down to the second sand layer. After the sheet piles were installed the soil was removed to a level of NAP -4.5 m. After removing the soil new sand was filled towards a level of NAP +0 m, creating a temporary land fill. In total 3 caissons were build and subsided, where one caisson has some extra areas for service and operation facilities of the underground system. Further it is used as the starting shaft for the two tunnel boring machines and last, it is used as a flood barrier. Inside the caisson a segment barrier is installed. The dimensions of the caisson are given in table D.2. Because of the resulting loads from the large structure on the subsoil and the visual impact to the environment, this caisson was built in two phases. First the section with the working chamber and metro-line section was subsided. In figure D.5 a photo the construction site in Amsterdam is given and in D.6 the plan and longitudinal section of the three caissons is shown.

Figure D.5: *Subsidence of a pneumatic caisson in Amsterdam*

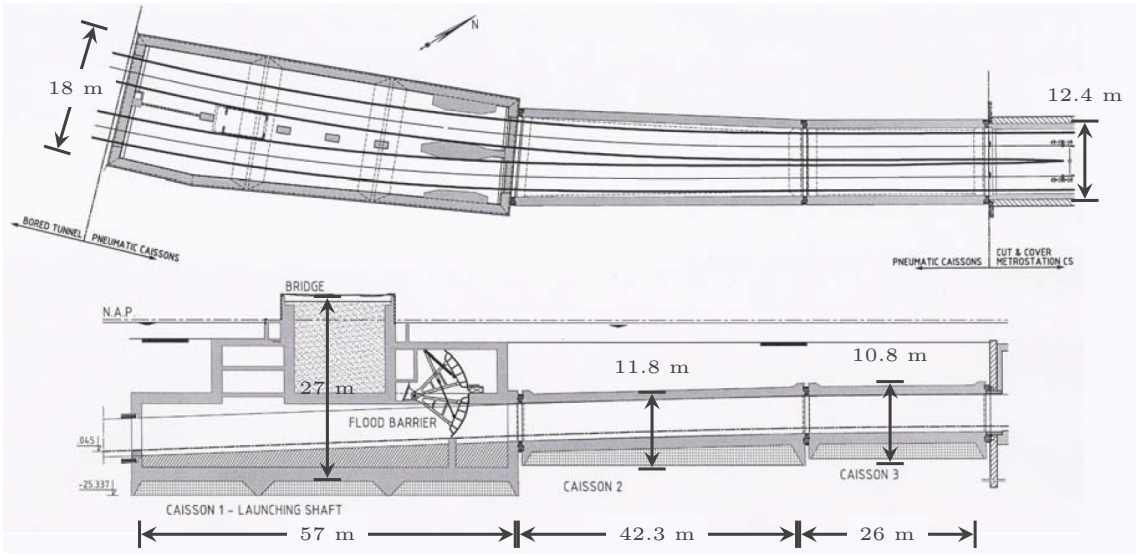

Figure D.6: *Plan and longitudinal section of the caissons*

D.3.3 OOSTLIJN, STATION NIEUWMARKT TOWARDS AMSTERDAM AMSTEL

Amsterdam has always had a good tram network, the necessity for a metro network was therefore less urgent than elsewhere. In contradiction to other European capitals. The Amsterdam metro is constructed more recently.

The city conducted various studies on the technical and financial feasibility of a new metro network. That produced a plan for a metro network of 78 kilometer in total which includes 25 kilometer of underground network

A part of this plan was the construction of the Oostlijn. In august 1975 the construction process began. The Oostlijn is 18 kilometer in length of which 3.5 kilometer is below surface level. From that 3.5 kilometer of metro tunnel below surface level 3 km is constructed as pneumatic caisson.

These caissons vary in dimensions. The dimensions of the caisson are given in table D.2. [Kamerling and van den Boogaard, 1986]

The construction of the underground part was executed with a pneumatic caisson construction . In large building pits the contractor made first the tunnel sections in the form of large rectangular concrete boxes. In figure D.7 a photo of the caissons can be seen. The tunnel segments where enclosed between sheet pile walls. Through an increased air pressure in the working chamber of the caisson the soil was removed under the caisson and the elements subsides to their final position at NAP -8.5 meter.

The construction of the tunnel was controversial, multiple houses at the Nieuwmarkt area were removed. Also there was a big overrun of the costs. From the original estimated 405 million to 860 million former Dutch guilders. [Stam, 2005]

Figure D.7: *An old photo from the pneumatic caissons on surface level used for the Oostlijn [Ouwendijk, 1977]*

Table D.2: *Summary: Dimensions of the caissons*

Project	**Length** [m]	**Width** [m]	**Height** [m]
Youngjong Grand Bridge	47	18	43
North-South metroline in Amsterdam	26 ~ 57	12.4 ~ 18	10.8 ~ 27
Oostlijn in Amsterdam	26 ~ 31	41 ~ 12	16 ~ 10.5

D.3.4 CONSTRUCTION OF THE DEURGANCKDOKSLUICE NEARBY ANTWERP

The construction of the second lock in the Waaslandhaven has many similarities with the prospective new lock at Terneuzen. The Waaslandhaven is located on the left bank in the port of Antwerp. In this case also large sea going vessels have to pass the lock. The new lock will become 500 meters in length and 68 meter width which are in a greater or lesser extent comparable with the lock in Terneuzen. Because the river Schelde is a tidal river also here different water levels on the outer lock head are present. In the docks behind the lock always a fixed water level is present. On this location a very thick layer of Boom Clay is reaching almost to the surface. Therefore the lock will be constructed in an open building pit with natural slopes. Due to the large number of similarities the dimensions of the Deurganckdok sluice will be taken as starting point for this masterthesis.

E

PLANNING AND COSTS

E.1 GLOBAL PLANNING OF NEW LOCK

E.1.1 CONSTRUCTION OF NEW LOCK WITH BUILDING PIT

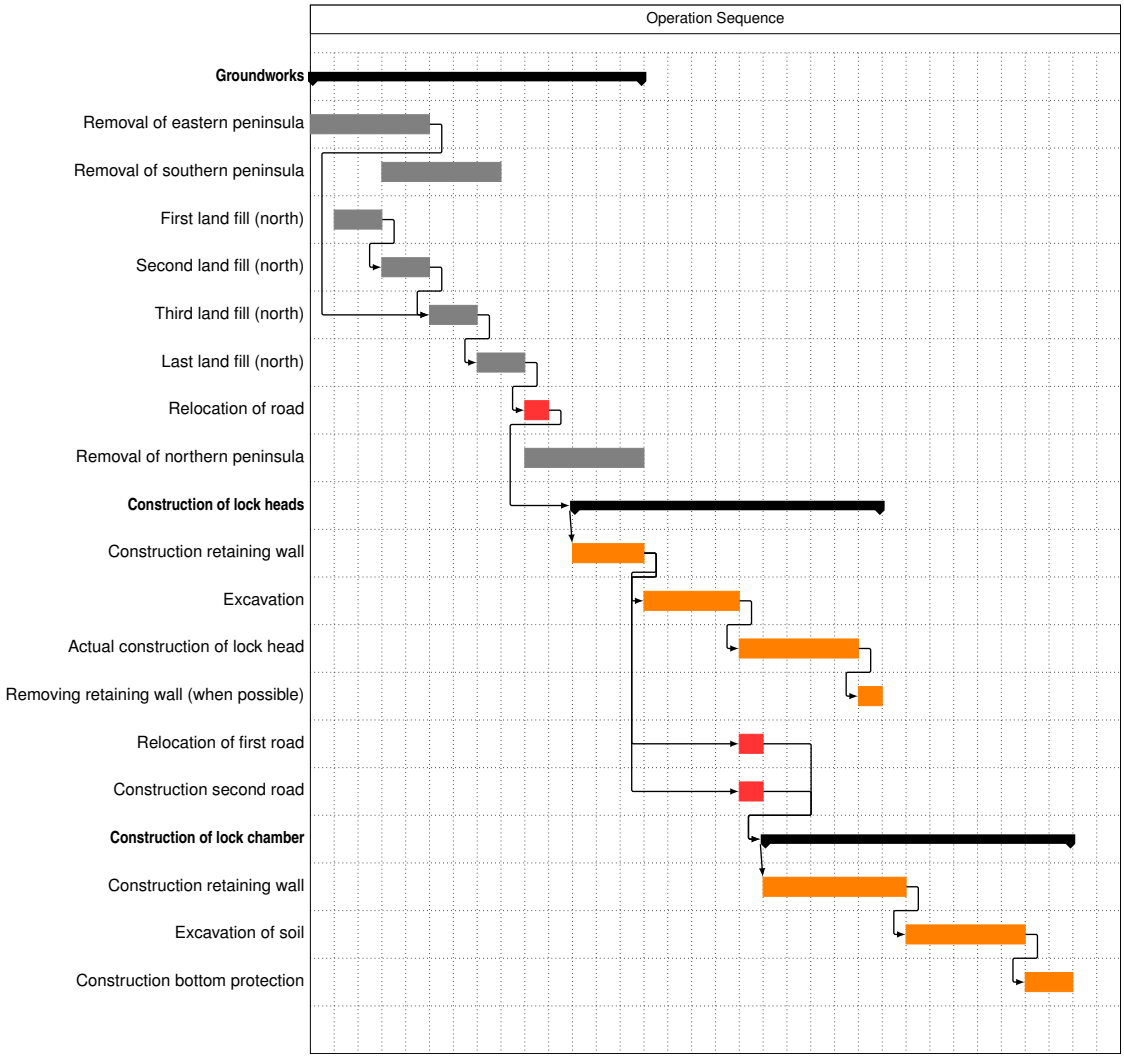

Figure E.1: *Global planning of the construction (Building Pit)*

E.1.2 CONSTRUCTION OF NEW LOCK WITH PNEUMATIC CAISSON

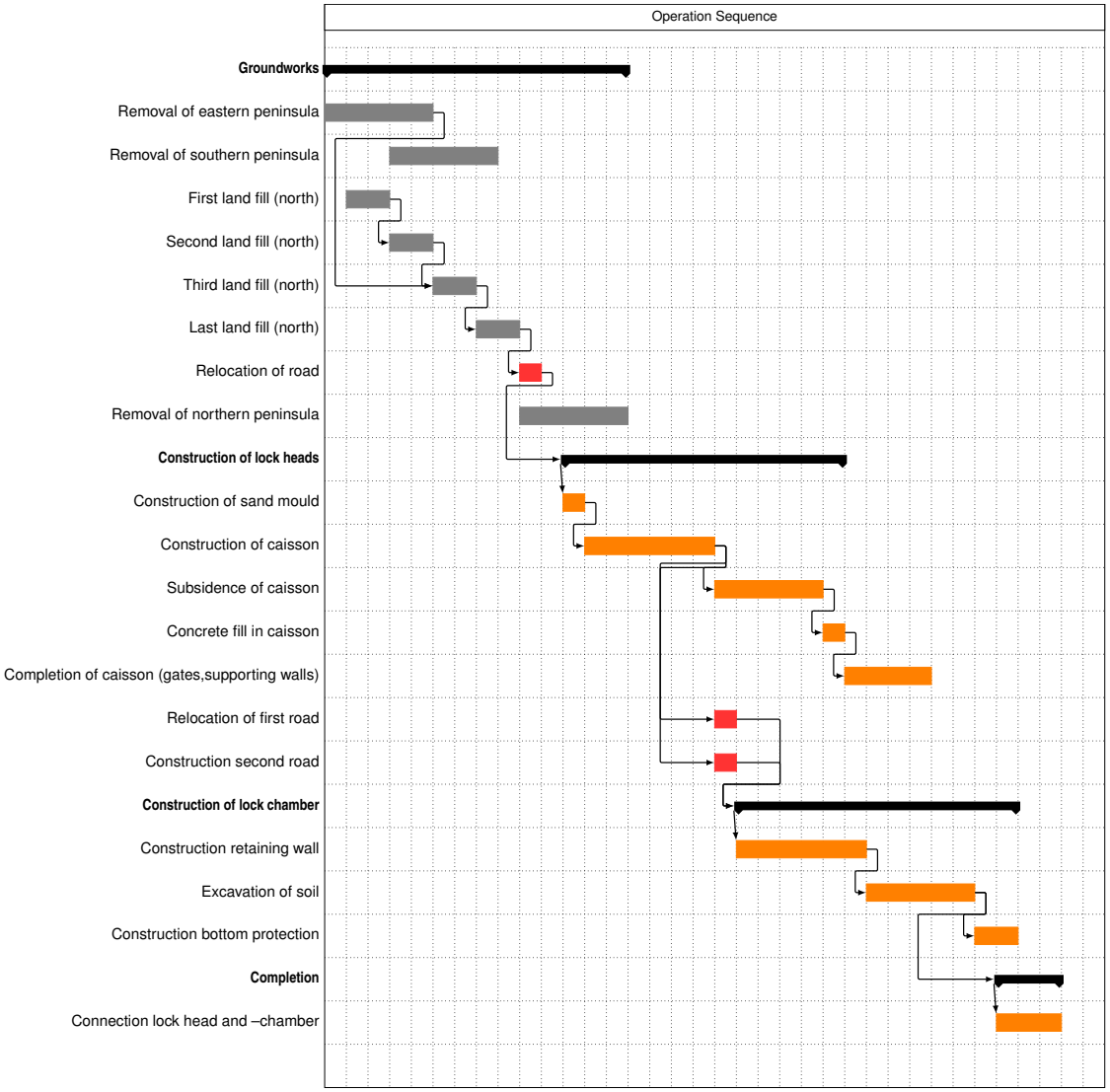

Figure E.2: *Global planning of the construction (Pneumatic Caisson)*

E.2 CONSTRUCTION TIME OF LOCK HEAD

In order to make a comparison between the different construction methods an estimation for the required construction time is given. In section E.2.1 the planning for the lock head constructed with a pneumatic caisson is given. Subsequently in section E.2.2 the planning of the lock head constructed with a traditional building pit is given.

E.2.1 PNEUMATIC CAISSON

The construction of the lock heads with pneumatic caisson(s) are subdivided in multiple phases which are listed below:

- Construction of the pneumatic caisson / Concrete works
- Subsidence of caisson
- Connection and completion of concrete works
- Installation of gates
- Installation of mechanical and electrical equipment
- Completion of the lock head

For each of these steps the required construction time is calculated in the following paragraphs.

CONCRETE WORKS

The construction of the pneumatic caissons starts around surface level. According to appendix F.1 a total of $V_{concrete} = 54000\ m^3$ of concrete is required. There are 21 working days per month. With the installation rate of 200 m^3/day, 270 working days or 13 months are required.

SUBSIDENCE OF THE CAISSON

The caisson must be subsided towards a level of NAP -27 meter. With an subsidence rate of 50 cm/day approximately 60 working days are required. This is equal to a time of 3 months.

CONNECTION AND COMPLETION OF CONCRETE WORKS

After subsidence of the caisson(s) the concrete works on the inside can start. For example the recesses for the lock gates can be constructed. In the same time the caissons are being connected, in the case of variant 2, the bulkheads can be removed. A global duration of 6 months is assumed.

INSTALLATION OF GATES, MECHANICAL AND ELECTRICAL EQUIPMENT

For the installation of gates, mechanical and electrical equipment 6 months of work are calculated. The largest part of the activities can already start during the concrete works.

COMPLETION OF THE LOCK HEAD

For the completion of the lock head another time of 6 months are included in the calculation. These can take place in the same time as the connection and completion of the concrete works.

When all the construction phases are summed up, a time of 22 months per lock head are required for the construction. All steps are schematised in figure E.3. In the red track the phasing of the optional second caisson of variant 2.

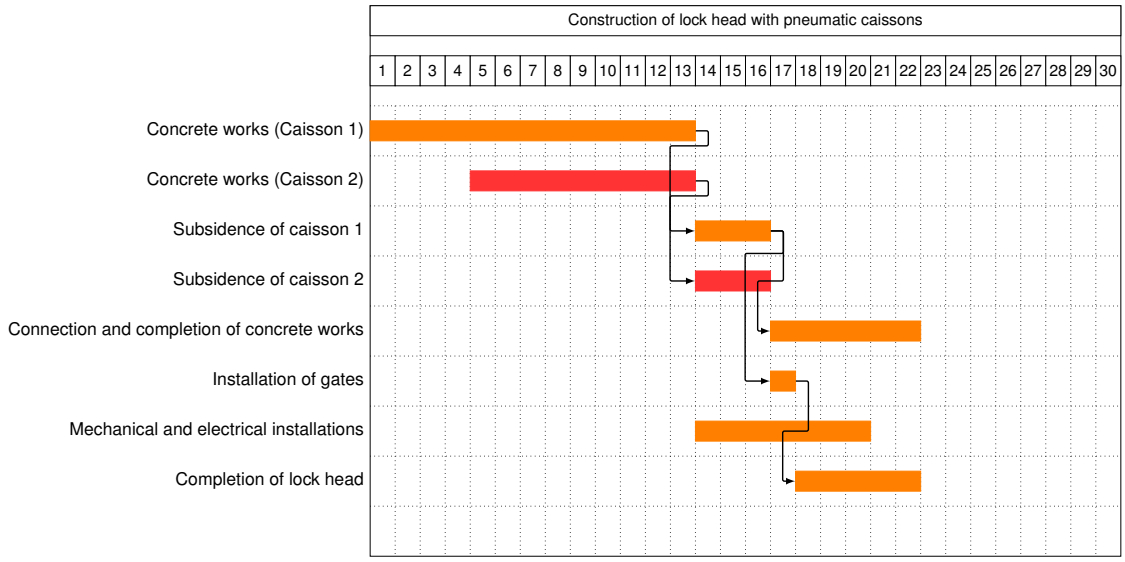

Figure E.3: *Construction planning of the pneumatic caissons*

E.2.2 TRADITIONAL BUILDING PIT

The construction of the building pit as well as the subsequent construction of the lock head are subdivided in multiple phases which are listed below:

- Installation of combi-walls and anchors
- Excavation of the building pit
- Installation of tension piles
- Casting of under water concrete
- Concrete works
- Installation of gates
- Installation of mechanical and electrical equipment
- Completion of the lock head

For each of these steps the required construction time is calculated in the following paragraphs.

INSTALLATION OF COMBI-WALLS AND ANCHORS

The building pit will be surrounded by combi-walls. The perimeter of the building pit ha a length of $l \cdot 2 + w \cdot 2 = 145 \cdot 2 + 45 \cdot 2 = 354$ m. The installation rate of the combi-wall has an average speed of 10 m/day is assumed. Therefore a total of 36 working days (*8 hours*) are required for the construction. The installation of the combi-walls takes globally 1.5 month.

EXCAVATION OF THE BUILDING PIT

After the combi-walls are installed the enclosed soil body must be excavated. The largest part of this excavation takes place in the wet. This can be done by a cutterhopper. A cutterhopper has a capacity of approximately 10.000 m^3/day. The total amount of soil, $V_{excavation}$, that has to be excavated inside the working chamber is equal to $V_{excavation} = l \cdot w \cdot h = 132 \cdot 45 \cdot (6 - -21) = 160380\ m^3$. A total of 16 working days are therefore required. The cutterhopper itself must also be build up before the excavations can start and must be removed afterwards. For the total excavation process 2 months of work are included in the calculation.

INSTALLATION OF THE TENSION PILES

The tension piles must keep the underwater concrete in position. On every $1.5 \times 1.5 = 2.25\ m^2$ one tension pile is installed. A total of $\frac{135 \cdot 45}{2.25} = 2700$ tension piles are required. With eight installation units with a capacity of 2 tension piles a day, 8 months are necessary for the installation.

UNDERWATER CONCRETE FLOOR

The height of the underwater concrete floor was assumed 3 meter in height. A total of $l \cdot w \cdot d = 132 \cdot 45 \cdot 2 = 11880\ m^3$ of underwater concrete is required. With an installation rate of 50 $m^3/hour$, 30 working are required. Including the time necessary to build up all the equipment, a total time of 2 months is assumed.

CONCRETE WORKS

After the construction of the building pit is finished the lock heads can be constructed. The same dimensions of the walls are applied as used in the design of the pneumatic caissons. The required amount of concrete is:

$$V_{concrete} = (45 + 2 \cdot 10 + 2 \cdot 67 + 45) \cdot 3.5 \cdot (6 - -19) + (132 \cdot 45 \cdot 2) = 33230\ m^3$$

With an installation rate of 200 m^3/day, the process takes up to 8 months.

INSTALLATION OF GATES, MECHANICAL AND ELECTRICAL EQUIPMENT

For the installation of gates, mechanical and electrical equipment 6 months of work are calculated. The largest part of the activities can already start during the concrete works.

COMPLETION OF THE LOCK HEAD

For the completion of the lock head and connection to the lock chamber an additional time of 6 months are included in the calculation.

When all the construction phases are summed up, a time of 30 months per lock head are required for the construction. All steps are schematised in figure E.4.

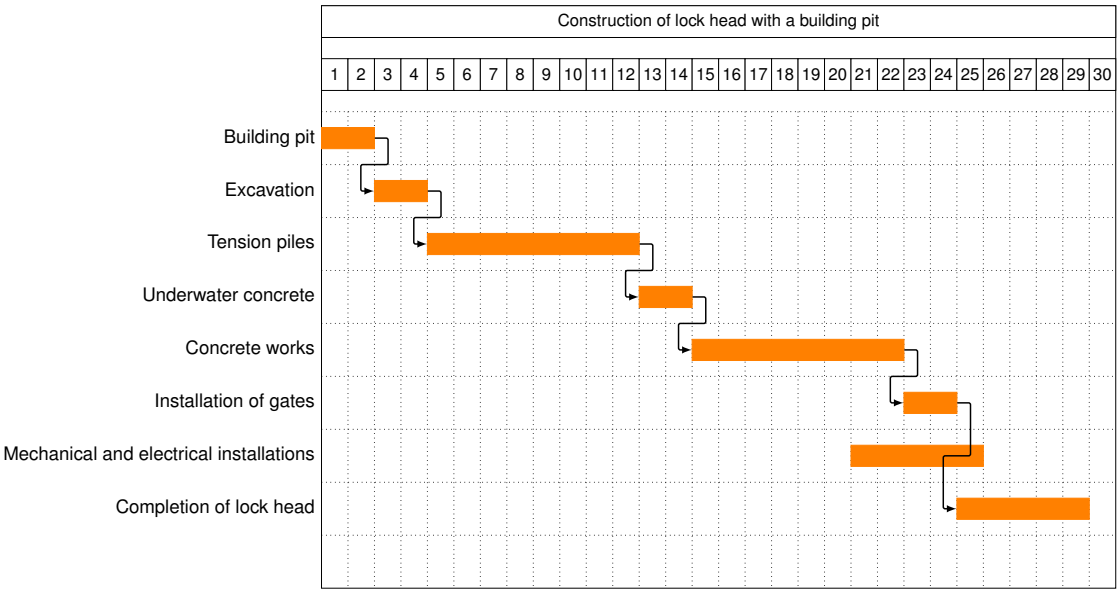

Figure E.4: *Construction planning of the lock head constructed in a traditional building pit*

E.3 GLOBAL COSTS OF LOCK HEAD

In table E.1 a global calculation is made for the costs of the three elaborated variants. To compare the variants only the costs related to the specified construction method are given and not for the complete lock. Therefore elements which are identical in every situation, such as, for example, the doors are not shown.

Table E.1: *Global estimated construction costs*

Variant 1 -One large pneumatic caisson divided into several compartments						
Description	*Quality*	*Unit*	*Unit price*			*Total*
Supplement and leveling of terrain	17.820	m^3	6	€/ m^3	€	106.920
Concrete works	62.250	m^3	450	€/ m^3	€	28.012.500
Underwater concrete below element	17.820	m^3	250	€/ m^3	€	4.455.000
Groundworks below caisson (NAP -27m)	1.96.020	m^3	80	€/ m^3	€	15.681.600
				Total	**€**	**48.256.020**
Variant 2 - Two pneumatic caissons which are subsided individually and divided into several compartments						
Description	*Quality*	*Unit*	*Unit price*			*Total*
Supplement and leveling of terrain	17.820	m^3	6	€/ m^3	€	106.920
Concrete works (Caisson 1)	10.507*	m^3	450	€/ m^3	€	4.728.150
Concrete works (Caisson 2)	40.352	m^3	450	€/ m^3	€	18.158.400
Underwater concrete below element (Caisson 1)	1.350*	m^3	250	€/ m^3	€	3.37.500
Underwater concrete below element (Caisson 2)	9.045	m^3	250	€/ m^3	€	2.261.250
Groundworks below caisson 1 (NAP -27m)	14.850*	m^3	80	€/ m^3	€	1.188.000
Groundworks below caisson 2 (NAP -27m)	99.495	m^3	80	€/ m^3	€	7.959.600
Excavation between caissons (NAP -25m)	76.725	m^3	6	€/ m^3	€	460.350
Concrete works immersable caisson	5.610	m^3	450	€/ m^3	€	2.524.500
Installation immersible caisson	50	% of production costs			€	1.262.250
				Total	**€**	**37.724.670**
Variant 3 - Reference design - Building pit						
Description	*Quality*	*Unit*	*Unit price*			*Total*
Supply and installation of combi-wall	16.275	m^2	500	€/ m^2	€	8.137.500
Anchors	868	st	1000	€/ st	€	868.000
Groundworks / Excavating building pit (NAP -22m)	276.640	m^3	6	€/ m^3	€	1.659.840
Supply and installation of tension piles	4.391	st	3000	€/ st	€	13.173.333
Supply and installation of underwater concrete	29.640	m^3	250	€/ m^3	€	7.410.000
De-watering building pit	9.880	m^3	125	€/ m^3	€	1.235.000
Concrete works	42.000	m^3	450	€/ m^3	€	18.900.000
Backfilling sand fill between structure and sheetpiles	98.500	m^3	12.5	€/ m^3	€	1.231.250
				Total	**€**	**52.614.923**

* The given quantities are exclude the solution to obtain a stable caisson. (*Section § 8.6*)

F

PNEUMATIC CAISSONS

F.1 SELF-WEIGHT OF THE PNEUMATIC CAISSON

Dimensions and self weight of the different options for the pneumatic caissons.

Variant 1

	Item	Length [m]		Width [m]		Height [m]		Volume/Surface		Unit Weight		Total [kN]
	Concrete											
	- Bottom slab	132	x	45	x	5	=	29700				
	- Cutting edge	354	x	0,85	x	3	=	902,7				
	Perimeter = 354 m, Avg width cutting edge = 0,5x(0,2+1,5)=0,85 m											
	- Walls	244	x	3,5	x	25	=	21350				
	Perimeter - 2 x 55 meter											
	- Compartment walls	1 x 132	x	1,7	x	3		673,2				
	- Compartment walls	6 x 45	x	1,7	x	3	=	1377				
	Avg width cutting edge = 2x0,5x(0,2+1,5)=1,7 m											
						SubTotal:		54002,9	m^3	x 25	=	1350072,5
	Bulkhead											
	-Temporary concrete	110	x	3	x	25		8250	x	x 25	=	206250
	= 2 x 55 meter											
										Total:		**1556323** kN

Variant 2

Caisson A

	Item	Length [m]		Width [m]		Height [m]		Volume/Surface		Unit Weight		Total [kN]
	Concrete											
	- Bottom slab	10	x	45	x	5	=	2250				
	- Cutting edge	110	x	0,85	x	3	=	280,5				
	Perimeter = 110 m, Avg width cutting edge = 0,5x(0,2+1,5)=0,85 m											
	- Walls	58	x	3,5	x	25	=	5075				
	45 + 2 x 6,5 meter											
	- Compartment walls	1 x 10	x	1,7	x	3		51				
	Avg width cutting edge = 2x0,5x(0,2+1,5)=1,7 m											
						SubTotal:		7656,5	m^3	x 25	=	191412,5
	Bulkhead											
	-Temporary concrete	38	x	3	x	25		2850	x	x25	=	71250
	= 45 -2 x 3,5 meter											
										Total:		**262663** kN

Caisson B

	Item	Length [m]		Width [m]		Height [m]		Volume/Surface		Unit Weight		Total [kN]
	Concrete											
	- Bottom slab	67	x	45	x	5	=	15075				
	- Cutting edge	224	x	0,85	x	3	=	571,2				
	Perimeter = 224 m, Avg width cutting edge = 0,5x(0,2+1,5)=0,85 m											
	- Walls	172	x	3,5	x	25	=	15050				
	= 2 x 67 + (45 - 2 x 3,5) = 172 m											
	- Compartment walls	1 x 67	x	1,7	x	3		341,7				
	- Compartment walls	3x 45	x	1,7	x	3	=	688,5				
						SubTotal:		31726,4	m^3	x 25	=	793160
	Bulkhead											
	-Temporary concrete	34,5	x	3	x	25		862,5	x	x 25	=	21562,5
	=45 -3 x 3,5 = 34,5m											
										Total:		**814723** kN

F.2 NET FORCE ON PNEUMATIC CAISSON

Construction Alternative 1

NAP		Selfweight	Friction	Bearing	Air	Ballast		w_ce	w_ce (new)	Net
level	m depth	kN	kN	kN	kN	m height	kN	m	m	
6	0							15,00		
5,5	0,5							15,75		
5	1							15,75		
4,5	1,5							15,75		
4	2							15,75		
3,5	2,5							15,75		
3	3							15,75		
2,5	3,5							15,75		
2	4	816323	-15472	-800851	0	0,0	0	15,75	6,36	0
1,5	4,5	811401	-18196	-781663	-11542	0,0	0	15,75	5,91	0
1	5	806480	-21095	-760267	-25117	0,0	0	15,75	5,49	0
0,5	5,5	801558	-24170	-736694	-40693	0,0	0	15,75	5,09	0
0	6	796637	-27421	-710974	-58241	0,0	0	15,75	4,71	0
-0,5	6,5	791715	-30847	-683137	-77731	0,0	0	15,75	4,34	0
-1	7	786794	-34449	-637501	-114844	0,0	0	8,92	3,10	0
-1,5	7,5	757094	-38226	-575963	-142904	0,0	0	8,09	2,69	0
-2	8	727394	-42179	-511917	-173298	0,0	0	7,36	2,29	0
-2,5	8,5	697694	-44911	-447054	-205728	0,0	0	6,72	1,93	0
-3	9	1407994	-53058	-1144801	-210135	0,0	0	2,50	2,50	0
-3,5	9,5	1378294	-56568	-1085640	-236086	0,0	0	2,36	2,36	0
-4	10	1348594	-60078	-1025429	-263087	0,0	0	2,21	2,21	0
-4,5	10,5	1318894	-63588	-963688	-291617	0,0	0	2,06	2,06	0
-5	11	1289194	-67098	-900291	-321804	0,0	0	1,89	1,89	0
-5,5	11,5	1259494	-70608	-835244	-353641	0,0	0	1,71	1,71	0
-6	12	1229794	-74118	-768608	-387067	0,0	0	1,53	1,53	0
-6,5	12,5	1223874	-77628	-727470	-418775	0,0	0	1,40	1,40	0
-7	13	1217954	-81138	-685185	-451630	0,0	0	1,27	1,27	0
-7,5	13,5	1212034	-84648	-641935	-485450	0,0	0	1,14	1,14	0
-8	14	1206114	-88159	-598341	-519614	0,0	0	1,02	1,02	0
-8,5	14,5	1200194	-91669	-554548	-553977	0,0	0	0,90	0,90	0
-9	15	1194274	-96760	-505856	-591658	0,0	0	0,76	0,76	0
-9,5	15,5	1188354	-100548	-464766	-623040	0,0	0	0,71	0,71	0
-10	16	1182434	-104336	-462267	-649677	0,4	33847	0,65	0,71	0
-10,5	16,5	1176514	-108124	-459808	-676276	0,8	67694	0,59	0,72	0
-11	17	1170594	-111913	-457388	-702834	1,2	101542	0,53	0,72	0
-11,5	17,5	1164674	-115701	-455009	-729353	1,6	135389	0,47	0,73	0
-12	18	1158754	-119489	-452670	-755830	2,0	169236	0,40	0,73	0
-12,5	18,5	1152834	-120399	-460510	-775008	2,4	203083	0,36	0,81	0
-13	19	1146914	-123836	-450142	-809866	2,8	236930	0,26	0,73	0
-13,5	19,5	1140994	-130284	-430667	-850819	3,2	270778	0,15	0,61	0
-14	20	1135074	-134124	-426633	-878941	3,6	304625	0,08	0,60	0
-14,5	20,5	1129154	-137964	-422548	-907114	4,0	338472	0,02	0,60	0
-15	21	1123234	-141804	-496958	-856790	4,4	372319	-0,10	1,24	0
-15,5	21,5	1117314	-145645	-490666	-887170	4,8	406166	-0,23	1,20	0
-16	22	1111394	-149485	-484254	-917669	5,2	440014	-0,36	1,16	0
-16,5	22,5	1105474	-153325	-477728	-948282	5,6	473861	-0,48	1,12	0
-17	23	1099554	-157165	-471094	-979003	6,0	507708	-0,59	1,08	0
-17,5	23,5	1093634	-161005	-464357	-1009827	6,4	541555	-0,70	1,04	0
-18	24	1087714	-164845	-457522	-1040749	6,8	575402	-0,81	1,01	0
-18,5	24,5	1081794	-168685	-450593	-1071765	7,2	609250	-0,91	0,97	0
-19	25	1075874	-172525	-443575	-1102871	7,6	643097	-1,01	0,94	0
-19,5	25,5	1069954	-176365	-436471	-1134062	8,0	676944	-1,11	0,91	0
-20	26	1064034	-180205	-429285	-1165335	8,4	710791	-1,20	0,87	0
-20,5	26,5	1058114	-176616	-399042	-1227094	8,8	744638	-0,98	0,66	0
-21	27	1052194	-179975	-395290	-1255415	9,2	778486	-1,07	0,65	0
-21,5	27,5	1046274	-183334	-391473	-1283799	9,6	812333	-1,16	0,64	0
-22	28	1040354	-186693	-387591	-1312249	10,0	846180	-1,25	0,64	0
-22,5	28,5	1034434	-190052	-383642	-1340767	10,4	880027	-1,35	0,63	0
-23	29	1028514	-193411	-379623	-1369354	10,8	913874	-1,44	0,62	0
-23,5	29,5	1022594	-196770	-375533	-1398012	11,2	947722	-1,54	0,62	0
-24	30	1016674	-200129	-371371	-1426743	11,6	981569	-1,63	0,61	0
-24,5	30,5	1010754	-203488	-367133	-1455548	12,0	1015416	-1,73	0,60	0
-25	31	1004834	-206847	-362819	-1484431	12,4	1049263	-1,83	0,60	0
-25,5	31,5	998914	-210206	-358425	-1513393	12,8	1083110	-1,93	0,59	0
-26	32	992994	-213565	-353950	-1542436	13,2	1116958	-2,03	0,58	0
-26,5	32,5	987074	-216924	-349392	-1571562	13,6	1150805	-2,13	0,57	0
-27	33	981154	-220283	-344747	-1600775	14,0	1184652	-2,24	0,57	0

Construction Alternative 2 - Caisson containing the gate recess

NAP		Selfweight	Friction	Bearing	Air	Ballast		w_ce	w_ce (new)	Net
level	m depth	kN	kN	kN	kN	m height	kN	m	m	
6	0							15,00		
5,5	0,5							10,00		
5	1							10,00		
4,5	1,5							10,00		
4	2							10,00		
3,5	2,5							10,00		
3	3							10,00		
2,5	3,5							10,00		
2	4	64538	-4808	-59730	0	0,0	0	10,00	2,77	0
1,5	4,5	63985	-5654	-57415	-916	0,0	0	10,00	2,55	0
1	5	63433	-6555	-54851	-2027	0,0	0	10,00	2,33	0
0,5	5,5	62880	-7511	-52039	-3331	0,0	0	10,00	2,13	0
0	6	62328	-8521	-48979	-4828	0,0	0	10,00	1,92	0
-0,5	6,5	61775	-9585	-45671	-6519	0,0	0	10,00	1,73	0
-1	7	61223	-10705	-41103	-9415	0,0	0	10,00	1,21	0
-1,5	7,5	58973	-11878	-35331	-11763	0,0	0	10,00	1,00	0
-2	8	56723	-13107	-29296	-14320	0,0	0	10,00	0,80	0
-2,5	8,5	54473	-13955	-23504	-17013	0,0	0	10,00	0,62	0
-3	9	250348	-16487	-228715	-5146	0,0	0	3,51	3,51	0
-3,5	9,5	248098	-17578	-224509	-6011	0,0	0	3,43	3,43	0
-4	10	245848	-18668	-220219	-6960	0,0	0	3,34	3,34	0
-4,5	10,5	243598	-19759	-215740	-8098	0,0	0	3,24	3,24	0
-5	11	241348	-20850	-211031	-9467	0,0	0	3,11	3,11	0
-5,5	11,5	239098	-21940	-206070	-11087	0,0	0	2,95	2,95	0
-6	12	236848	-23031	-200847	-12970	0,0	0	2,79	2,79	0
-6,5	12,5	235263	-24122	-196108	-15033	0,0	0	2,62	2,62	0
-7	13	233678	-25212	-191106	-17359	0,0	0	2,44	2,44	0
-7,5	13,5	232093	-26303	-185870	-19919	0,0	0	2,26	2,26	0
-8	14	230508	-27394	-180561	-22553	0,0	0	2,09	2,09	0
-8,5	14,5	228923	-28485	-175218	-25220	0,0	0	1,94	1,94	0
-9	15	227338	-30067	-168315	-28956	0,0	0	1,70	1,70	0
-9,5	15,5	225753	-31244	-163945	-30564	0,0	0	1,68	1,68	0
-10	16	224168	-32421	-159531	-32216	0,0	0	1,65	1,65	0
-10,5	16,5	222583	-33598	-155068	-33916	0,0	0	1,62	1,62	0
-11	17	220998	-34775	-150555	-35667	0,0	0	1,59	1,59	0
-11,5	17,5	219413	-35952	-145987	-37474	0,0	0	1,56	1,56	0
-12	18	217828	-37129	-141359	-39339	0,0	0	1,52	1,52	0
-12,5	18,5	216243	-37412	-139771	-39059	0,0	0	1,64	1,64	0
-13	19	214658	-38480	-132572	-43605	0,0	0	1,43	1,43	0
-13,5	19,5	213073	-40484	-122757	-49831	0,0	0	1,14	1,14	0
-14	20	211488	-41677	-117489	-52321	0,0	0	1,08	1,08	0
-14,5	20,5	209903	-42870	-112155	-54878	0,0	0	1,03	1,03	0
-15	21	208318	-44064	-126793	-37461	0,0	0	2,14	2,14	0
-15,5	21,5	206733	-45257	-119972	-41504	0,0	0	1,97	1,97	0
-16	22	205148	-46450	-113083	-45614	0,0	0	1,80	1,80	0
-16,5	22,5	203563	-47643	-106130	-49789	0,0	0	1,64	1,64	0
-17	23	201978	-48837	-99115	-54026	0,0	0	1,49	1,49	0
-17,5	23,5	200393	-50030	-92042	-58320	0,0	0	1,35	1,35	0
-18	24	198808	-51223	-84913	-62671	0,0	0	1,21	1,21	0
-18,5	24,5	197223	-52416	-77731	-67075	0,0	0	1,08	1,08	0
-19	25	195638	-53609	-70498	-71530	0,0	0	0,96	0,96	0
-19,5	25,5	194053	-54803	-63217	-76033	0,0	0	0,84	0,84	0
-20	26	192468	-55996	-55889	-80582	0,0	0	0,72	0,72	0
-20,5	26,5	190883	-54881	-47879	-88123	0,0	0	0,50	0,50	0
-21	27	189298	-55924	-41506	-91867	0,0	0	0,43	0,43	0
-21,5	27,5	187713	-56968	-35024	-95721	0,0	0	0,36	0,36	0
-22	28	186128	-58012	-28430	-99686	0,0	0	0,29	0,29	0
-22,5	28,5	184543	-59056	-30717	-101080	0,2	6310	0,22	0,32	0
-23	29	182958	-60099	-33044	-102434	0,3	12620	0,15	0,34	0
-23,5	29,5	181373	-61143	-35413	-103746	0,5	18930	0,08	0,37	0
-24	30	179788	-62187	-37823	-105017	0,6	25240	0,01	0,39	0
-24,5	30,5	178203	-63231	-40277	-106244	0,8	31550	-0,06	0,42	0
-25	31	176618	-64275	-42776	-107427	0,9	37859	-0,14	0,44	0
-25,5	31,5	175033	-65318	-45320	-108563	1,1	44169	-0,21	0,47	0
-26	32	173448	-66362	-47912	-109653	1,2	50479	-0,29	0,50	0
-26,5	32,5	171863	-67406	-50551	-110694	1,4	56789	-0,36	0,53	0
-27	33	170278	-68450	-53241	-111686	1,5	63099	-0,44	0,56	0

Construction Alternative 2 - Caisson containing the gate chamber

NAP		Selfweight	Friction	Bearing	Air	Ballast		w_ce	w_ce (new)	Net
level	m depth	kN	kN	kN	kN	m height	kN	m	m	
6	0							15,00		
5,5	0,5							14,20		
5	1							14,20		
4,5	1,5							14,20		
4	2							14,20		
3,5	2,5							14,20		
3	3							14,20		
2,5	3,5							14,20		
2	4	416910	-9790	-407120	0	0,0	0	14,20	5,74	0
1,5	4,5	414241	-11514	-396872	-5856	0,0	0	14,20	5,33	0
1	5	411572	-13348	-385455	-12769	0,0	0	14,20	4,94	0
0,5	5,5	408903	-15294	-372885	-20724	0,0	0	14,20	4,57	0
0	6	406234	-17351	-359176	-29706	0,0	0	14,20	4,22	0
-0,5	6,5	403565	-19519	-344343	-39703	0,0	0	14,20	3,88	0
-1	7	798709	-21798	-762210	-14700	0,0	0	8,43	8,43	0
-1,5	7,5	783634	-24188	-737100	-22345	0,0	0	7,63	7,63	0
-2	8	768559	-26690	-710518	-31351	0,0	0	6,93	6,93	0
-2,5	8,5	753484	-28418	-683531	-41534	0,0	0	6,32	6,32	0
-3	9	738409	-33573	-599580	-105255	0,0	0	2,33	2,33	0
-3,5	9,5	723334	-35794	-569225	-118314	0,0	0	2,20	2,20	0
-4	10	708259	-38015	-538331	-131912	0,0	0	2,07	2,07	0
-4,5	10,5	693184	-40236	-506645	-146302	0,0	0	1,92	1,92	0
-5	11	678109	-42457	-474100	-161551	0,0	0	1,77	1,77	0
-5,5	11,5	663034	-44679	-440697	-177658	0,0	0	1,61	1,61	0
-6	12	647959	-46900	-406467	-194592	0,0	0	1,44	1,44	0
-6,5	12,5	644776	-49121	-384955	-210700	0,0	0	1,32	1,32	0
-7	13	641594	-51342	-362838	-227414	0,0	0	1,20	1,20	0
-7,5	13,5	638411	-53563	-340212	-244636	0,0	0	1,07	1,07	0
-8	14	635229	-55784	-317404	-262040	0,0	0	0,96	0,96	0
-8,5	14,5	632046	-58005	-294492	-279549	0,0	0	0,85	0,85	0
-9	15	628864	-61226	-268795	-298842	0,0	0	0,72	0,72	0
-9,5	15,5	625681	-63624	-247289	-314769	0,0	0	0,67	0,67	0
-10	16	622499	-66021	-225465	-331013	0,0	0	0,62	0,62	0
-10,5	16,5	619316	-68418	-203304	-347594	0,0	0	0,56	0,56	0
-11	17	616134	-70815	-180786	-364533	0,0	0	0,50	0,50	0
-11,5	17,5	612951	-73212	-157888	-381851	0,0	0	0,44	0,44	0
-12	18	609769	-75609	-134587	-399572	0,0	0	0,38	0,38	0
-12,5	18,5	606586	-76184	-114724	-415678	0,0	0	0,35	0,35	0
-13	19	603404	-78360	-88799	-436245	0,0	0	0,25	0,25	0
-13,5	19,5	600221	-82440	-85336	-453478	0,5	21033	0,15	0,21	0
-14	20	597039	-84870	-86288	-467947	1,0	42066	0,09	0,21	0
-14,5	20,5	593856	-87299	-87251	-482404	1,5	63099	0,03	0,22	0
-15	21	590674	-89729	-104790	-480286	2,0	84132	-0,07	0,45	0
-15,5	21,5	587491	-92159	-105681	-494816	2,5	105165	-0,19	0,45	0
-16	22	584309	-94589	-106563	-509355	3,0	126198	-0,31	0,44	0
-16,5	22,5	581126	-97019	-107435	-523903	3,5	147231	-0,42	0,44	0
-17	23	577944	-99449	-108299	-538459	4,0	168264	-0,53	0,43	0
-17,5	23,5	574761	-101879	-109156	-553024	4,5	189297	-0,64	0,43	0
-18	24	571579	-104309	-110004	-567596	5,0	210330	-0,74	0,42	0
-18,5	24,5	568396	-106739	-110845	-582175	5,5	231363	-0,83	0,42	0
-19	25	565214	-109168	-111680	-596762	6,0	252396	-0,93	0,41	0
-19,5	25,5	562031	-111598	-112507	-611355	6,5	273429	-1,02	0,41	0
-20	26	558849	-114028	-113328	-625954	7,0	294462	-1,10	0,40	0
-20,5	26,5	555666	-111757	-111637	-647767	7,5	315495	-0,90	0,32	0
-21	27	552484	-113882	-113485	-661644	8,0	336528	-0,98	0,33	0
-21,5	27,5	549301	-116008	-115365	-675490	8,5	357561	-1,06	0,33	0
-22	28	546119	-118133	-117277	-689303	9,0	378594	-1,15	0,34	0
-22,5	28,5	542936	-120259	-119222	-703082	9,5	399627	-1,23	0,35	0
-23	29	539754	-122384	-121201	-716828	10,0	420660	-1,32	0,35	0
-23,5	29,5	536571	-124510	-123216	-730539	10,5	441693	-1,41	0,36	0
-24	30	533389	-126635	-125266	-744213	11,0	462726	-1,50	0,36	0
-24,5	30,5	530206	-128761	-127353	-757851	11,5	483759	-1,59	0,37	0
-25	31	527024	-130886	-129478	-771451	12,0	504792	-1,68	0,38	0
-25,5	31,5	523841	-133012	-131642	-785012	12,5	525825	-1,77	0,38	0
-26	32	520659	-135137	-133846	-798533	13,0	546858	-1,87	0,39	0
-26,5	32,5	517476	-137263	-136091	-812013	13,5	567891	-1,96	0,39	0
-27	33	514294	-139388	-138379	-825450	14,0	588924	-2,06	0,40	0

F.3 2D ANALYSIS OF CAISSON

To simplify the calculations the caisson will be seen in this section as thin walled two-dimensional structure in order to estimate the order of magnitude of the occurring forces and moments. The bottom slab is assumed 5 meters in height as first estimation for the calculations.

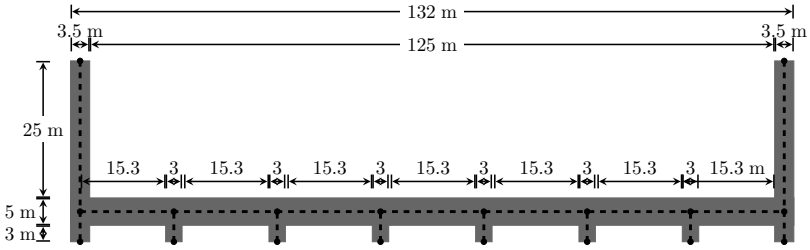

Figure F.1: *Cross section in x-direction*

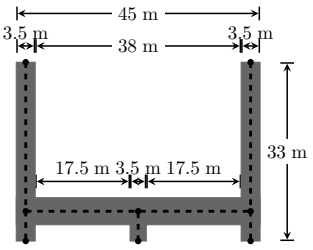

Figure F.2: *Y-direction*

In the 2D analysis the first load combination will be elaborated. An overview of the loads are given in figure F.3. The 2D schematisation has a depth of 1 meter and is constant in the plane perpendicular to the schematisation.

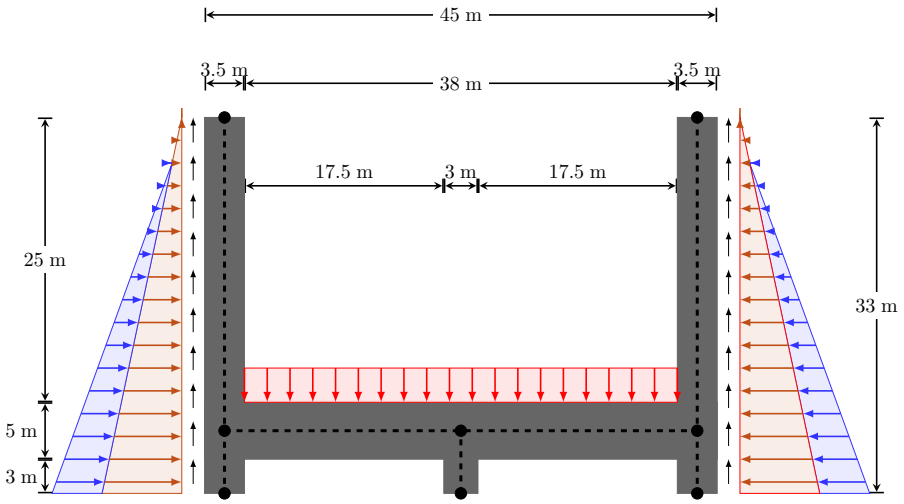

Figure F.3: *Overview of the different loads acting on the caisson at final depth (self-weight not schematised). The center lines pass through the center of the elements.*

To obtain a thin walled model it is assumed that the height of the bottom slab $h_{bottomslab} = 5$ m is divided over the height of the cutting edge ($3 + \frac{1}{2} \cdot 5 = 5.5$ m) and the caisson walls ($25 + \frac{1}{2} \cdot 5 = 27.5$ m).

As described in the previous sections the soil should be schematised as linear spring. Three different scenarios will be elaborated which represent an extreme situation:

- **Soil schematisation 1** - Constant spring stiffness, all values for the spring stiffness are $k = 27.4$ MN/m^3.

- **Soil schematisation 2** - A less stiffer soil layer is situated in the center of the structure $k = 27.4 \cdot 5 = 61.3\ MN/m^3$, a stiffer soil layer is situated on the edges of the structure, $k = \frac{27.4}{\sqrt{5}} = 12.3\ MN/m^3$.
- **Soil schematisation 3** - A stiffer soil layer is situated in the center of the structure $k = 61.3\ MN/m^3$, a less stiffer soil layer is situated on the edges of the structure, $k = 12.3\ MN/m^3$.

Because due to the irregular properties of the supports the forces are transmitted to the subsoil in different ways. The moment distribution along the structure is unique for each situation. In the first scenario, where soil properties are uniform distributed over the length of the structure, the caisson has a deformation shape as given in figure F.4.

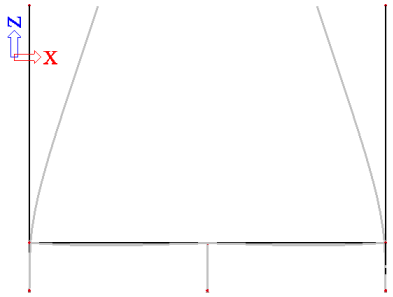

Figure F.4: *Deflection of the caisson using constant spring stiffness*

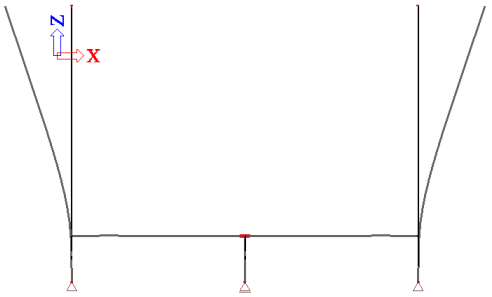

Figure F.5: *Deflection of the caisson using a stiffer spring stiffness in the center*

When the soil in the center part of the structure is stiffer and has more resistance against deformation the outer parts of the structure will deform more than the center part and an opposite deformation pattern will be the result. This is given in figure F.5. Therefore it can be expected that the deformations are smaller in the situation where the center part of the caisson is founded on a stiffer soil layer. Larger deflections can be expected in the case where the center part of the caisson is founded on weaker soil layers. In figure F.6 – F.8 the moment distribution is given for respectively soil schematisation 1, 2 and 3.

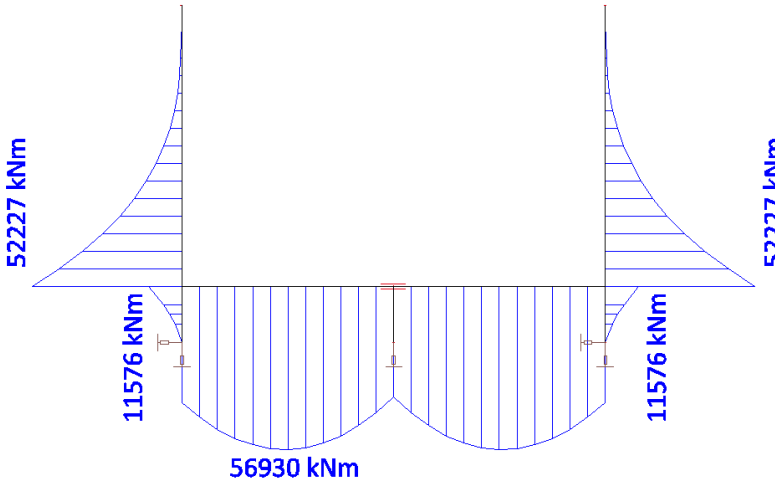

Figure F.6: *Moment distribution using constant spring stiffness*

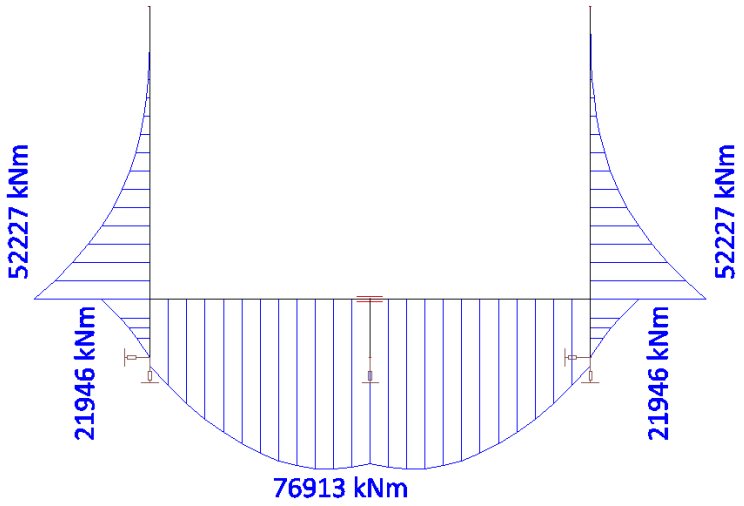

Figure F.7: *Moment distribution with a stiffer soil on the edges*

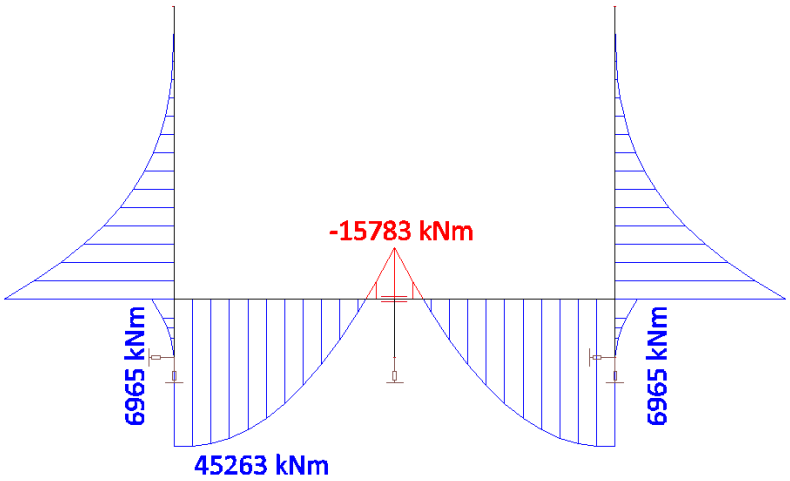

Figure F.8: *Moment distribution with a less stiffer soil on the edges*

The maximum bending moment in the bottom slab is not only dependent on the distributed load along the bottom slab but also from the fixing moment along the supports of the bottom slab. This moment is depending on the horizontal load from the soil against the caisson walls, water pressure forces acting on the outside and the friction force.

From the figures above it can be concluded that the bending moment will become larger with stiffer soil layers on the edges of the structure (figure F.7) and become less and even negative when the soil layer in the center of the structure is stiffer (figure F.8). The maximum deflections at the top of the structure and in the bottom slab are given in table F.1

Table F.1: *Maximum deflections in structure for the cross (x-)direction*

Schematisation	Max. Deflection at top [mm]	Max. Deflection at bottom slab [mm]
Soil schematisation 1	240	70.2
Soil schematisation 2	299.2	105.5
Soil schematisation 3	135.9	15.4

The calculation steps above are also performed for the longitudinal cross section. The moment distribution is given in figure F.9 – F.11. Also here it can be concluded that a stiffer soil layer in the center of a caisson has a positive influence to the deformation and bending moment distribution along the caisson.

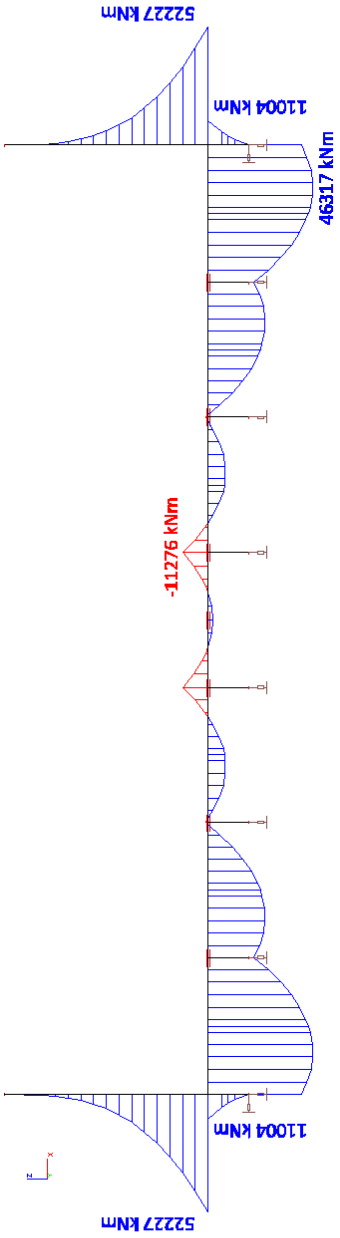

Figure F.9: *Moment distribution using constant spring stiffnesses*

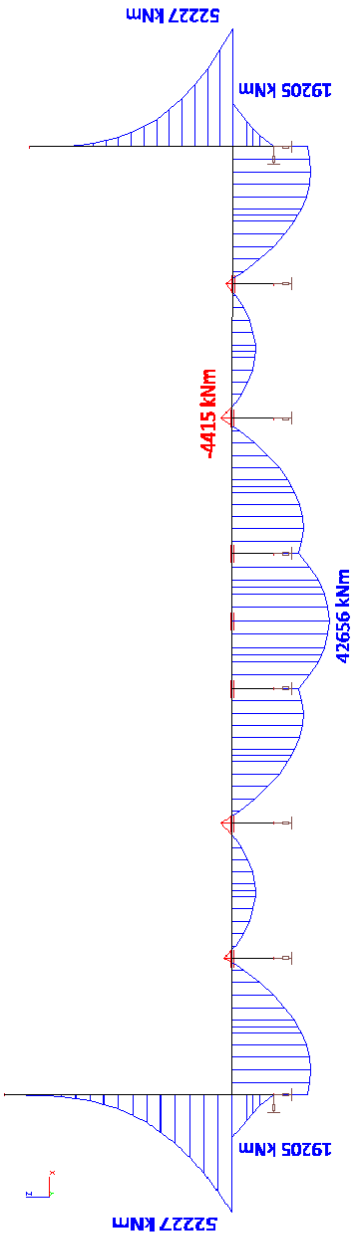

Figure F.10: *Moment distribution with a stiffer soil on the edges*

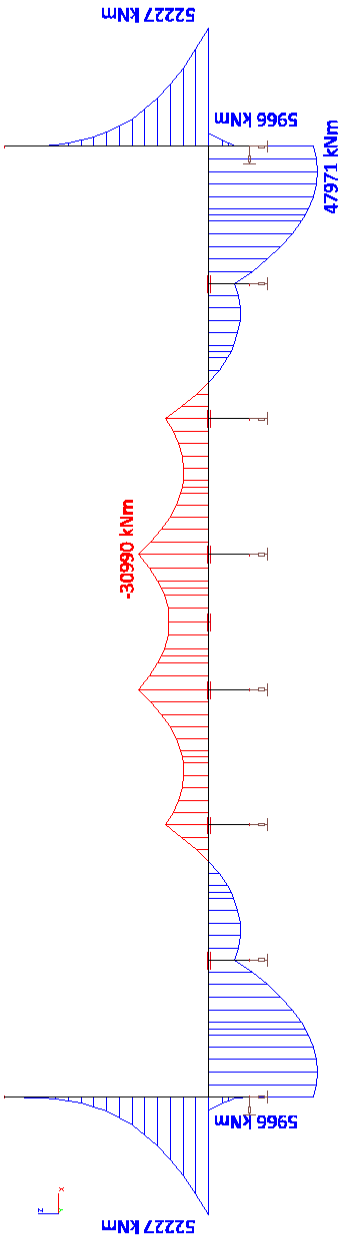

Figure F.11: *Moment distribution with a less stiffer soil on the edges*

The maximum deflections at the top of the structure and in the bottom slab are given in table F.2.

Table F.2: *Maximum deflections in structure for the longitudional (y-)direction*

Schematisation	Max. Deflection at top [mm]	Max. Deflection at bottom slab [mm]
Soil schematisation 1	299.6	115.4
Soil schematisation 2	336.8	337.2
Soil schematisation 3	135.8	145.1

F.4 SCHEMATISATION OF SOIL STIFFNESS

.

In this section the soil schematisation as elaborated in section 7.3.4 for the first variant as well as section 8.3 for the second variant is given.

F.4.1 VARIANT 1

In figure F.12 the soil schematisation for a homogeneously supported caisson is given. In figure F.13 for an caisson supported by a stiff soil on the edges.In figure F.14 for a caisson supported by a stiff soil in the center of the caisson and in figure F.15 for an caisson which is supported diagonally. The soil stiffness below the compartment walls is interpolated between the cutting edges.

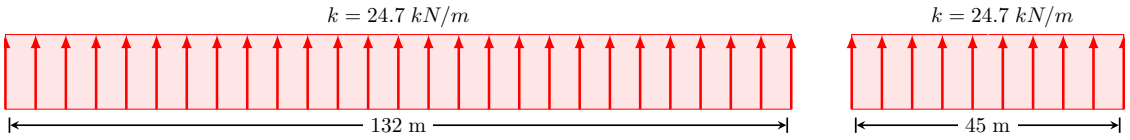

Figure F.12: *Distribution of the stiffness over the outer edge of the caisson (homogeneously supported)*

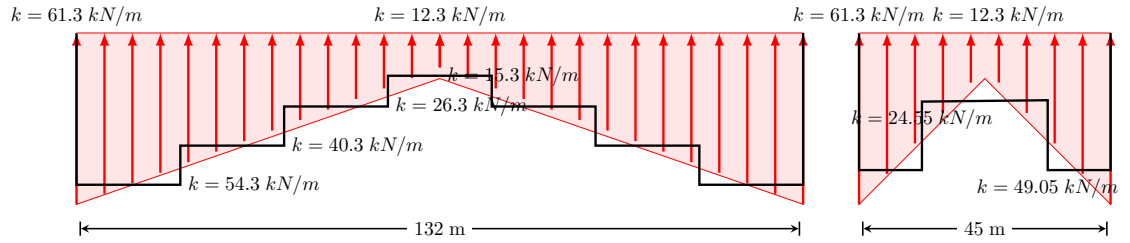

Figure F.13: *Distribution of the stiffness of the soil over the outer edge of the caisson for a caisson supported on the edges by a stiff soil layer as indicated for 7.12*

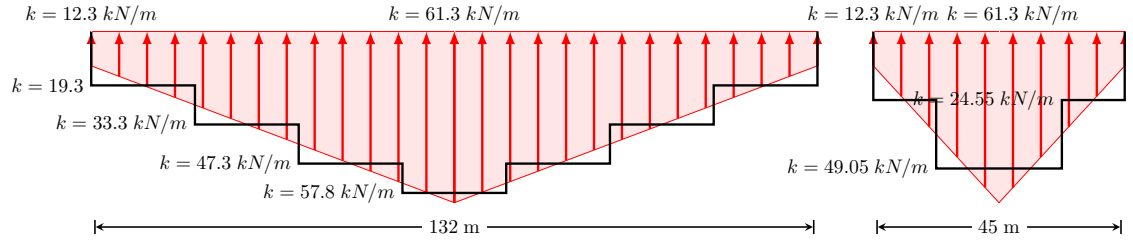

Figure F.14: *Distribution of the stiffness of the soil over the outer edge of the caisson for a caisson supported on the edges by a less stiffer soil layer as indicated for 7.13*

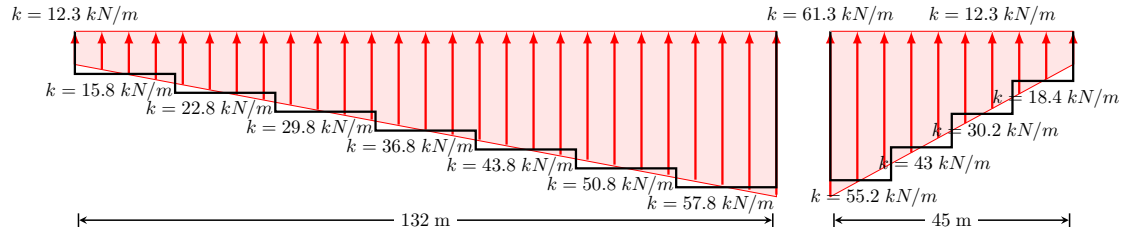

Figure F.15: *Distribution of the stiffness over the outer edge of the caisson for a caisson which is supported on a stiff soil layer diagonally as indicated for 7.14*

F.4.2 VARIANT 2

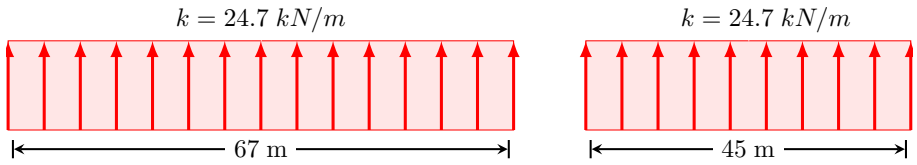

Figure F.16: *Distribution of the stiffness over the outer edge of the caisson (homogeneously supported)*

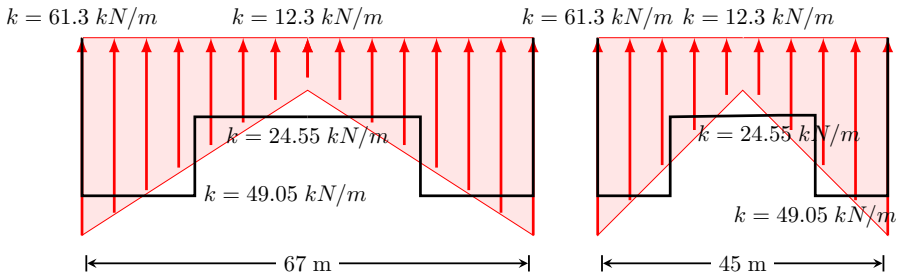

Figure F.17: *Distribution of the stiffness of the soil over the outer edge of the caisson for a caisson supported on the edges by a stiff soil layer as indicated for 7.12*

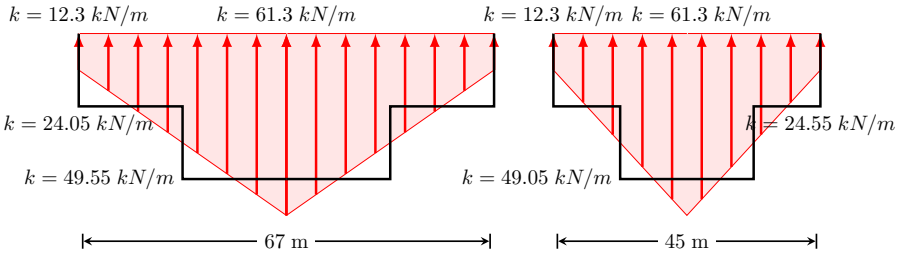

Figure F.18: *Distribution of the stiffness of the soil over the outer edge of the caisson for a caisson supported on the edges by a less stiffer soil layer as indicated for 7.13*

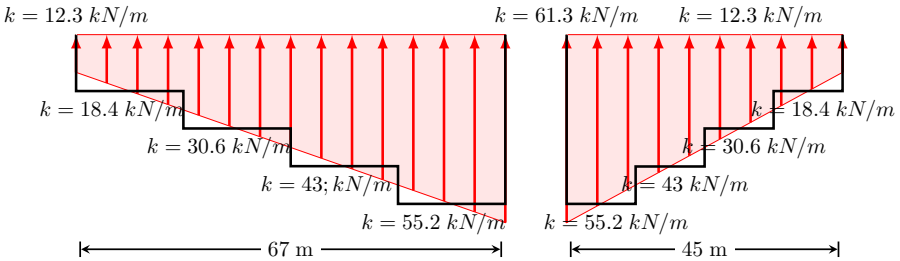

Figure F.19: *Distribution of the stiffness over the outer edge of the caisson for a caisson which is supported on a stiff soil layer diagonally as indicated for 7.14*

F.5 CHECK ON REINFORCEMENT

F.5.1 BENDING RESISTANCE

In this section the moments in the caisson wall from section 7.4 are elaborated. The construction is meanly below the water table. According to [NEN-EN 1992-1-1] the structure falls within the range of exposure class XS3, partially submerged in sea water. For the caisson walls and slabs a concrete cover of $c = 50$ mm is required. Because of the large forces and moments in the structure a concrete class C35/45 is used. Lower concrete classes do increase the amount of concrete required, higher concrete classes do decrease the amount of concrete but are more expensive. The choice of the right concrete class is therefore also dependent on availability and prices on the market. Afterwards the effect of another concrete class can be evaluated.

The assumption of a $h = 5000$ mm thick wall has been made. The effective width of the caisson wall is the width of the wall minus the concrete cover, the height of the possible present stirrups and reinforcement bars. For the first calculations the effective depth is set to $d = 4800$ mm. This assumption will be checked later on.

The walls of the caissons do have lengths between 45– and 132 meter. In the following equations we evaluate the wall per meter width. The width of the wall is therefore $b = 1000$ mm. In table F.3 all assumptions are summarised.

Table F.3: *Values of the different parameters.*

Concrete parameters (C35/45)		
f_{ck}	45	N/mm^2
f_{cd}	35	N/mm^2
f_{cm}	36	N/mm^2
$f_{ctm,fl}$	2.7	N/mm^2
E_{cm}	31000	kPa

Dimensions		
h	5000	mm
d	4800	mm
b	1000	mm
c	50	mm

Steel parameters (B500)		
f_{yk}	500	N/mm^2
f_{yd}	500/1.15=435	N/mm^2

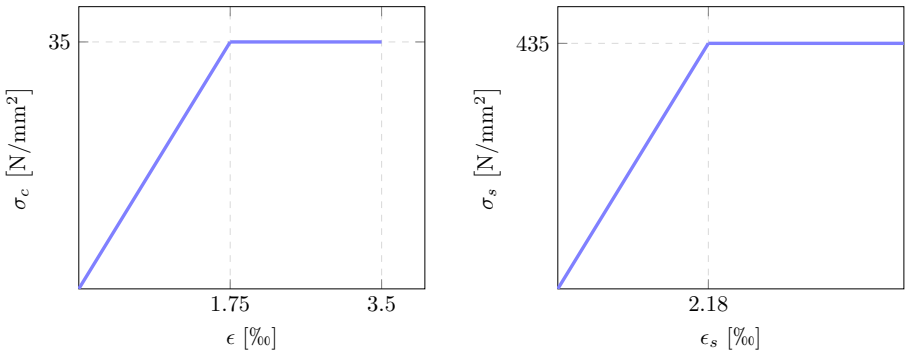

Figure F.20: *Mathematical σ - ϵ relations for concrete class C35/45 and steel quality B500B [Walraven, 2011]*

The σ - ϵ relations for concrete is given in figure F.20. The maximum force in the concrete compressive zone is equal to N_c when the maximum elongation ($\epsilon_{cu3} = 3.5‰$) is reached.

$$N_c = \frac{3}{4} \cdot x_u \cdot f_{cd} \cdot b \qquad \text{(Eq. 1)}$$

This force makes equilibrium with the force in the reinforcement steel (N_{yd})

$$N_{yd} = A_s \cdot f_{yd} \qquad \text{(Eq. 2)}$$

The first equation for equilibrium can be proposed:

$$N_c = N_{yd} - N_{ed} \qquad \Rightarrow \qquad \frac{3}{4} \cdot x_u \cdot f_{cd} \cdot b - N_{ed} = A_s \cdot f_{yd} \qquad \text{(Eq. 3)}$$

x_u is thereby:

$$x_u = \frac{A_s \cdot f_{yd} - N_{ed}}{\frac{3}{4} \cdot f_{cd} \cdot b} \qquad \text{(Eq. 4)}$$

Apart from the horizontal equilibrium also moment equilibrium is required. The resulting concrete compressive force acts at a distance of $0.39 \times x_u$ from the top of the cross section. The internal lever arm (z) is thereby:

$$z = d - 0.39 \cdot x_u \tag{Eq. 5}$$

The mathematical resistance moment is thereby:

$$M_{rd} = A_s \cdot f_{yd} \cdot z - N_{ed} \cdot (0.5 \cdot h - 0.39 \cdot x_u) \tag{Eq. 6}$$

The surface area of the reinforcement is thereby the only unknown.

A design moment of 52922 kNm/m is acting on the caisson bottom slab. The maximum occurring tensile force is $N_{ed} = 5526$ kN. For the reinforcement in the bottom of the slab $n = 7$ rows of ⌀32-150 are used. Between each layer of reinforcement bars an interspace of 75 mm is present. The new depth of the bottom slab can be calculated easily according to formula Eq. 7.

$$\begin{aligned} d &= h - c - \frac{n \cdot \varnothing + (n-1) \cdot 75}{2} \\ d &= 5000 - 50 - \frac{7 \cdot 32 + 6 \cdot 75}{2} = 4613 \text{ mm} \end{aligned} \tag{Eq. 7}$$

The total reinforcement area is

$$A_s = \frac{1}{4} \cdot \pi \cdot \varnothing^2 \cdot \frac{1000}{150} \cdot 7 = 37532 \text{ mm}^2 \tag{Eq. 8}$$

The reinforcement ratio can be calculated on the basis of the diameter, number of reinforcement bars and the new depth of equation Eq. 7

$$\rho = \frac{A_s}{b \cdot d} = \frac{37532}{1000 \cdot 4613} = 0.814\% \tag{Eq. 9}$$

The moment of resistance of the wall must be larger than the cracking moment to prevent brittle failure. ($M_{cr} \leqslant M_{rd}$). Only then failure of the wall will occur after major cracks are developed and large deformations have occurred by the yielding of the reinforcing steel. Before failure there is a visible warning.

$$\begin{aligned} M_{cr} &\leqslant M_{rd} \\ \frac{1}{6} \cdot b \cdot h^2 \cdot f_{ctm,fl} &\leqslant A_s \cdot f_{yk} \cdot d \cdot (1 - 0.52\rho \cdot \frac{f_{yk}}{f_{cm}}) \end{aligned} \tag{Eq. 10}$$

Therefore with $\rho = A_s/(b \cdot d)$ and approximately $h = 1.1 \cdot d$

$$\begin{aligned} \rho_{min} &= \frac{1 - \sqrt{1 - 0.42 \cdot f_{ctm,fl}/f_{cm}}}{1.04 \cdot f_{yk}/f_{cm}} \\ &= \frac{1 - \sqrt{1 - 0.42 \cdot 2.2/43}}{1.04 \cdot 500/43} = 0.089\ \% \end{aligned} \tag{Eq. 11}$$

Not only a minimum amount of reinforcement is required to prevent brittle failure, also a maximum amount of reinforcement is prescribed. The reinforcement must yield before failure of the concrete. This condition can be expressed in a limit value for the compression zone height of the concrete. With $\epsilon_{c3u} = 3.5$ ‰ and $\epsilon_{sy} = f_{yk}/E_s$.

$$\frac{x_u}{d} \leqslant \frac{3.5 \cdot 10^{-3}}{3.5 \cdot 10^{-3} + 2.5 \cdot f_{yk}/E_s} \tag{Eq. 12}$$

This leads to the requirement that $\frac{x_u}{d} \leqslant 0.45$. From the horizontal equilibrium it follows that:

$$0.75 \cdot x_u \cdot b \cdot f_{ck} = A_s \cdot f_{yk} \qquad \text{(Eq. 13)}$$

With $\rho = A_s/(b \cdot d)$ this is:

$$\begin{aligned} \rho_{max} &= 0.34 \cdot \frac{f_{ck}}{f_{yk}} \\ &= 0.34 \cdot \frac{45}{500} = 3.06 \end{aligned} \qquad \text{(Eq. 14)}$$

Equation Eq. 14 calculates the maximum reinforcement ratio based on the situation only tension reinforcement is used. When caissons with smaller inner dimensions are preferred then not only tensile reinforcement but also compressive reinforcement can be used. In that case more reinforcement can be used than allowed following the equation.

With help of the actual reinforcement surface the exact resistance moment can be calculated:

$$x_u = \frac{A_s \cdot f_{yd} - N_{ed}}{0.75 \cdot f_{cd} \cdot b} \quad \Rightarrow \quad x_u = \frac{37532 \cdot 435 - 5526}{0.75 \cdot 35 \cdot 1000} = 1082 \text{ mm} \qquad \text{(Eq. 15)}$$

For rectangular cross sections the resulting concrete compressive force N_c takes at a distance of $0.39 \cdot x_u$ from the upper side of the cross-section. The internal lever arm z is equal to:

$$z = d - 0.39 \cdot x_u = 4800 - 0.39 \cdot 1082 = 4192 \text{ mm} \qquad \text{(Eq. 16)}$$

At last the maximum mathematical moment of resistance can be calculated:

$$\begin{aligned} M_{rd} &= A_s \cdot f_{yd} \cdot z - N_{ed} \cdot (0.5 \cdot h - 0.39 \cdot x_u) \\ M_{rd} &= 37532 \cdot 435 \cdot 4192 - 5526 \cdot (0.5 \cdot 5000 - 0.39 \cdot 1082) = 56920 \text{ kNm} \end{aligned} \qquad \text{(Eq. 17)}$$

All forces and dimensions are schematised in figure F.21.

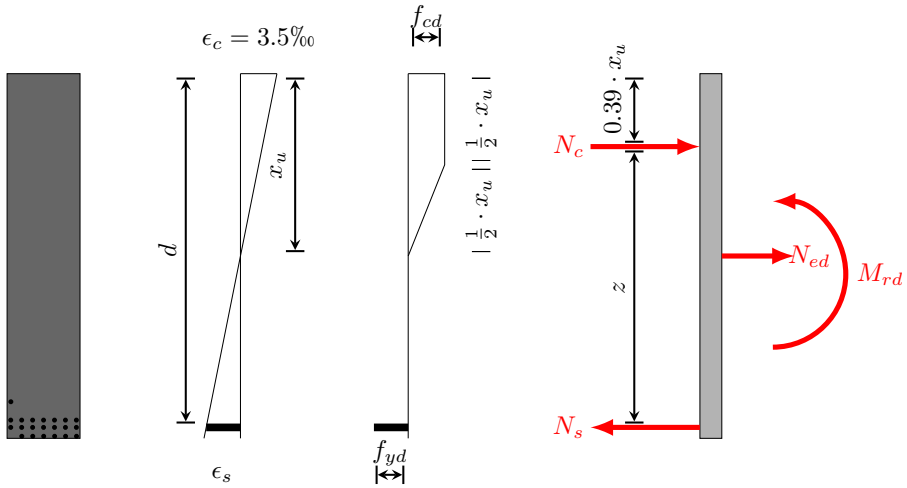

Figure F.21: *Schematisation of the forces in the cross section*

F.5.2 SHEAR RESISTANCE

Also without stirrups concrete has resistance against shear forces. The maximum shear forces the concrete can transfer will be calculated according equation Eq. 18 [NEN-EN 1992-1-1]

$$V_{Rd,c} = [C_{Rd,c} \cdot k \cdot (100 \cdot \rho_1 \cdot f_{ck})^{1/3} + k_1 \cdot \sigma_{cp}] \cdot b \cdot d \qquad \text{(Eq. 18)}$$

With a minimum value of:

$$V_{Rd,c} = (v_{min} + k_1 \cdot \sigma_{cp}) \cdot b \cdot d \qquad \text{(Eq. 19)}$$

Wherein:

k	$1 + \sqrt{\frac{200}{d}} \leqslant 2$	–
$C_{Rd,c}$	$\frac{0.18}{\gamma_c} = \frac{0.18}{1.5} = 0.12$	-
A_{sl}	Surface area of tension reinforcement.	mm^2
ρ_1	$\frac{A_{sl}}{b \cdot d} \leqslant 0.02$	%
σ_{cp}	N_{Ed}, minimum guaranteed value of normal stress, assumed $N_{Ed} = 0$	kN
k_1	0.15	–
v_{min}	$0.035 \cdot k^{3/2} \cdot f_{ck}^{1/2}$	-
d	Depth of concrete beam	-

The smaller the depth, d, of the concrete is the smaller the resistance against shear forces is. It should be noted that a decrease in depth also ensures a decrease in self weight and thereby a decrease in occurring shear forces. The maximum shear forces the concrete can handle without stirrups is given in table F.4.

Table F.4: *Maximum shear values*

	x-direction kN/m	**y-direction** kN/m
Bottom plate	1477	1504
Caisson wall	1016	1195

F.6 EFFECT OF UNEQUAL EXCAVATION OF WORKING CHAMBER

The effect of an unequal excavation of the working chamber will be calculated for the first caisson for a depth of 10.50 meters. (NAP -4.5 m). All governing vertical loads on the caisson given in equation 7.1 are known except on the resisting bearing force and air pressure which are dependent on the width of the cutting edge. Requiring $F_{net} = 0$. In the following sections the equilibrium in both directions will be elaborated.

CROSS SECTION

$$F_{net}(w_{ce}) = F_{selfweight} - [F_{friction} + F_{air}(w_{ce}) + F_{bearing}(w_{ce})]$$
$$= 1\,556\,322 - [108124 + (A_{bottom\,slab} - A_{foundation}) \times \underbrace{130}_{\sigma_{air}} + A_{foundation} \times \underbrace{379}_{\sigma_{bearing;max}} = 0 \qquad \text{(Eq. 20)}$$

In a compartimented caisson with 1 compartment wall in width and 6 compartment walls in length.

$$A_{foundation} = 132 \cdot 45 - [((2+6) \times w_{ce}) \cdot ((2+1) \times w_{ce})] \quad \text{(Eq. 21)}$$

w_{ce} is the only unknown parameter and therefore equation Eq. 20 can be solved: $w_{ce} = 2.30$ m. To analyse the effect of the increased horizontal soil pressure the extra excavation height on the right side of the caisson is set at $x = 0.50$ meter. See figure F.22.

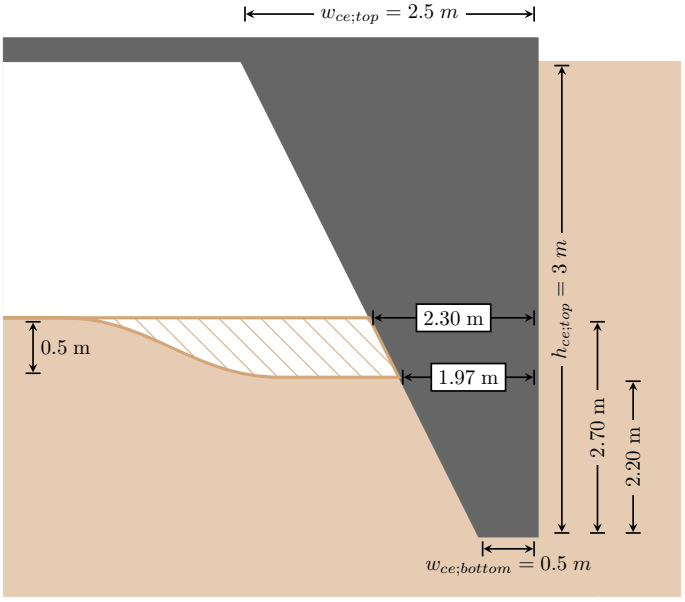

Figure F.22: *Schematisation of cutting edge with corresponding dimensions*

The new width of the cutting edge thereby becomes:

$$w_{ce;new} = w_{ce;original} - \frac{w_{ce;top} - w_{ce;bottom}}{h_{ce}} \cdot x = 2.30 - \frac{2.5 - 0.5}{3} \cdot 0.5 = 1.97 \text{ m} \quad \text{(Eq. 22)}$$

With the width cutting edge known all forces acting on the caisson can be calculated:

$$\begin{aligned} F_{air;left} &= \frac{1}{2} \cdot (A_{bottom\ slab} - A_{foundation}) \cdot \sigma_{air} \\ &= \frac{1}{2} \cdot (132 \cdot 45 - \left[\left(132 - \left((2+6) \times 2.30\right)\right) \cdot \left(45 - \left((2+1) \times 2.30\right)\right)\right]) \cdot 65 \\ &= 140555 \text{ kN} \end{aligned} \quad \text{(Eq. 23)}$$

And the air pressure on the other side can be calculated with the cutting edge on the right side. $w_{ce,new} = 1.97 \Rightarrow F_{air;right} = 147663$ kN.

The air pressure forces are acting on a distance $c_{air;left}$ and $c_{air;right}$ from the center of gravity:

$$\begin{aligned} c_{air;left} &= \frac{1}{2} \cdot (\frac{W}{2} - w_{ce;original}) = \frac{1}{2} \cdot (\frac{45}{2} - 2.30) = 10.10 \text{ m} \\ c_{air;right} &= \frac{1}{2} \cdot (\frac{W}{2} - w_{ce;new}) = \frac{1}{2} \cdot (\frac{45}{2} - 1.97) = 10.26 \text{ m} \end{aligned} \quad \text{(Eq. 24)}$$

The bearing capacity on the long side of the caisson can be calculated by multiplying the bearing capacity, length and cutting edge width.

$$\begin{aligned} F_{bearing;left} &= L \cdot w_{ce,original} \cdot \sigma_{max,d} \\ &= 132 \cdot 2.30 \cdot 663.0 = 201736 \text{ kN} \end{aligned} \tag{Eq. 25}$$

The bearing capacity on the right side can be calculated correspondingly: $w_{ce,new} = 1.97 \Rightarrow F_{bearing;right} = 172565$ kN. The bearing forces are acting on a distance $c_{bearing;left}$ and $c_{bearing;right}$ from the center of gravity:

$$\begin{aligned} c_{bearing;left} &= \frac{W}{2} - \frac{1}{2} \cdot w_{ce;original} = \frac{45}{2} - \frac{1}{2} \cdot 2.30 = 21.35 \text{ m} \\ c_{bearing;right} &= \frac{W}{2} - \frac{1}{2} \cdot w_{ce;new} = \frac{45}{2} - \frac{1}{2} \cdot 1.97 = 21.51 \text{ m} \end{aligned} \tag{Eq. 26}$$

The upward force from the cutting edge and compartment walls on the short side of the caisson can be calculated with:

$$\begin{aligned} F_{bearing;short\ side} &= (L - w_{ce;new} - w_{ce;original}) \cdot \sigma_{max;d} \cdot \frac{1}{2} \cdot (w_{ce;new} + w_{ce;original}) \cdot \\ &\quad (n_{cutting\ edge} + n_{compartment\ walls}) \\ &= (45 - 2.30 - 1.97) \cdot 663.0 \cdot \frac{1}{2} \cdot (2.30 + 1.97) \cdot (2 + 6) \\ &= 461898 \text{ kN} \end{aligned} \tag{Eq. 27}$$

The center of gravity of this force is situated at a distance of $c_{bearing;short}$ to the left of the center point of the caisson.

$$\begin{aligned} c_{bearing;short} &= 22.5 - (\frac{1}{3} \cdot 45 \cdot \frac{w_{ce;new} + 2 \cdot w_{ce;original}}{w_{ce;new} + w_{ce;original}}) \\ &= 22.5 - (\frac{1}{3} \cdot 45 \cdot \frac{1.97 + 2 \cdot 2.30}{1.97 + 2.30}) = 0.58 \text{ m} \end{aligned} \tag{Eq. 28}$$

The parameters $c_{bearing;short}$, $w_{ce;original}$ and $w_{ce;new}$ are given in figure F.23.

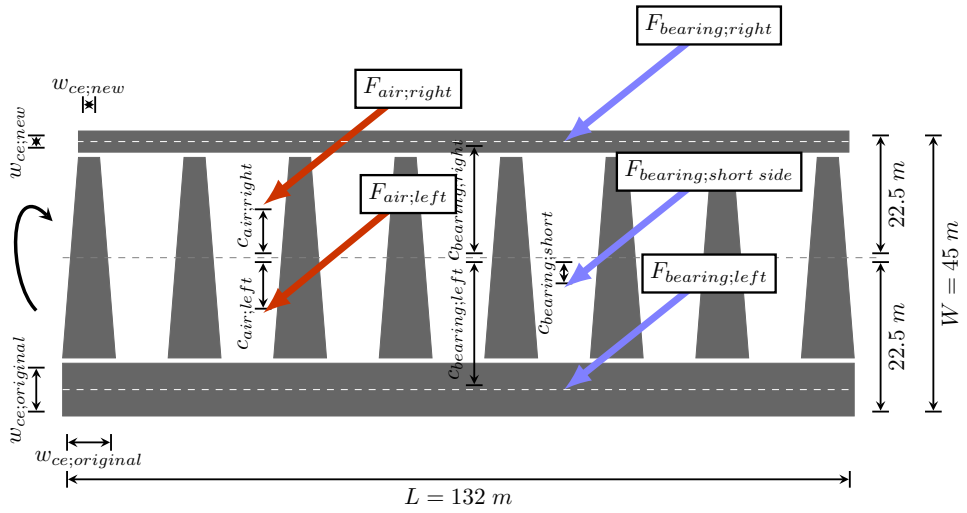

Figure F.23: *Schematisation of the foundation surface of the cutting edge and point of application of the bearing force on short side. (not on scale)*

At last the dimensions of the neutral soil pressure on the left side and the soil pressure on the right side will be calculated. On the left side the effective stress, which was given in figure 6.13, will be multiplied with the coefficient of neutral soil pressure K_n. This value can be calculated with equation 6.5. On the right side an increase force is available with a minimum value of the neutral soil stress and a maximum value of the passive soil stress. The results where given in figure 7.38. The corresponding moment can be calculated with equation Eq. 29 where $\sigma_{horizontal} = \sigma_{neutral}$ for the left side.

$$M_{horizontal} = \sum_{z=0}^{z=d} \sigma_{horizontal} \times (d - z) \tag{Eq. 29}$$

Because till this moment there is still no inclination and thereby no increase soil pressure the acting moment on both sides of the caisson is equal to $M_{horizontal;left} = M_{horizontal;right} =$ 14230 kNm.

With all forces known the total driving moment can be calculated:

$$\begin{aligned} M_{total} = {} & c_{bearing;left} \cdot F_{bearing;left} - c_{bearing;right} \cdot F_{bearing;right} \\ & + c_{bearing;short} \cdot F_{bearing;short\ side} + c_{air;left} \cdot F_{air;left} \\ & - c_{air;right} \cdot F_{air;right} + M_{horizontal;left} - M_{horizontal;right} \\ = {} & 767870\ \text{kNm} \end{aligned} \tag{Eq. 30}$$

The self weight of the caisson, used ballast weight and friction forces are going through the center of gravity and are thereby not included in the equation. Because $M_{total} \neq 0$ the caisson will tilt. The new width of the cutting edge after equilibrium can be calculated by requiring $M_{total} = 0$ and and where $w_{ce;new}$ is the only unknown. The equations Eq. 23–Eq. 30 can be recalculated. The new width of the cutting edge becomes $w_{ce;new} = 2.29$ m. This corresponds with an unilateral subsidence($w_{vertical}$) of:

$$w_{vertical} = \frac{w_{ce;new} - w_{ce;bottom}}{w_{ce;top} - w_{ce;bottom}} \cdot h_{ce;top} - \frac{w_{ce;original} - w_{ce;bottom}}{w_{ce;top} - w_{ce;bottom}} \cdot h_{ce;top} + 0.5$$
$$= \frac{2.29 - 0.5}{2.5 - 0.5} \cdot 3 - \frac{2.30 - 0.5}{2.5 - 0.5} \cdot 3 + 0.5 = 0.477 \text{ m} \quad \text{(Eq. 31)}$$

The situation is schematised and the dimensions are given in figure F.24a. The results over depth are given in figure F.25.

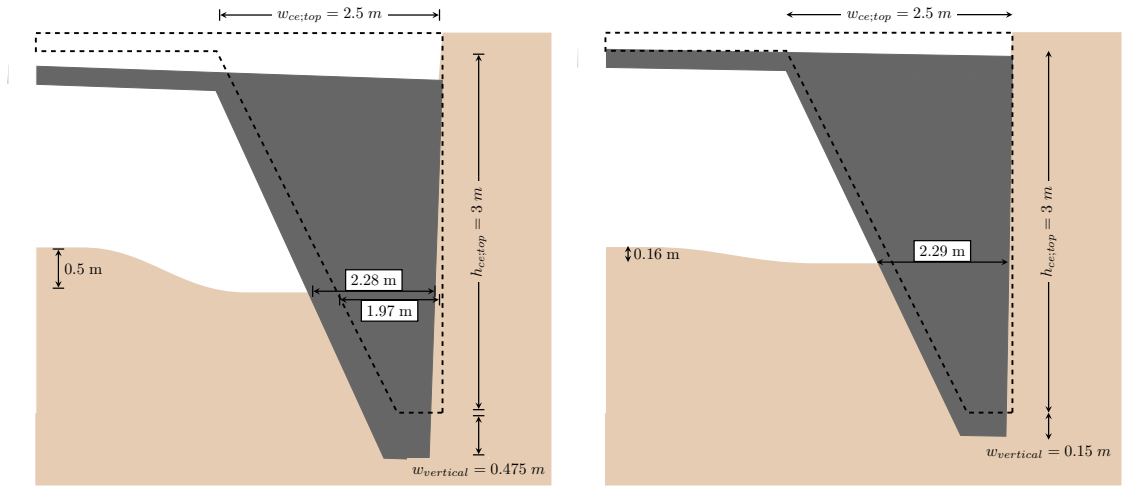

(a) *Schematisation of cutting edge in tilted position with corresponding dimensions for excavation of 50 cm*

(b) *Dimensions during a maximum inclination of* $w_{vertical} = 15\ cm$

Figure F.24: *Inclination of the cutting edge*

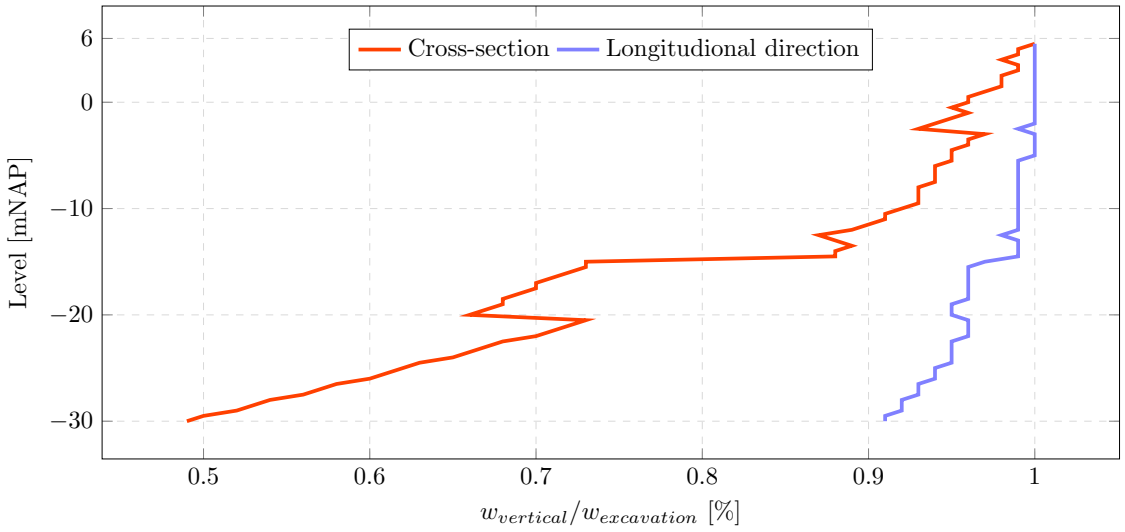

Figure F.25: *Unequal subsidence of the caisson by an unequal excavation of 50 cm*

This subsidence of 0.477 m is more than the maximum subsidence allowed of 0.15 meter. All the steps above are summarised in a flow chart given in figure F.26.

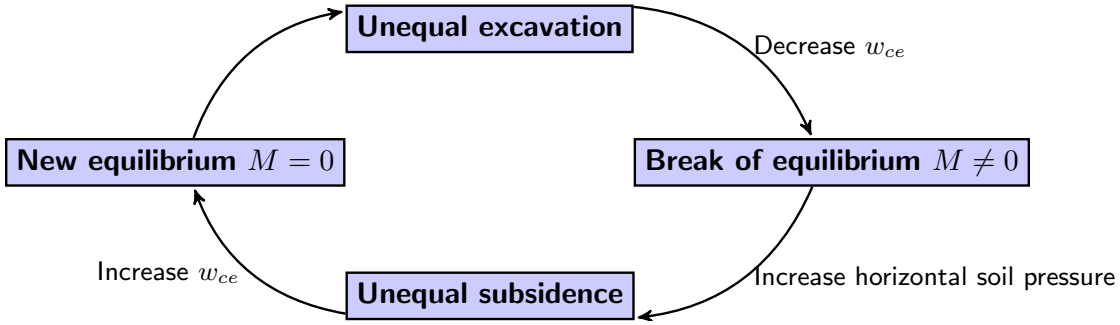

Figure F.26: *Flow chart of the different steps*

The question can also be reversed. The maximum differential excavation can be calculated whereby a maximum differential subsidence of $1:300 \Rightarrow 0.15$ cm occurs for the cross section and $1:300 \Rightarrow 0.44$ cm for the longitudinal section. Requiring $w_{vertical} = 0.15$ m and $M_{total} = 0$ gives a maximum excavation difference inside the working chamber of 0.16 meter where 0.5 meter was used for the previous calculations. This is schematised in figure F.24b. The maximum differential excavation $d_{excavation}$ is calculated in figure F.27.

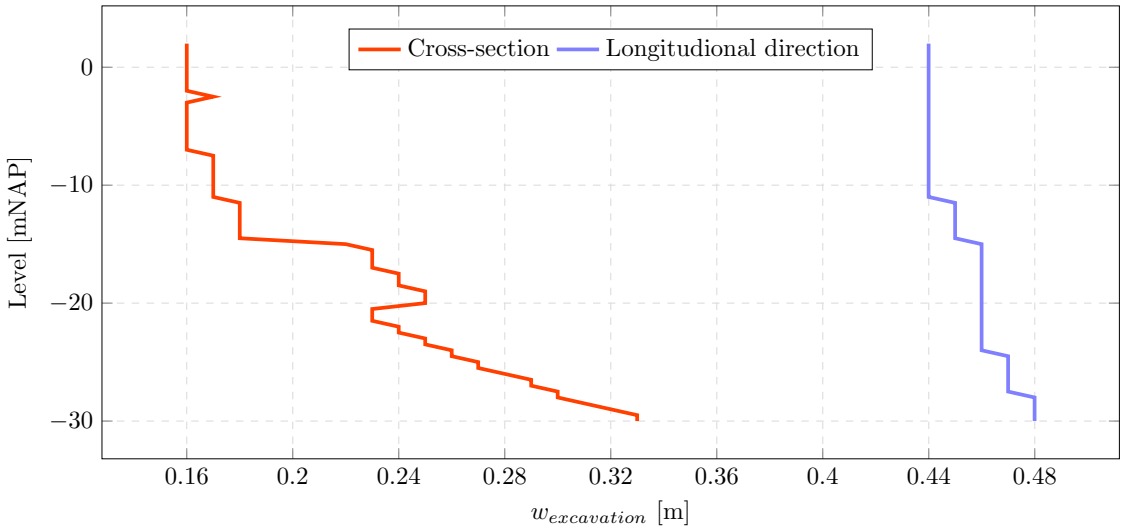

Figure F.27: *Maximum excavation difference for a differential settlement of* $w_{vertical} = 0.15$ m *for the x-direction or* $w_{vertical} = 0.44$ m *for the y-direction*

F.7 CONNECTION BETWEEN THE ELEMENTS

The lock head and –chamber can be constructed in different stages. When the pneumatic caissons are subsided to their final depth they should be connected to the lock chamber and to each other in the case multiple caissons are used for one lock head. In this master thesis the lock head

consist out of one large caissons or two multiple caissons divided by each other with a navigable section. However in other cases situations exists where caisson must be connected to each other. In that case the caissons should have an interspace of roughly 70 to 150 cm. There are multiple options to connect the different elements to each other below surface level.

- **Retaining wall** - A retaining wall which connects to the caissons.
- **Freezing** - By freezing the pore water between the soil particles the strength of the total soil body increases.
- **Jet Grouting** - Jet Grouting is method of ground improvement that does not penetrate the soil by means of impregnation or but uses high energy in the form of a high velocity jet of grout to destroy the soil structure and simultaneously mix cement grout into the soil. [Bachy, 2010]

F.7.1 RETAINING WALL

A retaining wall can be placed against the walls of the caissons. This retaining wall could be exist out of a sheet pile–, combi– or diaphragm wall. The soil in between the retaining wall and the bulkheads of the caisson can be excavated after finishing of the retaining wall. The groundwater table remains unchanged. After reaching the final depth an under water concrete floor will be cast. After hardening of this floor the water can be pumped out of this intermediate space and the bulkheads can be removed where after the final joint structure can be created. A schematisation is given in figure F.28.

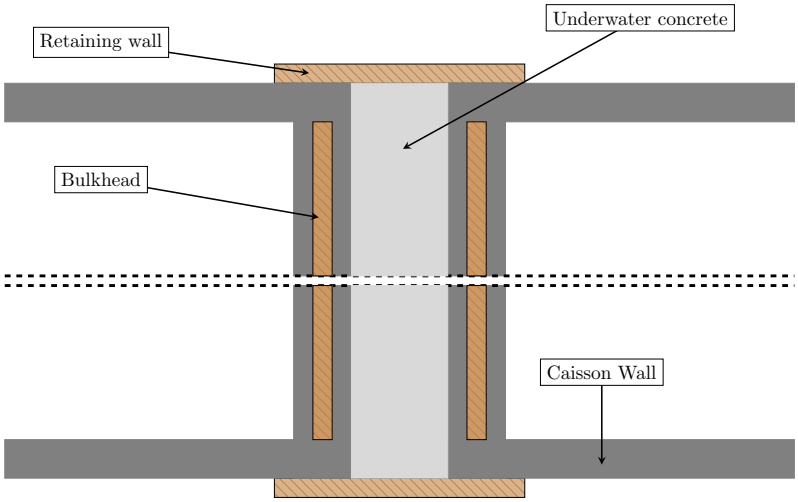

Figure F.28: *Top view of two caissons combined to each other*

F.7.2 FREEZING

The principle behind ground freezing is the use of refrigeration to convert pore water to ice particles. The ice becomes a bonding material, fusing together adjacent particles of soil to increase their combined strength and make them impermeable. Excavation and other work can

then proceed safely inside of, or next to, the barrier of strong, watertight frozen earth. Frozen ground is normally employed to provide one or more temporary functions such as support for an excavation, structural underpinning and groundwater control. Ground freezing is adaptable to practically any size, shape, or depth of excavation or structure and can be done with the same physical plant from site to site, despite wide variation in these factors. [Braun et al., 1979]

There are multiple freezing techniques available. They can be divided in three main groups: [Kleefmann, 2002]

- **Open circuits** - Freezing pipes are placed in the ground whereby liquid nitrogen is circulated. Due to the evaporation of the nitrogen, heat is extracted from the subsoil. Due to the low temperature of the nitrogen a high freezing rate can be achieved. Disadvantage of the open circuit is the high price of the system.
- **Closed circuits** - A primary circuit where freezing gasses likes freon, ammonia or carbon dioxide are brought to a liquid phase is combined with a secondary circuit where for example a brine solution is present. The primary circuit is a source of cooling for the secondary circuits which leads through the ground. With a closed circuit lower temperatures could be achieved but the freezing rate is lower in comparison with liquid nitrogen.
- **Combined circuits** - Combination of the above.

Retaining structures that are designed with freezing tecnhiques can act as water– and soil retaining structure. The soil must contain water, which is present in Terneuzen from a depth of NAP -2 meter. In the case of the lock in Terneuzen this freezing technique can be used to create a temporary retaining wall consisting out of frozen soil. In the meantime a permanent joint can be constructed between the both caissons and between the caisson and retaining wall of the lock chamber. A top and side view are schematised in respectively figure F.29 and F.30 where two caissons are combined to each other. Freezing pipes are installed both vertically, in the shape of an arc and horizontally where they can be installed trough the cutting edge. After the soil around the location of the joints is sufficient frozen the bulkheads can be removed and concrete joints can be constructed between the caissons. After finishing the freezing installation can be removed. In figure F.31a–F.31d the process of connecting two caissons with help of freezing pipes is given.

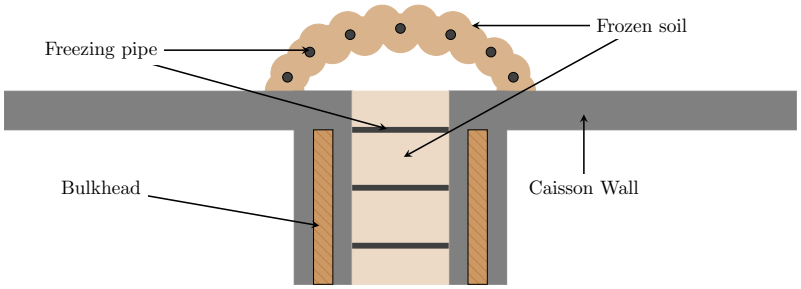

Figure F.29: *Top view of two caissons combined to each other with freezing techniques (not on scale)*

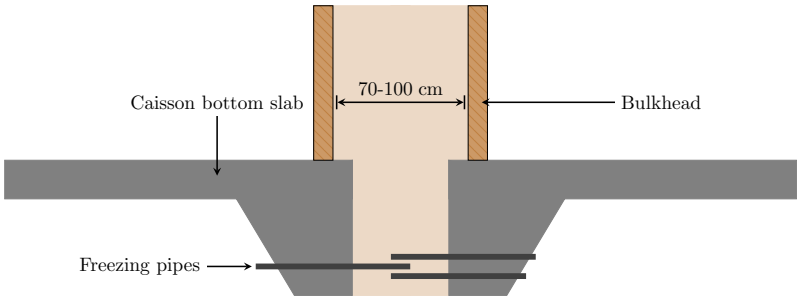

Figure F.30: *Side view of two caissons combined to each other with freezing techniques (not on scale)*

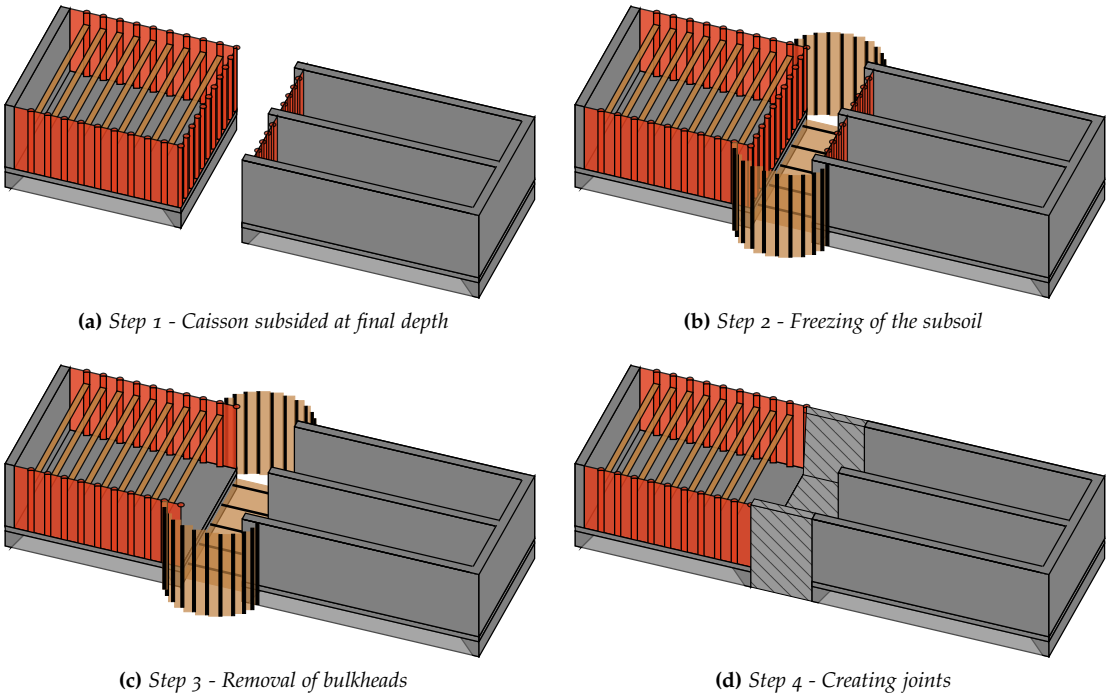

(a) *Step 1 - Caisson subsided at final depth*

(b) *Step 2 - Freezing of the subsoil*

(c) *Step 3 - Removal of bulkheads*

(d) *Step 4 - Creating joints*

Figure F.31: *Connection of two pneumatic caissons*

F.7.3 JET GROUTING

Jet grouting is one of the most popular ground improvement techniques, and is currently used all over the world for many different purposes, such as increasing the bearing capacity and reducing settlements of new and existing foundations, supporting for open and underground excavations and creating water cut-offs for dams. The method is based on high-speed grouting of water-cement mixtures and/or other fluids (air water) into the subsoil. The fluids are injected through small diameter nozzles placed on a grout pipe, which is continuously rotated at a constant rate and slowly released towards the ground surface. The jet propagates radially from the borehole axis and after some time the injected mortar solidifies underground eventually producing a cemented soil body of quasi cylindrical shape. [Modoni et al., 2006] There are

different jet grouting methods. Classified according to the number of fluids that are injected into the subsoil. In the same way as described in the previous section the jet grouting technique can be used to create impervious cut-off retaining walls and impervious bottoms. When multiple jet columns are combined a secant columns wall can be constructed which acts as temporary or final joint. In figure F.32 and F.33 respectively a top– and side view of the situation is given.

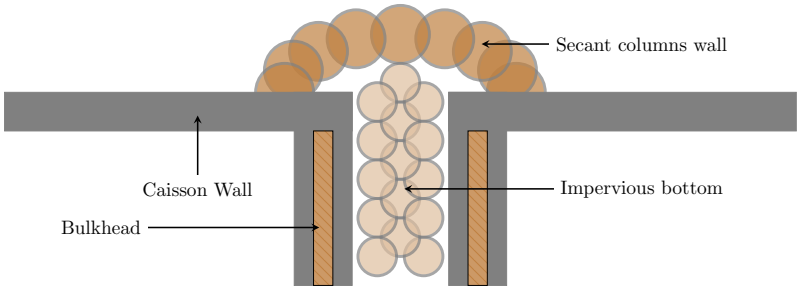

Figure F.32: *Top view of two caissons combined to each other with grouting techniques (not on scale)*

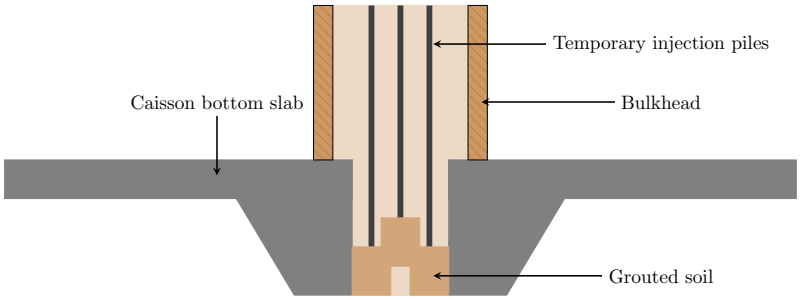

Figure F.33: *Side view of two caissons combined to each other with grouting techniques (not on scale)*

G

CALCULATION RESULTS

G.1 RESULTS FROM SCIA ENGINEER

All stiffness differences are based on $\lambda = 5$. *Explained in section 7.3.1*

G.1.1 VARIANT 1

Caisson bottom slab

Table G.1: *Maximum design moments in bottom slab for different load combinations and support reactions. Dimensions are listed in* kNm/m.

Caisson bottom slab	**mxD-**	**myD-**	**mxD+**	**myD+**
Load Combination 1				
Homogeneous supported	16099	45497	8567	6265
Caisson edges supported on stiff soil	21508	52961	14005	10880
Caisson edges supported on weak soil	9251	30405	7769	9300
Caisson diagonal supported	18847	51223	10146	7875
Load Combination 2				
Homogeneous supported	29904	24287	5563	6739
Caisson edges supported on stiff soil	27532	26198	6272	6272
Caisson edges supported on weak soil	30712	26166	1184	7717
Caisson diagonal supported	29968	24917	6223	7357
Maximum occurring moment	**30712**	**52961**	**14005**	**10880**

Table G.2: *Maximum tensile forces in bottom slab for different load combinations and support reactions. Dimensions are listed in* kN/m.

Caisson bottom slab	**Load combination 1**		**Load combination 2**	
	x	**y**	**x**	**y**
Homogeneous Supported	0	221	1238	1110
Caisson edges supported on stiff soil	1564	3676	1588	1759
Caisson edges supported on weak soil	0	1806	660	486
Caisson diagonal supported	0	2283	577	631

Caisson wall

Table G.3: *Maximum design moment in caisson wall for different load combinations and support reactions. Dimensions are listed in* kNm/m.

Caisson wall	**mxD-**	**myD-**	**mxD+**	**myD+**
Load Combination 1				
Homogeneous supported	30806	40525	14918	12492
Caisson edges supported on stiff soil	33548	38414	16701	14134
Caisson edges supported on weak soil	26139	41383	13612	11232
Caisson diagonal supported	31144	41568	15737	13470
Load Combination 2				
Homogeneous supported	13642	6703	7318	5724
Caisson edges supported on stiff soil	13521	6705	7220	5682
Caisson edges supported on weak soil	13064	6706	6871	5478
Caisson diagonal supported	14391	23484	7541	5951
Maximum occurring moment	**33548**	**41568**	**16701**	**14134**

Table G.4: *Maximum tensile forces in wall for different load combinations and support reactions. Dimensions are listed in* kN/m.

Caisson wall	**Load combination 1**		**Load combination 2**	
	x	**y**	**x**	**y**
Homogeneous Supported	0	4124	2563	7534
Caisson edges supported on stiff soil	1650	1456	1443	7129
Caisson edges supported on weak soil	7887	2086	3362	6637
Caisson diagonal supported	2810	536	2057	7473

Bulkhead

Table G.5: *Maximum design moment in bulkhead for different load combinations and support reactions. Dimensions are listed in* kNm/m.

Bulkhead	**mxD-**	**myD-**	**mxD+**	**myD+**
Load Combination 1				
Homogeneous supported	17494	26416	12825	10757
Caisson edges supported on stiff soil	19515	25110	13986	11864
Caisson edges supported on weak soil	17032	26991	12372	10326
Caisson diagonal supported	14084	27413	11775	9610
Maximum occurring moment	**19515**	**27413**	**13986**	**11864**

G.1.2 VARIANT 2

Caisson bottom slab

Table G.6: *Maximum design moments in bottom slab for different load combinations and support reactions for the smaller caisson covering the gate recess. Dimensions are listed in* kNm/m.

Caisson covering gate recess	**mxD-**	**myD-**	**mxD+**	**myD+**
Load Combination 1				
Homogeneous supported	16484	3643	0	0
Caisson edges supported on stiff soil	16811	4489	0	34
Caisson edges supported on weak soil	16297	3337	0	1792
Caisson diagonal supported	17508	4704	0	0
Load Combination 2				
Homogeneous supported	24577	14778	11078	18265
Caisson edges supported on stiff soil	22283	12028	9639	20205
Caisson edges supported on weak soil	30135	17483	11501	18800
Maximum occurring moment	**30135**	**17483**	**11501**	**20205**

Table G.7: *Maximum design moments in bottom slab for different load combinations and support reactions for the larger caisson covering the gate chamber. Dimensions are listed in* kNm/m.

Caisson covering gate chamber	**mxD-**	**myD-**	**mxD+**	**myD+**
Load Combination 1				
Homogeneous supported	9705	23811	3559	2713
Caisson edges supported on stiff soil	11292	24623	5847	5360
Caisson edges supported on weak soil	8708	23710	6096	5628
Caisson diagonal supported	14002	27313	8022	6186
Load Combination 2				
Homogeneous supported	6357	23637	3220	2781
Caisson edges supported on stiff soil	7385	23036	6141	3939
Caisson edges supported on weak soil	8149	25403	4279	3800
Caisson diagonal supported	3706	13013	5316	6018
Maximum occurring moment	**11292**	**25403**	**8022**	**6186**

Table G.8: *Maximum tensile forces in bottom slab for different load combinations and support reactions. Dimensions are listed in* kN/m.

Caisson bottom slab	**Load combination 1**		**Load combination 2**	
	x	**y**	**x**	**y**
Homogeneous Supported	772	3516	3404	3114
Caisson edges supported on stiff soil	3372	8069	4517	6598
Caisson edges supported on weak soil	0	939	2878	1689
Caisson diagonal supported	1481	3868	3300	2811

Caisson wall

Table G.9: *Maximum design moments in caisson wall for different load combinations and support reactions for the smaller caisson covering the gate recess. Dimensions are listed in* kNm/m.

Caisson for gate recess	**mxD-**	**myD-**	**mxD+**	**myD+**
Load Combination 1				
Homogeneous supported	11298	3683	7985	6666
Caisson edges supported on stiff soil	11291	3686	7992	6669
Caisson edges supported on weak soil	11306	3648	7979	6666
Caisson diagonal supported	11834	4152	12308	6814
Load Combination 2				
Homogeneous supported	2558	8652	2422	1691
Caisson edges supported on stiff soil	2583	8927	3362	1729
Caisson edges supported on weak soil	2558	8676	1678	1676
Maximum occurring moment	**11834**	**8927**	**12308**	**6814**

Table G.10: *Maximum design moments in caisson wall for different load combinations and support reactions for the larger caisson covering the gate chamber. Dimensions are listed in* kNm/m.

Caisson for gate chamber	**mxD-**	**myD-**	**mxD+**	**myD+**
Load Combination 1				
Homogeneous supported	17868	15712	12500	9778
Caisson edges supported on stiff soil	19021	14089	13271	10595
Caisson edges supported on weak soil	17390	17083	12172	9475
Caisson diagonal supported	24501	17774	13886	11486
Load Combination 2				
Homogeneous supported	13990	22343	7539	5914
Caisson edges supported on stiff soil	14119	23882	7734	5948
Caisson edges supported on weak soil	13611	22397	7302	5821
Caisson diagonal supported	11140	12785	7204	5091
Maximum occurring moment	**24501**	**23882**	**13886**	**11486**

Table G.11: *Maximum tensile forces in wallfor different load combinations and support reactions. Dimensions are listed in* kN/m.

Caisson wall	**Load combination 1**		**Load combination 2**	
	x	**y**	**x**	**y**
Homogeneous Supported	539	241	2606	5636
Caisson edges supported on stiff soil	1700	1043	1216	5088
Caisson edges supported on weak soil	939	1292	1915	2165
Caisson diagonal supported	825	1068	848	195

Bulkhead

Table G.12: *Maximum design moments in bulkhead for different load combinations and support reactions for the smaller caisson covering the gate recess. Dimensions are listed in* kNm/m.

Caisson for gate recess	**mxD-**	**myD-**	**mxD+**	**myD+**
Load Combination 1				
Homogeneous supported	8001	6660	8243	9072
Caisson edges supported on stiff soil	8004	6665	8238	9042
Caisson edges supported on weak soil	7998	6659	8252	9109
Caisson diagonal supported	8153	6805	7272	9700
Maximum occurring moment	**8153**	**6805**	**8252**	**9700**

Table G.13: *Maximum design moments in bulkhead for different load combinations and support reactions for the larger caisson covering the gate chamber. Dimensions are listed in* kNm/m.

Caisson for gate chamber	**mxD-**	**myD-**	**mxD+**	**myD+**
Load Combination 1				
Homogeneous supported	15162	3713	4576	3776
Caisson edges supported on stiff soil	16153	3854	5803	4302
Caisson edges supported on weak soil	14727	3675	3964	3677
Caisson diagonal supported	20602	4221	9259	5081
Maximum occurring moment	**20602**	**4221**	**9259**	**5081**

G.2 OVERVIEW OF REINFORCEMENT

Input					
Variant 1 - Caisson bottom slab					
M	30712	52961	14005	10880	kNm/m
N	1588	3676	1588	3676	kN/m
Location	Bottom	Bottom	Top	Top	
Direction	x	y	x	y	
b	1000	1000	1000	1000	mm
d	5000	5000	5000	5000	mm
Reinforcement					
diameter	32	32	32	32	mm
hoh	150	150	150	150	mm
rows	4	7	2	2	-
Output					
i	118	118	118	118	mm
As	21447	37532	10723	10723	mm^2
c_xy	32		32		
c_extra	160,5	321	53,5	53,5	mm
d_act	4742	4613	4849	4881	mm
xu	775,6	1267,4	308,2	98,9	mm
z	4440	4120	4729	4842	mm
rho	0,452%	0,814%	0,221%	0,220%	
Mrd	37909	59854	18267	13526	kNm/m
Med/Mrd(N)	81%	88%	77%	80%	

Input					
Variant 1 - Caisson wall					
M	33548	41568	16701	14134	kNm/m
N	7887	7534	7887	7534	kN/m
Location	Bottom	Bottom	Top	Top	
Direction	x	y	x	y	
b	1000	1000	1000	1000	mm
d	3500	3500	3500	3500	mm
Reinforcement					
diameter	32	40	32	32	mm
hoh	150	125	150	125	mm
rows	8	5 *	5	3	-
Output					
i	118	85	118	93	mm
As	42893	50265	26808	19302	mm^2
c_xy	40		32		
c_extra	374,5	230	214	107	mm
d_act	3020	3200	3188	3327	mm
xu	1078,9	1435,6	377,8	86,0	mm
z	2600	2642	3041	3294	mm
rho	1,421%	1,571%	0,841%	0,580%	
Mrd	37993	48755	22803	14707	kNm/m
Med/Mrd(N)	88%	85%	73%	96%	

Input					
Variant 2 - Caisson bottom slab					
M	11299	25403	6096	6186	kNm/m
N	3372	8069	3372	8069	kN/m
Location	Bottom	Bottom	Top	Top	
Direction	x	y	x	y	
b	1000	1000	1000	1000	mm
d	5000	5000	5000	5000	mm
Reinforcement					
diameter	32	32	32	32	mm
hoh	150	150	150	150	mm
rows	2	5	2	3	-
Output					
i	118	118	118	118	mm
As	10723	26808	10723	16085	mm^2
c_xy	32		32		
c_extra	53,5	214	53,5	107	mm
d_act	4849	4720	4849	4827	mm
xu	129,4	359,6	129,4	-107,8	mm
z	4798	4580	4798	4869	mm
rho	0,221%	0,568%	0,221%	0,333%	
Mrd	14110	34341	14110	13540	kNm/m
Med/Mrd(N)	80%	74%	43%	46%	

Input					
Variant 2 - Caisson wall					
M	29968	52922	14005	10880	kNm/m
N	4517	6598	4517	6598	kN/m
Location	Bottom	Bottom	Top	Top	
Direction	x	y	x	y	
b	1000	1000	1000	1000	mm
d	3500	3500	3500	3500	mm
Reinforcement					
diameter	32	40	32	32	mm
hoh	150	125	150	150	mm
rows	6	6	3	3	-
Output					
i	118	85	118	118	mm
As	32170	60319	16085	16085	mm^2
c_xy	40		32		
c_extra	267,5	287,5	107	107	mm
d_act	3127	3143	3295	3327	mm
xu	949,4	1967,7	248,3	39,6	mm
z	2757	2377	3198	3312	mm
rho	1,029%	1,919%	0,488%	0,483%	
Mrd	32329	55848	14900	11715	kNm/m
Med/Mrd(	93%	95%	94%	93%	

fck	20	N/mm2	fyk	500 N/mm2
fcd	13,3	N/mm2	fyd	434,78 N/mm2
fctm,fl	2,2	N/mm2		
fcm	43	N/mm2		
c	50	mm		

G.3 OVERVIEW OF ADJUSTED REINFORCEMENT

Input					
Variant 1 - Caisson bottom slab					
M	30712	52961	14005	10880	kNm/m
%	27%	29%	17%	30%	
M+%	39004	68320	16386	14144	kNm/m
N	1588	3676	1588	3676	kN/m
Location	Bottom	Bottom	Top	Top	
Direction	x	y	x	y	
b	1000	1000	1000	1000	mm
d	5000	5000	5000	5000	mm
Reinforcement					
diameter	32	32	32	32	mm
hoh	150	150	150	150	mm
rows	**5**	**9**	2	**3**	-
Output					
i	118	118	118	118	mm
As	26808	48255	10723	16085	mm^2
c_xy	32		246		
c_extra	214	428	53,5	107	mm
d_act	4688	4506	4635	4827	mm
xu	1009,3	1734,8	308,2	332,6	mm
z	4295	3831	4515	4698	mm
rho	0,572%	1,071%	0,231%	0,333%	
Mrd	46721	73673	17269	24138	kNm/m
Med/Mrd(	83%	93%	95%	59%	

Input					
Variant 1 - Caisson wall					
M	33548	41568	16701	14134	kNm/m
%	4%	2%	5%	6%	
M+30%	34890	42399	17536	14982	kNm/m
N	7887	7534	7887	7534	kN/m
Location	Bottom	Bottom	Top	Top	
Direction	x	y	x	y	
b	1000	1000	1000	1000	mm
d	3500	3500	3500	3500	mm
Reinforcement					
diameter	32	40	32	32	mm
hoh	150	125	150	125	mm
rows	**11**	5	5	**4**	-
Output					
i	118	85	118	93	mm
As	58978	50265	26808	25736	mm^2
c_xy	500		353		
c_extra	535	230	214	160,5	mm
d_act	2399	3200	2867	3274	mm
xu	1780,0	1435,6	377,8	366,5	mm
z	1707	2642	2720	3131	mm
rho	2,458%	1,571%	0,935%	0,786%	
Mrd	35424	48755	19061	22923	kNm/m
Med/Mrd(N)	98%	87%	92%	65%	

Input					
Variant 2 - Caisson bottom slab					
M	11299	25403	6096	6186	kNm/m
%	11%	6%	30%	40%	
M+30%	12542	26927	7925	8660	kNm/m
N	3372	8069	3372	8069	kN/m
Location	Bottom	Bottom	Top	Top	
Direction	x	y	x	y	
b	1000	1000	1000	1000	mm
d	5000	5000	5000	5000	mm
Reinforcement					
diameter	32	32	32	32	mm
hoh	150	150	150	150	mm
rows	**3**	5	2	3	-
Output					
i	118	118	118	118	mm
As	16085	26808	10723	16085	mm^2
c_xy	460		246		
c_extra	107	214	53,5	107	mm
d_act	4367	4720	4635	4827	mm
xu	363,1	359,6	129,4	-107,8	mm
z	4226	4580	4584	4869	mm
rho	0,368%	0,568%	0,231%	0,333%	
Mrd	21599	34341	13113	13540	kNm/m
Med/Mrd(N)	58%	78%	60%	64%	

Input					
Variant 2 - Caisson wall					
M	29968	52922	14005	10880	kNm/m
%	4%	5%	4%	5%	
M+30%	31167	55568	14565	11424	kNm/m
N	4517	6598	4517	6598	kN/m
Location	Bottom	Bottom	Top	Top	
Direction	x	y	x	y	
b	1000	1000	1000	1000	mm
d	3500	3500	3500	3500	mm
Reinforcement					
diameter	32	40	32	32	mm
hoh	150	125	150	150	mm
rows	**9**	6	**4**	3	-
Output					
i	118	85	118	118	mm
As	48255	60319	21447	16085	mm^2
c_xy	615		246		
c_extra	428	287,5	160,5	107	mm
d_act	2391	3143	3028	3327	mm
xu	1650,5	1967,7	482,0	39,6	mm
z	1749	2377	2840	3312	mm
rho	2,018%	1,919%	0,708%	0,483%	
Mrd	31692	55848	19424	11715	kNm/m
Med/Mrd(N)	98%	99%	75%	98%	

fck	20	N/mm2	fyk	500 N/mm2
fcd	13,3	N/mm2	fyd	434,8 N/mm2
fctm,fl	2,2	N/mm2		
fcm	43	N/mm2		
c	50	mm		

G.4 FRICTION FORCES & AIR PRESSURE

NAP	depth	gamma	theta	c	level	total	water	effective	kn	fs	level	Ffriction	Ffriction;without	level
6	0	17,5	25	0	6	0	0	0,00	0,58	0,00	6	0,00	0,00	6
5,5	0,5	17,5	25	0	5,5	8,75	0	8,75	0,58	1,51	5,5	0,76	0,76	5,5
5	1	17,5	25	0	5	17,5	0	17,50	0,58	3,02	5	3,02	3,02	5
4,5	1,5	17,5	25	0	4,5	26,25	0	26,25	0,58	4,54	4,5	6,81	6,81	4,5
4	2	17,5	25	0	4	35	0	35,00	0,58	6,05	4	12,10	12,10	4
3,5	2,5	17,5	25	0	3,5	43,75	0	43,75	0,58	7,56	3,5	18,91	18,91	3,5
3	3	17,5	25	0	3	52,5	0	52,50	0,58	9,07	3	27,22	27,22	3
2,5	3,5	16	21	3	2,5	61,25	0	61,25	0,64	9,80	2,5	34,30	34,30	2,5
2	4	16	21	3	2	69,25	0	69,25	0,64	11,08	2	44,31	44,31	2
1,5	4,5	16	21	3	1,5	77,25	5	72,25	0,64	11,56	1,5	49,98	52,01	1,5
1	5	16	21	3	1	85,25	10	75,25	0,64	12,04	1	55,65	60,19	1
0,5	5,5	16	21	3	0,5	93,25	15	78,25	0,64	12,52	0,5	61,32	68,85	0,5
0	6	16	21	3	0	101,25	20	81,25	0,64	13,00	0	66,99	77,99	0
-0,5	6,5	16	21	3	-0,5	109,25	25	84,25	0,64	13,48	-0,5	72,66	87,61	-0,5
-1	7	16	21	3	-1	117,25	30	87,25	0,64	13,96	-1	78,33	97,71	-1
-1,5	7,5	16	21	3	-1,5	125,25	35	90,25	0,64	14,44	-1,5	84,00	108,28	-1,5
-2	8	16	21	3	-2	133,25	40	93,25	0,64	14,92	-2	89,67	119,34	-2
-2,5	8,5	16	21	3	-2,5	141,25	45	96,25	0,64	15,40	-2,5	95,34	130,88	-2,5
-3	9	17,1	32	0	-3	149,25	50	99,25	0,47	18,22	-3	110,39	163,99	-3
-3,5	9,5	17,1	32	0	-3,5	157,8	55	102,80	0,47	18,87	-3,5	116,74	179,30	-3,5
-4	10	17,1	32	0	-4	166,35	60	106,35	0,47	19,53	-4	123,10	195,25	-4
-4,5	10,5	17,1	32	0	-4,5	174,9	65	109,90	0,47	20,18	-4,5	129,46	211,86	-4,5
-5	11	17,1	32	0	-5	183,45	70	113,45	0,47	20,83	-5	135,81	229,11	-5
-5,5	11,5	17,1	32	0	-5,5	192	75	117,00	0,47	21,48	-5,5	142,17	247,02	-5,5
-6	12	17,1	32	0	-6	200,55	80	120,55	0,47	22,13	-6	148,53	265,58	-6
-6,5	12,5	17,1	32	0	-6,5	209,1	85	124,10	0,47	22,78	-6,5	154,89	284,80	-6,5
-7	13	17,1	32	0	-7	217,65	90	127,65	0,47	23,44	-7	161,24	304,66	-7
-7,5	13,5	17,1	32	0	-7,5	226,2	95	131,20	0,47	24,09	-7,5	167,60	325,18	-7,5
-8	14	17,1	32	0	-8	234,75	100	134,75	0,47	24,74	-8	173,96	346,35	-8
-8,5	14,5	17,1	32	0	-8,5	243,3	105	138,30	0,47	25,39	-8,5	180,31	368,17	-8,5
-9	15	19,1	37	0	-9	251,85	110	141,85	0,40	25,94	-9	186,26	389,09	-9
-9,5	15,5	19,1	37	0	-9,5	261,4	115	146,40	0,40	26,77	-9,5	193,34	414,96	-9,5
-10	16	19,1	37	0	-10	270,95	120	150,95	0,40	27,60	-10	200,41	441,65	-10
-10,5	16,5	19,1	37	0	-10,5	280,5	125	155,50	0,40	28,44	-10,5	207,49	469,18	-10,5
-11	17	19,1	37	0	-11	290,05	130	160,05	0,40	29,27	-11	214,57	497,55	-11
-11,5	17,5	19,1	37	0	-11,5	299,6	135	164,60	0,40	30,10	-11,5	221,65	526,74	-11,5
-12	18	19,1	37	0	-12	309,15	140	169,15	0,40	30,93	-12	228,73	556,77	-12
-12,5	18,5	17,1	32	0	-12,5	318,7	145	173,70	0,47	31,89	-12,5	236,31	589,96	-12,5
-13	19	17,1	32	0	-13	327,25	150	177,25	0,47	32,54	-13	242,67	618,29	-13
-13,5	19,5	19,1	37	0	-13,5	335,8	155	180,80	0,40	33,06	-13,5	248,50	644,71	-13,5
-14	20	19,1	37	0	-14	345,35	160	185,35	0,40	33,89	-14	255,58	677,88	-14
-14,5	20,5	19,1	37	0	-14,5	354,9	165	189,90	0,40	34,73	-14,5	262,65	711,88	-14,5
-15	21	19,1	37	0	-15	364,45	170	194,45	0,40	35,56	-15	269,73	746,72	-15
-15,5	21,5	19,1	37	0	-15,5	374	175	199,00	0,40	36,39	-15,5	276,81	782,38	-15,5
-16	22	19,1	37	0	-16	383,55	180	203,55	0,40	37,22	-16	283,89	818,88	-16
-16,5	22,5	19,1	37	0	-16,5	393,1	185	208,10	0,40	38,05	-16,5	290,97	856,22	-16,5
-17	23	19,1	37	0	-17	402,65	190	212,65	0,40	38,89	-17	298,04	894,38	-17
-17,5	23,5	19,1	37	0	-17,5	412,2	195	217,20	0,40	39,72	-17,5	305,12	933,37	-17,5
-18	24	19,1	37	0	-18	421,75	200	221,75	0,40	40,55	-18	312,20	973,20	-18
-18,5	24,5	19,1	37	0	-18,5	431,3	205	226,30	0,40	41,38	-18,5	319,28	1013,86	-18,5
-19	25	19,1	37	0	-19	440,85	210	230,85	0,40	42,21	-19	326,36	1055,35	-19
-19,5	25,5	19,1	37	0	-19,5	450,4	215	235,40	0,40	43,05	-19,5	333,43	1097,68	-19,5
-20	26	19,1	37	0	-20	459,95	220	239,95	0,40	43,88	-20	340,51	1140,83	-20
-20,5	26,5	19	23	90	-20,5	469,5	225	244,50	0,61	40,85	-20,5	332,13	1082,41	-20,5
-21	27	19	23	90	-21	479	230	249,00	0,61	41,60	-21	338,89	1123,13	-21
-21,5	27,5	19	23	90	-21,5	488,5	235	253,50	0,61	42,35	-21,5	345,65	1164,60	-21,5
-22	28	19	23	90	-22	498	240	258,00	0,61	43,10	-22	352,40	1206,83	-22
-22,5	28,5	19	23	90	-22,5	507,5	245	262,50	0,61	43,85	-22,5	359,16	1249,80	-22,5
-23	29	19	23	90	-23	517	250	267,00	0,61	44,60	-23	365,92	1293,53	-23
-23,5	29,5	19	23	90	-23,5	526,5	255	271,50	0,61	45,36	-23,5	372,68	1338,01	-23,5
-24	30	19	23	90	-24	536	260	276,00	0,61	46,11	-24	379,43	1383,24	-24
-24,5	30,5	19	23	90	-24,5	545,5	265	280,50	0,61	46,86	-24,5	386,19	1429,22	-24,5
-25	31	19	23	90	-25	555	270	285,00	0,61	47,61	-25	392,95	1475,96	-25
-25,5	31,5	19	23	90	-25,5	564,5	275	289,50	0,61	48,36	-25,5	399,70	1523,45	-25,5
-26	32	19	23	90	-26	574	280	294,00	0,61	49,12	-26	406,46	1571,68	-26
-26,5	32,5	19	23	90	-26,5	583,5	285	298,50	0,61	49,87	-26,5	413,22	1620,67	-26,5
-27	33	19	23	90	-27	593	290	303,00	0,61	50,62	-27	419,97	1670,41	-27
-27,5	33,5	19	23	90	-27,5	602,5	295	307,50	0,61	51,37	-27,5	426,73	1720,91	-27,5
-28	34	19	23	90	-28	612	300	312,00	0,61	52,12	-28	433,49	1772,15	-28
-28,5	34,5	19	23	90	-28,5	621,5	305	316,50	0,61	52,87	-28,5	440,25	1824,15	-28,5
-29	35	19	23	90	-29	631	310	321,00	0,61	53,63	-29	447,00	1876,90	-29
-29,5	35,5	19	23	90	-29,5	640,5	315	325,50	0,61	54,38	-29,5	453,76	1930,40	-29,5
-30	36	19	23	90	-30	650	320	330,00	0,61	55,13	-30	460,52	1984,65	-30

NAP	depth	water	air
6	0	0	0
5,5	0,5	0	0
5	1	0	0
4,5	1,5	0	0
4	2	0	0
3,5	2,5	0	0
3	3	0	0
2,5	3,5	0	0
2	4	0	0
1,5	4,5	5	5
1	5	10	10
0,5	5,5	15	15
0	6	20	20
-0,5	6,5	25	25
-1	7	30	30
-1,5	7,5	35	35
-2	8	40	40
-2,5	8,5	45	45
-3	9	50	50
-3,5	9,5	55	55
-4	10	60	60
-4,5	10,5	65	65
-5	11	70	70
-5,5	11,5	75	75
-6	12	80	80
-6,5	12,5	85	85
-7	13	90	90
-7,5	13,5	95	95
-8	14	100	100
-8,5	14,5	105	105
-9	15	110	110
-9,5	15,5	115	115
-10	16	120	120
-10,5	16,5	125	125
-11	17	130	130
-11,5	17,5	135	135
-12	18	140	140
-12,5	18,5	145	145
-13	19	150	150
-13,5	19,5	155	155
-14	20	160	160
-14,5	20,5	165	165
-15	21	170	170
-15,5	21,5	175	175
-16	22	180	180
-16,5	22,5	185	185
-17	23	190	190
-17,5	23,5	195	195
-18	24	200	200
-18,5	24,5	205	205
-19	25	210	210
-19,5	25,5	215	215
-20	26	220	220
-20,5	26,5	225	225
-21	27	230	230
-21,5	27,5	235	235
-22	28	240	240
-22,5	28,5	245	245
-23	29	250	250
-23,5	29,5	255	255
-24	30	260	260
-24,5	30,5	265	265
-25	31	270	270
-25,5	31,5	275	275
-26	32	280	280
-26,5	32,5	285	285
-27	33	290	290
-27,5	33,5	295	295
-28	34	300	300
-28,5	34,5	305	305
-29	35	310	310
-29,5	35,5	315	315
-30	36	320	320

G.5 HORIZONTAL AND ROTATIONAL FORCE ON CAISSON

NAP	x	effective stress	theta	Kn	sigma hor
6	0	0	26	0,56	0
5,5	0,5	8,6	26	0,56	4,830008138
5	1	17,2	26	0,56	9,660016275
4,5	1,5	25,8	26	0,56	14,49002441
4	2	34,4	26	0,56	19,32003255
3,5	2,5	43	26	0,56	24,15004069
3	3	51,6	26	0,56	28,98004883
2,5	3,5	60,2	21	0,64	38,62624944
2	4	68,3	21	0,64	43,82346905
1,5	4,5	71,4	21	0,64	45,8125284
1	5	74,5	21	0,64	47,80158776
0,5	5,5	77,6	21	0,64	49,79064712
0	6	80,7	21	0,64	51,77970647
-0,5	6,5	83,8	21	0,64	53,76876583
-1	7	86,9	21	0,64	55,75782518
-1,5	7,5	90	21	0,64	57,74688454
-2	8	93,1	21	0,64	59,7359439
-2,5	8,5	96,2	21	0,64	61,72500325
-3	9	99,3	28	0,53	52,68147382
-3,5	9,5	103,6	28	0,53	54,9627461
-4	10	107,9	28	0,53	57,24401838
-4,5	10,5	112,2	28	0,53	59,52529066
-5	11	116,5	28	0,53	61,80656294
-5,5	11,5	120,8	28	0,53	64,08783522
-6	12	125,1	28	0,53	66,3691075
-6,5	12,5	129,4	28	0,53	68,65037978
-7	13	133,7	28	0,53	70,93165206
-7,5	13,5	138	28	0,53	73,21292434
-8	14	142,3	28	0,53	75,49419662
-8,5	14,5	146,6	28	0,53	77,7754689
-9	15	150,9	31	0,48	73,1807545
-9,5	15,5	155,65	31	0,48	75,48432364
-10	16	160,4	31	0,48	77,78789278
-10,5	16,5	165,15	31	0,48	80,09146193
-11	17	169,9	31	0,48	82,39503107
-11,5	17,5	174,65	31	0,48	84,69860022
-12	18	179,4	31	0,48	87,00216936
-12,5	18,5	184,15	27	0,55	100,5476495
-13	19	188,35	27	0,55	102,8408894
-13,5	19,5	192,55	31	0,48	93,37941868
-14	20	197,4	31	0,48	95,73148401
-14,5	20,5	202,25	31	0,48	98,08354935
-15	21	207,1	31	0,48	100,4356147
-15,5	21,5	211,95	31	0,48	102,78768
-16	22	216,8	31	0,48	105,1397454
-16,5	22,5	221,65	31	0,48	107,4918107
-17	23	226,5	31	0,48	109,843876
-17,5	23,5	231,35	31	0,48	112,1959414
-18	24	236,2	31	0,48	114,5480067
-18,5	24,5	241,05	31	0,48	116,900072
-19	25	245,9	31	0,48	119,2521374
-19,5	25,5	250,75	31	0,48	121,6042027
-20	26	255,6	31	0,48	123,9562681
-20,5	26,5	260,45	25	0,58	150,3790737
-21	27	264,6	25	0,58	152,7752079
-21,5	27,5	268,75	25	0,58	155,1713422
-22	28	272,9	25	0,58	157,5674764
-22,5	28,5	277,05	25	0,58	159,9636106
-23	29	281,2	25	0,58	162,3597448
-23,5	29,5	285,35	25	0,58	164,755879
-24	30	289,5	25	0,58	167,1520132
-24,5	30,5	293,65	25	0,58	169,5481474
-25	31	297,8	25	0,58	171,9442817
-25,5	31,5	301,95	25	0,58	174,3404159
-26	32	306,1	25	0,58	176,7365501
-26,5	32,5	310,25	25	0,58	179,1326843
-27	33	314,4	25	0,58	181,5288185

SUM H	136334
SUM M	1499670
M/V	7,15239076